DEVELOPMENT OF A DRY POWDER INHALER AND NEBULISED NANOPARTICLES-BASED FORMULATIONS OF CURCUMINOIDS FOR THE POTENTIAL TREATMENT OF LUNG CANCER

Y. AL AYOUB

PhD

UNIVERSITY OF BRADFORD

2017

Development of a Dry Powder Inhaler and Nebulised Nanoparticle-Based Formulations of Curcuminoids for the Potential Treatment of Lung Cancer

Development of Drug Delivery Formulations of Curcuminoids to the Lungs using Air Jet Milling and Sonocrystallisation Techniques for Dry Powder Inhaler Preparations; and Nanoemulsion and Microsuspension for Nebuliser Formulations

Yuosef AL AYOUB

Submitted for the Degree of

Doctor of Philosophy

School of Pharmacy

University of Bradford

2017

Abstract

Development of a Dry Powder Inhaler and Nebulised Nanoparticle-Based Formulations of Curcuminoids for the Potential Treatment of Lung Cancer

Yuosef AL Ayoub

Keywords: Curcumin, Demethoxycurcumin, Bisdemethoxycurcumin, Dry Powder Inhaler, Air Jet Milling, Sonocrystallisation, Nebuliser, Nanoemulsion, Microsuspension, Particles Aerodynamic Characterisations.

Abstract:

Curcuminoids have strong anticancer activities but have low bioavailability. The highest rate of cancer deaths comes from lung tumours; therefore, inhaled curcuminoids could treat lung cancer locally. To date, there are no nebulised formulations of curcuminoids, and there are no inhalable curcuminoids particles without excipients using air jet mill and sonocrystallisation methods for DPI formulations. It is the first time; the aerodynamic parameters of curcumin, demethoxycurcumin and bisdemethoxycurcumin were measured individually using NGI. The size, shape, free surface energy, and the crystal polymorphism of the produced inhalable curcuminoid particles were characterised using laser diffraction, SEM, IGC, DSC and XRPD, respectively. Several DPI formulations with a variable particle size of curcuminoids were prepared in two drug-carrier ratios (1:9 and 1:67.5). The best performance of the DPI formulations of the sonocrystallised particles, which exist in crystal structure form1, were obtained from ethanol- heptane, as illustrated FPF 43.4%, 43.6% and 43.4% with MMAD of 3.6µm, 3.5µm and 3.4µm, whereas the best DPI formulation of the air jet milled particles was presented FPF 38.0%, 38.9%, and 39.5% with MMAD of 3.6µm, 3.4µm and 3.2µm for curcumin, demethoxycurcumin and bisdemethoxycurcumin, respectively.

Nebulised curcuminoids using nanoemulsion and microsuspension formulations were prepared. The physical properties, such as osmolality, pH and the viscosity of the aerosolised nanoemulsion and the microsuspension formulations were determined. The FPF% and MMAD of nebulised nanoemulsion ranged from 44% to 50% and from 4.5µm to 5.5µm respectively. In contrast, the FPF% of microsuspension ranged from 26% to 40% and the MMAD from 5.8µm to 7.05µm. A HPLC method was developed and validated in order to be used in the determination of curcuminoids from an aqueous solution.

List of Publications

1. “Development of a dry powder inhaler formulation of curcumin for lung cancer treatment” Yuosef AL Ayoub1, Khaled Assi1, Anant Paradkar1, Mohammad Amin1, abstract in Journal of Aerosol Medicine and Pulmonary Drug Delivery 28(3): A40-A40 · June 2015
2. Development and evaluation of nanoemulsion and microsuspension nebulised formulations of curcuminoids for lung delivery with new approach of understanding the aerosol performance of nanoparticles (submitted to the International Journal of Nanomedicine).
3. Development and evaluation a dry powder inhaler of curcuminoids particles produced using sonocrystallisation technique for lung delivery (under preparation).

Acknowledgment

All praise and thanks to Allah, the most gracious and the most merciful.

I would like to dedicate this research to the memory of my mother, who was taken from me as she was killed in a mortar attack in Syria. The memory of her warmth, kindness and constant encouragement are the reasons I continue to do better.

To my father who passed away before seeing this and who believed in my abilities and pushed me to do the best as I can from an early age, his words are still alive to encourage me.

I thank my wife and all my siblings, who have supported and encouraged me throughout this challenging time. The smiles of my two children, Nour and Hiba, made the journey all the more pleasant.

I would like to express my sincere and special thanks to Dr. Khaled Assi, my supervisor, for his encouragement and unwavering support throughout the duration of my PhD. This research would not have been possible without him.

Last but not least, I thank my co-supervisor Prof. Anant Paradakr, his guidance and support have been invaluable throughout this project.

Table of Contents

Abstract ……i

List of Publications ……ii

Acknowledgment……iii

Table of Contents…….. iv

List of Figures……viii

List of Tables……xvii

Chapter 1: Literature review.....2

1.1. General introduction.....2

1.2. An overview on the respiratory system 5

1.3. Lung cancer 6

1.3.1. Aetiology of lung cancer.....8

1.3.2. Pathophysiology of lung cancer 11

1.3.3. Types of lung cancer.....14

1.3.4. Chemotherapy via inhalation for lung cancer 17

1.3.5. Curcumin.....20

1.4. Pulmonary drug delivery 27

1.5. Method of producing particles for pulmonary delivery.....28

1.5.1. Air jet milling:.....28

1.5.2. Sonocrystallisation 30

1.5.3. Other methods 34

1.6. Factors affecting deposition of drug particles in the lungs 35

1.6.1. Particle size.....35

1.6.2. Inhalation technique.....35

1.7. Method of administration of inhaled drugs 36

1.7.1. Dry powder inhalers (DPIs) 36

1.7.2. Metered dose inhalers (MDIs).....38

1.7.3. Nebulisers.....39

1.8. Curcumin formulations 39

1.9. Nanoparticles genotoxicity 41

1.10. In vitro method of assessment of drug deposition in the lung (using impaction method) 42

1.11. Principles of operation of cascade Impactor 43

1.11.1. Next Generation Impactor 45

1.12. Hypothesis 47

1.13. Aims and Objectives 48

1.14. Thesis structure 49

Chapter 2: Materials and Methods 51

2.1 Materials 51

2.2 Instruments and Apparatus 52

2.2.1 Apparatus used in high performance liquid chromatography (HPLC) 52

2.2.2 Apparatus used in particle size reduction (air jet mill) 52

2.2.3 Ultrasound instrument 53

2.2.4 Apparatus used in particles characterisation and analysis 53

2.2.5 Apparatus and software used to evaluate the in vitro particle deposition of dry powder inhalers and nanoemulsion formulations 53

2.2.6 General laboratories apparatus 54

2.3 Methods 54

2.3.1 Air jet milling for particle size reduction of curcuminoids 54

2.3.2 Sonocrystallisation of curcuminoids 55

2.3.3 Nanoemulsion preparations for nebulisation of curcuminoids 56

2.3.4 Powder particles characterisation 56

2.3.5 Thermal method of analysis 56

2.3.6 X-ray powder diffraction (XRPD) 58

2.3.7 Particle size analysis 59

2.3.8 Scanning electron microscope (SEM) 60

2.3.9 Powder surface free energy characterisation 61

2.3.10 Surface energy calculation method 62

2.3.11 High performance liquid chromatography (HPLC) 65

Chapter 3: Development and validation of HPLC methods for the determination of curcuminoids in aqueous solution 70

3.1 HPLC assay for curcuminoids using conventional mobile phase 70

3.1.1 Introduction 70

3.1.2 Method 71

3.1.3 Method development 72

3.1.4 Method validation 73

3.1.5 Conclusion 77

3.2 HPLC assay for curcuminoids using microemulsion mobile phase 77

3.2.1 Introduction 77

3.2.2 HPLC conditions 80

3.2.3 Method development 81

3.2.4 Factors affecting the HPLC separation using microemulsion 83

3.2.5 Method validation 89

3.2.6 Conclusion 93

Chapter 4: Production of inhaled curcumin particles using air jet milling technique 95

4.1. Introduction 95

4.2. Methods 96

4.2.1. Method of milling a start material of curcumin using jet mill 96

4.2.2. Surface energy analysis 98

4.2.3. Surface energy calculation method 99

4.2.4. Blending of micronized curcumin with α-lactose 99

4.2.5. Aerodynamic particle size characterisation 100

4.2.6. HPLC method 103

4.3. Results and discussion 104

4.3.1. Particle size analysis 104

4.3.2. Morphology of the air jet milled curcumin particles using scanning electron microscope (SEM) 105

4.3.3. Thermal analysis of milled curcumin particles (DSC) 108

4.3.4. X-ray powder diffraction (XRPD) 109

4.3.5. Surface energy analysis of curcumin powder 110

4.3.6. Dry powder inhaler preparations and Drug content uniformity 112

4.3.7. Aerodynamic characterisation of DPI of curcumin formulations 115

4.4. Conclusion 120

Chapter 5: Sonocrystallisation of curcumin for inhalation application ... 123

5.1. Introduction 123

5.2. Methods 125

5.2.1. Sonocrystallisation of curcumin 125

5.3. Results and discussion 127

5.3.1. Particle size analysis using laser diffraction 127

5.3.2. Morphology of sonocrystallised curcumin particles using scanning electron microscope (SEM) 133

5.3.3. Differential scanning calorimetry (DSC) 139

5.3.4. X-ray powder diffraction (XRPD) 146

5.3.5. Surface energy analysis of curcumin particles 152

5.3.6. Dry powder inhaler preparations 157

5.3.7. Aerodynamic characterisation using next generation impactor 158

5.4. Conclusion 167

Chapter 6: Development and evaluation of nanoemulsion and microsuspension formulations of curcuminoids for lung cancer using nebuliser 171

6.1. Introduction 171

6.2. Methods 173

6.2.1. Nanoemulsion Preparation 173

6.2.2. Microsuspension preparation 174

6.2.3. Osmolality and PH 175

6.2.4. Physical stability studies 175

6.2.5. Particles size measurement 176

6.2.6. Zeta potential determination.....176

6.2.7. Density 176

6.2.8. Viscosity.....176

6.2.9. CEN method for measuring aerosol output 177

6.2.10. Aerodynamic diameter measurements and particles lungs depositions.....178

6.2.11. Genotoxicity 179

6.3. Results and discussions.....181

6.3.1. Nanoemulsion preparation and optimization 181

6.3.2. Osmolality 184

6.3.3. pH 186

6.3.4. Viscosity.....187

6.3.5. Density 188

6.3.6. Particle size analysis using malvern (zetasizer) 189

6.3.7. Zeta potential 191

6.3.8. Physical stability results 192

6.3.9. Aerosol output using the jet nebuliser 193

6.3.10. Aerodynamic particles size characterisation 201

6.3.11. Genotoxicity of curcumin nanoemulsion 218

6.4. Conclusion 221

Chapter 7: General conclusion and future work 225

7.1 General Conclusion 225

7.2 Future Work.....229

Chapter 8: References 232

8.1 References 232

List of Figures

Figure 1. 1 The branching patterns of the airway from the conducting to the transitional and to the respiratory airway zones 6
Figure 1. 2 Normal goblet cells (Almeida and Barry 2010).....12
Figure 1. 3 Stratified squamous epithelium (Almeida and Barry 2010) 12
Figure 1. 4 Hyperplasia (b) and Dysplasia (c) (Almeida and Barry 2010) 14
Figure 1.5 Percentage of the lung cancer types (adapted from mechanismsinmedicine.com).....15
Figure 1. 6 Site of the squamous cell carcinoma in the central lung and the mucociliary epithelial cell (adopted from www.urac.org (American Accreditation HealthCare Commission).....15
Figure 1. 7 Site of adenocarcinoma in the lung periphery and alveolar type II cells (adopted from www.urac.org (American Accreditation HealthCare Commission).....16
Figure 1. 8 Sit of the large cell carcinoma is either in the central & peripheral lung area or squamous & glandular features (adopted from www.urac.org (American Accreditation HealthCare Commission).....16
Figure 1. 9 Site of the small cell carcinoma in the central of the lung (adopted from www.urac.org (American Accreditation HealthCare Commission).....17
Figure 1. 10 Chemical structures of curcuminoids 25
Figure 1. 11 Crystal packing of curcumin polymorphs (Cambridge Structural Database), F1 is curcumin form1, F2 is curcumin form 2, and F3 is curcumin form 3.....27
Figure 1. 12 Schematic diagram of a spiral jet mill (Brodka-Pfeiffer et al. 2003) 30
Figure 1. 13 Solubility diagram shows metastable zone 32
Figure 1. 14 Formation of transient and stable cavitation bubbles by ultrasound (Leonelli and Mason 2010) 34
Figure 1. 15 Schematic diagram of the disintegration of spherical pellets through a specific disintegration mechanism, Reproduced from (Chrystyn 2003) 37
Figure 1. 16 Principle of cascade impactor operation (Reproduced from Copley, 2008).....44
Figure 1. 17 Next Generation Impactor, (a) NGI including pre-separator and induction port, (b) NGI (open view) showing nozzles & collection cups, (c) NGI

(open view) showing cup tray removed, (d) Collection cups showing typical deposition pattern (Reproduced from Copley, 2008) 46
Figure 2. 1 A spiral jet mill (FPS,Italy).....54
Figure 2. 2 Schematic diagram of DSC.....57
Figure 2. 3 Schematic diagram of particles size analyser via laser diffraction ..59
Figure 2.4 Schematic diagram of SEM (Adapted from www.purdue.edu/REM/rs/sem.htm) 60
Figure 3.1 Chromatograms of curcumin (C), demethoxycurcumin (DC), and bisdemethoxycurcumin (BDC) with emodin using conventional HPLC method 73
Figure 3. 2 Calibration curve of curcumin (RC), demethoxycurcumin (RD) and bisdemethoxycurcumin (RB) using mobile phase of 55%:45%v/v (acetonitrile: phosphate buffer).....74
Figure 3. 3 Separation of curcuminoids using microemulsion using isopropyl myristate as oil phase, C is curcumin, DC is demethoxycurcumin and BDC is bisdemethoxycurcumin. 82
Figure 3. 4 Chromatograms of curcuminoids using microemulsion as an eluent, C is curcumin, DC is demethoxycurcumin, and BDC is bisdemethoxycurcumin. 83
Figure 3.5 The effect of SDS concentrations on the retention time of curcuminoids, SDS is sodium dodecyl sulphate, C is curcumin, DC is demethoxycurcumin, and BDC is bisdemethoxycurcumin. 85
Figure 3.6 The effect of butanol concentrations on the retention time of curcuminoids, C is curcumin, DC is demethoxycurcumin, and BDC is bisdemethoxycurcumin. 86
Figure 3.7 The effect of IPM concentrations on the retention time of curcuminoids, IPM is isopropyl myristate oil C is curcumin, DC is demethoxycurcumin, and BDC is bisdemethoxycurcumin. 87
Figure 3.8 The effect of buffer concentrations on the retention time of curcuminoids, C is curcumin, DC is demethoxycurcumin, and BDC is bisdemethoxycurcumin. 88
Figure 3. 9 The effect of temperature on the retention time of curcuminoids, C is curcumin, DC is demethoxycurcumin, and BDC is bisdemethoxycurcumin. 89
Figure 3. 10 Calibration curves of curcuminoids using microemulsion mobile phase, C is curcumin, DC is demethoxycurcumin and BDC is bisdemethoxycurcumin 90

List of Figures

Figure 4. 1 The component of the next generation impaction (NGI). 102
Figure 4. 2 Setting up the NGI for DPIs characterisation 102
Figure 4. 3 SEM images of micronized curcumin particles, A is unprocessed curcumin particles, B, C and D milled curcumin particles with D_{50} of 2.5µm, E and F micronized curcumin particles with D_{50} of 3.5µm. 107
Figure 4. 4 DSC thermograms of the jet milled curcumin particles, A is unprocessed powder, and B and C are micronized curcumin particles with D_{50} on 2.5µm and 3.5µm, respectively 108
Figure 4. 5 Diffractograms of curcumin powder form1 (A), B is unprocessed curcumin; C and D are milled curcumin particles D_{50} of 2.5µm and 3.5µm, respectively. 110
Figure 4.6 The non-dispersive (specific energy), dispersive and total free surface energy of unprocessed and milled curcumin particles with particle size. 112
Figure 4. 7 The work of adhesion of unprocessed and milled curcumin particles, and work of adhesion of processed curcumin particles (2.5µm and 3.5µm) with α-lactose. 112
Figure 4. 8 Mass distribution DPI formulation (1:9 drug:carrier ratio) of curcumin particles (D_{50}=3.5µm) among NGI stages from easyhaler device at flow of 45 L/m for 5.5 second, C is curcumin, DC is demethoxycurcumin and BDC is bisdemethoxycurcumin. 117
Figure 4. 9 Mass distribution DPI formulation (1:67.5 drug:carrier ratio) of curcumin particles (D_{50}=3.5µm) among NGI stages from easyhaler device at flow of 45 L/m for 5.5 second, C is curcumin, DC is demethoxycurcumin and BDC is bisdemethoxycurcumin. 117
Figure 4. 10 Mass distribution DPI formulation (1:9 drug:carrier ratio) of curcumin particles (D_{50}=2.5µm) among NGI stages from easyhaler device at flow of 45 L/m for 5.5 second, C is curcumin, DC is demethoxycurcumin and BDC is bisdemethoxycurcumin. 118
Figure 4. 11 Mass distribution DPI formulation (1:67.5 drug: carrier ratio) of curcumin particles (D_{50}=2.5µm) among NGI stages from easyhaler device at flow of 45 L/m for 5.5 second, C is curcumin, DC is demethoxycurcumin and BDC is bisdemethoxycurcumin. 119
Figure 5.1 SEM images of sonocrystallised curcumin particles which precipitated from different organic solvents with water and heptane.....139

Figure 5. 2 SEM images of curcumin particles which precipitated from ethanol and water without ultrasound. *Before-sono is the curcumin particles prepared without ultrasound,*After-sono is the formed particles sonicated for 15 minutes. 139
Figure 5. 3 DSC thermograms of precipitated curcumin particles from ethanol-water at different ultrasound amplitude 141
Figure 5.4 DSC thermograms of precipitated curcumin particles from ethanol-water at different sonication time 141
Figure 5. 5 DSC thermograms of precipitated curcumin particles from isopropanol-water at different ultrasound amplitude 142
Figure 5.6 DSC thermograms of precipitated curcumin particles from isopropanol-water at different sonication time.....143
Figure 5. 7 DSC thermograms of precipitated curcumin particles from acetone-water at different sonication time 144
Figure 5. 8 DSC thermograms of sonocrystallised curcumin particles from ethanol, isopropanol and acetone as good solvents and heptane as an antisolvent.....145
Figure 5. 9 XRPD patterns of curcumin polymorphs reproduced from Cambridge Crystallographic Data Centre (CCDC) 147
Figure 5. 10 XRPD patterns of sonocrystallised curcumin particles from ethanol-water at different ultrasound amplitude 148
Figure 5. 11 XRPD patterns of sonocrystallised curcumin particles from ethanol-water at different times of sonication.....148
Figure 5. 12 XRPD patterns of sonocrystallised curcumin particles from isopropanol-water at different ultrasound amplitude 149
Figure 5.13 XRPD patterns of sonocrystallised curcumin particles from isopropanol-water at different times of sonication.....150
Figure 5. 14 XRPD patterns of sonocrystallised curcumin particles from acetone-water at different times of sonication.....150
Figure 5. 15 XRPD patterns of sonocrystallised curcumin particles from ethanol, acetone and isopropanol and heptane as an antisolvent. 151
Figure 5. 16 Surface energy of sonocrystallised curcumin, sono8: particles precipitated from isopropanol-water; sono2: particles precipitated from ethanol-water; sono14: particles precipitated from acetone-water.....153

Figure 5. 17 Surface energy of sonocrystallised curcumin, sono16: particles precipitated from ethanol-heptane; sono17: particles precipitated from acetone-heptane. 154
Figure 5. 18 Surface energy of lactose (lactohale200) which is used in DPI formulations of curcumin 154
Figure 5. 19 The work of adhesion between sonocrystallised curcumin and lactose, sono16: particles precipitated from ethanol-heptane, sono17: particles precipitated from acetone-heptane. 155
Figure 5. 20 The work of cohesion between sonocrystallised curcumin, sono16: particles precipitated from ethanol-heptane, sono17: particles precipitated from acetone-heptane 155
Figure 5. 21 Mass distribution of DPI formulation (sono17-2) of sonocrystallised curcumin particles from acetone-heptane (sono17). BDC: Bisdemethoxycurcumin, DC: Demethoxycurcumin, C: curcumin. 159
Figure 5. 22 Mass distribution of DPI formulation (sono17-1) of sonocrystallised curcumin particles from acetone-heptane (sono17). BDC: bisdemethoxycurcumin, DC: demethoxycurcumin, C: curcumin 160
Figure 5. 23 Mass distribution of DPI formulation (sono16-2) of sonocrystallised curcumin particles from ethanol-heptane (sono16). BDC: bisdemethoxycurcumin, DC: demethoxycurcumin, C: curcumin 162
Figure 5. 24 Mass distribution of DPI formulation (sono16-2) of sonocrystallised curcumin particles from ethanol-heptane (sono16). BDC: bisdemethoxycurcumin, DC: demethoxycurcumin, C: curcumin 163
Figure 5. 25 drug particles distributed on a carrier surface at low and high concentration of drugs particles in dry powder inhaler formulations....166
Figure 5. 26 drug detachments from the carrier surface during inhalation 167
Figure 6.1 Schematic diagram of aerosol output system, adapted from Boe (Boe et al. 2001) 178
Figure 6.2 NGI and nebuliser set up 179
Figure 6.3 Schematic structure of glass slide preparation for comet assay 181
Figure 6.4 An example of illustrative data analysis obtained from malvern zeta sizer for NE11 190
Figure 6.5 Schematic diagram of physical instability of emulsion 193

Figure 6.6 The relationships between the suspension concentrations and the Fine Particle Fraction of curcuminoids. BDC*: Bisdemethoxycurcumin. DC*: Demethoxycurcumin. C*: Curcumin. FPF*: Fine Particle Fraction. 203
Figure 6.7 The relationships between the suspension concentrations and the Mass Median Aerodynamic Diameters (MMAD) of curcuminoids. BDC*: Bisdemethoxycurcumin. DC*: Demethoxycurcumin. C*: Curcumin.....203
Figure 6.8 The mean (n=3, SD) of mass distribution of curcuminoids from suspension 3 in NGI using jet nebuliser at flow 15 L/min.....204
Figure 6.9 The mean (n=3, SD) of mass distribution of curcuminoids from suspension 2 in NGI using jet nebuliser at flow 15 L/min. 204
Figure 6.10 The mean (n=3, SD) of mass distribution of curcuminoids from suspension 1 in NGI using jet nebuliser at flow 15 L/min. 205
Figure 6.11 Nebulised droplets form microsuspension formulations at low drug concentration (A) and at high drug concentration (B).....206
Figure 6.12 The relationships between the drug nanoemulsion concentrations (using oleic acid oil) and the Fine Particle Fraction of curcuminoids. BDC*: Bisdemethoxycurcumin. DC*: Demethoxycurcumin. C*: Curcumin. FPF*: Fine Particle Fraction. 208
Figure 6.13 The relationship between the nanoemulsion concentrations (using oleic acid oil) and the Mass Median Aerodynamic Diameters (MMAD) of curcuminoids. BDC*: Bisdemethoxycurcumin. DC*: Demethoxycurcumin. C*: Curcumin. 208
Figure 6.14 The mean (n=3, SD) of mass distribution of curcuminoids nanoemulsion (NE11, with oleic acid oil) in NGI using jet nebuliser at flow 15 L/min. 209
Figure 6.15 The mean (n=3, SD) of mass distribution of curcuminoids nanoemulsion (NE10, with oleic acid oil) in NGI using jet nebuliser at flow 15 L/min 209
Figure 6.16 The mean (n=3, SD) of mass distribution of curcuminoids nanoemulsion (NE9, with oleic acid oil) in NGI using jet nebuliser at flow 15 L/min. 210
Figure 6.17 The relationship between the drug nanoemulsion concentrations (using limonene oil) and the Fine Particle Fraction of curcuminoids. BDC*: Bisdemethoxycurcumin. DC*: Demethoxycurcumin. C*: Curcumin. FPF*: Fine Particle Fraction 212

Figure 6.18 The relationship between the drug nanoemulsion concentrations (using limonene oil) and the Mass Median Aerodynamic Diameters (MMAD) of curcuminoids. BDC*: Bisdemethoxycurcumin. DC*: Demethoxycurcumin. C*: Curcumin. 212
Figure 6.19 The mean (n=3, SD) of mass distribution of curcuminoids nanoemulsion (NE5, with limonene oil) in NGI using jet nebuliser at flow 15 L/min. 213
Figure 6.20 The mean (n=3, SD) of mass distribution of curcuminoids nanoemulsion (NE4, with limonene oil) in NGI using jet nebuliser at flow 15 L/min. 213
Figure 6.21 The mean (n=3, SD) of mass distribution of curcuminoids nanoemulsion (NE3, with limonene oil) in NGI using jet nebuliser at flow 15 L/min. 214
Figure 6.22 Comparison of fine particle fraction (FPF) between nanoemulsion formulations (NE5: limonene oil, NE11: oleic acid oil) and suspension 3 of curcuminoids for the same concentration (100µg/ml). BDC*: bisdemethoxycurcumin, DC*: demethoxycurcumin.....215
Figure 6.23 Comparison of fine particle fraction (FPF) between nanoemulsion formulations (NE4: limonene oil, NE10: oleic acid oil) and suspension 2 of curcuminoids for the same concentration (250µg/ml). BDC*: bisdemethoxycurcumin, DC*: demethoxycurcumin. 215
Figure 6.24 fine particle fraction (FPF) comparison between nanoemulsion formulations (NE5: limonene oil, NE11: oleic acid oil) and suspension 3 of curcuminoids for the same concentration (100µg/ml). BDC*: bisdemethoxycurcumin, DC*: demethoxycurcumin. 216
Figure 6.25. Nebulised droplets from nanoemulsion formulation (A) and from microsuspension formulation (B).....217
Figure 6.26 Effect of curcuminoids nanoemulsion (with limonene oil) formulations on lymphocyte's DNA 219
Figure 6.27 Effect of curcuminoids nanoemulsion (with oleic acid oil) formulations on lymphocyte's DNA 220
Figure 6. 28 Lymphocyte DNA under a fluorescence microscope after treatment with curcuminoids nanoemulsion formulations, A & C: treated with curcuminoids nanoemulsion using oleic acid oil at concentrations 1 & 5 µg/ml. B &D: treated

with curcuminoids nanoemulsion using limonene oil at concentration 1 & 5 µg/ml. E is an example of positive control, and F is a negative control. 221

List of Tables

Table 1. 1 Advantages and disadvantages of DPI 37
Table 1. 2 Lung cancer types and their distribution in the lungs and the corresponding cut off diameters (CFD) of Next Generation Impactor (NGI) at flow 15 and 45 L/min.....46
Table 3.1 Regression coefficient, intercept, and the slope of curcuminoids components using 55%:45%v/v of acetonitrile: phosphate buffer mobile phase, flow rate 1 ml/min, λ=420nm, injection volume: 30µl.....74
Table 3.2 Limit of detection and limit of quantification of curcuminoid using the conventional method.....75
Table 3.3 Inter-day and intra-day precision data using the conventional method 76
Table 3.4 Accuracy data of the conventional method 77
Table 3. 5 Linearity data of curcuminoids components using microemulsion mobile phase.....90
Table 3. 6 Limit of detection and Limit of quantification data of curcuminiods using microemulsion mobile phase.....91
Table 3. 7 Inter-day and intra-day precision data of curcuminoids using the microemulsion mobile phase.....92
Table 3. 8 Accuracy data of curcuminoids using microemulsion mobile phase 93
Table 4. 1 The jet mill parameters setting, grinding pressure (GP) and Injection pressure.....98
Table 4. 2 The mean (n=3) and the standard deviation (SD) of the curcumin particles size before and after milling.....104
Table 4.3 The mean relative standard deviation (RSD%) for the mixing content uniformity of micronized curcumin (D_{50}=3.5µm) with lactose at different times (n=3), F1 is DPI formulation 1, which contains 1:9, curcumin: lactose w/w.....113
Table 4.4 The mean relative standard deviation (RSD%) for the mixing content uniformity of micronized curcumin (D_{50}=3.5µm) with lactose at different times (n=3), F2 is DPI formulation 2, which contains 1:67.5, curcumin: lactose w/w. 114
Table 4.5 The mean relative standard deviation (RSD%) for the mixing content uniformity of micronized curcumin (D_{50}=2.5µm) with lactose at 5 mins (n=3), F3&F4 are DPI formulations, which contain1:9 and 1:67.5, curcumin:lactose w/w, respectively.....114

Table 4.6 The aerodynamic parameters of DPI formulations (of curcumin particles (D_{50}=3.5µm) from easyhaler device at flow of 45 L/m for 5.5 second. 116

Table 4.7 The aerodynamic parameters of DPI formulations (of curcumin particles (D_{50}=2.5µm) from easyhaler device at flow of 45 L/m for 5.5 second. 118

Table 5.1 Parametrs of sonocrystallisation of curcumionds from ethano and water 125

Table 5.2 Parameters of sonocrystallisation of curcuminoids from isopropanol and water 126

Table 5.3 Parameters of sonocrystallisation of curcuminoids from acetone and water 126

Table 5.4 Parameters of sonocrystallisation of curcuminoids using different solvent and heptane as antisolvent 126

Table5.5 The mean size and the standard deviation (n=3) of the sonocrystallised curcumin particles which precipitated from ethanol and water. 127

Table5. 6 The mean size and the standard deviation (n=3) of the sonocrystallised curcumin particles which precipitated from isopropanol and water. 129

Table 5.7 The mean size and the standard deviation (n=3) of the sonocrystallised curcumin particles which precipitated from acetone and water. 130

Table 5. 8 The mean size and the standard deviation (n=3) of the sonocrystallised curcumin particles which precipitated from different solvents and heptane. 132

Table 5. 9 Endothermic peak temperature for precipitated curcumin particles from ethanol-water. 140

Table 5. 10 Polymorph transformation and melting temperature of precipitated curcumin particles from isopropanol-water 143

Table 5. 11 Endothermic peak temperature of precipitated curcumin particles from acetone-water 144

Table 5. 12 Endothermic peak temperature of sonocrystallised curcumin particles from ethanol, isopropanol and acetone as good solvents and heptane as an antisolvent 145

Table 5. 13 The mean (n=3) of the aerodynamic parameters of DPI formulation of curcuminoids of sono17 (sonocrystallised curcumin particles precipitated from acetone-heptane).....159
Table 5. 14 Aerodynamic characterisation of DPI formulation of curcuminoids of sono16 (sonocrystallised curcumin particles precipitated from ethanol-heptane) 162
Table 6. 1 Nanoemulsion compositions (NE: Nanoemulsion) 174
Table 6. 2 Results of visual observation for nanoemulsion reported in table 6.1 182
Table 6.3 Osmolality results for the nanoemulsion and suspension preparations and Sodium chloride concentrations in each formulation.....185
Table 6.4 pH results of nanoemulsion and suspension formulations 186
Table 6.5 Viscosity results of nanoemulsion and suspension formulation using viscometer.....187
Table 6. 6 Density results of both preparations nanoemulsion and suspension 188
Table 6.7 Particles size results and polydispersity index for nanoemulsion and suspension formulations using Zetasizer 189
Table 6.8 Zeta potential data for nanoemulsion and suspension formulations191
Table 6.9 The percentage of bisdemethoxycurcumin (BDC) that was nebulised from jet nebuliser at dose of 100µg/ml, 250µg/ml and 500µg/ml of 5ml of curcuminiods (n=3) 194
Table 6.10 The nebulisation time and the percentage of inhaled and exhaled BDC per minute using jet nebuliser.....195
Table 6.11 The percentage of demethoxycurcumin (DC) that nebulised from jet nebuliser at dose of 100µg/ml, 250µg/ml and 500 µg/ml of 5ml of curcuminoids 196
Table 6.12 The nebulisation time and the percentage of inhaled and exhaled DC per minute using jet nebuliser 197
Table 6.13 The percentage of curcumin (C) that nebulised from jet nebuliser at dose of 100µg/ml, 250µg/ml and 500µg/ml of 5 ml of curcuminoids 198
Table 6.14 The nebulisation time and the percentage of inhaled and exhaled curcumin (C) per minute using jet nebuliser.....199
Table6.15 The mean (n=3) of the aerodynamic data of suspension formulations using jet nebuliser at flow 15 L/min 202

Table 6.16 The mean (n=3) of the aerodynamic characterisation of curcuminoids nanoemulsion nanoemulsion with oleic acid oil formulations using jet nebuliser at flow 15 L/min 207
Table 6.17 The mean (n=3) of the aerodynamic characterisation of curcuminoids nanoemulsion with limonene oil formulations using jet nebuliser at flow 15 L/min.....211

List of Abbreviations

NE	Nanoemulsion
BDC	Bisdemethoxycurcumin
C	Curcumin
CFD	Cut off diameter
CEN	European Committee for Standardization, French: Comité Européen de Normalisation
DC	Demethoxycurcumin
DLS	Dynamic light scattering
DMSO	Dimethyl sulfoxide
DNA	Deoxyribonucleic acid
DPI	Dry powder inhaler
DSC	Differential scanning calorimetry
EDTA	Ethylenediaminetetraacetic acid
ETS	Environmental tobacco smoke
FDA	Food and Drug Administration
FPF	Fine particle fraction
GSD	Geometric standard deviation
HPLC	High performance liquid chromatography
ICH	International Conference on Harmonisation

IGC	Inverse gas chromatography
IPM	Isopropyl myristate
LOD	Limit of detection
LOQ	Limit of quantification
MELC	Microemulsion liquid chromatography
Min(s)	Minute (s)
mJ/M2	Millijoule per meter square
MMAD	Mass median aerodynamic diameter
NCSLC	Non-cell small lung cancer
NGI	Next generation impactor
NSCLC	Non-small cell lung cancer
ORR	Overall response rate
PDI	Polydispersity index
XRRD	Powder X-ray diffraction
RSD	Relative standard deviation
SCLC	Small cell lung cancer
SD	Standard deviation
SDS	Sodium dodecyl sulphate (SDS)
SEM	Scanning electron microscope
SONO	Sonocrystallisation

t_r	Measured retention time of a probe
t_n	Net retention time of a probe
γ_S^d	Dispersive surface component of a solid
γ_S^+	Electron acceptor component of a solid
γ_S^-	Electron donor component of a solid
γ_l^d	Dispersive surface component of a liquid
γ_l^+	Electron acceptor component of a liquid
γ_l^-	Electron donor component of a liquid
γ_s^{sp}	The specific free energy of a solid
γ_s^{total}	Total free surface energy of a solid
γ_s^{sp}	Specific free energy of a solid
α_{Ci}	Cross–sectional area of a n-alkane probe
$t_{p,ref}$	Net retention time of theoretical n-alkane reference of a polar probe
$l+$	Monopolar electron acceptor probe (e.g. chloroform)
t_{nl+}	Net retention time of $l+$
$t_{nl+,ref}$	Net retention time of theoretical n-alkane reference of $l+$
γ_{l+}^d	Dispersive component of $l+$

List of Abbreviations

a_{l+}	Cross–sectional area of $l+$
$l-$	Monopolar electron donor probe (e.g., ethyl acetate)
t_{nl-}	Net retention time of $l-$
$t_{nl-,ref}$	Net retention time of theoretical n-alkane reference of $l-$
γ_{l-}^{d}	Dispersive component of $l-$
a_{l-}	Cross–sectional area of $l-$
γ_{CH_2}	Dispersive free energy of methylene group
α_{CH_2}	Cross section area of methylene group
$K_{CH_2}^{a}$	Dispersive retention factor
K_{l+}^{a}	Electron acceptor retention factor
K_{l-}^{a}	Electron donor retention factor
T	Column temperature (in Kelvin)
k	Boltzmann constant = $1.380648813 \times 10^{-23}$ J K^{-1}
W_c	Work of cohesion between particles of the same material
W_a	Work of adhesion between particles of the different materials

CHAPTER ONE

Literature review

Chapter 1: Literature review

1.1. General introduction

Lung cancer is becoming the second most distributed diseases amongst other cancer types in worldwide. It is responsible for the highest rate of cancer deaths (Hitzman et al. 2006; Eramo et al. 2008; El-Gendy and Berkland 2009). Inappropriate treatment or insufficient drug delivery to the site of the disease after oral or intravenous administration is a possible cause of lung cancer treatment failure; it may also be the cause of the efficacy limitation of some chemotherapy, as well as the late detection of the disease. In addition, lung cancer treatment has had no significant progress in the recent years and the remedy rate continues to be the lowest one among all cancers or malignancies (Maillet et al. 2008; El-Gendy and Berkland 2009).

Curcumin is currently the drug which has shown to have a strong effect on treatment of cancers in cell culture (Kunnumakkara et al. 2008; Sa and Das 2008; Huang et al. 2013; Lee et al. 2015; Seo et al. 2016). Interestingly, curcumin has the ability to inhibit cell cancer throughout interactions with multiple molecular targets (Nagabhushan and Bhide 1992; Anand et al. 2008; Chen et al. 2008; Kunnumakkara et al. 2008; Kasi et al. 2016). Most of these molecular targets play a significant role in cancer initiation or development. Moreover, curcumin has proved its ability to inhibit most of the mechanism of cancer development (Maheshwari et al. 2006). Curcumin demonstrates that it can be safe even when consumed at a high dose up to 10 g/day (Sharma et al. 2005; Goel et al. 2008). However, curcumin is poorly soluble in water, which limits its absorption to the body; hence reduces its pharmacological activity (Anand et al. 2007). These solubility problems could be solved by enhancing

the drug formulations using different technique in drug production such as solid dispersion system (Paradkar et al. 2004; Anand et al. 2007; Anand et al. 2010). Moreover, curcumin undergoes first pass metabolism, in liver, when it is administrated orally. This significantly reduces the ability of the drug to reach the site of action, resulting in decreasing the effect of the drugs (Pond and Tozer 1984; Anand et al. 2007).

In lung cancer, the chemotherapy agents are given intravenously. But this administration route causes a high drug concentrations in the systemic circulations, which leads to some side effects and low drug concentrations in the respiratory tract (Guilleminault et al. 2011). The drugs that treat lung disease, such as asthma and chronic obstructive pulmonary disease (COPD) are usually administrated via the airways. The advantage of this route is that curcumin will be directly delivered to tumour site in the bronchi, bronchioles or deep lungs. Theoretically, the airways drug delivery should ensure longer contact of intended target to higher concentration of the drugs, while reducing the systemic side effect. Therefore, the patients should benefit from low minimum drug concentrations in the systemic circulation and other body tissues. Hence, the airways could be an attractive route of administration for curcumin in lung cancer, as other routes of administrations have shown a limited success.

Dry powder inhalers (DPIs) are considered a good drug delivery method for the inhalation. This is due to the improved stability of dry powders as well as the ease of use of the device (Bosquillon et al. 2001; Chougule et al. 2007; El-Gendy and Berkland 2009). The dry powder inhalers have been reported to offer a novel formulation for localising chemotherapy in the treatment of lung cancer (El-Gendy and Berkland 2009). However, the DPI has some

disadvantages such as inability to be used by children and for elderly patients; thus, the recommended formulation for those patients is nebulised formulations. Therefore, the formulation of curcumin in a nebulised form will also be examined in this thesis.

In pulmonary drug delivery, particles size of the drug is a vital factor that determines the aerosol distribution in the lungs (Labiris and Dolovich 2003). In order to allow the dry powders to penetrate the respiratory system and to deposit in the lungs, the size of the drug particles must be in the range of 1-5μm in aerodynamic diameter. Aerosol particles larger than 5μm commonly stay in the oral cavity, where they will be swallowed and passed through the digestive system. However, the particles smaller than 1μm will be exhaled, this is because they settle down very slowly (Ahmad et al. 2009).

Producing drug particles in inhaled range size can be a challenge for the formulator. The traditional method to operate the powders for inhalation is the milling technique. In this project, Air Jet mill has been used to obtain curcumin powders in the desired size. Also, a simple and rapid crystallisation method using ultrasound was utilised to produce inhalable curcumin particles.

The nebulised formulations of curcumin were obtained using suspension formulation technique which is the most common and available method for water insoluble drugs. In addition, solution formulation of curcumin was prepared in nanoemulsion form. The advantage of later formulation is that it provides a soluble form of curcumin which improves its anti-inflammatory activity (Wang et al. 2008).

1.2. An overview on the respiratory system

The respiratory system is composed of upper and lower part. The upper respiratory system includes the nose, pharynx, larynx, and trachea. The function of this part is to warm and provide moisture to the air entering as well as to filter it. The moisture of the air is raised, in this region, from 40-60% to 99%, as relative humidity, and is warmed from 20ºC up to 37ºC.

The lower respiratory system includes the bronchi and the lungs. The bronchi rise from the trachea enters the left and the right lung. The bronchi are further divided into smaller branches inside the lungs to form structures known as bronchioles. These become narrower, shorter and more numerous as they go deeper in to the lung. The bronchi are lined by pseudostratified ciliated epithelial cells which create mucous. This part from the trachea to the terminal bronchioles is called the conduction zone in which the inspired air reaches to the gas-exchange zone of the lung. The terminal bronchioles end by respiratory bronchioles (connected with alveolar duct) which end with alveolar sacs. The respiratory zone consists of respiratory bronchioles, alveolar duct and alveolar sacs. The gas exchange occurs at the respiratory zone (Levitzky 2007).

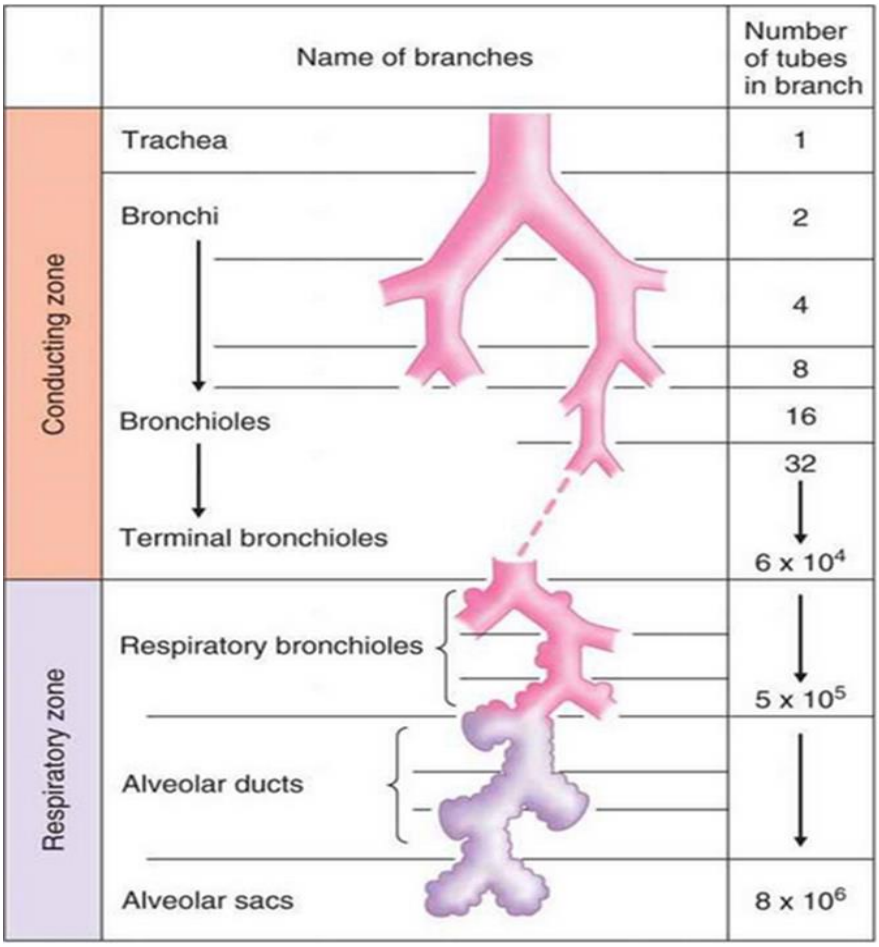

Figure 1. 1 The branching patterns of the airway from the conducting to the transitional and to the respiratory airway zones

1.3. Lung cancer

Cancer, in the most basic sense, is the abnormal, uncontrolled growth of previously normal cells. The alteration in the genetic information causes cells to stop carrying out their function properly. The transformation in the cells comes from modification to their DNA that accumulates over time. A primary feature of cancer cells is the ability of these cells to rapidly divide, which results in accumulation of cancer cells also known as a tumour. As the proliferation of these ‘abnormal’ cells occurs the tumour grows and where it does not spread to the surrounding tissue, is known as benign. Benign tumours are usually harmless. However, a benign tumour can still be harmful if the tumour

compresses the surrounding tissue against a tough surface in the body. For example, a benign brain tumour can place pressure on the brain tissue forcing it against the skull and as a result could potentially cause paralysis, loss of hearing or sight and dizziness (Hansen 2008; Almeida and Barry 2010).

A malignant tumour however, is when the tumour spreads to a far-away tissue. It usually grows at a fast rate and can be fatal. Metastasis is a process of spreading cancerous cells from their original primary tumour to another distance organ in where it will multiply and make secondary tumour (Hansen 2008; Almeida and Barry 2010).

Lung cancer is a disease characterised by uncontrolled cell growth in the lung tissues. Lung cancer is also used to describe tumours which take place in the epithelial lining of the respiratory tract such as bronchi, bronchioles and alveoli (Ellison-Loschmann 2004; Harwood et al. 2005).

Lung cancer is the most common cause of the cancer related deaths in the world. More than 15% of the death in the world is related to the lung cancer. In addition lung cancer causes more deaths than any of the other most common cancers combined (colon, breast and prostate) (Jemal et al. 2008). It is the second most frequently diagnosed cancer in both males and females after prostate and breast cancer.

In the United states, according to American Cancer Society, the estimated deaths in 2012 due to lung cancer is higher than colon, breast, pancreases and prostate cancers combined (Siegel et al. 2012). According to the National Cancer Institute, the records of lung cancer enlarged by 28% between 1973 and 1997 compare to an overall raise of 23.4% in all sites of cancers combined.

The number of people who died from lung cancer has increased by approximately 4.3% between 1999 and 2008 (American Cancer Society 2012).

According to a cancer research reported in 2012 in the UK, about 41,500 people had lung cancer in 2009. Approximately 23,000 cases were diagnosed in males and 18,400 in females. This makes lung cancer the second common cancer in men after prostate cancer and the third common cancer in women after the breast and bowel cancer. In the 1950s, for every case of lung cancer in females there were six cases in the male population; however, this ratio has now dramatically changed, with a ratio of 3 females in every four males being diagnosed with lung cancer.

1.3.1. Aetiology of lung cancer

The major increase of lung cancer diagnosis has been a result of several environmental and lifestyle issues. One of the most important of these issues is tobacco smoke with almost 85% to 90% of lung cancer patients are smokers. However, lung cancer can also be diagnosed in patients who have never smoked; suggesting that there are other factors such as environmental tobacco smoke (ETS), environmental and domestic air pollution, work-related risk factors, asbestos exposure, and viruses which could have an effect on the incidence of lung cancer (Hansen 2008).

Smoking is the most common cause of lung and other types of cancers. Cigarette smoke consists of a mixture of different compounds and more than 4000 compounds have been found in the gas phase of the smoke. Reports have found that up to 70 of these compounds have potential to cause cancer in the lungs (carcinogenic). Examples of theses carcinogens are polycyclic hydrocarbons (PAHs), heterocyclic hydrocarbons, N –nitrosamines, aromatic

amines, N -heterocyclic amines, aldehydes and several organic and inorganic compounds (Hansen 2008). Lung tumour arises from the attachment of tobacco carcinogens to the cell's nuclear DNA, which can result in either killing the cell or cause a genetic mutation. This binding with DNA is irreversible. Once the mutation inhibits programmed cell death, the cell can survive to become a cancer cell (Feng et al. 2006). Acrolein is a major cigarette-related lung cancer agent: Preferential binding at p53 mutational hotspots and inhibition of DNA repair (Feng et al. 2006).

In addition to this, there are some metals, such as nickel, cadmium and chromium in the gas phase of the smoke (Cella et al. 1993; Morita et al. 2003; Hansen 2008). Their role in lung carcinogenesis still not fully understood. However, it has been reported that chromium, cadmium and nickel produce lung tumour in rat after inhalation (Scagliotti et al. 2002; Paccagnella et al. 2004; Hansen 2008). Induction DNA damage in the lung cells may be the reason for their ability to carry out lung carcinogenesis (Hansen 2008).

Environmental tobacco smoke, (ETS), or passive smoking, is a mixture of exhaled mainstream smoke and sidestream smoke diluted in air (Hansen 2008). There are differences in the level of particular compounds that present in sidestream and mainstream smoke. For instance, with a cigarette filtration, the level of PAHs in mainstream smoke is ten times less than those in sidestream smoke (Paccagnella et al. 2004; Hansen 2008). There are many studies that indicate a high level of risk for lung cancer incidence in those who are exposed to ETS and who had never smoked before. Mutations (at P53 and KRAS) have been found in lung cancer of ETS-exposed non-smoking patients, which are the

same mutations, occurred in smoker patients, although with a lower frequency (Sculier 1995; Boussat et al. 2000; Hansen 2008)

Air pollution is a term used to describe the quality of the air. It is a complex mixture of gaseous substance that causes harm to humans and other living organisms. Air pollutants come from various sources, in particular factories and heavy traffic. These involve polycyclic hydrocarbons (PAHs), petroleum vapours, benzene, ethylene oxide and metals. It has been reported that residents in urban areas with high levels of exposure to the pollutions have an increase in lung cancer incidence than those in rural areas by 1.5 times (Sculier and Markiewicz 1993; Hansen 2008). In other reports in 2011, it was found that the risk of lung tumour increased in people who settle in areas with high levels of nitrogen oxide. Also in the same study, the incidence was higher for non-smokers than smokers (Raaschou-Nielsen et al. 2011). Work place exposure is reported to be a risk factor for lung cancer (Gustavsson et al. 2000). The international agency for research on cancer has addressed 12 workplace exposure factors as carcinogenic in the lungs. These factors are Aluminium production, arsenic, asbestos, bis-chloromethyl ether, beryllium, cadmium, hexavalent chromium, coke and coal gasification fumes, crystalline silica, nickel, radon, and soot. In addition, diesel exhaust is identified as carcinogen for the lungs (Tomatis et al. 1978; Steenland et al. 1996; Smoke and Smoking 2004). The duration and intensity of exposure to asbestos fibres could cause a lung tumor (Ayres et al. 2009). The European Union has banned all use of asbestos and extraction, manufacture and processing of asbestos products (European Parliament 2010)

Oncogenic viruses are viruses that can cause a cancer. These viruses could be included in lung cancer aetiology (Hansen 2008). There are some studies which have researched papilloma viruses, however the detection frequency of the virus in bronchial carcinoma are significantly changeable, ranging from zero to 100% in many reports (Booth et al. 2004; Hansen 2008). Regarding other oncogenic viruses such as Epstein–Barr virus, human cytomegalovirus, human herpes virus-8, and simian virus 40, the evidence is rare (Uchitomi et al. 2003; Hansen 2008).

In conclusion, the aetiology factors on lung cancer can be divided into two factors; major and minor. Tobacco smoking, either active smoking or ETS, all have a major role in the aetiology lung cancer due to the previously addressed fact that tobacco has a large number of carcinogenic substances. Another aetiology factors such as air pollution, occupations and viruses, which although seem minor, can still have a significant value in lung carcinogenesis.

1.3.2. Pathophysiology of lung cancer

The pathophysiology of lung cancer is a complex multistep process which includes alterations in the intact bronchial mucosa through lesions, involving cell hyperplasia, metaplasia and dysplasia.

The respiratory tract is lined by epithelial cells which undergo changes in structure and hence function when exposed to noxious substances in the air. These epithelial cells, which form a surface layer of the trachea, bronchi and some of the bronchioles, consist of pesudostratified columnar cells. Amongst these cells are specialized cells known as goblet cells which is presented in figure 1.2 (Almeida and Barry 2010).

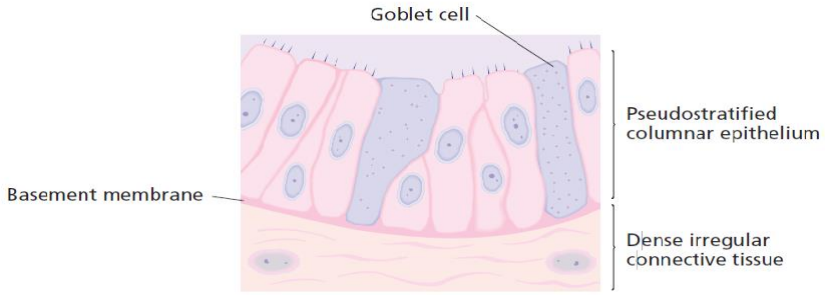

Figure 1. 2 Normal goblet cells (Almeida and Barry 2010)

Goblet cells produce sticky and thick mucus, which traps dust and microorganisms and prevent them from going deeper into the lungs. The cilia, which are short hair-like structures present on the surface of the columnar epithelial cells, will trap substances that will then be swept back up to the throat.

Exposure to chemicals or irritant and carcinogens from the tobacco over a long period of time will cause inflammation of the respiratory epithelium then paralyzes the cilia on the surface of the epithelium. This permits the mucus with its trapped compounds to accumulate in the respiratory tract and move further down to the lungs. It is found that in a tobacco smoker, the pseudstratified columnar epithelium is being replaced by stratified squamous epithelium which is showed in figure 1.3.

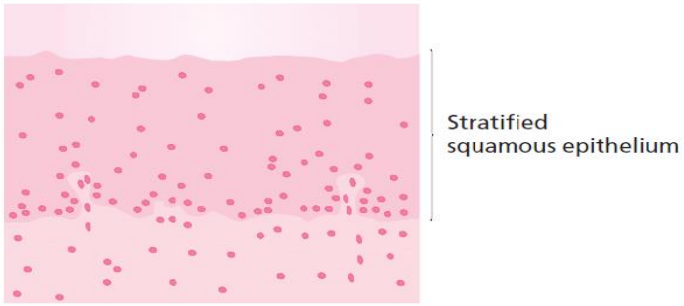

Figure 1. 3 Stratified squamous epithelium (Almeida and Barry 2010)

Stratified squamous cells normally exist in the inner digestive system and outer layer of the skin but not in respiratory system. This process of replacing a mature normal cell type by another mature normal cell type is called metaplasia. The replaced/second types of cells are normal cells but are present in the incorrect location and as a result will not carry out the function required. Nevertheless this process is reversible, when the stimulus that initiated the transformation is absent, healthy cells should return back to their original structure and function. However, permanent alterations may arise resulting from genetic mutations in oncogenes and tumour suppressor genes; this may enhance these types of cells and cause them to become cancerous.

In addition to this, mutations in oncogenes and suppressor genes will enhance hyperplastic growth as a result of losing regulations at the 'checkpoint' of the cell cycle. Hyperplasia is an increase in the number of cells with normal organisation growth in response to a certain stimuli, which can be seen in figure 1.4 b. Dysplasia is increasing in cell number with disorganisation growth, which is presented in figure 1.4 c (Almeida and Barry 2010).

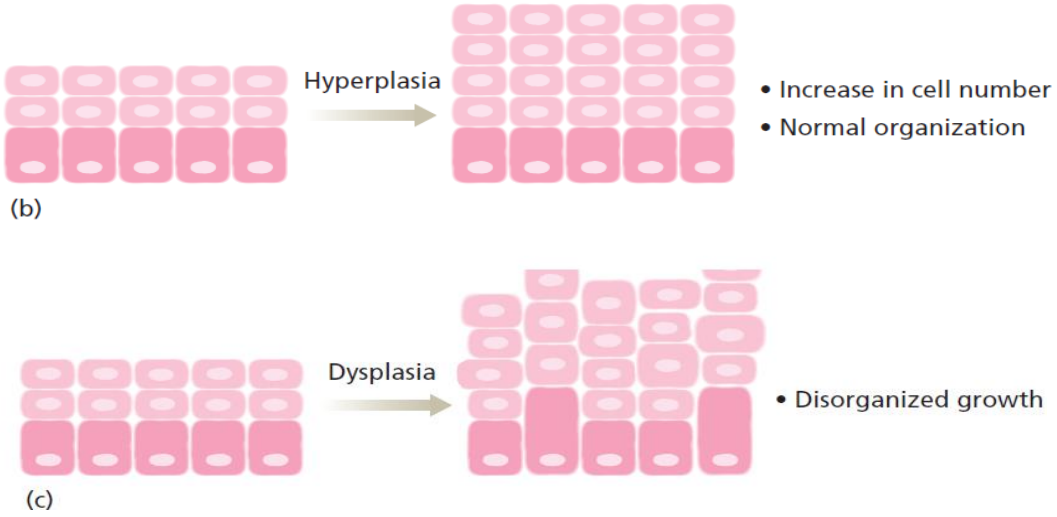

Figure 1. 4 Hyperplasia (b) and Dysplasia (c) (Almeida and Barry 2010)

In conclusion, the pathophysiology of lung cancer development is complex and not fully understood. Genetic alterations and mutations carry out significant roles in lung carcinogenesis. Tobacco still has the most important sources of carcinogens which is the trigger for lung cancer.

1.3.3. Types of lung cancer

There are two main types of tumours in the lung, each with different treatment and different expected survival rate. They are non- small cell lung cancer (NSCLC) and small cell lung cancer (SCLS). This classification depends on the appearance of their cellular structure under a microscope.

1.3.3.1. Non-small cell lung cancer (NSCLC)

Around 85% of lung cancers are NSCLCs, which are characterised by slow growth and do not spread as much as SCLCs. The expected survival rate for NSCLCs is five years of 60% if early diagnosed and 40% if late diagnosed. There are three subtypes of NSCLs and their named (subtypes) is based on the kind of cells in which the tumour develops and vary in their size and shape as presented in figure 1.5

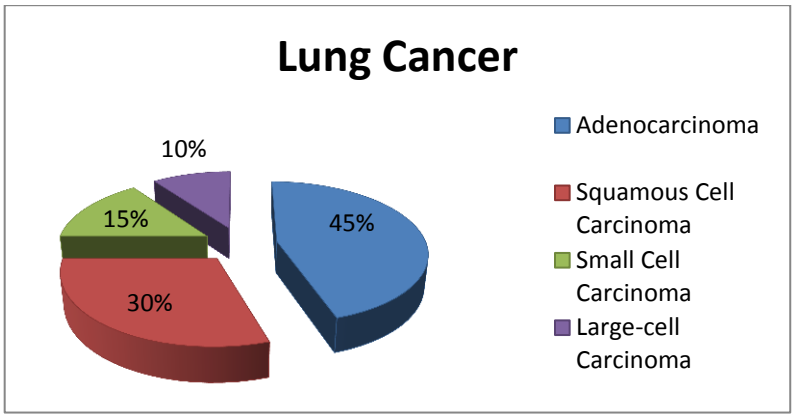

Figure 1.5 Percentage of the lung cancer types (adapted from mechanismsinmedicine.com)

Squamous or epidermoid carcinoma usually arises close to the bronchus and grows slowly. (The main site of SCLC is in mainstream and segmental bronchi (Hansen 2008). Adenocarcinomas vary in size and grow near the outside surface of the lung. Large cell undifferentiated carcinomas might appear at any part of the lung and spread very quickly (Almeida and Barry 2010). (See figures 1.6, 1.7 and 1.8)

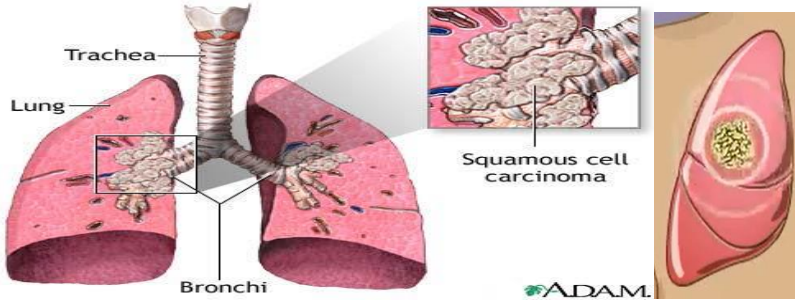

Figure 1. 6 Site of the squamous cell carcinoma in the central lung and the mucociliary epithelial cell (adopted from www.urac.org (American Accreditation HealthCare Commission)

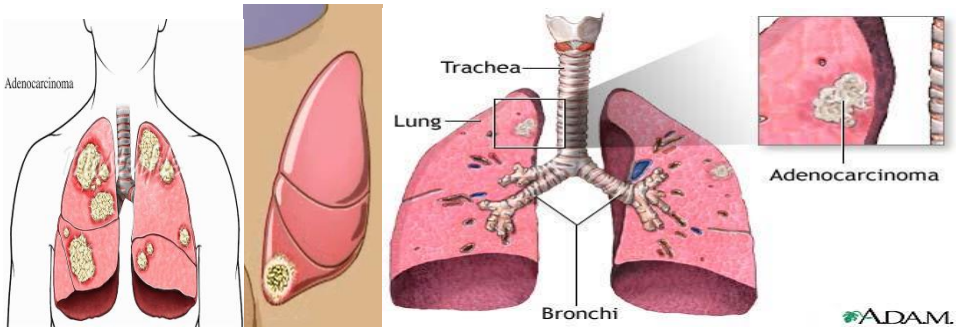

Figure 1. 7 Site of adenocarcinoma in the lung periphery and alveolar type II cells (adopted from www.urac.org (American Accreditation HealthCare Commission)

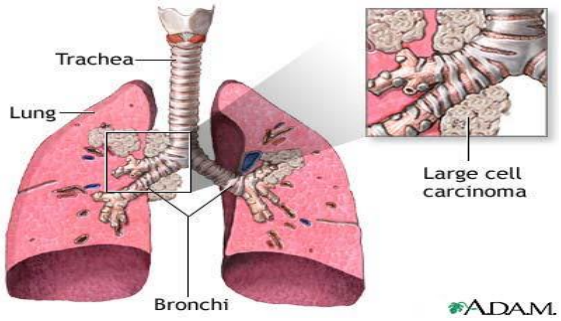

Figure 1. 8 Sit of the large cell carcinoma is either in the central & peripheral lung area or squamous & glandular features (adopted from www.urac.org (American Accreditation HealthCare Commission)

1.3.3.2. Small cell lung cancer (SCLC)

This is also known as oat cell cancer. It is less common than NSCLC forming only 15% of all lung cancers, but it is more fatal. It starts in bronchi and grows at a significantly high rate (faster than NSCLC) and more readily able to metastasize to other organs, the site of the small cell carcinoma is presented in figure1.9.

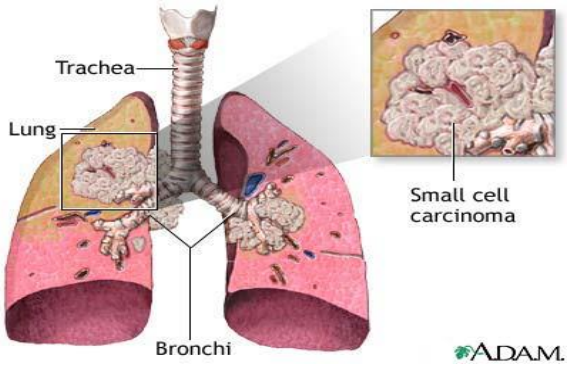

Figure 1. 9 Site of the small cell carcinoma in the central of the lung (adopted from www.urac.org (American Accreditation HealthCare Commission)

1.3.4. Chemotherapy via inhalation for lung cancer

Chemotherapy used in lung cancer to prolong survival time of patients. There are many different types of drugs for cancers with different mechanism of action but most of these drugs have many side effects and high level of toxicity on different organs of the body which affect the life style of the patients.

1.3.4.1. Cisplatin

Cisplatin is an alkylating drug that inhibits DNA synthesis (Ritter 2008). It is considered as a cornerstone from first line drugs that are used in the treatment lung cancer. As much as 83% response has been achieved using this drug in treatment of SCLC. However, most of the patients relapse (Johnson 1999b; Schultheis et al. 2001).

Clinical studies have proved that adding other anticancer drug platinum compounds increases the therapeutic effect of these compounds and hence increases the life expectancy of the patients with lung cancer. The reasons for using the combinations may reduce the resistance of the tumour cells to the Cisplatin. Examples of some agents that are used in combination are Etoposid,

Mitomycine, Gemcitabine, and Paclitaxel (Johnson 1999b; Sculier and Fry 2004).

Cisplatin has a high toxicity profile, causing such as nephrotoxicity and neurotoxicity. This toxicity prevents its use for long durations. Carboplatin is an analogue derivative to Cisplatin with slightly different toxicity. The toxicity has been reduced but it is still highly toxic to the blood (Sculier and Fry 2004). Some clinical studies (on NSCLC) showed no differences between these two drugs in the presence of Etoposide (Johnson 1999a; Schultheis et al. 2001) in terms of survival. However, the response to carboplatin was decreased. Another trial using combination with Paclitaxel showed no difference between Cisplatin and Carboplatin in terms of survival and response rate (Johnson 1999a; Schultheis et al. 2001).

1.3.4.2. Etoposide

This is an alkaloid substance which acts as a cytotoxic agent by inhibiting DNA Topoisomerase enzyme II. This enzyme is very important in cleavage of DNA strands. It is a vital enzyme for both RNA transcription and DNA replication (Ritter 2008).

Etoposide is the most effective medicine in the treatment of SCLC. It has been reported that its response rate was 86% (Johnson 1999a; Schultheis et al. 2001). Etoposide, combined with Cisplatin was also recommended by Sunderom in the treatment of SCLC (Morita et al. 2003; Hansen 2008) and it showed that this combination was more effective than Vincristine, Epirubicin and Cyclophosphamide in the treatment SCLC. Furthermore, the Etoposide-Cisplatin regimen (IV) has been compared with Topotecan-Cisplatin regimen (orally) in clinical studies. The results of this research showed that there was no

difference in the survival rate between these two regimens in treatment of SCLC, (9.3) vs. (9.1) months (Thongprasert et al. 1999; Hansen 2008).

However, Etoposide alone is not effective in treatment of NSCLC. Clinical studies have compared Etoposide-Cisplatin with other anticancer drugs such as Vindesine, Vinblastine, Gemcitabine and Paclitaxel. A significant reduction in overall response rate (ORR) was found in the regimen of Etoposide-Cisplatin compared with the other regimen (Sculier and Fry 2004).

1.3.4.3. Topotecan

This is an alkaloid compound that has anticancer properties by inhibition DNA Topoisomerase enzyme I. Topoisomerase Enzyme I is a vital enzyme for DNA unwinding in the replication process and RNA transcription. Apoptosis or programmed cell death is the most likely way of its cell killing (Ritter 2008).

Topotecan is used in the treatment of SCLC and it is the only one which has been approved by the FDA as second line therapy for this disease. Clinical studies have been carried out on this drug; one of these trials presented a 22% of response for this drug in 30 weeks (Ardizzoni et al. 1997; Schultheis et al. 2001). However, topotecan has many side effects as other cancer medications such as myelosuppression, diarrhoea and alopecia (Ritter 2008).

1.3.4.4. Paclitaxel

Paclitaxel is an antimicrotubule agent that is used in the treatment of different types of cancers including lung cancer (NSCLC). It works by inhibiting cell mitosis by binding to B-subunit of tubulin (Ritter 2008). Tubulin is a protein which plays an important role in maintaining cell structure, intracellular

transport, formation of the mitotic spindle, as well as other cellular processes (Desai and Mitchison 1997).

There are very few studies using paclitaxel in clinical trials. However, one study showed that when paclitaxel was used as a single agent a response of 29% in 24 patients within a period of 3 weeks (Smit et al. 1998; Schultheis et al. 2001).

Other studies have compared a combination of paclitaxel-cisplatin (or paclitaxel_carboplatin) with other anticancer drugs such as gemcitabine_cisplatin and docetaxel- cisplatin (Sculier and Fry 2004). The results have shown no improvement in survival rate or in ORR with paclitaxel_cisplatin. The response rate for paclitaxel_cisplatin regimen was 21%, whereas in case of gemcitabine_cisplatin and docetaxel_platin the response rates were 22% and 17% respectively (Sculier and Fry 2004).

In another trial, a comparison between carboplatin_paclitaxel with cisplatin_vinorelbine was carried out by Kelly (Sculier and Fry 2004). The data as shown in other trials showed no major difference. The response rate was 26% with 8.6 months survival rate for the first combination and 28% and 8.1 months for the second one.

1.3.5. Curcumin

Turmeric is a rhizome from the herb Curcuma longa Linn, which was used in Ayurveda and Chinese medicine to prevention and cure of human illnesses. Turmeric powder is used in cooking and it is the main ingredient of “curry spice” preparations. Turmeric powder is yellow pigmented and has 2% to 9% of curcuminoids; the word “curcuminoid” indicates a group of compounds such as curcumin, demethoxycurcumin and bisdemethoxycurcumin (Priyadarsini 2014).

Out of these compounds, curcumin is about (77%), demethoxycurcumin (17%), and bisdemethoxycurcumin (3%) (Jadhav et al. 2007; Shanmugam et al. 2015). Curcumin is a polyphenol compound which entitles in Ayurvedic medicine as an effective medicine for various disorders such as asthma, bronchial hyperactivity, allergy, cough and hepatic disease (Ammon and Wahl 1991). There are many reports of its anti-infectious (Chan et al. 2005), anti-oxidant (Rao 1997), anti-inflammatory (Brouet and Ohshima 1995; Dikshit et al. 1995), hepatoprotective (Kiso et al. 1983), cardioprotective (Venkatesan 1998), thrombosuppressive (Srivastava et al. 1985), anti-arthritic (Dcodhar et al. 2013), chemopreventive, and anti-carcinogenic (Chen et al. 2006; Divya and Pillai 2006) properties. Curcumin has also been shown to modulate multiple cellular molecular targets (Chattopadhyay et al. 2004; Shishodia et al. 2007a; Shanmugam et al. 2011).

1.3.5.1. Pharmacological activity of curcumin on cancer

There are many studies have shown the ability of curcumin to inhibit tumours. It can carry out this inhibition in cell cultures by transcription factors activation, tyrosine kinase enzyme inhibition (Bharat B. Aggarwal July 24, 2006).

Genes which contribute to cell growth as well as carcinogenesis and angiogenesis are regulated by transcription factors such as nuclear factor-kB (NF-kB) and other factors. NF-KB has very important roles in cancer formation and also in cancer promotion. It can be activated in lung cancer through tobacco exposure. The activation of these factors can be inhibited strongly by curcumin (Shishodia et al. 2007b; Goel et al. 2008).

Tyrosine kinase enzymes play important roles in cell cancer proliferation and in modulating DNA synthesis and genes transcriptions(Ritter 2008). These enzymes are stimulated by mutations (Goel et al. 2008). A certain number of

these enzymes have been found in NSCLC, in particular the epidermal growth factor receptor (EGFR)(Hansen 2008). Studies have proven that curcumin totally inhibits protein kinase activity *in vitro* using cell line (Srivastava et al. 1995; Nirmala and Puvanakrishnan 1996; Tikhomirov and Carpenter 2003; Goel et al. 2008).

More enzymes are included in cancers, cyclooxygenase-2 has been found in different type tumours in human, such as breast, colon and lung cancer. A considerable amount of research has been focused on development of selective cox-2 inhibitors in the past, because it has been thought that these drugs have a significant impact on inhibition of carcinogensis (Grosser 2006; Goel et al. 2008). Most studies have indicated that curcumin is able to inhibit cox-2 through the down regulation of the NF-kB which is vital for cox-2 activation (Goel et al. 2008).

Tumour suppressor gene P53 is a transcription factor. It has many functions in terms of cell process. These processes are genomic stability, cell cycle regulator, cellular response to DNA damage and apoptosis (cell programmed death) (Aggarwal et al. 2007). The P53 gene is able to stimulate other genes to induce apoptosis. It is also able to inhibit cell growth with damaged DNA (Furukawa et al. 2001; Aggarwal et al. 2007). Dysfunction of the P53 gene leads cells to produce errors and mutations as well as malignant transformations (Sculier and Fry 2004). In lung cancer, P53 becomes mutated as a result of mutations in other genes. Mutant P53 causes abnormal and uncontrolled cell growth and forms tumours (Aggarwal et al. 2007). It has been reported that P53 mutations are the most common point of mutation in lung cancer and its incidence around 40% (Sculier and Fry 2004). This mutation is

present in SCLC in 90%, but only 50% and 35% in carcinoma and adenocarcinoma, respectively (Sculier and Fry 2004). Preclinical studies have found that curcumin is a potent inhibitor to mutant P53 (Natarajan and Bright 2002; Aggarwal et al. 2007).

Applying curcumin locally on skin showed that curcumin prevented or inhibited tumour formation by carcinogens. A trial on rodents involved curcumin being applied on the skin five minutes before cancer intonation by a carcinogen such as benzo[a]pyrene or DMBA. The tumour was then improved by another carcinogen such as o-tetradecanoylphorbol-13-acetate. The results showed that curcumin was able to inhibit carcinogenesis by inhibiting inflammation. This inflammation is induced by arachidonic acid, formation of hydrogen peroxidase and ornithine decarboxylase activity/transcription (Conney 2003; Aggarwal et al. 2007).

Also curcumin was topically applied on the buccal pouch of Syrian/Golden Hamster where oral cancer was caused by a carcinogen as DMBA (12, 7, 12-dimethylbenz[a]antracene). The results from this experiment suggested that curcumin inhibits the formation of oral tumour locally. In addition to this, the effect of curcumin has been improved by adding or consuming green tea as a chemo-preventive agent (Li et al. 2002; Aggarwal et al. 2007).

In certain clinical studies, curcumin was applied topically in oral cancer by Kuttan, the results of this study showed that a 10% decreasing in lesion size (Sharma et al. 2004; Aggarwal et al. 2007). It has been reported that some clinical trials were conducted for using curcumin in the treatment of patients with advanced colon cancer for four months (Sharma et al. 2004; Sharma et al. 2005). It was found that five patients out of 15 had a stable disease for up to

four months, and another patient had a significant decrease in carcinoembryonic antigen (colon cancer biomarker).

It could be concluded that curcumin has potential ability in the treatment or inhibition of cancers through different modes of action. A possible cause for the importance of curcumin in the treatment of tumours may be due to the wide variety of mechanisms of inhibitions cells of cancer.

1.3.5.2. Pharmacokinetics of curcumin (absorption, metabolism, and safety)

Curcumin exerts poor oral bioavailability in both humans and rats. This may be attributed to low absorption of curcumin from the gut. As a result most of the ingested amount of curcumin is excreted in faeces unchanged. Intravenous injection of curcumin in rodents underwent first-pass metabolism and half of it was excreted in the bile within 5 hours. This may be due to the low absorption and rapid metabolism of curcumin (Wahlström and Blennow 1978; Goel et al. 2008). The major metabolites (via reduction and glucuronides) of curcumin in the bile are tetrahydrocurcumin_glucuronides (THG) and hexahydrocurcumin (HHC) (Holder et al. 1978; Goel et al. 2008). Studies have indicated that the liver is the main site of metabolism of curcumin in both humans and rats (Wahlström and Blennow 1978; Garcea et al. 2004; Hoehle et al. 2006; Goel et al. 2008).

Curcumin has not shown any toxicity to either humans or animals even at high doses (Shankar et al. 1980; Aggarwal et al. 2003; Shen and Ji 2007). It has been found to be very safe when used in humans, as it has been administrated up to 10 g/day resulting in no toxicity (Chainani-Wu 2003; Shen and Ji 2007). Moreover, the consumption of curcumin over a long period of time by many populations in some countries is an indication of its safety.

1.3.5.3. Physiochemical properties of curcumin

Curcumin is considered as a polyphenol compound with chemical formula C_{21} H_{20} O_6 and molecular weight of 368.37 g/mol. The substituted phenol groups are attached with unsaturated carbon chain with a diketon group as it is shown in figure1.10. The hydroxyl group of the benzene ring, the β-diketon moiety and the double bond of the alkene group are responsible for the curcuminoids activities (Osawa and Namiki 1985; Ruby et al. 1995).

It is a lipophilic compound which is very poorly soluble in water at acidic and neutral pH medium. It is sensitive to changes in the pH, as while it is stable at pH levels ranging from 1-7, it becomes degradable above this limit (Oetari et al. 1996; Wang et al. 1997; Goel et al. 2008). It is also photosensitive, as changes in the light affect the stability of curcumin especially the solution form.

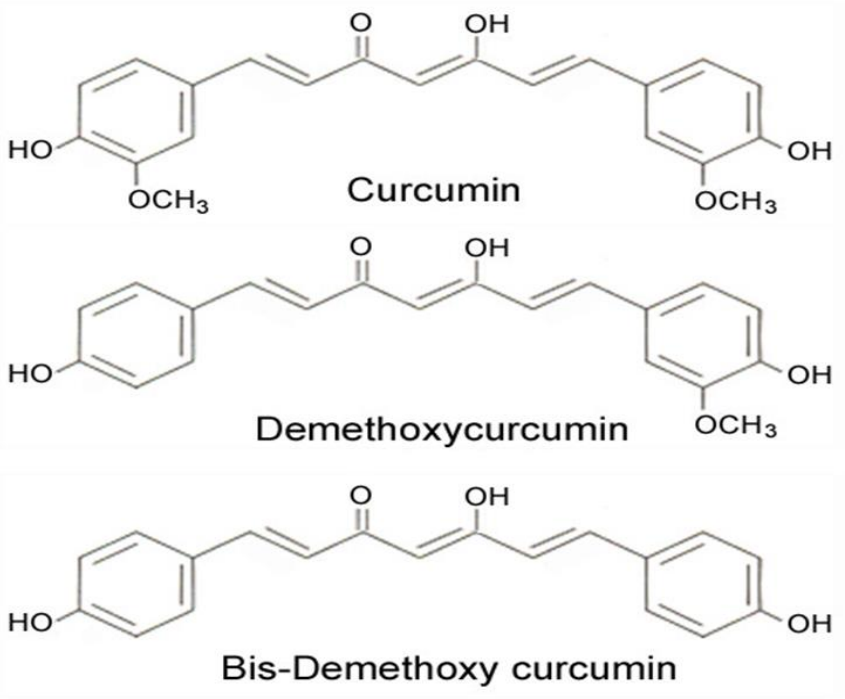

Figure 1. 10 Chemical structures of curcuminoids

Commercial curcumin powder presents in crystalline form. Crystal structure of curcumin exists in three different forms (Sanphui et al. 2011), forms 2 and 3 are known as orthorhombic structure whereas form 1 is monoclinic structure (Sanphui et al. 2011). The variation between Form 1 and Forms 2 and 3 of curcumin is mainly the conformation of a curcumin molecule and its interaction through hydrogen bonding with neighbouring curcumin molecules (Sanphui et al. 2011; Thorat et al. 2014). In Form 1, the curcumin molecule has a curved and twisted conformation as a result of hydrogen bounding between neighbouring curcumin molecules (Sanphui et al. 2011; Thorat et al. 2014). In form 2 and 3, they have a linear and planar conformation (Sanphui et al. 2011). The difference between forms 2 and 3 is only the keto-enol orientation of curcumin molecules packed in the unit cell (Sanphui et al. 2011; Thorat et al. 2014). In form 2 the keto-enol groups in 2 molecules are *cis* in orientation, whereas in form 3 are in *trans* in orientation (Sanphui et al. 2011; Thorat and Dalvi 2015). Also the colour of the curcumin polymorph is distinguishable visually, as form 1 has a yellow-orange and form 2 and 3 have a red-orange colour (Liu et al. 2015). The onset melting point of curcumin form 1 is about 177ºC, whereas the form 2 and 3 are 171ºC and 168ºC, respectively (Sanphui et al. 2011).

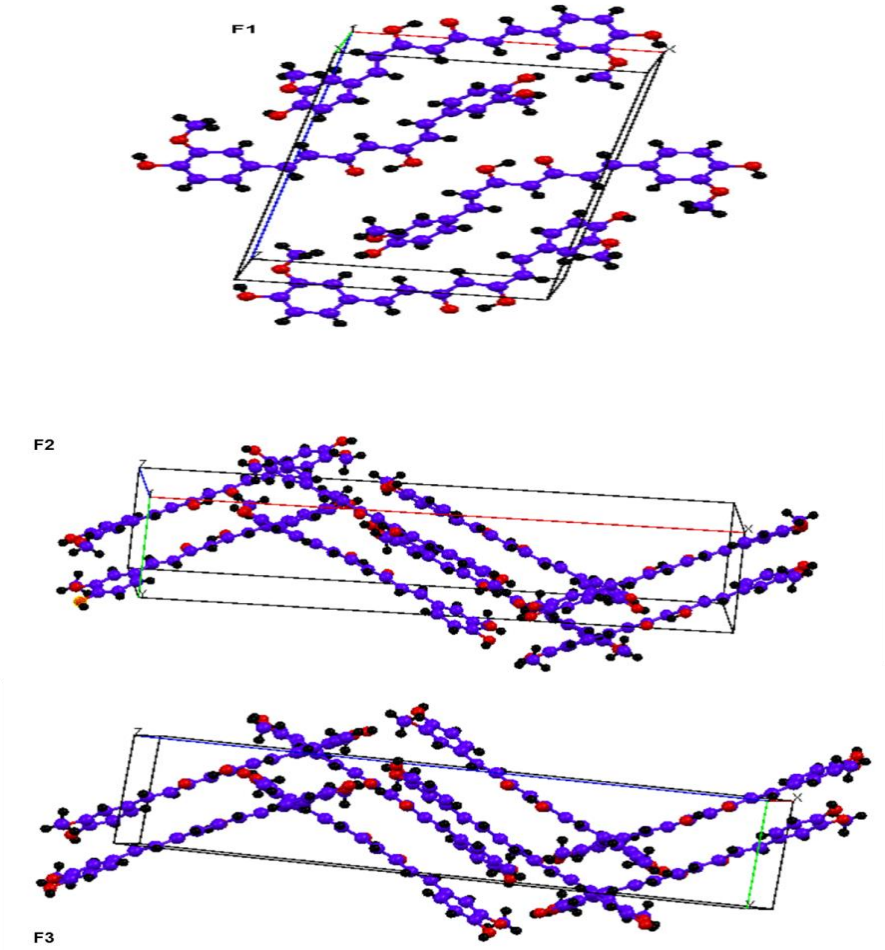

Figure 1. 11 Crystal packing of curcumin polymorphs (Cambridge Structural Database), F1 is curcumin form1, F2 is curcumin form 2, and F3 is curcumin form 3

1.4. Pulmonary drug delivery

Drugs delivered to the lungs are generally used in the treatment of respiratory diseases such as bronchial asthma. Hence, they act locally. They can also be used systemically, as in the case of the treatment migraine with ergotamine (Aulton 2009). Administration of medication through the inhalation route has some advantages over the oral route. For example, administration through the inhalation route results in a more rapid onset of action with topical delivery to the respiratory system. This allows reducing medications dose, which could minimise the adverse effects of the drugs. It avoids the first pass effect in liver

and in intestine that reduce the absorption of drugs. As well as this, the lungs provide a large surface area which is lipophilic in nature that helps to increase the absorption of poorly water soluble drugs.

For respiratory drug delivery to take place, it is vital that the drug particles have very specific properties. These properties are important in allowing the drug to deposit in the correct location (in the bronchioles) and hence producing the desirable effect of the medications.

1.5. Method of producing particles for pulmonary delivery

The size of the particles is the most important factor that must be considered in production of inhaled preparation. The required particles size for inhalation is about 1 to 5µm. There are different methods of producing such particles, these methods including milling, sonocrystallisation and others.

1.5.1. Air jet milling:

Milling is the most common technique in particle size reduction, and it is the most traditionally used method in inhalable particles productions. Milling of powder is divided to wet-milling or dry milling. In the wet milling, a spherical metal beads and vehicle (such as organic solvent or water with stabiliser) are used to produce the desirable particles. Particle size reduction is obtained due to collision between the metal balls and drug powder. This process has few disadvantages such as contaminations of the drug; this is resulting from impact between the instrument walls and used metal beads. Furthermore, high energy (temperature) could be produced during milling process which could leads to amorphous formations. This technique may need another process step, such as spry drying or freeze drying, to obtain the final products. In the dry milling methods, compressed air or gas such as nitrogen, can be used to decrees the

particles size. The mechanism of the size reduction in this technique is based on particle-particle and particles instrument walls impactions. Figure 1.12 shows a schematic diagram of air jet mill micronizer, which is composed of grinding, injection (feed) air, material feed channels, venturi system and collection container. The feed material is transferred from inlet funnel into the grinding chamber through air vacuum which is created by venturi system from the injection pressure. The compressed air is forced into the grinding chamber through nozzles at high velocity. This high velocity of the air accelerates particles which leads to particles-particles collision and particles instrument wall impactions. Centrifugal force that developed inside the mill holds coarser particles in the outer area of the grinding chamber, until they are milled to finer particles, and allows the smaller particles to move towards the center and into the collection container at the bottom of the mill. The advantages of this technique, it is being simple, low metal contaminations, suitable for heat sensitive compounds, and less heat energy produced, due to absences of mechanical moving parts. Furthermore, it is very simple, easy to operate and inexpensive technique.

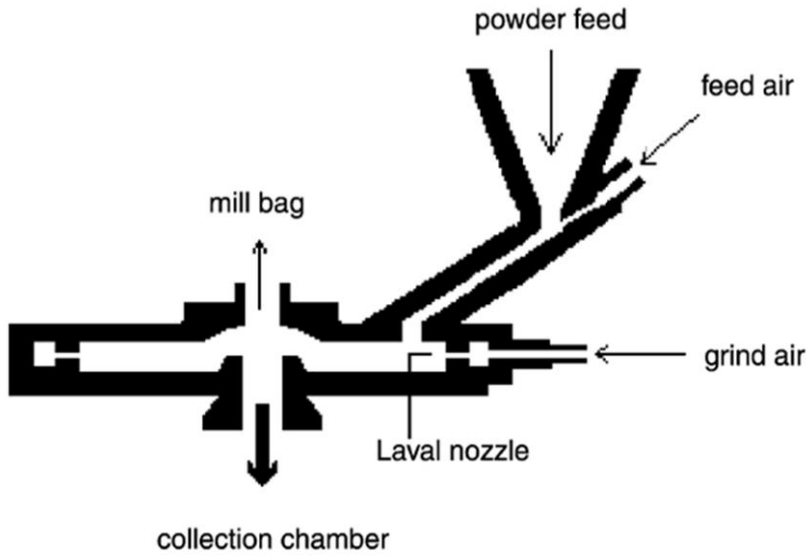

Figure 1. 12 Schematic diagram of a spiral jet mill (Brodka-Pfeiffer et al. 2003)

1.5.2. Sonocrystallisation

Crystallisation is the formation of highly organised solid particles within a homogeneous phase (Deora et al. 2013). Crystals can be grown from a liquid phase within a solution. Any liquid solution which is saturated with a solute at a given temperature can be considered to be in a thermodynamic equilibrium (Deora et al. 2013). However, when the concentration of the solute in the solution exceeds its saturated (or equilibrium) concentration, crystallisation may occur (Deora et al. 2013). The crystallisation process is one of the most important techniques used in particle engineering and pharmaceutical industries as a method of production, purification and modification. Crystallisation is usually achieved throughout supersaturation, nucleation and crystal growth (Brito and Giulietti 2007; Bund and Pandit 2007). Supersaturation is an essential step in the crystallisation process and it is the driving force for nucleation and crystal growth (Visser 1982). A supersaturation solution can be defined as a solution that contains dissolved solutes other than can be found in saturation conditions (Mullin 2001). The supersaturation solutions are usually

thermodynamically unstable, therefore the system will move back to the true saturation level, which then requires the excess of the dissolved solute to precipitate (Aulton 2009). The solute remains dissolved in the solution until a high level of supersaturation is achieved to induce a spontaneous nucleation; this extent of the supersaturation level is called a metastable zone width as shown in the solubility diagram in figure 1.13. The solubility diagram presents three zones which are the stable, metastable and unstable zones, in the last two zones (unstable and the metastable) the supersaturation solution is formed. In the unstable zone, nucleation spontaneously occurs, whereas in the metastable zone, no nucleation occurs which indicates the supersaturation itself is insufficient to form crystals (Shi et al. 1989; Shi et al. 2005).

Nucleation is a small mass of the solute formation on which further crystal growth occurs (Aulton 2009). The nucleation is calcified as a primary and secondary nucleation, in the primary nucleation the nucleation occurs spontaneously or by adding foreign imputers or due to the wall of the container. In the secondary nucleation, a pre-existing solute of the same material is added to the solution to work as a templet (De Castro and Priego-Capote 2007). Once the nuclei are formed and being stable in a supersaturation system, they begin to grow to form crystals in a visible size (Rodríguez-hornedo and Murphy 1999). A period of time elapses between the supersaturation solution achievement and the appearance of the crystal, this lag of time is usually called “induction time or period” (De Castro and Priego-Capote 2007; Patel and Murthy 2009).The induction time could be controlled or influenced by the supersaturation level, agitation, and viscosity (De Castro and Priego-Capote 2007).

Crystal growth is bringing more molecules of the solute to the nucleation site to form a defined shape and size of crystals (Aulton 2009).

Crystallisation from solution remains the most used technique industrially. Typically, a supersaturation solution can be achieved by evaporation, cooling or by addition of another solvent, which is miscible with solution but it does not solubilise the solute; the second solvent is called an anti-solvent. The rate of the supersaturation, nucleation and crystal growth are critical in determination of the crystal properties such as size and shape (Deora et al. 2013).

Sonocrystallisation is the use of ultrasound during crystallisation. Involving (application of) ultrasound irradiations on crystallisation has enhanced the crystallisation process by inducing rapid nucleation, narrowing metastable zone width, decreasing the induction time, producing uniform particle shape; inhibiting particle agglomeration and narrowing particle size distributions.

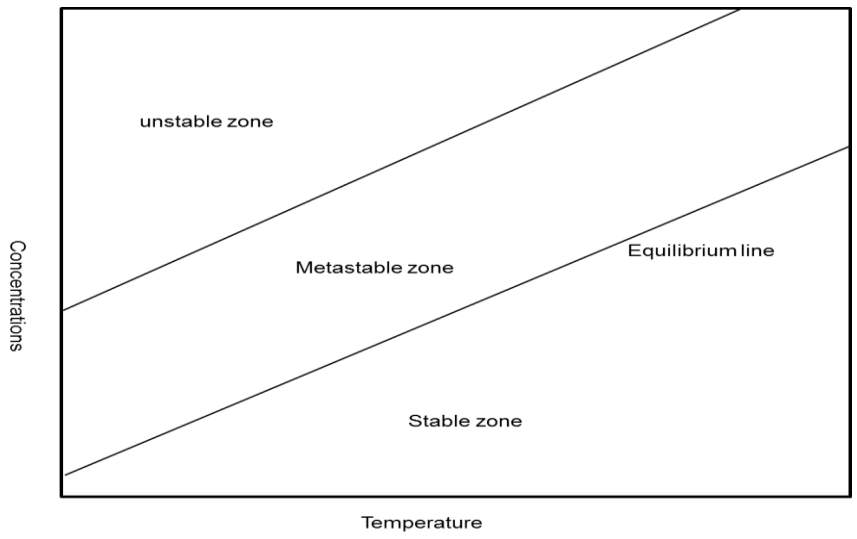

Figure 1. 13 Solubility diagram shows metastable zone

1.5.2.1. Mechanism by which ultrasound induces crystallisation

Ultrasound produces waves that travel throughout the liquid forming a cavitation bubble with high energy and pressure (Richards and Loomis 1927; Suslick 1998; Leonelli and Mason 2010; Deora et al. 2013). These waves are transmitted as a series of compression and rarefaction cycles affecting the liquid molecules (Suslick 1998; Leonelli and Mason 2010). A distance between the molecules is created on a rarefaction cycle which leads to forming a void; this is as a result of the rarefaction negative pressure that exceeds the attractive forces of the molecules (Hu et al. 2006; Leonelli and Mason 2010). This cavity contains a small amount of vapour from the surrounded solvent, so it does not collapse on compression but it continues to grow in successive compression and rarefaction cycles to form acoustic cavitation bubbles (Leonelli and Mason 2010) as shown in figure 1.14. There are many of these bubbles, some of them are relatively stable (called transmission cavitation) and others keep expanding further to an unstable size and then collapse violently (called transient cavitation) (Leonelli and Mason 2010; Deora et al. 2013), producing a high local temperature (5000 K) and pressure of 2000 atms and heat cool rate of 10^{10} k/s (Suslick 1998; De Castro and Priego-Capote 2007). Moreover, US irradiation induces acoustic streaming which can be described as a steady fluid motion created under the influence of high amplitude acoustic waves, when they propagate through a dissipative fluid medium (Rayleigh 1884).

The acoustic streaming and cavitation bubbles (microstreaming), and highly localized temperature and pressure within the fluid; bring considerable benefits to the crystallization process, such as rapid induction of primary nucleation, reduction of crystal size, inhibition of agglomeration, and manipulation of crystal size distribution (De Castro and Priego-Capote 2007). As the number of primary

nuclei increases, the amount of solute on each primary nucleus decreases, thus decreasing the size of the final crystal (Louhi-Kultanen et al. 2006).

Localised high pressure, agitation and temperature are attributed to influencing the nucleation during crystallisation as a result of increasing molecules which collide and increase the supersaturation level (Cains et al. 1998; De Castro and Priego-Capote 2007; Patel and Murthy 2009).

The induction time and Metastable Zone Width has been reported to be influenced during ultrasound irradiation. This is by reducing the induction time and metastable zone width during crystallization (Thompson and Doraiswamy 2000; Lyczko et al. 2002; Guo et al. 2005).

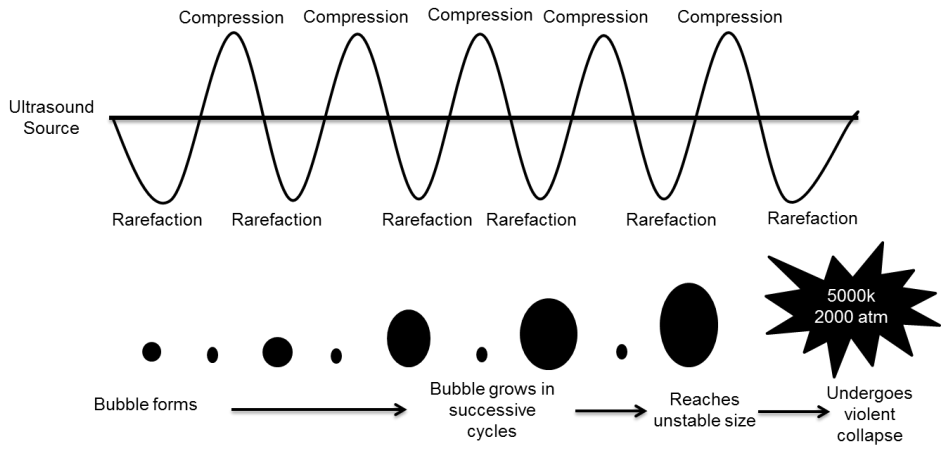

Figure 1. 14 Formation of transient and stable cavitation bubbles by ultrasound (Leonelli and Mason 2010)

1.5.3. Other methods

There are few other methods can be used to produces inhalable particles. These techniques are the spray drying and supercritical fluids. They are usually costly and complicated. The spray drying consumes high energy which could produce amorphous products which are usually unstable. The supercritical fluid process a long time is required for particles productions.

1.6. Factors affecting deposition of drug particles in the lungs

1.6.1. Particle size

The size of the inhaled particles is the most important factor that effects the deposition of these particles in the respiratory tract. Aerodynamic diameter is the physical diameter of a unit density sphere and is usually used to determine or measure the particle size of the aerosols. The size distribution is interpreted by geometric standard deviation (GSD).

Particles need to be less than about 1- 5μm in aerodynamic diameter size to penetrate the airways (Bates et al. 1966; Telko and Hickey 2005). When the particles are greater than 5μm, they are more likely to settle in the upper respiratory tract. This includes the mouth and pharynx, so would be swallowed (Rees et al. 1982), whereas particles less than 0.5μm may not deposit in the lungs at all. It was found that particles with less than 2μm are more likely to deposit in the alveoli. As a result of these findings it has been recommended that for a potential lung deposition to take place, particles should be within the range of 1-5μm aerodynamic diameters (Usmani et al. 2003; Telko and Hickey 2005).

1.6.2. Inhalation technique

Inhalation technique is another factor which affects the deposition of the drug particles in the lungs. The interaction between the inhaler-formulation and the patient inhalation manoeuvre (scheme) have an effect on the volume of inhaled air, the flow of the inhalation, breath holding after inhalation and the lung volume at the beginning of the inhalation. All of these factors aid in the deposition of the drug particles in the patients lungs (Timsina et al. 1994; Yakubu 2009).

Also in DPIs (Dry Powder inhalers), the flow and the time of the inspiration, the acceleration rate, the resistance to the flow of the inhaler device as well as the powder formulation are the most important factors that may affect the particle depositions (De Boer et al. 1996; Yakubu 2009).

1.7. Method of administration of inhaled drugs

1.7.1. Dry powder inhalers (DPIs)

DPIs are made of four function parts: the powder reservoir, metering system, the disintegration principles and a mouthpiece. There are two types of DPIs which are single dose inhaler and multi-dose inhalers.

Currently there are two types of DPI formulation available on the market; spherical pellets and adhesive mixture. The spherical pellets formulation consists of agglomerated micronized particles which form a large spherical unit without binding agent. Lactose as a diluent may be added to the formulation when the dose is too low. This formulation of DPI needs to be disintegrated completely during the inhalation into fine particles in a respiration size to penetrate the respiratory system. The adhesive mixture formulation contains micronized drug particles and a coarse lactose carrier. The drug particles are attached to the surface of the carrier. This attachment of the drug-carrier must be released and free up the drug particles to penetrate the airways during the inhalation process. For the disintegration of the particles or for the drugs particles to be released from the surface of the carrier need a source of energy. This source of the energy is obtained from the patient's inspiration flow.

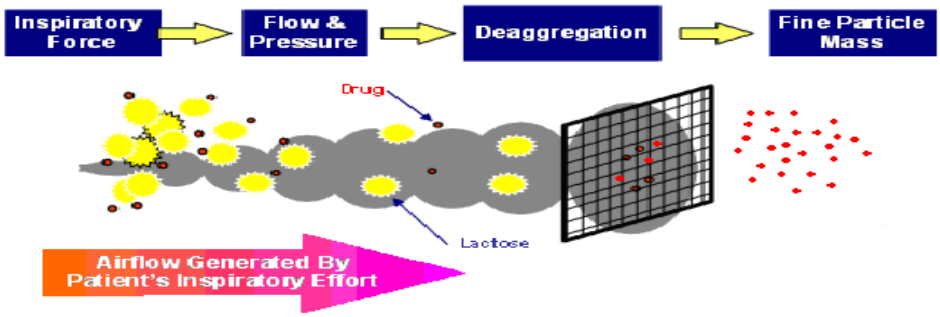

Figure 1. 15 Schematic diagram of the disintegration of spherical pellets through a specific disintegration mechanism, Reproduced from (Chrystyn 2003)

Table 1. 1 Advantages and disadvantages of DPI

Advantages of DPIs	Disadvantages of DPIs
• Free of propellants • No need for patient co-ordination • Very rare for formulation problems • Good drug stability.	• Performance based on the patients inspiratory flow • Resistance to airflow of the device • Difficulties to be protected from the environment effect • Difficulties to obtain dose uniformity and expensive

1.7.1.1. Single dose inhaler system

In this system, a specific amount (pre-metred dose) of the formulation of the dry powder is filled in a hard gelatine capsule. This capsule is loaded in inhaler devices such as Aerolizer. The capsules will be pierced at both ends before the inhalation. The disadvantage of this particular system is that some patients

experience a difficulty of the loading procedure, especially those who are elderly.

1.7.1.2. Multi-dose inhaler system

In this system of inhalers two different types exist. These types are reservoir system and multi unite dose. In the former design, the formulation of the drug is stored in a container from which a single precise doses could be measured by a special dose metering unite. Accurate metering dose in this type of inhaler needs careful manipulation of the devices by the patients. An example for this system is the Easyhaler device. In the latter system, the formulation as single doses unit is filled in an appropriate dose compartment, such as a blister disk. Examples for these inhalers are Diskhaler and Accuhaler.

1.7.2. Metered dose inhalers (MDIs)

MDI or Pressurized Metered Dose Inhaler (pMDIs) is still the most commonly used inhalation formulation of medicines (Vaswani and Creticos 1998; Yakubu 2009). MDI is composed of a canister in which the drug is dissolved or suspended in a liquid propellant. The predetermined dose is released on actuation of a metering valve which is fitted on the canister. The propellant produces a force to de-aggregate the particles and release them at high velocity which causes a high deposition in the oropharynges and also the cooling sensation contributes to the oropharynges deposition (Fink 2000; Yakubu 2009). Using MDI needs a co-ordination between the start of the inhalation and the actuation to produce the dose, which might be quite difficult to carry out correctly in children and elderly people(Crompton 1982; Yakubu 2009).

1.7.3. Nebulisers

Nebulisers, the oldest system for delivery of liquids to lungs, are devices that are able to convert a solution or suspension of medicines to aerosols mist in micron size which is suitable for inhalation. It is used for patients who are unable to use the MDI or DPI and it is more convenient for elderly patients and children (Fink 2000; Yakubu 2009).

1.8. Curcumin formulations

Development of curcumin complex formulation to avoid the low solubility of curcumin and poor bioavailability is an unmet challenge. Various attempts have been made to enhance curcumin solubility; this includes encapsulate curcumin in liposome (Torchilin 2005; Malam et al. 2009; Torchilin 2009), polymers as solid dispersion (Paradkar et al. 2004; Teixeira et al. 2016) and cyclodextrin (Tønnesen et al. 2002). These approaches have shown some degree of improvement but do not provide a practical and easy solution to the existing problem. Moreover, these formulations were intended for oral administrations as they are not suitable for inhalation.

Inhalable curcumin particles have been recently reported in three articles as dry powder inhalers. These particles were prepared by supercritical fluid (Kurniawansyah et al. 2015), spray drying and freeze drying (Yu et al. 2016) and mechanical milling followed by spry drying (Hu et al. 2015). However, stabilisers and formulation enhancers such as polyvinylpyrrolidone 40K (1:1 w/w curcumin-PVP), Hydroxybutyl-β-cyclodextrin (1:4 w/w, curcumin- HB-β-CD) (Kurniawansyah et al. 2015), chitosan (1:1.16 curcumin-chitosan) (Yu et al. 2016), and Tween 80 (6.25%) (Hu et al. 2015) have been used to produce these inhaled curcumin particles, which are not proved by FDA (Myrdal et al.

2014; FDA 2016) and therefore, these formulations are not safe for lungs. Tween 80 and PVP 30K are approved by FDA at level of, 0.02% and 0.0001% respectively (Myrdal et al. 2014). There is no reported method for producing curcumin using either air jet milling or sonocrystallisation for dry powder inhaler formulation and with use of no excipients. There is only one study that used ultrasound in crystallisation of curcumin, in which curcumin polymorphs were investigated under using ethanol as organic solvent and water as antisolvent with different types of polymers (PVP, HMPC and BSA) and surfactants (tween 80 and SDS) but the inhalation performance of the sonocrystallised curcumin particles was not assessed (Thorat and Dalvi 2014; Thorat and Dalvi 2016).

Curcuminoids nanoemulsion for lung delivery has not been reported before. Therefore, one of the aims of this work is to prepare curcuminoids nanoemulsion for the potential treatment of lung cancer and other lung disease. Nanoemulsion formulations of curcumin have been reported to enhance the curcuminoids bioavailability and its activity when it has been applied locally onto skin or taken orally (Wang et al. 2008; Cui et al. 2009; Liu et al. 2011; Hu et al. 2012).

At the present, there is only a single formulation type for nebulisation of poorly water soluble compounds. Suspension formulations of water insoluble drugs (such as budesonide and beclomethasone) have been marketed and used by patients. In nebulised suspensions, large aerosols are required to carry the micron sized particles in suspension, therefore, it is likely that some aerosols droplets will contain no or small number of suspended drug (Knoch and Keller 2005). Moreover, this formulation is usually associated with limited bioavailability, as the drug is in suspended in solid form, and low deposition

pattern (Patravale and Kulkarni 2004). These formulations require shake before their use and show inconsistency when they used in different nebulisers (Nikander et al. 1999), therefore, an alternative formulation to nebulise water insoluble drug is required.

Nanoemulsion is a preparation that provides a complete incorporation of water insoluble drugs in aqueous formulation, which could be nebulised. Nanoemulsion is a nanometre sized droplet of one liquid dispersed in another immiscible liquid, and it is generally optically transparent and thermodynamically stable(Bryant and Altria 2004). Nanoemulsion drug delivery systems have been used in different administration route, such as oral, parenteral and topical (Lawrence and Rees 2012). In addition to its small particles size (1-100nm), the nanoemulsion has the ability to solubilise both hydrophilic and hydrophobic drugs, hence increasing the bioavailability of the drug (Lawrence and Rees 2012). There are few studies investigated nanoemulsions for respiratory drug delivery for water insoluble drugs such as budesonide, amphotericin B and ibuprofen (Amani et al. 2010; Nasr et al. 2012; Nesamony et al. 2014), but these formulations contain high amount of surfactant and hence this limits their safety on the lungs. Therefore, it has been proposed in this project to prepare a curcuminoid nanoemulsion using an extremely low amount of surfactant to avoid the formulation toxicity and to make it safer for inhalation.

1.9. Nanoparticles genotoxicity

There are some reports have shown that nanoparticles exert genotoxicity to cells by damaging their DNA (Chan 2006; Magdolenova et al. 2013). This is attributed to a direct interaction of the nanoparticles with genetic material, or indirect damage from nanoparticle-induced reactive oxygen species, or by

releasing toxic ions (Kisin et al. 2007; Barnes et al. 2008). Nanoparticles, due to their unique size, have the ability to cross the cellular membrane and may reach the nucleus by diffusion across the nuclear membrane or by transportation through nuclear pore complex, and directly interact with DNA (Barillet et al. 2010). Nanoparticles with size 8nm to 10nm enter through a nuclear pore, whereas larger nanoparticle size 15nm to 60nm may access to the DNA in the dividing cells during the mitosis when the nuclear membrane dissolves (Xing-Jie Liang 2008; Singh et al. 2009; Magdolenova et al. 2013). The nanoemulsion preparations is considered to be a nanoparticles based formulation, so their genotoxicity has been reported in this work. This could provide information in regard of the safety of the nanoemulsion preparation for further studies in future.

1.10. *In vitro* method of assessment of drug deposition in the lung (using impaction method)

In vitro lung drug deposition assessment is being used to assure the quality of dry powder inhaler formulation performance and to give a prediction of the particles deposition in the lung *in vivo* using parameters such as aerodynamic particle size distributions, fine particle dose fraction (FPD%) and total emitted dose. There are many different methods used *in vitro* to predict the particles deposition. However, the most common method is the inertial impaction method using cascade Impactors.

The drug particles in the dry powder inhalers have an uneven shape, weight and surface area. This could be impossible to be described accurately by one variable. Therefore, particles are usually described by their aerodynamic diameter which is the diameter of a unit density sphere that has the same

settling velocity in air as the particle. The aerodynamic diameter takes into consideration the density, shape and size of the particles (Hickey 2003; Yakubu 2009). The mass median aerodynamic diameter (MMAD) of an aerosol is the diameter that separates the mass of particles equally by 50%.(i.e. 50% of the particles mass can be separated). According to BP and EP, the MMAD can be measured by plotting the cumulative particles mass versus the cut-off diameter on a log probability graph (Pharmacopoeia 2001). Geometric Standard Deviation (GSD) is used to determine the particles polydispersity (also described as the spread) of an aerosol. For the monodispersed inhalation particles, GSD is 1 and for the heterodisperse aerosol GSD is greater than 1.2. Fine Particle Dose represents the amount of the particles in the aerosol with an aerodynamic diameter less than 5µm which is able to penetrate the lungs (Newman et al. 1991a). As the label claims of many inhalers vary, for the simple comparison in terms of the performance, FPD is usually expressed as a percentage of the emitted dose to give the fine particle fraction (FPF%). The fraction dose gives an estimate of the fraction of the dose that has the ability to penetrate into the lungs (Fink 2000; Barry and O'Callaghan 2003).

1.11. Principles of operation of cascade Impactor

'Impactor' is a term used for the instrument where the particles can impact on a dry impaction plate or cup. Cascade Impactors act on the inertial impaction technique. The Impactor has a different number of stages and in each one there is a single or series of nozzles. The particles in the air stream are passed through these nozzles to the collection surface of the corresponding stage. Particles impacting on a particular stage are based on their aerodynamic particles size. The particles with sufficient inertia will impact at that stage, whereas the particles with small aerodynamic diameter and insufficient inertia

will continue flowing in the air stream and pass onto another stage where the process is repeated.

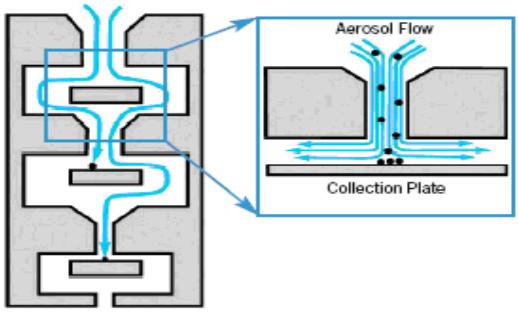

Figure 1. 16 Principle of cascade impactor operation (Reproduced from Copley, 2008)

In some cases, particles might jump in response to impact when coming into contact with the surface of the collection plate or the stage. This might cause the particles to re-entrain into the air stream and to be carried into a lower stage. This particular issue could take place with DPI and some MDIs. This problem can be avoided by coating the collection plate or the stages with suitable surface coating (Allen 1990).

The Impactor stages are assembled in order of decreasing particle size. The nozzles of the stages are getting decreased from one to another one, which increases the air velocity further and the finer particles are collected. The remaining particles are collected on a final filter. At the end of the procedure, the amount of particles in each stage collection plate is recovered using a proper solvent and then analysed using HPLC to determine the mass of the drug. Then, the fine particle dose, fine particle fraction and mass median aerodynamic diameter (MMAD) were calculated as well as the geometric standard deviation (GSD).

1.11.1. Next Generation Impactor

The Next Generation Impactor has been designed particularly for pharmaceutical inhaler testing. This cascade is provided with 7 stages, as shown in figure 1.17, and is designed to be operated at any inlet flow rate from 30 L/min to 100 L/min for dry powder, and 15 L/min for nebulisers. The cut-off size at flow rate of 45 L/min and 15 L/min is presented in table 1.1. The NGI has several features to enhance its utility for inhaler testing:

- Particles deposited on collection cups are held in a tray which can be separated from the impactor as a single unit, facilitating quick sample recovery.
- The user can add up to approximately 40mL of an appropriate solvent directly to the cups for more efficiently.
- The Micro-orifice Collector (MOC), in the collection cup, captures extremely small particles normally collected on the final filter in other impactors.
- The particles captured in the MOC cup can be analysed in the same manner as the particles collected in the other impactor stage cups (Marple et al. 2003; Yakubu 2009).

Figure 1. 17 Next Generation Impactor, (a) NGI including pre-separator and induction port, (b) NGI (open view) showing nozzles & collection cups, (c) NGI (open view) showing cup tray removed, (d) Collection cups showing typical deposition pattern (Reproduced from Copley, 2008)

Table 1. 2 Lung cancer types and their distribution in the lungs and the corresponding cut off diameters (CFD) of Next Generation Impactor (NGI) at flow 15 and 45 L/min.

Lung cancer types	**Locations**	**CFD at flow 45 L/min**	**CFD at flow 15 L/min**
1. Small cell carcinoma	Secondary bronchus (Central zone)	S3 & S4 (3.3-.1µm)	S5 (3.3-2.1µm)
2. Non-small cell lung cancer			
2.1. Squamous carcinoma	Primary bronchus (Central zone)	S3 (4.7-3.33µm)	S4 (4.7-3.33µm)
2.2. Adenocarcinoma	Tertiary bronchus (peripheral zones)	S4 & S5 (2.1-1.1 µm)	S6 (2.1-1.1 µm)
2.3. Large cell carcinoma	Secondary or tertiary bronchus	S3, S4& S5	S5 & S6

S: The stages of Next Generation cascade Impactor, CFE: Cut off diameter of NGI stages

1.12. Hypothesis

Lung cancer is the most common cause of cancer related death in the world. It is still the second most commonly diagnosed cancer in both men and women. Lung cancer is responsible for more than 15% of deaths worldwide. The incidence of lung cancer related deaths is higher than that of three other common cancers combined (colon, breast and prostate cancer).

Studies have shown that curcumin is a potent anticancer and antioxidant compound. In addition, it is a very safe herbal drug even when consumed at high concentrations, as no side effects were reported when it was taken at quantities of up to 10g/day (Anand et al. 2007). However, the poor bioavailability of curcumin limits its use in clinical settings (Anand et al. 2007). The low bioavailability is a result of low absorption of curcumin because it is poorly soluble in water and also due to the first pass metabolism in the liver.

Pulmonary delivery of curcumin as a dry powder inhaler and liquid- based formulation (nanoemulsion) would be beneficial, as curcumin will be directly delivered to the cancer cells in the bronchi, bronchioles or deep lungs. This will ensure longer contact of these cells to higher concentration of curcumin, while reducing the systemic side effect by minimizing the drug amount in the systemic circulations and other body tissues. The lung acts as a good medium for lipophilic drugs, as well as this; the first pass effect will be avoided through administration of drugs via inhalation. The nanoemulsion nebulised formulation will introduce curcumin in liquid form to the cancer cells. This may increase the curcumin effect at tumour site of the lungs. This is more likely to produce the desired effect when compared to other routes of administration.

1.13. Aims and Objectives

The aims of this research are:

- To formulate and optimise a dry powder inhaler of curcumin without any formulation enhancers, such as polymers or surfactants, by air jet mill microniser and sonocrystallisation.
- To develop and evaluate a nebulised formulation of curcumin using nanoemulsion (with minimum amount of surfactants) and microsuspension formulations.

The objectives of this work are:

- Development and validation HPLC method using microemulsion as mobile phase, and a conventional HPLC method for assay of curcuminoids.
- Reduce the particle size of the raw materials of curcuminoids using air jet mill microniser into the optimum size, which is required for the DPI formulations. Mixing the micronized particles of curcuminoids with a carrier in different ratios for the best lung deposition. Determine the *in vitro* lung deposition of the micronized curcuminoids using NGI.
- Sonocrystallisation of curcuminoids to obtain a suitable particles size for inhaler formulation of curcumin. Mixing the sonocrystallised curcumin with lactose in different ratios. *In vitro* assessment and evaluation of dry powder inhaler formulations performance using NGI.
- Preparation of nanoemulsion of curcuminoids with a very low amount of surfactant for nebulisation, and *in vitro* aerosols characterisation of the nanoemulsion formulation using NGI.

1.14. Thesis structure

This thesis consists of eight chapters:

- Chapter 1 involves a general introduction and back ground about lung cancer, curcumin and pulmonary drug delivery.
- Chapter 2 includes the general methods and materials used in this work
- Chapter 3 provides the development and the validation of HPLC methods using a conventional and nanoemulsion mobile phases for curcuminoids assay.
- Chapter 4 describes the air jet milling method of raw material of curcuminoids, product characterisation, and the lungs deposition of DPI formulations, which are prepared from milled particles of curcuminoids.
- Chapter 5 presents the sonocrystallisation procedure of curcumin, characterisation of the processed materials and the lung deposition behaviour of DPI formulations, which are prepared from sonocrystallised particles, using NGI.
- Chapter 6 describes the nanoemulsion preparations, the formulation characterisation, and the aerosols performance of the nebulised formulations using NGI, as well as the genotoxicity of the nanoemulsion formulations.
- Chapter 7 is the general conclusion and the future work
- Chapter 8 is the references

CHAPTER TWO

Materials and Methods

Chapter 2: Materials and Methods

2.1 Materials

- Acetonitrile, HPLC grade, (Fisher Scientific, UK).
- 1-Butanol, HPLC grade, 99%, (Alfa Aesar, UK).
- Ethanol, HPLC grade, 99% ,(Alfa Aesar, UK)
- Acetone, HPLC grade, (Fisher Scientific, UK).
- Isopropanol, HPLC grade, (Fisher Scientific, UK).
- Heptane, HPLC grade, (Sigma-Aldrich, UK)
- Hexane, HPLC grade, (Sigma-Aldrich, UK)
- Octane, HPLC grade, (Sigma-Aldrich, UK)
- Nonane, HPLC grade, (Sigma-Aldrich)
- Chloroform, HPLC grade, (Fisher Scientific, UK).
- Ethyl acetate HPLC grade, (Fisher Scientific, UK).
- Isopropyl myristate, (Alfa Aesar, UKC)
- Sodium dodecyl sulphate (SDS), (Alfa Aesar, UK)
- Potassium dihydrogen phosphate, (Alfa Aesar, UK)
- Orthophosphoric acid, (Fisher Scientific ,UK)
- Glycerol 99%, (Alfa Aesar, UK)
- Brij® L23, (Sigma-Aldrish, UK)
- α-Lactose monohydrate (Lactohale LH200), (DFE Pharma, Germany)
- Pure and commercial curcuminoids, (Alfa Aesar, UK)
- Oleic acid oil, 99%, (Alfa Aesar, UK)
- Limonene oil, 97%, (Sigma-Aldrich, UK)
- Polysorbate 80 (Tween 80), (Alfa Aesar, UK).
- Sodium chloride, (Sigma-Aldrich, UK)

- Low-melting point agarose, (Sigma-Aldrich, UK)
- EDTA, (Sigma-Aldrich, UK)
- Tris base, (Sigma-Aldrich, UK)
- DMSO, (Sigma-Aldrich, UK)
- Tirton X-100, (Sigma-Aldrich, UK)
- NaOH, (Sigma-Aldrich, UK)
- EDTA phythaemagglutinin (PHA), (Sigma-Aldrich, UK)
- RPMI 1640 medium (with L glutamine and 25mm Hepes), (Sigma-Aldrich, UK)
- Compressed air

2.2 Instruments and Apparatus

2.2.1 Apparatus used in high performance liquid chromatography (HPLC)

- Pump and autosampler: Hewlett packard 1050 system with a multiple solvent delivery system connected to an auto sampler with a variable injection loop
- Detectors: Variable wavelength UV detector HP 1050 series
- Integrators: Prime multichannel data station (Ver 4.2.0) (HPLC technologies, Herts, UK)
- HPLC columns: Phenomenex C18 magellen, 250mm X 4.6mm i.d X 5µm (Phenomenex, Macclesfield, Chesire, UK). Phenomenex, Gemini-NX C18, 250mm X 4.6mm i.d X 5µm (Phenomenex; Torrance, USA).

2.2.2 Apparatus used in particle size reduction (air jet mill)

- Spiral air jet mill, FPS 241, (FPS, Italy).

2.2.3 Ultrasound instrument

- Sonics vibra-cell (VCX 500 with net power output ~ 500 W, attached to a sonotrode with a tip diameter of 13 mm)

2.2.4 Apparatus used in particles characterisation and analysis

- Laser diffraction particle size analyser, sympatec HELOS (H2419) & RODOS/M
- DLS (Dynamic light scattering), Zetasizer Nano ZS (Malvern Instruments, Uk)
- Differential scanning calorimeter (DSC), Serial NO 2000-0843, (TA Instruments, West Sussex, UK).
- Powder x-ray diffractometer (PXRD), serial NO 202288, (Bruker, Kahlsruhe, Germany).
- Scanning electron microscope (SEM), Serial No XTE 235/D 7875, (FEI, Cambridge, UK).
- Carbon coater (Emitech, Kent, UK).
- Inverse gas chromatography (IGC), surface measurement system Ltd (SMS), UK)

2.2.5 Apparatus and software used to evaluate the *in vitro* particle deposition of dry powder inhalers and nanoemulsion formulations

- Next generation cascade impactor (Copley Scientific, Nottingham, UK)
- Critical flow controller model TPK , (Coply Scientific Ltd, Nottingham, UK).
- Electronic flow meter model DFM, (Coply Scientific Ltd, Nottingham, UK).
- Copley inhaler testing data analysis software (CITDAS), version 2.00, (Coply Scientific Ltd, Nottingham, UK).
- Inhaler device: Easyhaler.

- Nebuliser : sidestream jet nebuliser

2.2.6 General laboratories apparatus

- Ultrasonic bath (Decon Laboratories, Hove, UK).
- Syringe filter 0.22 micrometer pores size, (Scientific Resources Inc, NJ, UK) used for HPLC samples filtration.
- Nylfao®, nylon membrane filters 0.45µm pore size (Pall Gelman) used for HPLC mobile phase filtration.
- Thermo-micro balance
- ELGA ultrapure water dispensing system, (High Wycombe, UK).
- pH meter

2.3 Methods

2.3.1 Air jet milling for particle size reduction of curcuminoids

The imcronisiation of raw material of curcumin was assessed using FPS spiral jet mill (FPS, Italy).

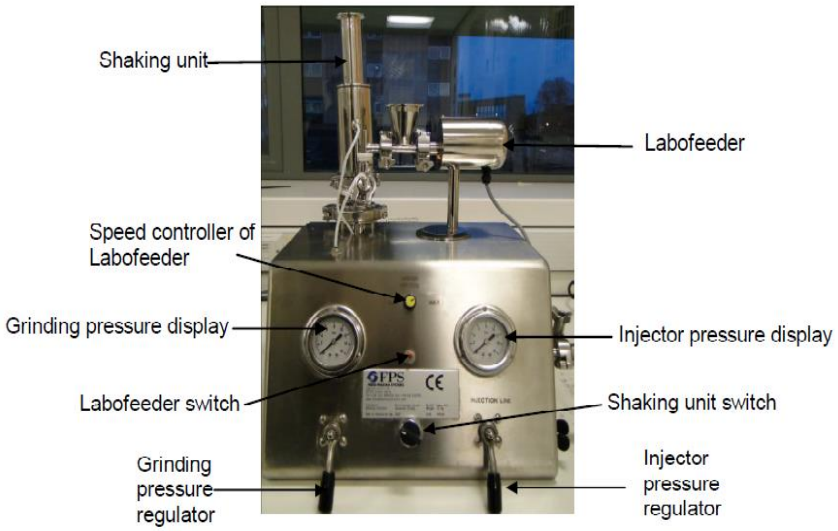

Figure 2. 1 A spiral jet mill (FPS,Italy)

The FPS spiral jet mill is made of a labofeeder and labomill. The labofeeder was connected with labomill and the then connected to power supply . All the parts of the spiral jet mill were held together by connection clamps. The injector, grinder and shaking lines of the labomill were appropriately attached too. A champer filter provided from the manufacturer was placed in the vibration part of the apparatus. The labofeeder was controlled by a switch placed on the front of the sprial jetmill. The sample feed rate was operated by a speed controller which was set at the moderate rate for each of the samples. The products were collected from the container after micronse 5g of the sample was produced. The gas which was used in this work was compressed air and adjusted up to 10 bar pressure. The injection pressure line was then opened to the required level and then the grinding pressure was opened too. The pressure of these two lines was controlled through an injector/grinding pressure regulator on the front of the sprial jetmill. The pressure reading was recorded from the injector/grinding pressure display. The labofeeder was then switched on and the sample started passing from the sample unit to to the mill chamber. The products were then collected from a container placed in the bottom of the mill and stored in silica discade to prevent moisture affecting the sample before the characterisation test is carried out.

2.3.2 Sonocrystallisation of curcuminoids

Appropriate amount of curcumin was dissolved in organic solvents (good solvent) by increasing the solvent temperature accordingly. Known volume of the antisolvent (bad solvent) was placed in a jacket vessel at adjusted temperature of five Celsius degrees, the ultrasound system were adjusted at the required sonication time and amplitude power, the ultrasound probe was

immersed just below the bad solvent surface. The drug solvent, after it has been filtered, was added into the antisolvent and the ultrasound switched on at the simultaneously with addition of drug solvent. The ultrasound was removed and cleaned after completion the sonication process. The drug suspension was filtered using filter paper and left to dry at room temperature. The powder was collected and kept for characterisations.

2.3.3 Nanoemulsion preparations for nebulisation of curcuminoids

Nanoemulsion of curcuminoids was prepared by dissolving sufficient amount of the drug in a pre-measured and mixed amount of oil, surfactant and co-surfactant. The mixture of the drug with nanoemulsion ingredients was then mixed well till the drug was dissolved, and then known amount of ultrapure water was added slowly into the previous mixture with vigorous shaking till a clear solution was seen. The nanoemulsion was sonicated using a sonication bath for about 10 mins. Suitable amount of sodium chloride was added into the nanoemulsion preparation for osmolality adjustment. 5ml of the nanoemulsion formulation was filtered into jet nebuliser chamber for aerolisation characterisation.

2.3.4 Powder particles characterisation

2.3.5 Thermal method of analysis

- **Differential scanning calorimetry (DSC):**

It is a widely used technique in thermal analysis to study and evaluate any phase transition and changes in polymorphic structure of a substance after processing or during storage. It is the measurement of the variation of the total energy which is required to increase the temperature of a sample and is used

as an inert reference as a function of temperature. Both the sample of interest and the reference are kept up at the same temperature during the experiment. The temperature program in the DSC experiment is programmed in such a way that the temperature of sample holder increases linearly as a function of time.

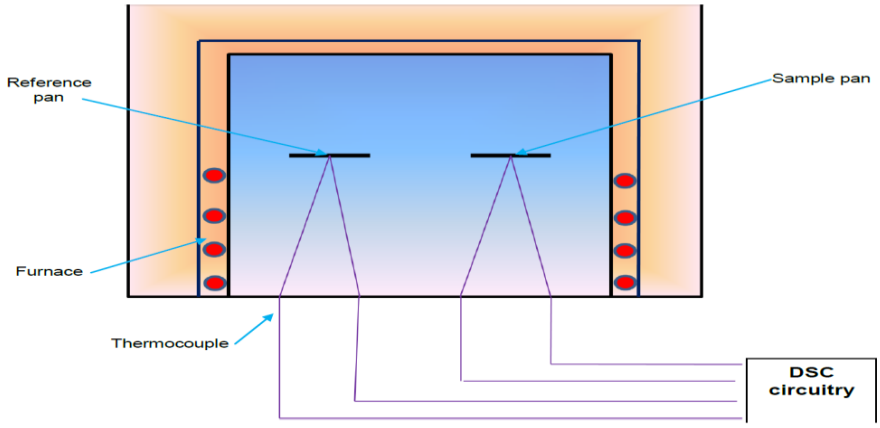

Figure 2. 2 Schematic diagram of DSC

The mechanism of DSC process is as follows, when the physical state of the sample undergoes to transformation such as phase transition through the process, a heat will be needed to flow to or from the sample in order to keep the sample and the reference at the same temperature. The flow of the heat to or from the sample depends on whether the process is endothermic or exothermic. An example being if a sample which is in its solid state changes to a liquid state, which would require a higher rate of heat flow maintain a temperature close to that of the reference. This is a result of the heat absorbed by the sample due to endothermic phase transition from solid phase to a liquid phase. Similarly, when the sample undergoes an exothermic transition, for example in the case of crystallisation, less heat is required to increase the sample temperature. This

variation in heat flow between the sample and the reference will be measured by DSC and it represents the amount of absorbed and/ or released heat in the phase transitions.

In this work, DSC module of the TA Instrument Q2000 Series Thermal analysis System (TA Instrument, West Sussex, UK) was used in DSC analysis. Samples were weighed into an aluminium pan. An aluminium lid, with a central hole, was crimped on to the pan. The samples were then heated under nitrogen gas stream from 25-250ºC using heat rates of 10ºC/min. All the samples were analysed in duplicate. The temperature scale was calibrated using a pure indium standard (melting point 156.60ºC) and was confirmed using a zinc standard (melting point 419.5ºC).

In this study, DSC analysis is used to see if the polymorphic structure of the produced curcumin remains stable after processing the raw material by Air Jet mill micronizer and sonocrystallisation.

2.3.6 X-ray powder diffraction (XRPD)

XRPD is a great tool for crystalline solid evolution. By XRPD, the solid structure and the packing between molecules can be completely determined. Any change in crystallinity state or polymorphic form can be detected by XRPD. This data is often very helpful when trying to understand the chemistry solid state of the substances of drugs.

In this experiment XRPD analysis is used to see if the polymorphic structures of the processed material stay stable after reducing the raw material particle size by Jet mill micronizer and sonocrystallisation.

2.3.7 Particle size analysis

Particle size was assessed for both the raw materials and the processed one using a Laser Diffraction Particle Size Analyser (Sympatec HELOS & RODOS dry dispersion unit, Sympatec Instruments, UK). Approximately 15-20mg of the sample was fed into the analyser by using an ASPIROS unit, under air pressure of 4 bars at a speed of 30 mm/sec. Trigger conditions were at five seconds at an optical concentration of one percent (1%).

In laser diffraction, as the particles pass through a laser beam, light is scattered in response to the particles at an angle which is directly related to their sizes, figure 2.3. The scattering angle increases logarithmically with decrease in particles size. The particle distribution in laser diffraction is based on the comparison of the scattering pattern of the samples with a suitable optical model. This model considers measured particles as spherical (Aulton 2009). Measurement of non-spherical particles in laser diffraction may show an oversized and hence have exaggerated size distribution. This is due to the deviation from the spherical model used in the processing of data.

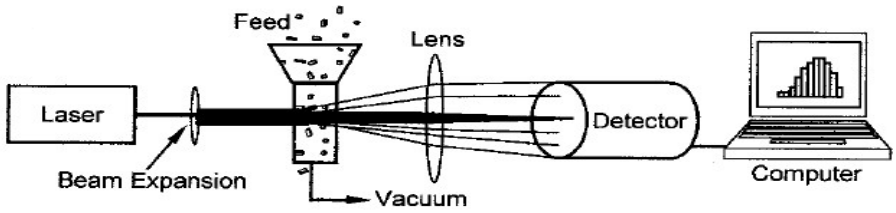

Figure 2. 3 Schematic diagram of particles size analyser via laser diffraction

2.3.8 Scanning electron microscope (SEM)

Scanning electron microscope can give a high resolution image using electron beams instead of light for particle surface texture, topography, shape and size. SEM was performed using a Quanta 400 SEM (FEI Company, Cambridge, UK).

Electron beams are produced from an electron gun placed at the top of the microscope and follow a vertical path through electromagnetic fields and lenses, which point the beams down to the sample, under a vacuum. When the beams hit the sample, electrons and x-rays are reflected from the sample. Theses reflections are collected by detectors and a screen similar to a television screen produce the sample image (Mohamed 2009).

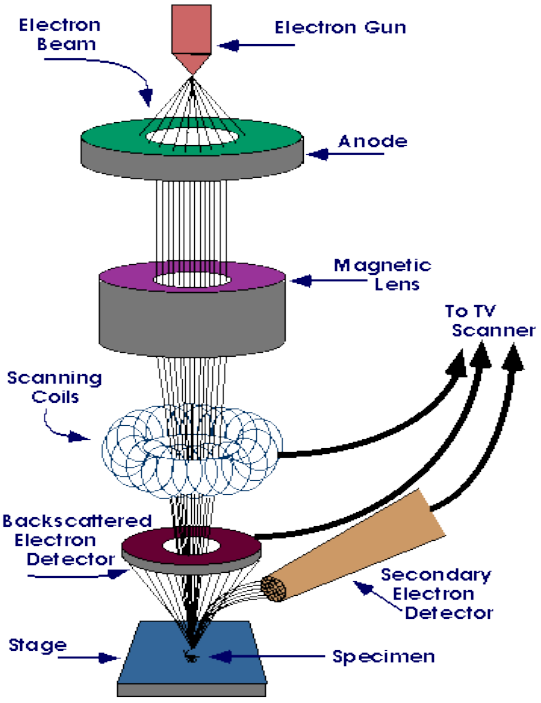

Figure 2.4 Schematic diagram of SEM (Adapted from www.purdue.edu/REM/rs/sem.htm)

All samples were coated with a thin layer of gold using Sputter Coater. This is due to the use of conditions under a vacuum and electrons so there becomes a need to make the non-metal samples conductive by covering them with a thin layer of conductive materials. When using sputter coater an electric field and argon gas are used.

2.3.9 Powder surface free energy characterisation

The free surface energy of curcumin was characterised using inverse gas chromatography (IGC) by injecting a series of n-alkanes (hexane to nonane) and two polar probes (ethyl acetate and chloroform). In this work, surface energy of curcumin particles was correlated to its aerodynamic performance during inhalation.

The surface free energy or surface energy (γ) is defined as the energy that creates a unit area of surface. The total free surface energy is composed of different physical forces and it is usually divided into several components (Grimsey et al. 2002) . Materials have non-polar (dispersive) forces, and most of the materials have polar forces such as hydrogen bonding or acid base forces (Fowkes 1964; Grimsey et al. 2002). Therefore, the surface free energy is split into dispersive (γ^{d}) and polar (specific γ^{sp}) components, thus the total free energy is the sum of both energies of the dispersive and the specific energy (Fowkes 1964; Van Oss et al. 1988) as it is shown in (eq. 1)

$$\gamma_s^{total} = \gamma_s^{d} + \gamma_s^{sp} \qquad (1)$$

Where, γ_s^{total} is the total free surface energy of the solid, γ_S^{d} dispersive surface component of a solid, γ_s^{sp} is specific free energy of the solid.

2.3.10 Surface energy calculation method

To obtained dispersive and specific components of a powder using inverse gas chromatography, a series of homologous n-alkane (hexane to nonane) and two polar probes (i.e. ethyl acetated and chloroform) are injected into a packed column with the sample of interest and the elution time (tr) of the probes is recorded, the retention time measures a magnitude of interaction between the injected probes (non-polar and polar probes) and the stationary phase (packed samples).

The methods reported by Mohammad (Mohammad 2013; Mohammad 2015) were used to calculate the surface energies of the processed curcumin samples. These methods describe the surface properties using the dispersive retention factor $K_{CH_2}^{a}$, the electron acceptor retention factor K_{l+}^{a}, and the electron donor retention factor K_{l-}^{a}, which are calculated using the measured retention times of probes:

- The dispersive retention factor is calculated from the following eq. (2)

$$\ln t_n = (\ln K_{CH_2}^{a})\, n + C \quad (2)$$

Where t_n is the net retention time of the n-alkane probes, n is the carbon number of the homologous n-alkanes, $K_{CH_2}^{a}$ is the dispersive retention factor of the analysed powder and C is a constant.

The t_n is calculated from the (eq. 3)

$$t_n = (t_r - t_0) \quad (3)$$

Where, t_r and t_0 (Dead time) are the retention times of the n-alkanes and a non-adsorbing marker, respectively.

The t_0 is calculated according to the following eq. 4

$$t_0 = \frac{tr_{ci+2}tr_{ci} - (tr_{ci+1})^2}{tr_{ci+2} + tr_{ci} - 2tr_{ci+1}} \quad (4)$$

The γ_s^d of the powder is determined using eq. 5

$$\gamma_s^d = \frac{0.477\ (T \ln K_{CH_2}^a)^2}{(\alpha_{CH_2})^2\ \gamma_{CH_2}}\ \text{mJ.m}^{-2} \quad (5)$$

The parameters of CH_2 are calculated from Eq. 6

$$(\alpha_{CH_2})^2\ \gamma_{CH_2} = -1.869T + 1867.194\ \ \text{Å}^4.\text{mJ.m}^{-2} \quad (6)$$

Where, T is the sample column temperature in kelvin

- The electron acceptor and donner retention factors, K_{l+}^a and K_{l-}^a , are calculated using eq. 7 and 8

$$K_{l+}^a = t_{nl+}/t_{nl+,ref} \quad (7)$$

$$K_{l-}^a = t_{nl-}/t_{nl-,ref} \quad (8)$$

$l+$ Monopolar electron acceptor probe (e.g., dichloromethane or chloroform), $l-$ is Monopolar electron donor probe (e.g., ethyl acetate or toluene), t_{nl+} and $t_{nl+,ref}$ are the retention time of l_+ and its theoretical n-alkane reference, respectively, t_{nl-} and $t_{nl-,ref}$ are the retention time of l_- and its theoretical n-alkane reference, respectively.

The $t_{nl-,ref}$, $t_{nl+,ref}$ are calculated from eq. 9 and 10

$$\ln t_{nl+,ref} = \ln t_{nCi} + \left(\frac{\alpha_{l+}\left(\gamma_{l+}^d\right)^{0.5} - \alpha_{Ci}\left(\gamma_{Ci}^d\right)^{0.5}}{\alpha_{CH_2}\left(\gamma_{CH_2}\right)^{0.5}}\right) \ln K_{CH_2}^a \quad (9)$$

$$\ln t_{nl-,ref} = \ln t_{nCi} + \left(\frac{\alpha_{l-}\left(\gamma_{l-}^{d}\right)^{0.5} - \alpha_{Ci}\left(\gamma_{Ci}^{d}\right)^{0.5}}{\alpha_{CH_2}\left(\gamma_{CH_2}\right)^{0.5}} \right) \ln K_{CH_2}^{a} \qquad (10)$$

Where α_{CH_2} , γ_{CH_2}, α_{Ci} , γ_{Ci}^{d}, α_{l+} , γ_{l+}^{d}, , α_{l-} and γ_{l-}^{d} are the cross–sectional area and the dispersive free energy of a methylene group, an n-alkane, l_+ and l_-, respectively. t_{nCi} is the retention time of the n-alkane.

The retention factors are then used to calculate the electron donner (γ_S^-) and acceptor (γ_S^+) and component of a solid:

$$\gamma_s^- = \frac{0.477\ (T \ln K_{l+}^{a})^2}{(\alpha_{l+})^2\ \gamma_{l+}^{+}}\ \text{mJ.m}^{-2} \qquad (11)$$

$$\gamma_s^+ = \frac{0.477\ (T \ln K_{l-}^{a})^2}{(\alpha_{l-})^2\ \gamma_{l-}^{-}}\ \text{mJ.m}^{-2} \qquad (12)$$

Where, γ_{l+}^{+} is the electron acceptor component of l_+ , γ_{l-}^{-} is the electron donor component of l_-, and T is the sample column temperature in kelvin. The units of α are Å2 and of γ are mJ.m^{-2} in all equations.

The parameters of polar probes are still under debate and different values were reported (Schultz et al. 1987; Van Oss et al. 1988; Della Volpe and Siboni 1997; Della Volpe et al. 2004; Das et al. 2010; Shi and Qi 2012). In this work, we considered the values which were recently used for ethyl acetate (γ_{l-}^{-}= 19.20 mJ/m^2, γ_{l-}^{d}= 19.60 mJ/m^2, α_{l-}= 48.0 Å^2) and for chloroform (γ_{l+}^{+}= 3.80 mJ/m^2, γ_{l+}^{d}= 25.90 mJ/m^2, α_{l+}= 44.0 Å^2) (Das et al. 2010; Mohammad 2013).

- The specific free energy of the solid particles is calculated as shown in eq.11

$$\gamma_s^{sp} = 2(\gamma_s^- . \gamma_s^+)^{0.5}$$

- Work of cohesion (W_c) between curcumin particles is calculated eq.

$$W_c = 2\gamma^{total}$$

- Work of adhesion (W_a) between curcumin and lactose carrier particles is calculated as shown in eq. 12 of the different materials

$$W_a = 4\left[\frac{\gamma_1^d \cdot \gamma_2^d}{\gamma_1^d + \gamma_2^d} + \frac{\gamma_1^{sp} \cdot \gamma_2^{sp}}{\gamma_1^{sp} + \gamma_2^{sp}}\right]$$

γ_1^d , γ_1^{sp} are dispersive and the specific energy of curcumin particles, γ_2^d , γ_2^{sp}, are dispersive and the specific energy of lactose carrier particles, respectively

2.3.11 High performance liquid chromatography (HPLC)

1.14.1.1. Preparation of conventional mobile phase

The conventional mobile phase was prepared by mixing (55% V/V) of acetonitrile HPLC grade with (45% V/V) of phosphate buffer solution of 10mM in a volumetric flask. This solution was then filtered under vacuum using 45mm nylon filter and degassed by sonication under vacuum for 15 minutes.

1.14.1.2. Preparation of microemulsion mobile phase

A microemulsion mobile phase was prepared by weighing a phosphate buffer solution (% w/w), surfactant (% w/w), oil (% w/w), and co-surfactant (% w/w) in a volumetric flask with shaking to obtain an optically transparent solution. This mixture was then sonicated for 15 minutes to assure that all ingredients were dissolved. This microemulsion was then filtered under vacuum using a 0.45µm

nylon filter to remove any particles that could block the HPLC system. The mobile phase is degassed by sonication under vacuum for 15 minutes.

1.14.1.3. Analytical method validation

The HPLC methods were developed and validated according to ICH and FDA guidelines. The validation parameters that were assessed are as follows:

2.3.5.1.1 Linearity:

A linearity curve is the relationship between the instrument response and known concentrations of the analytes. According to ICH (1996) and FDA (2001), the linearity is the ability of the analytical method to give results which are directly proportional to the defined concentrations of the analytes. The linearity is usually determined by a series of five different concentrations of analytes with a replicate measurement.

The regression line is represented by the following equation: $y=mx + c$

Whereas C is the intercept point with y-axis, M is the slope of the regression line. The correlation coefficient (R^2) represents the degree of linearity of the relationship (the relationship between the obtained results and their concentrations). When the coefficient R^2 produces a value of one, this suggests that complete linearity relationship exists.

2.3.5.1.2 Sensitivity:

The sensitivity is represented by the Limit of Detection (LOD) and the Limit of Quantification (LOQ). Limit of Detection is the lowest concentration of the sample or the analytes which could be detected by the analytical method but

not necessary to quantify it. LOD is determined by using the standard deviation (ICH 1996).

$$\mathrm{LOD} = \frac{3.3\ \sigma}{S}$$

Where, σ is the standard deviation of Y-intercept and S is the slope of the calibration curve.

Limit of Quantification is the lowest amount of the sample which can be quantified by the applied assay with an acceptable level of accuracy and precision. LOQ is determined by the following equation:

$$\mathrm{LOQ} = \frac{10\ \sigma}{S}$$

Where, σ is the standard deviation of Y-intercept and S is the slope of the calibration curve.

2.3.5.1.3 Precision:

The precision is the closeness of the agreement (degree of scatter) between a series of measurements obtained from multiple sampling of the same homogeneous sample under the prescribed conditions. It is determined by using a minimum of five determinations for each concentration. It is recommended to use three concentration levels in the range of expected concentration. Precision is divided into intra-day precision (within the days) and inter-day precision (between the days). The precision is expressed as the relative standard deviation as a percentage (RSD%) which is known as coefficient variation (CV).

2.3.5.1.4 Accuracy:

The accuracy of analytical methods expresses the closeness of agreement between the obtained values and the true values of the analytes. According to ICH (1996) and FDA (2000) guidelines, it is measured by a minimum of five determinations for each concentration.

1.14.1.4. Preparation of phosphate buffer solution for mobile phase

Appropriate amount of buffer salts was weighed and transferred to a volumetric flask. ELGA deionised water was then added and the solution was sonicated before being made up to the required volume. The pH of the buffer was then corrected by using an appropriate acidic or alkali solution before filtrations through a 0.45µm membrane filter. The pH meter was calibrated at pH 4.0 and 7.0 using commercial buffer solutions.

1.14.1.5. Stock solution preparation

A suitable amount of curcumin powder was weighed and transferred to a volumetric flask. Then the mixture of acetonitrile and phosphate buffer solution was added and sonicated for 10 minutes to aid dissolution of curcumin. The solution was made up to the required volume which was then filtered through a syringe filter (0.33µm diameter) to remove any un-dissolved materials.

CHAPTER THREE

Development and Validation of HPLC Methods for the Determination of Curcuminoids in Aqueous Solution

Chapter 3: Development and validation of HPLC methods for the determination of curcuminoids in aqueous solution

3.1 HPLC assay for curcuminoids using conventional mobile phase

3.1.1 Introduction

High performance liquid Chromatography is the most widely used technique for qualitative and quantitative determination of drugs in separation science. Compounds to be separated are distributed between a stationary phase and a mobile phase which carries the solutes through the column. Reversed phase chromatography is the most popular for separation of drugs and their related substances. In the reversed phase chromatography, a polar mobile phase and non-polar stationary phase are utilised where the separation of samples is related to their affinity for both the stationary phase and the mobile phase.

Several HPLC methods were reported for curcuminoids determinations and separations. However, most of these methods have some disadvantages, such as unsatisfactory separation times (Kulyal et al. 2016), poor resolution (Wichitnithad et al. 2009) and/or complicated solvent mixtures (Jayaprakasha et al. 2002) and high flow rate (Jadhav et al. 2007; Wichitnithad et al. 2009). Some of these methods were applied only for curcumin determination without considering demethoxycurcumin and bisdemethoxycurcumin (Ma et al. 2007; Li et al. 2009; Kim et al. 2016).

In this work the conventional HPLC method is developed and validated to separate the three components of the curcuminoids, curcumin (C), demethoxycurcumin (DC) and bisdemethoxycurcumin (BDC), using emodin as an internal standard, with a good resolutions and proper separation time and

flow rate. This method will be used for determination of curcuminoids amount in Next Generation Impactor stages.

3.1.2 Method

1.14.1.6. HPLC conditions:

Stationary phase (column): Phenomenex C18µm

Mobile phase: Acetonitrile and 10mM orthophosphate buffer (55%:45% v/v) adjusted to pH 3.0. The mobile phase was filtered through 0.45µm nylon filter and degassed under vacuum in ultrasonic bath for 15 mins before use.

Internal standard: Emodin 40µg/ml

Flow rate: 1 ml/min

Detector: UV set at wavelength of λ= 420nm

Integrator: Prim software (HPLC technology Ltd)

Injection volume: 30µL

Standard solution: 10mg of pure curcumin, demethoxycurcumin and bisdemethoxycurcumin powder were accurately weighed and dissolved in 100ml flask of mobile phase solution and stored in a refrigerator. From the stock solution, serial dilution was made using aqueous solution of internal standard to prepare the standard solutions with the following concentrations 2.5, 10, 20, 40, 60 and 80µg/ml and 40µg/ml for Emodin. The prepared samples were stored in light resistant volumetric flask and kept in refrigerator.

3.1.3 Method development

Curcumin, demethoxycurcumin and bisdemethoxycurcumin are non-polar compounds and very similar in their structure with a difference in the presence or absence of methoxy groups ($O–CH_3$), so this means they are very similar in their polarity too. Optimising the mobile phase condition was very critical, mobile phases with varying compositions were prepared (70%:30%, 60%:40% and 50%:50% as acetonitrile: buffer solution (v:v). the results showed that the amount of acetonitrile had a dramatic effect on the separations of the compounds. This might be attributed to the fact that acetonitrile is very selective for the methoxy group in each of these compounds. Poor separation and peaks overlapping was observed by increasing the acetonitrile above 55% (v/v). On the other hand, increasing in the retention time was observed in decreasing the acetonitrile below 55% (v/v). Furthermore the buffer concentration affected the separation too, peaks interfering observed by raising the buffer concentration above 10mM, where there was a slight increase in the retention time with decreasing the buffer concentration below 10mM.

The separation of the mixture of three pure curcuminoids including the internal standard was achieved in 13 minutes as shown in the figure 3.1. The retention time for curcumin, demethoxycurcumin and bisdemethoxycurcumin was at 7.8, 7.2 and 6.7 minutes, respectively, whereas the retention time for emodin (IS) was at 12.5 min. The resolution between the curcuminoids peaks was more than 1.5.

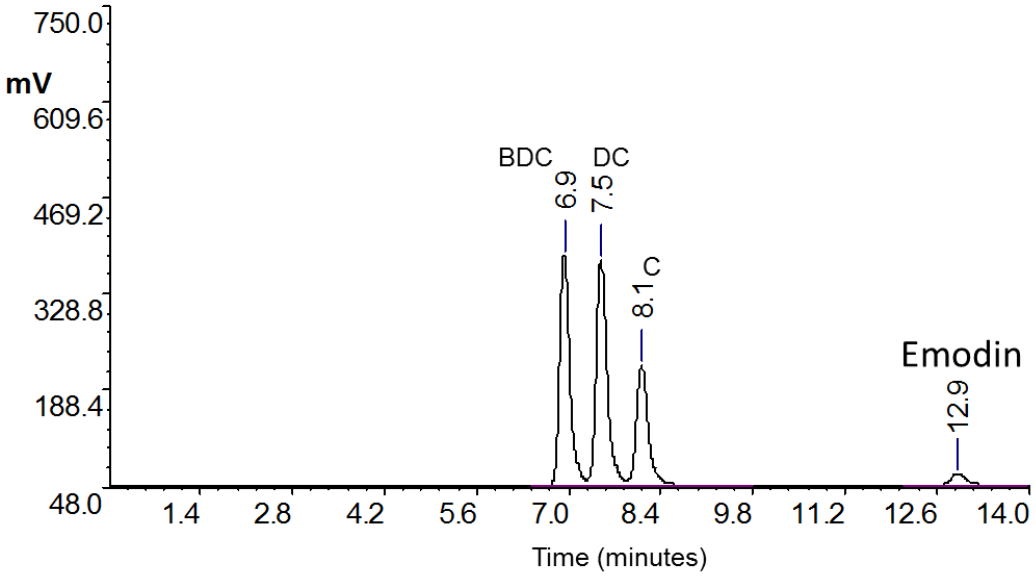

Figure 3.1 Chromatograms of curcumin (C), demethoxycurcumin (DC), and bisdemethoxycurcumin (BDC) with emodin using conventional HPLC method

3.1.4 Method validation

The method was validated for the determination of curcuminoids in aqueous samples. The method validation was based on ICH guidelines (ICH 1996).

1.14.1.7. Linearity

To determine the linearity of the HPLC response, different concentrations of curcumin, demethoxycurcumin and bisdemethoxycurcumin solutions ranging from 2.5µg/ml to 80µg/ml were prepared. The samples including emodin 40µg/ml as internal standard were injected twice. Blank samples were analysed during the experiment. The plots of the results showed a linear relationship between the response (peak eras) and the concentrations, Figure 3.2. The regression coefficient R^2 for curcumin, demethoxycurcumin and bisdemethoxycurcumin are shown in Table 3.1.

Table 3.1 Regression coefficient, intercept, and the slope of curcuminoids components using 55%:45%v/v of acetonitrile: phosphate buffer mobile phase, flow rate 1 ml/min, λ=420nm, injection volume: 30µl

Drugs	R^2	Intercept	Slope
Curcumin	0.99	0.27	0.09
Demethoxycurcumin	0.99	0.3	0.15
Bisdemethoxycurcumin	0.99	0.15	0.139

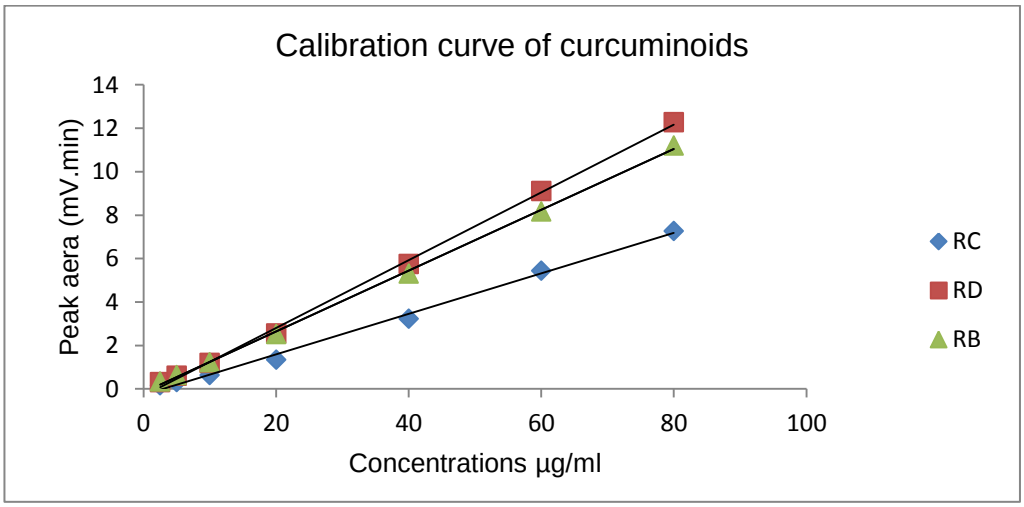

Figure 3. 2 Calibration curve of curcumin (RC), demethoxycurcumin (RD) and bisdemethoxycurcumin (RB) using mobile phase of 55%:45%v/v (acetonitrile: phosphate buffer)

1.14.1.8. Sensitivity

Sensitivity is represented by the limit of detection and the limit of quantitation.

LOD and LOQ were calculated using the following equations:

$$LOD = \frac{3.3\ \sigma}{S}$$

$$LOQ = \frac{10\ \sigma}{S}$$

Where, σ is the standard deviation of Y-intercept and S is the slope of the calibration curve.

The LOD and the LOQ data are illustrated in Table 3.2.

Table 3.2 Limit of detection and limit of quantification of curcuminoid using the conventional method

	Curcumin	Demethoxycurcumin	Bisdemethoxycurcumin
LOD	1.16µg/ml	1.48µg/ml	1.20µg/ml
LOQ	3.54µg/ml	4.50µg/ml	3.64µg/ml

1.14.1.9. Precision

The precision is expressed as the relative standard deviation (RSD%). It was tested by six determinations at three levels of known concentrations, low (10µg/ml), medium (40µg/ml) and high (80µg/ml) levels in the range of the calibration curve. These experiments were repeated for five days under the same conditions to determine the inter-day precision. Both inter- and intra-day precisions were determined by calculating the relative standard deviation (RSD%). The lower the RSD% value the better the performance of the method. RSD% data for both inter-day and intra-day are shown in table (3.3).

Table 3.3 Inter-day and intra-day precision data using the conventional method

inter-day RSD%			
Sample concentrations	Curcumin	Demethoxycurcumin	Bisdemethoxycurcumin
10µg/ml	0.47	0.2	0.15
40µg/ml	0.15	0.11	0.1
80µg/ml	0.15	0.12	0.08
intra-day RSD %			
Sample concentrations	Curcumin	Demethoxycurcumin	Bisdemethoxycurcumin
10µg/ml	0.35	0.33	0.27
40µg/ml	0.11	0.14	0.17
80µg/ml	0.15	0.13	0.17

1.14.1.10. Accuracy

Accuracy of analytical method measures the closeness of the test results to the true concentration of the analytes. This test needs three different known concentrations (low, medium, high) within the linearity range to be analysed each one six times. The accuracy was then calculated by dividing each value of six samples of each level by the true concentration, the accuracy results of this method are addressed in Table 3.4.

Table 3.4 Accuracy data of the conventional method

Accuracy			
Actual concentrations	Curcumin	Demethoxycurcumin	Bisdemethoxycurcumin
10µg/ml	97.06	101.69	103.51
40µg/ml	96.85	102.52	99.96
80µg/ml	97.75	97.27	102.158

3.1.5 Conclusion

In conclusion, the conventional method for curcuminoids separation using acetonitrile and phosphate buffer solution (10mM) as a mobile phase(55%:45%) with internal standard (emodin) was linear, sensitive, precise and accurate. The analysis time was 13 minutes. The compounds were very sensitive to the concentration of acetonitrile and to the buffer solution.

3.2 HPLC assay for curcuminoids using microemulsion mobile phase

3.2.1 Introduction

Microemulsion is a nanometre sized droplet of one liquid suspended or dispersed in another immiscible liquid. Microemulsion is usually composed of oil dispersed in water or water dispersed in oil. The oil and water are completely immiscible and this is because there is a high surface tension between them (Bryant and Altria 2004). Therefore adding a surfactant to reduce this surface tension will allow an emulsion to form. Nevertheless, for a microemulsion to be created the surface tension needs further reducing to zero, this can be approached by adding a small chain of alcohol, which is called co-surfactant, such as 1-butanol (Bryant and Altria 2004).

Microemulsion is generally optically transparent and thermodynamically stable. The ratios of oil-water-surfactant and co-surfactant must be correct to obtain a stable microemulsion system; otherwise the microemulsion will not be formed or will decompose into two layers water and oil in short time. So the composition ratio of microemulsion needs to be taken into consideration. There has been an increase using microemulsion in HPLC as an eluent and in separation science and this is due to its selectivity compared to conventional method.

There are two types of microemulsion used as mobile phase in HPLC, oil in water and water in oil. The oil in water microemulsion is where the oil is dispersed in a continuous phase (water), and this type is used in a reversed phase chromatography. The other type is water in oil microemulsion, in this type the water is dispersed in the oil phase as droplets and it used for normal phase chromatography.

The mechanism of separation in HPLC is due to the partitioning of the solutes between the stationary phase and the mobile phase. This theory is being altered in the use of microemulsion as an eluent; this is because of a surfactant layer is adsorbed onto the stationary phase surface. Also a second partitioning mechanism is created, which is where the solutes partition into the droplets from both the stationary and the mobile phase. In O/W microemulsion, water-insoluble substances are involved in the oil droplets. The retention of the hydrophobic compounds is highly influenced by the partitioning into oil droplets of the microemulsion. Water-soluble substances stay in the aqueous phase and the retention is mostly controlled by the interaction of the solutes with the stationary phase. The hydrophobic droplets are also allocated to the surface of

the stationary phase and thereby affect solutes selectivity and the retention (El-Sherbiny et al. 2003; Marsh et al. 2005).

Berthed used O/W microemulsion of heptane, 1-pentanol, SDS and aqueous orthophosphate buffer in separation of series of alkyl benzenes and in quick screen of 11 drugs used illegally in sport (Berthod et al. 1992; Marsh et al. 2005).

Alex March (2005) also studied the use of microemulsion of Octane, 1-n Butanol, SDS and aqueous orthophosphate buffer in separation of different compounds, such as a wide range of acidic, basic and neutral drugs and excipients, and the effect of each parameter on the retention (Marsh et al. 2005)

El-Sherbiny (2005 and 2007) worked on the evaluation of the use of the microemulsion as an eluents in HPLC for the separation of flunarizine in the presences of some of its degradation components and on determination of loratadine and desloratadine in a pharmaceutical dosage form using octane, n-butanol, SDS and aqueous orthophosphate buffer (El-Sherbiny et al. 2005; El-Sherbiny et al. 2007).

Mohammad Althanyan (2011) used octane, 1-n-butanol, SDS and aqueous orthophosphate buffer , as microemulsion, in determination of some inhaled drugs such as formoterol and salmeterol in urine samples (Althanyan et al. 2011). Another microemulsion was also prepared by using ethyl acetate, Brij35, 1-butanol and aqueous orthophosphate buffer for determination of terbutaline sulphate in urine samples (Althanyan et al. 2016).

AL-Jammal (2015) and Li (2016) have used a microemulsion as a mobile phase, which is composed of octane, 1-n-butanol, SDS and aqueous

orthophosphate buffer, in determination of nifedipine and hydrochlorothiazide and losartan in pharmaceutical preparations such as tablet (AL-Jammal et al. 2015; Li et al. 2016)

In this work, microemulsion of isopropyl myristate, 1-n-butanol, SDS and aqueous orthophosphate buffer, is used to separate curcumin, demethoxycurcumin and bisdemethoxycurcumin to benefit from the advantage of using microemulsion over the conventional method.

The microemulsion has two phases, so it has a great capacity of solubility for both hydrophilic and hydrophobic analytes (Marsh 2005), which can provide fast separations. For oil in water microemulsion, the retention time of the lipophilic substances can be reduced compared to conventional methods in which the organic solvent gradients are necessary (Marsh 2005). Also in O/W microemulsion, the majority composition is water which is around 90% and just ten percentages is organic solvent including the surfactants, whereas in the conventional method that was developed for the determination of curcuminoids contains more than 50% of organic solvent which is more expensive and environmentally unfriendly.

In this part, it is proposed to study the application of microemulsion for the analysis of curcuminoids in aqueous solution and to examine the effects of experimental parameters on the separation of curcuminoids.

3.2.2 HPLC conditions

The experiments were carried out under the following conditions:

Stationary phase (column): Phenomenex C18

Mobile phase: 0.8% isopropyl myristate (IPM), 9% 1-n-butanol, 2.7% SDS and 88.7% (10mM) phosphate buffer solution (all w/w).

Flow rate: 1 ml/min

Detector: UV set at wavelength λ=420nm

Injection volume: 30μL

3.2.3 Method development

The first few experiments were carried out using the typical microemulsion mobile phase in which the octane was used as the oil. It was reported that this mobile phase separates a variety of drugs (Miola et al. 1998; Altria 1999; Mahuzier et al. 2001). It is usually composed of 0.8% octane (as an oil phase), 3.3% surfactant (SDS), 6.6% co-surfactant (butan-1-ol) and 89.3% phosphate buffer solution 5mM (as aqueous phase). However, this mobile phase was unable to separate the curcuminoids components. This might be attributed to the low solubility of the solutes in the oil phase. The limited solubility of curcuminoids in the octane was very clear after dissolving a few milligrams of the curcuminoid samples in the oil. Hence, octane oil was replaced with isopropyl myristate (IPM); The IPM was able to solubilise the curcuminoids more than octane. IPM was also used in some drug delivery formulations of microemulsion of curcumin (Chen et al. 2005). The new mobile phase with isopropyl myristate was able to separate the solutes with acceptable retention time as shown in figure 3.3.

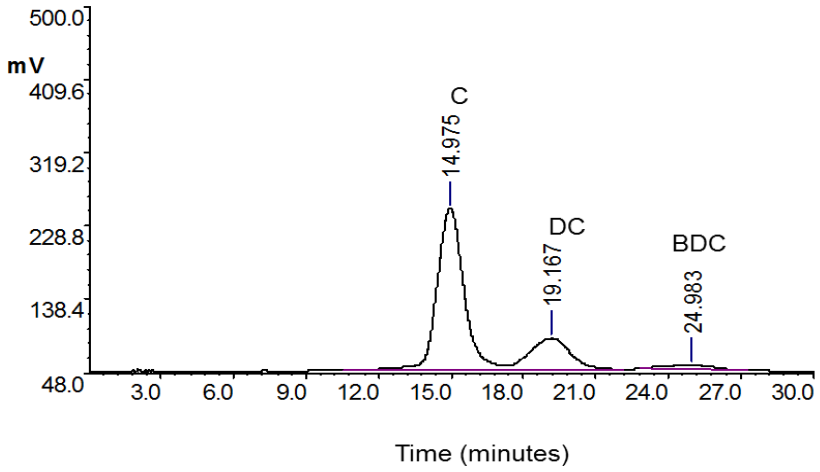

Figure 3. 3 Separation of curcuminoids using microemulsion using isopropyl myristate as oil phase, C is curcumin, DC is demethoxycurcumin and BDC is bisdemethoxycurcumin.

The components concentrations of the new mobile phase were optimised to reduce the retention time of the solutes. The optimum concentrations of the new mobile phase components were as follows:

0.5% IPM, 2.7% surfactant (SDS), 9% co-surfactant (butan-1-ol) and 87.8% phosphate buffer solution 10mM (pH.3). The amount of individual components of the mobile phase was prepared as w/w. The optimised mobile phase significantly reduced the retention time of the solutes. Figure 3.4 shows the reduction in the retention time. The concentrations of these parameters have been studied in detail in the next section.

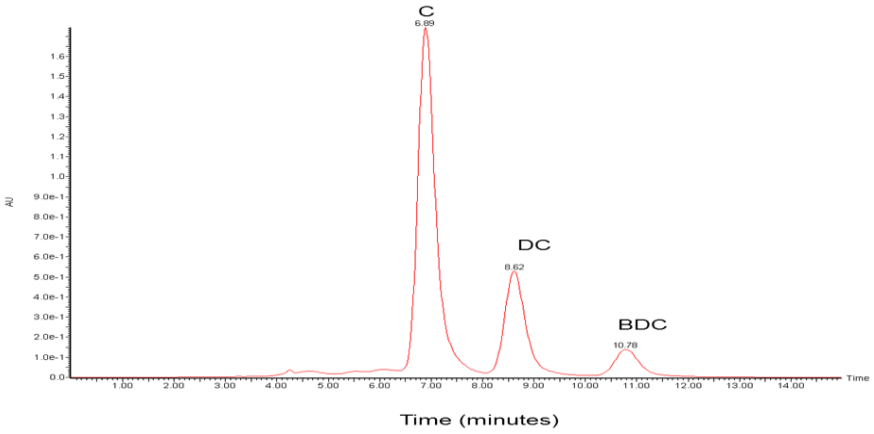

Figure 3. 4 Chromatograms of curcuminoids using microemulsion as an eluent, C is curcumin, DC is demethoxycurcumin, and BDC is bisdemethoxycurcumin.

3.2.4 Factors affecting the HPLC separation using microemulsion

There are five parameters that affect the separation of curcuminoids using microemulsion as the mobile phase. These parameters comprise of surfactant, co-surfactant, oil and buffer solution and temperature. It was found that the concentrations of these parameters affect the retention time and the resolution of the compounds.

1.14.1.11. Surfactant concentration

The effect of different concentrations of SDS on the retention time of solutes was studied. It was found that as the SDS concentration is increased, the retention time of the curcuminoids decreases and it was noticed that the peak resolutions is sensitive to the SDS. This is because of the fact that an increase in the surfactant concentration increases the distribution of the solutes into the microemulsion, as well as increases the volume of the microemulsion in the mobile phase (El-Sherbiny et al. 2003; Marsh 2005). This effect is more applicable for the solutes that have a greater affinity to the oil droplets; this means that the hydrophobic solutes will be more affected by changing the

surfactant concentration than the hydrophilic ones (El-Sherbiny et al. 2003; Marsh 2005). The analytes with no affinity to the oil droplets will not be affected by changing the concentration of the surfactant, and also the retention of the more hydrophobic compounds will be influenced to a superior degree due to their distribution into the droplets (El-Sherbiny et al. 2003; Marsh 2005; McEvoy et al. 2006). Furthermore, it was reported that surfactants could adsorb on the column's stationary phase and modify the surface of the stationary phase (Berthod et al. 1992). Hence, this influences the partitioning properties between the solutes and the stationary phase.

The effect of SDS concentration on the separation of curcuminoids was assessed by preparing several mobile phases with different concentration of SDS ranging from 1.5% to 2.8%. It was found that the retention time of curcumin, demethoxycurcumin and bisdemethoxycurcumin decreased with increasing the SDS concentration. Increasing the concentration of SDS above 2.8% led to an increase in the back pressure of the column which caused a halt in the system. Nevertheless, the microemulsion was not formed when decreasing the concentration of SDS below 1.5%. Figure 3.5 presents the effect of the SDS concentrations on the retention time of the compounds.

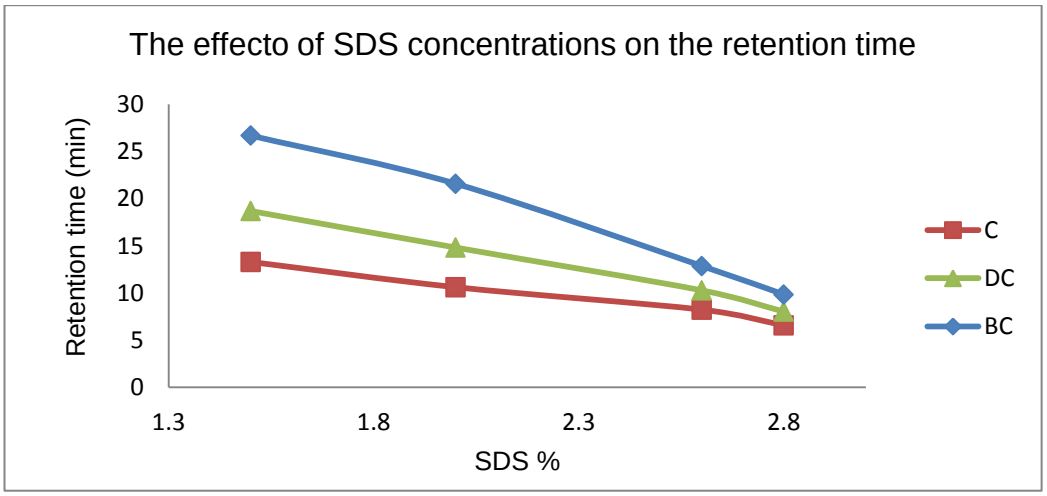

Figure 3.5 The effect of SDS concentrations on the retention time of curcuminoids, SDS is sodium dodecyl sulphate, C is curcumin, DC is demethoxycurcumin, and BDC is bisdemethoxycurcumin.

1.14.1.12. Co-surfactant concentration

The use of co-surfactants such as butan-1-ol can also influence the satiability and the formation of the microemulsion system. Figure 3.6 illustrates the effect of changing the concentrations of buatn-1-ol. It was found that raising the concentration of the co-surfactant from 6.6% to 11% w/w reduced the retention time of the curcuminoids components. However, a further increase in the concentrations led to a loss in the separation resolution of the solutes and an increase in the column pack pressure in the system. The reduction in the retention time of the solutes is attributed to the increase in the organic phase of the microemulsion system (Marsh 2005; McEvoy et al. 2006) and therefore enhancing the solubility of these solutes in the mobile phase by increasing the microemulsion solubilisation capacity (Garti et al. 2001; Althanyan 2011).

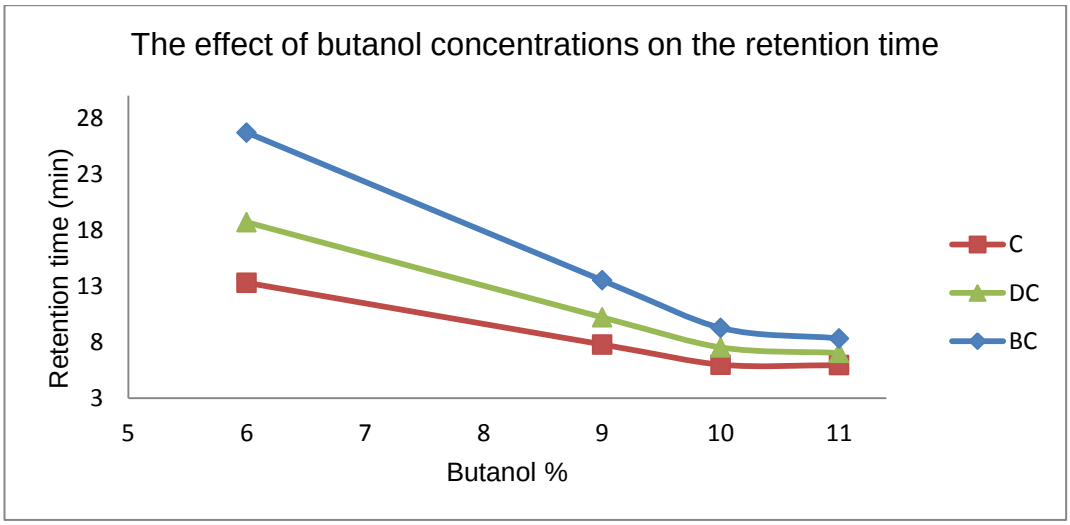

Figure 3.6 The effect of butanol concentrations on the retention time of curcuminoids, C is curcumin, DC is demethoxycurcumin, and BDC is bisdemethoxycurcumin.

1.14.1.13. Oil concentration

The oil is dispersed as micro-droplets in a continuous water phase to form microemulsion with aids of surfactant/co-surfactant which are located on the interfaces between the oil and water (Mason et al. 2006; Althanyan 2011). The concentrations and the type of the oil used in the HPLC microemulsion have a noticeable effect on the retention time of the analytes. This effect is based on the nature of the analytes. The effect of oil concentration on the separation of curcuminoids has been examined in the range from 0.3% to 0.8% w/w. Figure 3.7 demonstrates the effect of these concentrations on the retention time of the curcuminoids. The results show that increasing the concentration of the oil decreases the retention time of the curcumin, demethoxycurcumin and bisdemethoxycurcumin. This could be attributed to the increase of the solubility of the solutes in the mobile phase. Increasing the oil above 0.5% has a slight influence on the retention time.

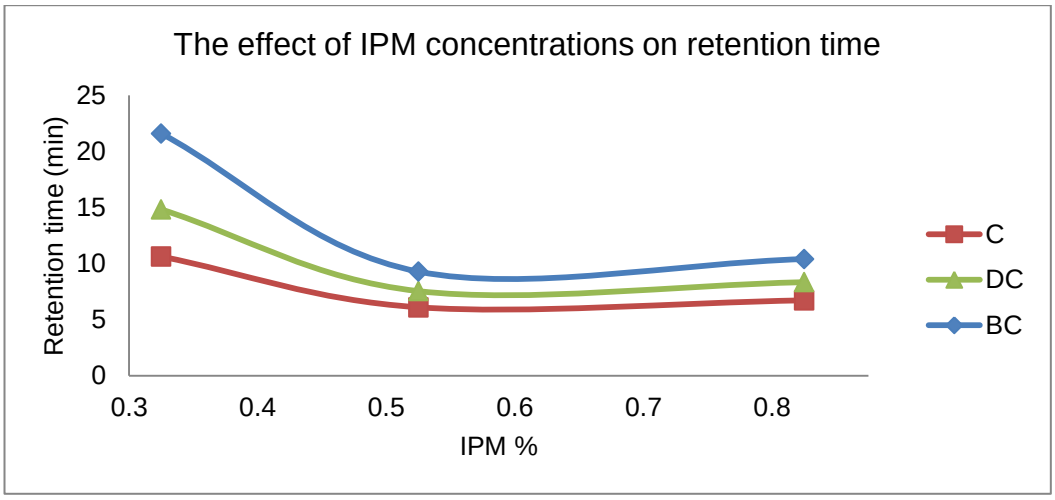

Figure 3.7 The effect of IPM concentrations on the retention time of curcuminoids, IPM is isopropyl myristate oil C is curcumin, DC is demethoxycurcumin, and BDC is bisdemethoxycurcumin.

1.14.1.14. Buffer concentration

The effect of phosphate buffer concentrations on separation of the curcuminoids solutes was investigated at three levels 10, 15 and 20mM. Figure 3.8 illustrates the effect of changing the buffer concentrations on the retention time of the solutes. The retention time decreased when the concentration of the buffer solution of the mobile phase increased. These results are in agreement with those reported by Mao et al. (2001). However, the study reported by Mao et al. was carried out using conventional mobile phase; this shows that the retention time of solutes decreased with increasing buffer concentrations, whether the mobile phase is a microemulsion or conventional (Mao and Carr 2001).

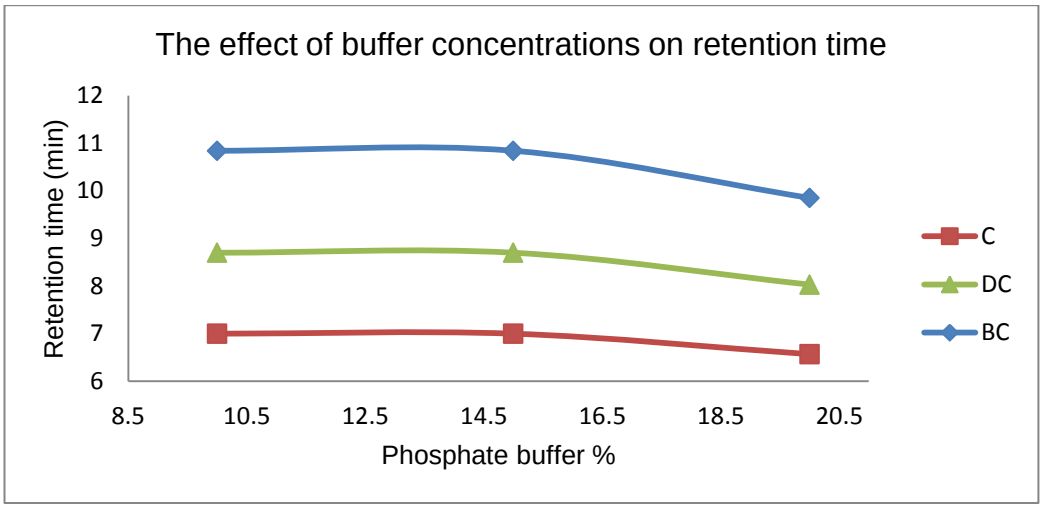

Figure 3.8 The effect of buffer concentrations on the retention time of curcuminoids, C is curcumin, DC is demethoxycurcumin, and BDC is bisdemethoxycurcumin.

1.14.1.15. Temperature

The effect of the column's temperature was investigated at three different temperatures ranging from 25°C to 45°C. Figure 3.9 displays the effect of increasing the temperature on the separation time of curcuminoids solutes. It was found that increasing the temperatures decreases the retention time. Increasing the temperature lowers the viscosity of the microemulsion and hence reduces the column back pressure. This decrease in the viscosity may influence the distribution and the solubility of the solutes in the microemulsion system and hence decrease the retention time.

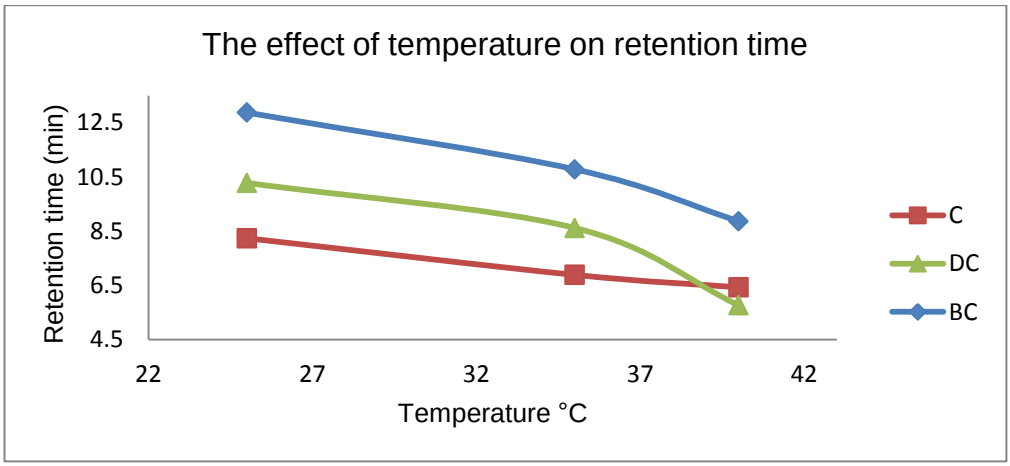

Figure 3. 9 The effect of temperature on the retention time of curcuminoids, C is curcumin, DC is demethoxycurcumin, and BDC is bisdemethoxycurcumin.

3.2.5 Method validation

The method was validated for the determination of curcuminoids in aqueous solution. The method validation was based on ICH guidelines (ICH 1996).

1.14.1.16. Linearity

To determine the linearity of HPLC response, different concentrations of curcumin, demethoxycurcumin and bisdemethoxycurcumin solutions ranging from 2.5µg/ml to 80µg/ml were prepared. The samples including emodin 40µg/ml as internal standard were injected twice. Blank samples were analysed during the experiment. The calibration curve showed a linear relationship between the response (peak area) and the concentrations, Figure 3.10. Regression coefficients R^2 are shown in Table 3.5.

Table 3. 5 Linearity data of curcuminoids components using microemulsion mobile phase

Samples	R^2	Intercept	slope
Curcumin	0.99	0.33	0.09
Demethoxycurcumin	0.99	0.44	0.15
Bisdemethoxycurcumin	0.99	0.17	0.13

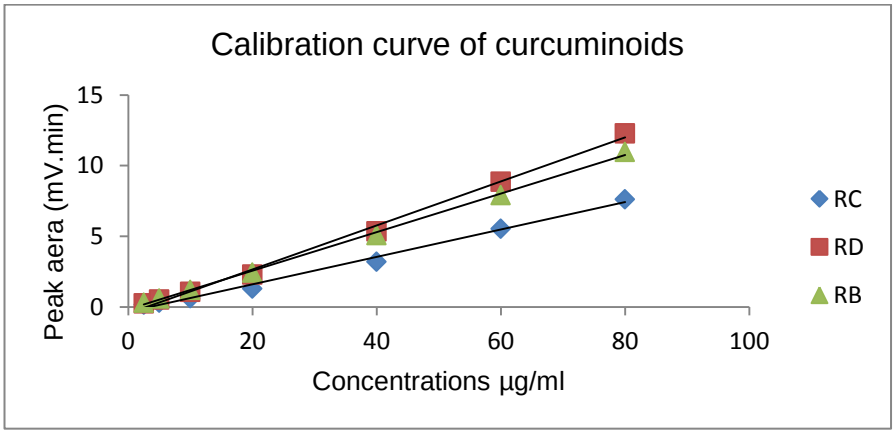

Figure 3. 10 Calibration curves of curcuminoids using microemulsion mobile phase, C is curcumin, DC is demethoxycurcumin and BDC is bisdemethoxycurcumin

1.14.1.17. Sensitivity

Sensitivity is represented by the limit of detection and the limit of quantitation.

LOD and LOQ were calculated using the following equations:

$$LOD = \frac{3.3\ \sigma}{S}$$

$$LOQ = \frac{10\ \sigma}{S}$$

Where, σ is the standard deviation of Y-intercept and S is the slope of the calibration curve.

The LOD and the LOQ data showed in Table (3.6).

Table 3. 6 Limit of detection and Limit of quantification data of curcuminiods using microemulsion mobile phase

	Curcumin	Demethoxycurcumin	Bisdemethoxycurcumin
LOD	1.20µg/ml	0.81µg/ml	0.70µg/ml
LOQ	3.63µg/ml	2.47µg/ml	2.14µg/ml

1.14.1.18. Precision

The precision is expressed as the relative standard deviation (RSD%). It was tested by six determinations at three levels of known concentrations, low (10µg/ml), medium (40µg/ml) and high (80µg/ml) levels in the range of the calibration curve. These experiments were repeated for five days under the same conditions of the HPLC to determine the inter-day precision. Both inter- and intra-day precision were determined by calculating the relative standard deviation (RSD%). The lower RSD% value the better is the precision of the method. RSD% data for both inter-day and intra-day are shown in table 3.7.

Table 3. 7 Inter-day and intra-day precision data of curcuminoids using the microemulsion mobile phase

Inter-day RSD%			
Sample concentrations	Curcumin	Demethoxycurcumin	Bisdemethoxycurcumin
10µg/ml	0.52	0.34	0.33
40µg/ml	0.57	0.3	0.42
80µg/ml	0.5	0.5	0.62
Intra-day RSD%			
Sample concentrations	Curcumin	Demethoxycurcumin	Bisdemethoxycurcumin
10µg/ml	0.25	0.72	0.76
40µg/ml	0.58	0.57	0.5
80µg/ml	0.42	0.37	0.36

1.14.1.19. Accuracy

Accuracy of analytical method measures the closeness of the experimental value to the true concentration of the analytes. The accuracy of the method was assessed at three different concentration levels (low, medium, and high) within the linearity range and each level was repeated six times. The accuracy was then calculated by dividing each value of six samples of each level by the true concentration. The accuracy results of this method are shown in Table 3.8.

Table 3. 8 Accuracy data of curcuminoids using microemulsion mobile phase

Accuracy			
Actual concentrations	Curcumin	Demethoxycurcumin	Bisdemethoxycurcumin
10µg/ml	96.25	101.84	97.78
40µg/ml	98.38	96.5	99.15
80µg/ml	100.8	99.06	99.02

3.2.6 Conclusion

The separation of curcuminoids was achieved by using two HPLC methods, which are the conventional and microemulsion methods. Both methods showed good results in terms of sensitivity, linearity, precision and accuracy. The microemulsion method was more sensitive for both demethoxycurcumin and bisdemethoxycurcumin than conventional methods. There was no difference in the sensitivity of both methods for curcumin. The results appear to be much closer to each other in both methods regarding the precision, the accuracy and the linearity.

In the conventional method, the separation time for curcuminoid components including the internal standard was 13 minutes. On the other hand, 18 minutes was required to complete the separation in the microemulsion method. In the conventional technique, about 50% of the mobile phase is organic solvent, whereas about 90% of the mobile phase in the microemulsion is aqueous solution, which is inexpensive and environmentally friendly.

CHAPTER FOUR

Production of Inhaled Curcuminoids Particles using Air Jet Milling Technique

Chapter 4: Production of inhaled curcumin particles using air jet milling technique

4.1. Introduction

Air jet milling method is the simplest milling technique used to reduce size of powder particles. A compressed air is used in this process to accelerate the particles speed and leads to particles-particles and particles instrument wall collisions and impactions, which in turns cause a break of the particles to a smaller size (Letang et al. 2002; Protonotariou et al. 2015). Also attrition occurs at solid surfaces of the particles as they move rapidly, in the high velocity of stream air, against each other, resulting in shear forces that could break the particles down (Loh et al. 2015). Air jet micronisation has many advantages over other mechanical milling methods, such as absence of product contamination with metal (Shariare 2011), and it is suitable for heat sensitive components, as less temperature is generated during the milling (Saleem and Smyth 2010).

It has been reported that air jet microniser reduces the particle size of salbutamol sulfate (Brodka-Pfeiffer et al. 2003; Shariare et al. 2011a), and fenoterol hydrobromide (Brodka-Pfeiffer et al. 2005) below 5µm that allow them to be suitable for dry powder inhaler formulation. In DPI preparation, the API must be in respirable size of 1-6µm for optimal lung deposition (Pritchard 2001; Telko and Hickey 2005). Therefore, air jet mill has been used to investigate its ability to produce inhalable curcumin particles.

In this work, inhaled curcumin particles were prepared and formulated by a simple method without any excipients or additives, which makes these DPI formulations safer and available for patients. Also in this work, the aerodynamic

behaviour of all curcuminoids components (curcumin, demethoxycurcumin and bisdemethoxycurcumin) was determined.

The processed curcumin particles have been characterised for their size, shapes, polymorphism alterations and the inhalation performance. The laser diffraction and scanning electron microscope were used to determine the size and shape of milled curcumin particles, respectively. The differential scanning calorimetry and XRPD were utilised to assess any changes in curcumin polymorphism after comminution. The inverse gas chromatography was used to examine the free surface energy of the powder before and after milling, and to correlate the surface energy with inhalation profile of curcumin particles. Dry powder inhalers (DPI) formulations were prepared by mixing the micronized curcumin particles with α-lactose monohydrate at two different ratios (1:9 and 1:67.5 curcumin:lactose). Several formulations were prepared for two different sizes of micronized curcumin particles that have a D_{50} of 3.5µm and 2.5µm. DPI formulations were then characterised using Next Generation Impactor. The FPF%, MMAD and GSD were determined for each of curcuminoids components (curcumin, demethoxycurcumin and bisdemethoxycurcumin).

4.2. Methods

4.2.1. Method of milling a start material of curcumin using jet mill

Curcuminoids' powder was micronized by FPS spiral jet mill (FPS, Italy).The micronisation process was manipulated by changing grinding pressure (GP), injection pressure (IP) as it is shown in table 4.1. The pressure of these two lines was controlled through an injector/grinding pressure regulator with pressure display on the front of the spiral jet mill. A compressed air was used to create these pressures and it is adjusted up to 10 bars pressure. The injection

pressure line was first opened to the required level and then the grinding pressure was opened too. The lowest and the highest pressure level of both injection and grinding that can be used in this machine are two and seven bar. During conduction the experiments, firstly, both lines of the jet mill were gradually increased from 2 bars to 6 bars, secondly, the injection pressure was kept at 7 bars and then the grinding pressure increased gradually from 2 to 4 bars as it can be seen in experimental parameter table 4.1. In operating the jet mill, the injection pressure needs to be either equal to or higher than grinding pressure, otherwise high vacuum pressure will be generated inside the microniser which leads the product to disperse to the filter. In each run of the experiments, 5g of curcuminoids was used and then collected after one minute intervals from a container at the bottom of the spiral jet mill. The feed rate was kept constant to a medium level for all the experiments. This is because it has been reported that feed rate has no effect on the particles size reduction of powder (Brodka-Pfeiffer et al. 2003).

Table 4. 1 The jet mill parameters setting, grinding pressure (GP) and Injection pressure.

Experiment No	GP (Bar)	IP (Bar)
1	2	2
2	3	3
3	4	4
4	5	5
5	6	6
6	2	7
7	3	7
8	4	7

4.2.2. Surface energy analysis

Surface energy, of curcumin and lactose powder, was determined by an automated inverse gas chromatography (IGC) system (Surface Measurement Systems Ltd, London, UK). Powder samples were filled into a pre-silanised standard glass column (3mm internal diameter and 30cm long; SMS). All samples columns were packed by tapping for around 5 min using a jolting volumeter (Surface Measurement Systems Ltd, London, UK). For each samples, the experiment was repeated five times. Prior each first measurement of each sample, the system was conditioned for 2 hours, at temperature of 30ºC and 0% relative humidity. Non polar and polar probes were injected into the packed samples using helium as carrier gas (mobile phase) with a flow rate of

10 ml/min at temperature 30ºC. Several non-polar probes were used including hexane, heptane, octane and nonane while the polar probes were chloroform and ethyl acetate (Schultz et al. 1987; Van Oss et al. 1988; Van Oss 1993). The net retention time of non-polar solvents were used to calculate the dispersive energy, whereas, net retention time of the polar probes were used to measure the specific surface energy of powder (Mohammad 2013).

4.2.3. Surface energy calculation method

See section 2.3.9.

4.2.4. Blending of micronized curcumin with α-lactose

The dry powder inhaler formulations of curcumin were prepared for the different sizes of micronized curcuminoids (D_{50}=3.5µm and 2.5µm) by mixing the particles of each of the sizes with α-lactose monohydrate (Lactohale200® 50-100µm) as a carrier. In DPI formulations, α-lactose is used as a carrier in order to enhance the performance and flowability of the formulation (Telko and Hickey 2005; Kou et al. 2012). Lactose is considered to be an inert compound with non-toxicology profile (Pilcer et al. 2012). Lactose particles characteristics such as size, shape and surface morphology have an effect on the DPI performance (Kou et al. 2012). It has been reported by Steckel and Muller that the drugs concentrations to the lactose (carrier) have an effect on the fine particle fraction and the drug deposition in the lung (Steckel and Muller 1997; Adi et al. 2008; Kou et al. 2012). Therefore, two different formulations of curcuminoids-lactose concentrations were prepared. The ratios of these formulations were 1:9 and 1:67.5 (curcuminoids-lactose w/w). Each of these formulae (2g) was mixed for a different length of time to obtain the most homogeneity sample using a tumbling shaker mixer. The blending times were one, five, ten and thirty minutes. The

homogeneity (uniform) mixing was then examined by taking three samples from each formulation and analysed by HPLC. The percentage RSD (relative standard deviation, n=3) for each mixing time was calculated individually. One gram of powder of the most uniform formulation after blending was transferred into an Easyhaler device to assess the aerodynamic particles characterisation using Next Generation Impactor (NGI).

4.2.5. Aerodynamic particle size characterisation

Procedure to setup the next generation impactor (NGI): The next generation impactor has been designed to have 7 stages with a Micro-orifice collector. It can be operated at inlet flow rate from 30 L/min to 100 L/min. It is composed of three parts: the bottom part which is a frame that holds the impaction cups, the upper part which is the seal part holding the nozzles and finally the lid that has the inter-stage passages as shown in figure 4.4. The collection cups were coated with glycerol and allowed to dry for about 10 minutes before running the experiment. The cups were placed in the bottom frame and the lid of the impactor was closed. An amount of 15ml of suitable solvent was placed into the central cup of the pre-separator. The use of the pre-separator is recommended by USP (United States Pharmacopeia Convention. 2004) for dry powder inhaler testing in order to entrain the active ingredient that is attached to the larger carrier particles (United States Pharmacopeia Convention. 2004). The induction port was then connected to the pre-separator which was also connected to impactor body. A suitable mouth piece adaptor was connected to the induction port to ensure there was no loss in the sample between the inhaler devices and the induction tube. A vacuum pump was connected to the NGI, to obtain the desired flow rate throughout the flow controller. The inhalation flow rate was determined to be equivalent to 4kpa pressure drop across the inhaler device

(United States Pharmacopeia Convention. 2004). This was equal to a flow rate of 45 L/min. A calibrated electronic flow meter was used to measure the flow rate each time before the inhaler devices connected to the induction port. The inhalation time was calculated by using the following equation (European Directorate for the Quality of Medicines & HealthCare. 2008):

$$T = (60\ sec\ x\ V) / Q$$

T = Time duration consistent for withdrawal of 4 litres of air from the inhaler

Q = Airflow which produces a pressure drop of 4 KPa

V = 4 L to be drawn through the inhaler

According to the above equation the time required for the flow rate of 45 L/min is 5.5 seconds.

Dry powder inhaler formulations of curcumin were loaded into the Easyhaler, which was then connected to the induction port through an air tight chamber to ensure that it was in isolation from the atmosphere pressure as it is presented in figure 4.2 (Yakubu 2009). The dose was discharged from the Easyhaler into the NGI at flow rate of 45 L/min for 5.5 seconds. An experiment was carried out for each formulation three times. The deposited particles in the stages was then recovered by HPLC mobile phase and was analysed using HPLC.

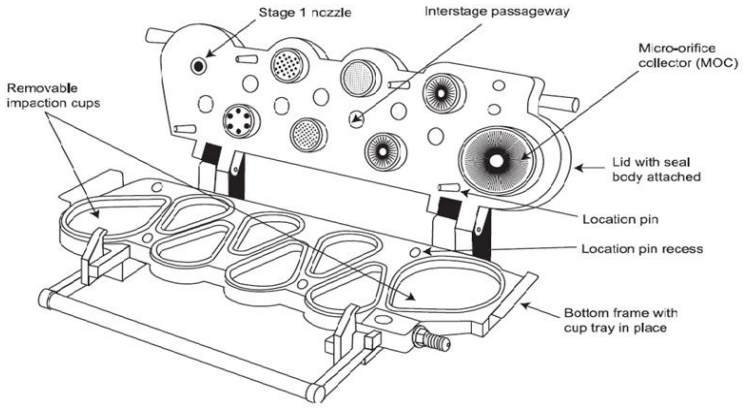

Figure 4. 1 The component of the next generation impaction (NGI).

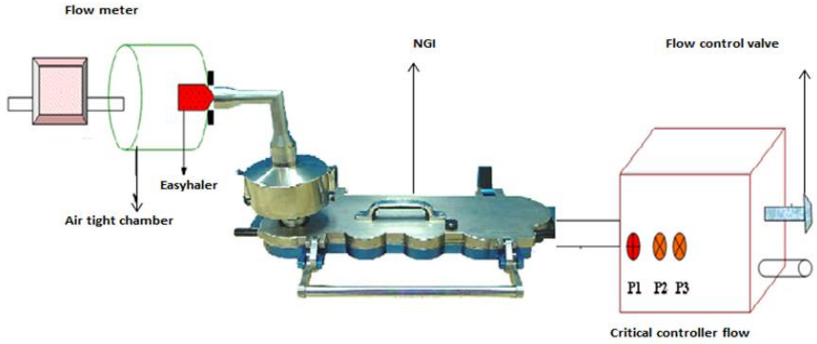

Figure 4. 2 Setting up the NGI for DPIs characterisation

Calculations of FPF%, MMAD and GSD:

The aerodynamic parameters, for each DPI formulations, have been calculated using Copley Inhaler testing data analysis software (CITDAS). The deposition profile and the aerodynamic characterisation of curcumin (C), demethoxycurcumin (DC) and bisdemethoxycurcumin (BDC) were determined for each formulation.

These parameters were calculated as follows:

I. Fine particle fraction (FPF):

$$FPF = (FPD/Total\ delivered\ dose) * 100\%$$

Where fine particle dose (FPD), as specified by CITDAS, is the amount of the drug with aerodynamic diameter less than 5μm. The fine particle dose (FPD) is the amount with particles that correspond to a size less than 5μm (Telko and Hickey 2005).The total delivered dose is the total amount of the drug that deposited in throat, pre-separator and the NGI stages.

II. The Mass median aerodynamic diameter (MMAD):

MMAD was calculated from the logarithm of the ECD (effective cut-off diameter) corresponding to 50% undersize particles (on probability scale).

III. The Geometric standard deviation (GSD):

GSD was calculated from the following equation:

$$GSD = \sqrt{((d84.13\% / d15.87\%))}$$

Where d84.13%, and d15.87% are the aerodynamic particle size at 15.87% and at 84.13% less than the stated size, respectively for the cumulative size distribution.

The mean and SD of the FPF, MMAD, and GSD were determined for each formulation using Microsoft excel.

4.2.6. HPLC method

The HPLC method for determining the amount of curcuminoids in each stage of NGI has been described in chapter 3. Section3.1

4.3. Results and discussion

4.3.1. Particle size analysis

The mean size of the milled curcumin particles, D_{10}, D_{50} and D_{90}, are presented in table 4.2.

Table 4. 2 The mean (n=3) and the standard deviation (SD) of the curcumin particles size before and after milling.

Experiment No	D_{10} (µm) +/- SD	D_{50} (µm) +/- SD	D_{90} (µm) +/- SD
1	0.82 +/- 0.04	2.44 +/- 0.55	5.86 +/- 1.31
2	0.89 +/- 0.06	2.23 +/- 0.42	5.54 +/- 1.57
3	0.70 +/- 0.11	1.90 +/- 0.75	3.94 +/- 0.87
4	0.79 +/- 0.01	1.85 +/- 0.02	3.96 +/- 0.12
5	0.82 +/- 0.1	1.79 +/- 0.03	3.60 +/- 0.08
6	0.96 +/- 0.01	3.21 +/- 0.03	7.71 +/- 0.45
7	0.91 +/- 0.02	2.65 +/- 0.06	5.83 +/- 0.04
8	0.84 +/- 0.04	1.88 +/- 0.13	4.75 +/- 0.81
Start material	1.49 +/-0.48	7.85 +/- 2.77	41.3 +/- 12.54

It is clear that the jet mill micronizer using compressed air was able to reduce the particle size of curcumin (D_{50}) down below 5µm. The size was further reduces by increasing the grinding and injection pressure. In the experiments (1 to 4) in which both grinding and injection pressure raised from 2 bars to 6 bars gradually, the D_{50} of the particles was decreased simultaneously from 7.82µm to 1.79µm. Keeping the feed pressure (injection pressure) to the maximum (7

bars) while raising the grinding pressure gradually, from 2 bars to 4 bars, showed a reduction in the curcumin particles size from 7.95µm to 1.88µm. The data above indicates that increasing the grinding pressure (GP) decreases the particle size. This may be as a result of the increasing particles and particles collisions and particles instrument wall impactions, which in turn leads to break the curcumin particles down (Brodka-Pfeiffer et al. 2003). This observation was in agreement with a reported study on particles size of reduction using the jet mill microniser (Shariare et al. 2011b; Protonotariou et al. 2015; Angelidis et al. 2016; Kou et al. 2016). It has been observed that when grinding pressure increased more than 6 bars, the yield of the product was reduced. This may be due to the high vacuum inside the microniser that was generated by grinding pressure which caused the product to disperse to the filter. This work shows the ability of jet mill to reduce curcumin raw material with a particle size of 7.85µm (D_{50}) and 41.3µm (D_{90}) to inhalable particle size (D_{50} below 5µm). The micronized curcumin particles with size of (D_{50}) 3.5µm and 2.5µm were chosen for further characterisation and for dry powder inhaler formulations.

4.3.2. Morphology of the air jet milled curcumin particles using scanning electron microscope (SEM)

The morphology (particle shape) of pulverised curcumin particles were analysed using SEM. Figure 4.3 shows SEM images of the unprocessed and the triturate curcumin particles. Raw curcumin particles exhibit irregular shapes (Figure 4.3A). The milled curcumin (2.5µm) formed agglomerated particles as shown in figure 4.1 B, C and D, compared to the unprocessed curcumin. The particle shape of the micronized curcumin looks like partially rounded. The micronized particles with a size of 3.5µm (D_{50}) shows to be less agglomerated compared to the particles with size of 2.5µm. this could be attributed to the difference in their

particles size, since the smaller particles gain high energy and (including) static charges as they have intense energy during the milling process, therefore, particles aggregate to lower their total surface energy (Van Eerdenbrugh et al. 2008; Loh et al. 2015).

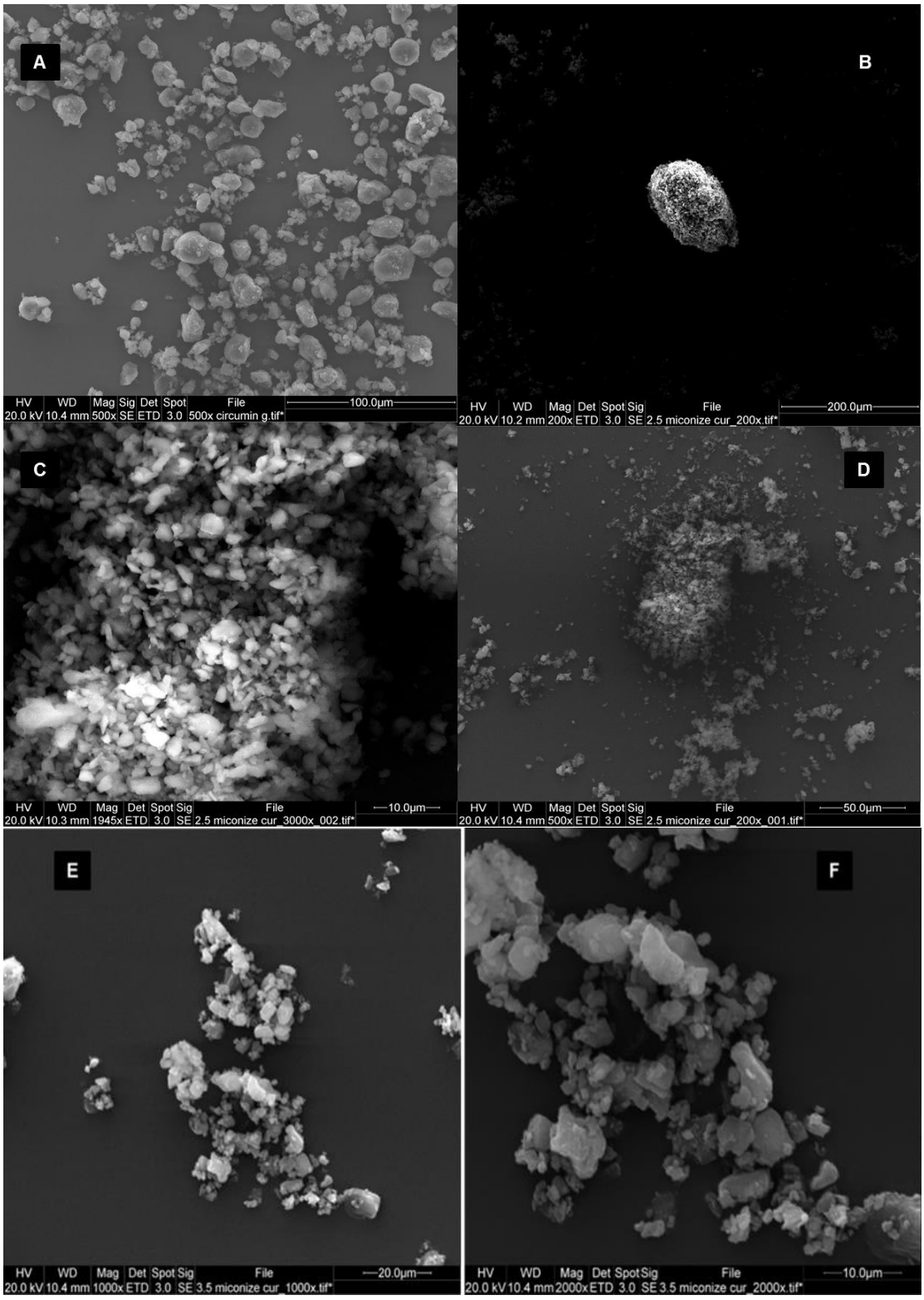

Figure 4. 3 SEM images of micronized curcumin particles, A is unprocessed curcumin particles, B, C and D milled curcumin particles with D_{50} of 2.5µm, E and F micronized curcumin particles with D_{50} of 3.5µm.

4.3.3. Thermal analysis of milled curcumin particles (DSC)

Different scanning calorimetry (DSC) was used to examine any changing in the melting point of the comminuted curcumin particle prepared as well as unprocessed material. The unprocessed curcumin particle has endothermic peak at 175ºC (Sanphui et al. 2011; Liu et al. 2015) which represents melting point of curcumin polymorph 1 as shown in figure 4.4A. The DSC results of micronized curcumin are presented in figure 4.4. It shows that milled curcumin particles with the different sizes (2.5µm and 3.5µm) have the same endothermic peak at 176ºC, which is in agreement with endothermic peak of the unprocessed particles. This endothermic peak represents the melting temperature of curcumin polymorph 1 (Sanphui et al. 2011; Thorat and Dalvi 2016).

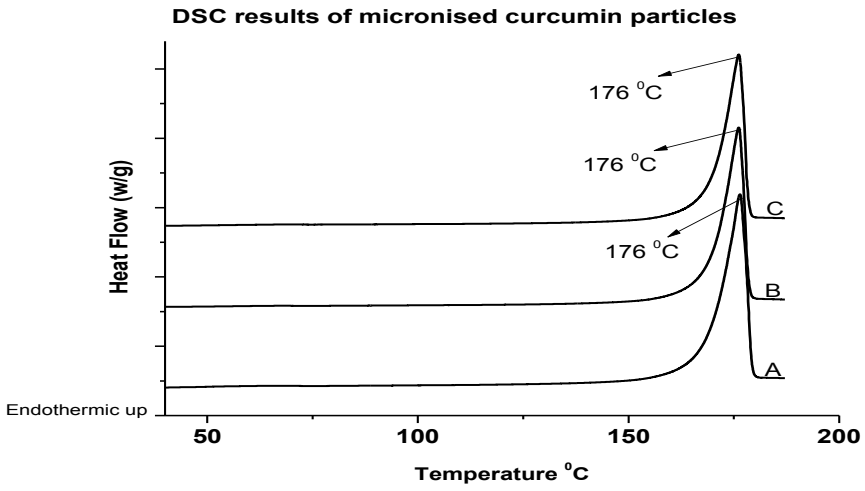

Figure 4. 4 DSC thermograms of the jet milled curcumin particles, A is unprocessed powder, and B and C are micronized curcumin particles with D_{50} on 2.5µm and 3.5µm, respectively

4.3.4. X-ray powder diffraction (XRPD)

XRPD was used to determine any changes in curcumin crystal structure. Curcumin crystal structure presents in three different polymorphs, commercial curcumin usually exhibit form 1 which is monoclinic structure, the other two forms are known as orthorhombic structures (Sanphui et al. 2011). Commercial curcumin form 1 was reported to have characteristic peaks in 2θ region at 8.90° and 17.0° (Sanphui et al. 2011; Liu et al. 2015; Thorat and Dalvi 2015).

The XRPD pattern of commercial material and the processed particles of curcumin alongside with curcumin polymorph 1 as a reference, which is obtained from Cambridge Structure Database (CSD), are illustrated in figure 4.5. The results indicate that milled curcumin particles with different sizes have form1 as the unprocessed material compared with XRPD patterns reference form1. The obtained data from diffractometer are in agreement with DSC results which are both proved that no alteration on curcumin polymorphs. This finding shows that the energy that used in jet mill was just enough to reduce the particles size of curcumin powder without producing any change in curcumin polymorphism, whereas in mechanical milling (milling using beads) curcumin has converted to amorphous form (Liu et al. 2013). In mechanical milling, when drug particles reached a certain critical size, the extra milled energy cause defect and disordering in drug crystal structure (Boldyrev 2004), which leads to the disappearance of the ordering positions of atoms or molecules in the crystals, these defect could impact the entire crystal resulting in complete amorphization) formed around crystalline core (Hersey and Krycer 1980; Loh et al. 2015). The amorphous state of a drug improved its solubility and the dissolution rate (Yu 2001). However, amorphous forms are usually unstable and

usually are converted to a crystalline forms leading to alteration of the particle size distribution and the performance of the drug (Guinot and Leveiller 1999).

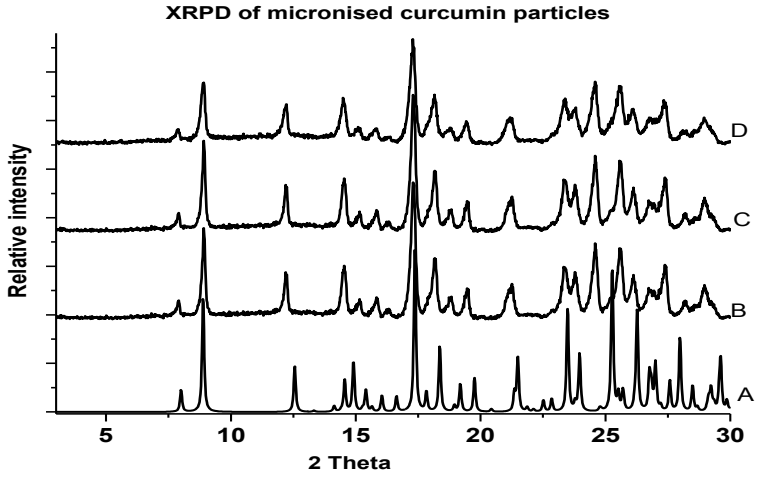

Figure 4. 5 Diffractograms of curcumin powder form1 (A), B is unprocessed curcumin; C and D are milled curcumin particles D_{50} of 2.5µm and 3.5µm, respectively.

4.3.5. Surface energy analysis of curcumin powder

The free surface energy of both raw and triturate curcumin powder were characterised using inverse gas chromatography (IGC). The specific, dispersive and total surface energy of unprocessed and processed curcumin are presented in figure 4.6. The work of cohesion and the work of adhesion between pulverised curcumin (2.5µm and 3.5µm) and α-lactose are illustrated in figure 4.7. The milled curcumin has shown a lower total free surface energy compared to the unprocessed materials. The dispersive components of micronized and the raw powder exhibit almost no changes as the raw curcumin has 38 mJ/m^2 whereas the micronized curcumin has 36 mJ/m^2 and 37 mJ/m^2 for particles of 3.5µm and 2.5µm (D_{50}), respectively. Polar surface energy was

reduced significantly after milling. A further reduction in non-dispersive energy was also noticed when the particles size of curcumin was further reduced. The analysed non-dispersive component of unprocessed curcumin was 16.0mJ/m^2 whereas the milled particles with D_{50} of 3.5µm and 2.5µm were 4.0mJ/m^2 and 0.98mJ/m^2, respectively. This reduction is attributed to particles agglomeration after comminution; also the further reduction attributed to extra particles agglomerations. This was confirmed by the SEM images in figure 4.3. It seems that the particles have agglomerated towards the polar surface sites, as it has more energy than non-polar sites of the particles surface which prevented the polar probes to interact with these sites, whereas the non-polar sites facing the outer surface. This finding is similar to the results reported on the surface energy of lactose, when the surface energy was measured after storage at 75% relative humidity for three months, there was increase in the polar surface energy and reduction in the dispersive energy. This was due to the interaction of the moisture with polar sites which prevented the polar probes to access the polar sites of the lactose, and hiding the nearer non-polar sites, which led to the reduction in the dispersive energy of lactose (Newell et al. 2001; Das et al. 2009).

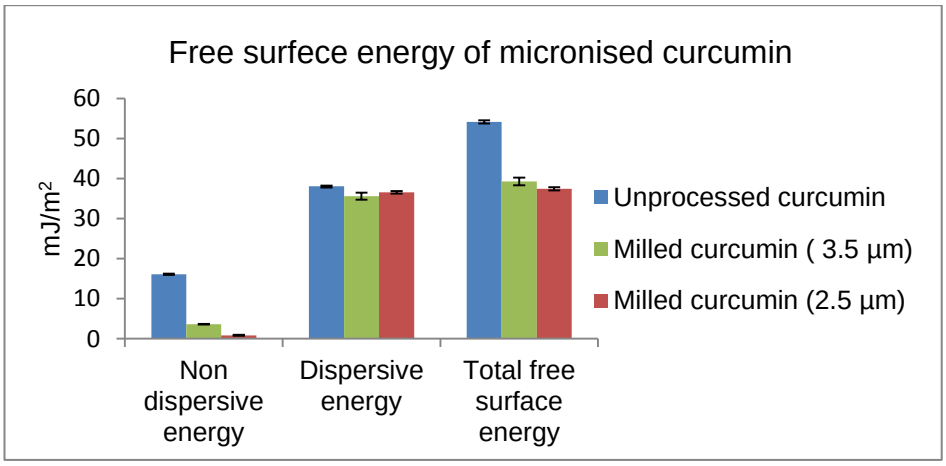

Figure 4.6 The non-dispersive (specific energy), dispersive and total free surface energy of unprocessed and milled curcumin particles with particle size.

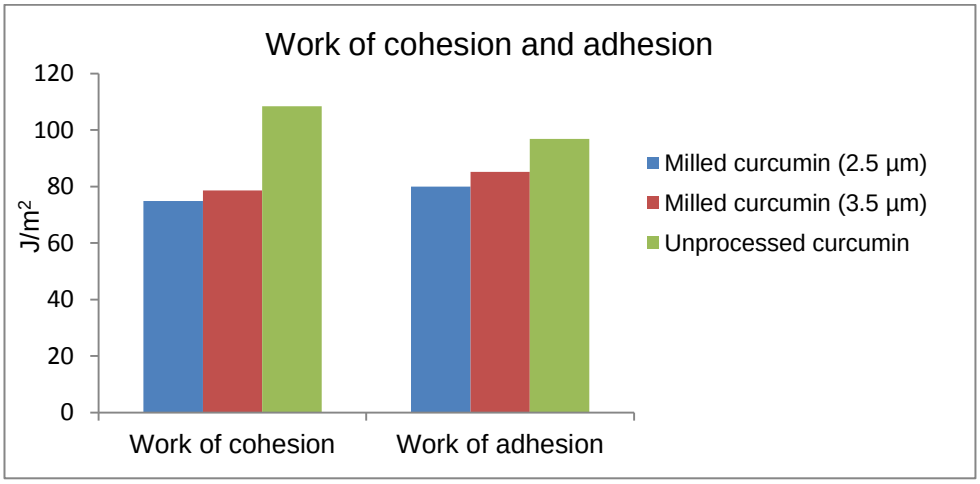

Figure 4. 7 The work of adhesion of unprocessed and milled curcumin particles, and work of adhesion of processed curcumin particles (2.5µm and 3.5µm) with α-lactose.

4.3.6. Dry powder inhaler preparations and Drug content uniformity

DPIs of curcumin (as mentioned in section 4.2.4) were prepared by blending each of processed curcumin particles (D_{50}=3.5µm and 2.5µm) with α-monohydrate lactose as a carrier (lactohale 201) at two ratios 1:9 and 1:67.5 curcumin:lactose (w/w). F1 and F2 are the DPIs formulations, which were prepared by using processed curcumin of D_{50} =3.5µm at ratio of 1:9 and 1:67.5

drug:carrier w/w, respectively. F3 and F4 are the DPIs formulations, which were prepared by using processed curcumin of D_{50}=2.5µm at ratio of 1:9 and 1:67.5 drug: carrier w/w, respectively.

The relative standard deviation (RSD%) for the drug content uniformity of F1 and F2 is presented in tables 4.3 and 4.4. The optimum mixing time was found to be 5 mins which was then used to assess the content uniformity of formulations F3 and F4 as shown in table 4.5.

Table 4.3 The mean relative standard deviation (RSD%) for the mixing content uniformity of micronized curcumin (D_{50}=3.5µm) with lactose at different times (n=3), F1 is DPI formulation 1, which contains 1:9, curcumin: lactose w/w.

RSD% of F1 (D_{50} 3.5µm, ratio 1:9)				
Time	1 min	5 mins	10 mins	30 mins
Bisdemethoxycurcumin	7.32	1.8	35.48	8.43
Demethoxycurcumin	7.21	1.62	35.08	8.35
Curcumin	7.22	2.2	34.55	8.78

Table 4.4 The mean relative standard deviation (RSD%) for the mixing content uniformity of micronized curcumin (D_{50}=3.5µm) with lactose at different times (n=3), F2 is DPI formulation 2, which contains 1:67.5, curcumin: lactose w/w.

RSD% of F2 (D_{50} 3.5µm, ratio 1:67.5)				
Time (min)	1 min	5 mins	10 mins	30 mins
Bisdemethoxycurcumin	8.36	2.45	4.08	5.83
Demethoxycurcumin	8.94	1.93	4.68	5.47
Curcumin	8.78	2.06	4.61	5.33

Table 4.5 The mean relative standard deviation (RSD%) for the mixing content uniformity of micronized curcumin (D_{50}=2.5µm) with lactose at 5 mins (n=3), F3&F4 are DPI formulations, which contain1:9 and 1:67.5, curcumin:lactose w/w, respectively.

RSD% of F3&F4 (D_{50} 2.5µm, ratios 1:9 &1:67.5)		
DPI formulations	F3	F4
Time (min)	5 mins	5 mins
Bisdemethoxycurcumin	3.06	2.7
Demethoxycurcumin	2.93	2.52
Curcumin	3.25	2.81

The results obtained from F1 have shown that the lowest value of RSD% is after 5 minutes of blending, whereas the highest value of RSD was after 30 minutes, which indicates that the drug and the lactose are not well uniform and getting separated. The values which were obtained after 1 and 30 minutes were

slightly close to each other; this shows the same degree of homogeneity for these samples. In F2, the lowest value of RSD percentage was for the sample blended for 5 minutes, which is closer to the results in F1.Therefore, the optimum mixing time was considered to be 5 minutes and this is because it has the lowest RSD value among the sample mixing time.

In F3 and F4, The RSD of blending was found to be 3.25% and 2.8% for curcumin, respectively. It is slightly higher than RSD% which was obtained for F1 and F2. This may be attributed to the high energy of the agglomerated particles of curcumin which was obtained from the further reduction in the particle size of curcumin (Ward and Schultz 1995; Taylor et al. 1999). This energy may have an effect on the de-agglomeration of particles on the lactose surface in mixing as well as during the inhalation process. Therefore, increasing the concentration of lactose may aid the drug particles to de-agglomerate and to distribute among the lactose itself.

Overall, the homogeneity profile of mixing of curcumin with α-lactose was slightly improved as the concentration of the curcumin related to lactose decreased (Ward and Schultz 1995; Taylor et al. 1999). The mixing profile showed that the most acceptable percentage RSD in the four DPI formulations was with the blending time of 5 minutes.

4.3.7. Aerodynamic characterisation of DPI of curcumin formulations

The aerodynamic characterisation of the DPI formulations of milled curcuminoids of particle size of (D_{50}) 3.5µm (F1&F2) and 2.5µm (F3&F4) are presented in tables 4.6 and 4.7, respectively. The drug mass distribution of both DPI formulations (D_{50} =3.5µm and 2.5µm) for the two ratio of drug-carrier (1:9 and 1:67.5) throughout the NGI stages is shown in figures 4.8, 4.9, 4.10 and

4.11, respectively. F1 & F2 are the formulations contained curcumin particles size of D_{50} =3.5µm for drug:carrier ratio of 1:9 and 1:67.5, respectively. F3 &F4 are the formulations contained curcumin particles size of D_{50} =2.5µm for curcumin:lactose ratio of 1:9 and 1:67.5, correspondingly.

The FPFs of F1 are 30.1%, 32.63% and 30.4%, whereas FPFs of F2 are 32.7%, 33.6% and 33.2% for bisdemethoxycurcumin, demethoxycurcumin and curcumin respectively. The MMAD of F1 was around 4.6µm whereas in F2 is about 4.0µm, it is clear that there is slight improvement in FPF and MMAD for F2 compared to F1. The FPF of the DPI formulations of F3&F4, for bisdemethoxycurcumin, bisdemethoxycurcumin and curcumin, are 36.0%, 34.6%, 36.5%, 39.5%, 38.9% and 38.0%, respectively. The MMAD of F3 was ranging from 3.36µm to 3.7µm, whereas in F4 was ranging from 3.2µm to 3.6µm.

Table 4.6 The aerodynamic parameters of DPI formulations (of curcumin particles (D_{50}=3.5µm) from easyhaler device at flow of 45 L/m for 5.5 second.

Aerodynamic parameters of curcuminoids DPI Formulations 1&2 (D0 3.5µm)				
Drug	Formulations	FPF%	MMAD (µm)	GSD
Bisdemethoxycurcumin	F1(1 to 9)	30.16	4.54	1.87
	F2 (1 to 67.5)	32.78	4.21	2.69
Demethoxycurcumin	F1 (1 to 9)	32.63	4.66	1.77
	F 2 (1 to 67.5)	33.68	3.94	2.31
Curcumin	F 1(1 to 9)	30.43	4.76	1.67
	F 1(1 to 67.5)	33.28	4.18	2.13

FPF% is fine particle fraction, MMAD is the mass median aerodynamic diameter, and GSD is the geometric standard deviation.

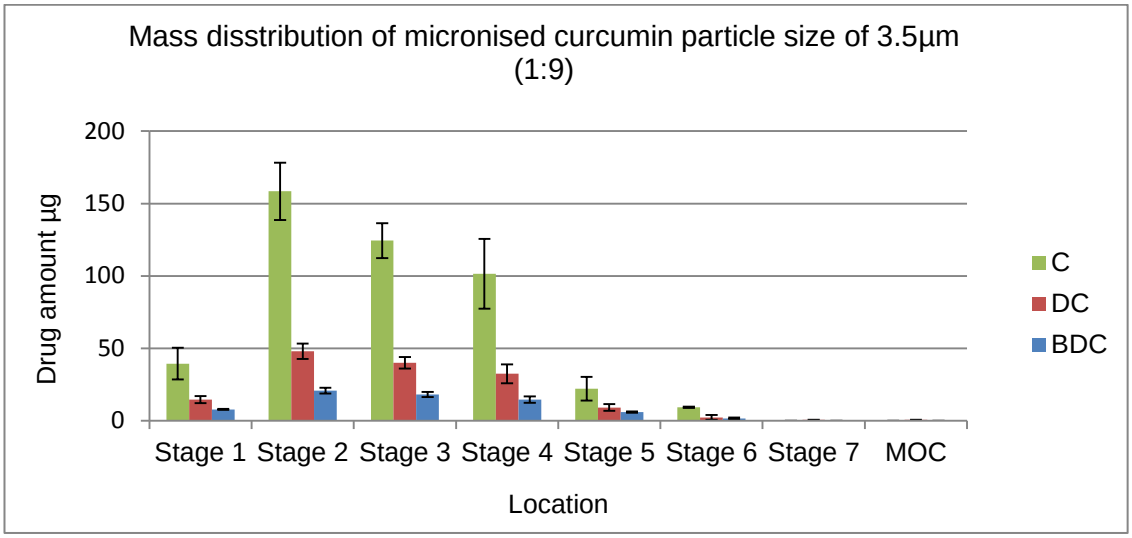

Figure 4. 8 Mass distribution DPI formulation (1:9 drug:carrier ratio) of curcumin particles (D_{50}=3.5µm) among NGI stages from easyhaler device at flow of 45 L/m for 5.5 second, C is curcumin, DC is demethoxycurcumin and BDC is bisdemethoxycurcumin.

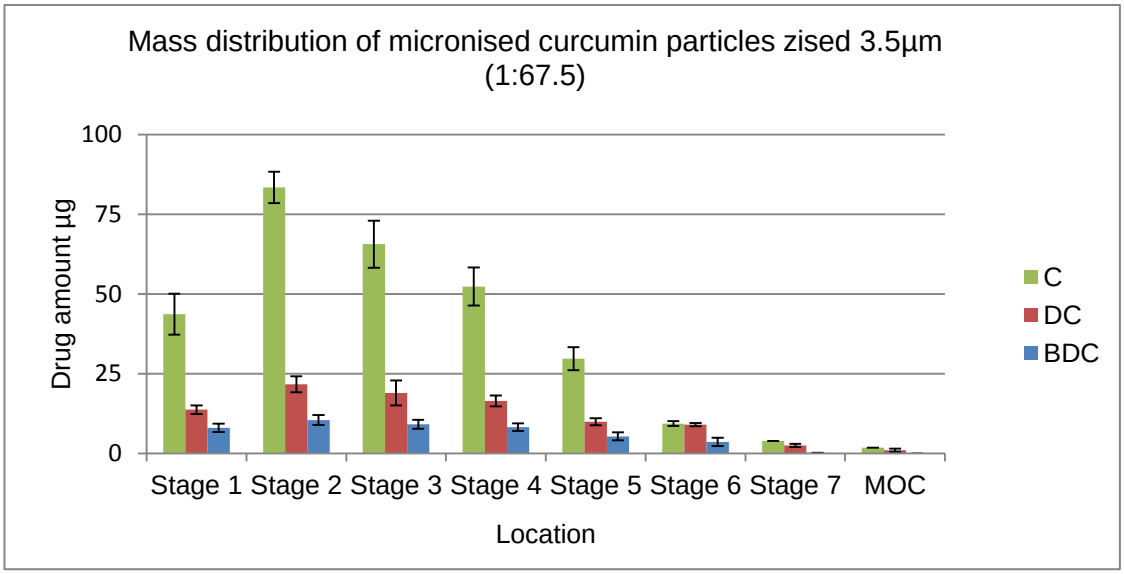

Figure 4. 9 Mass distribution DPI formulation (1:67.5 drug:carrier ratio) of curcumin particles (D_{50}=3.5µm) among NGI stages from easyhaler device at flow of 45 L/m for 5.5 second, C is curcumin, DC is demethoxycurcumin and BDC is bisdemethoxycurcumin.

Table 4.7 The aerodynamic parameters of DPI formulations (of curcumin particles (D_{50}=2.5µm) from easyhaler device at flow of 45 L/m for 5.5 second.

Aerodynamic parameters of curcuminoids DPI Formulations 3&4(D0 2.5µm)				
Drug	Formulations	FPF%	MMAD (µm)	GSD
Bisdemethoxycurcumin	F3 (1:9)	36.03	3.36	2.18
	F4 (1:67.5)	39.54	3.20	2.54
Demethoxycurcumin	F3 (1:9)	34.67	3.55	2.03
	F4 (1:67.5)	38.90	3.44	2.39
Curcumin	F3 (1:9)	36.52	3.79	2.29
	F4 (1:67.5)	38.00	3.66	2.05

FPF% is fine particle fraction, MMAD is the mass median aerodynamic diameter and GSD is the geometric standard deviation.

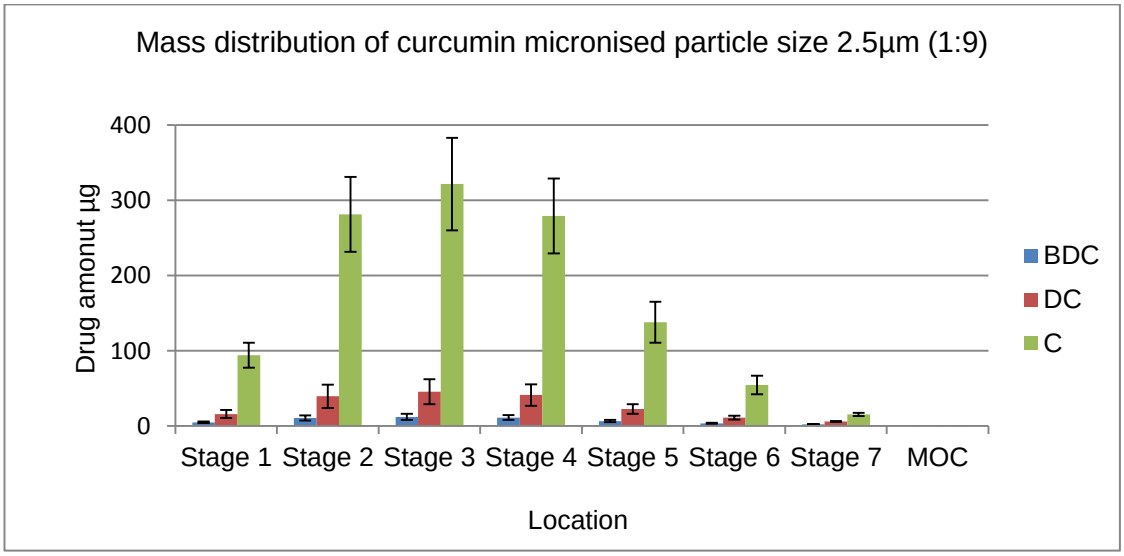

Figure 4. 10 Mass distribution DPI formulation (1:9 drug:carrier ratio) of curcumin particles (D_{50}=2.5µm) among NGI stages from easyhaler device at flow of 45 L/m for 5.5 second, C is curcumin, DC is demethoxycurcumin and BDC is bisdemethoxycurcumin.

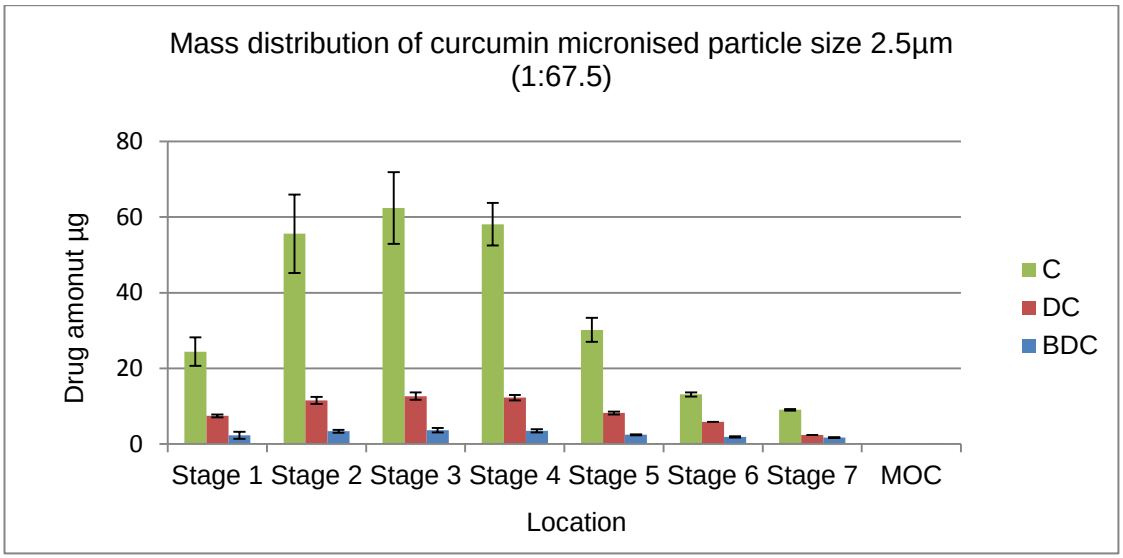

Figure 4. 11 Mass distribution DPI formulation (1:67.5 drug: carrier ratio) of curcumin particles (D_{50}=2.5µm) among NGI stages from easyhaler device at flow of 45 L/m for 5.5 second, C is curcumin, DC is demethoxycurcumin and BDC is bisdemethoxycurcumin.

The results of both formulations, with different particle size, have shown that the low drug concentration (1:67.5 drug: lactose) has a slight improve in the FPF% and MMAD. This enhancement in the performance of the DPI preparation ,of the drug: lactose ratio 1:67.5, is resulted from the reduction in the formation of the agglomeration drug particles in the formulation as the drug has an opportunity to disperse more among the carrier surface (Steckel and Muller 1997). This finding is in agreement with a reported study on the effect of the drug concentrations on the FPF of the DPI preparation of budesonide, which showed that as drug concentration increased from 1% to 5% and 9%, the FPF of budesonide reduced from 32% to 21% (Steckel and Muller 1997). Also, other studies, on budesonide and salmeterol xinafoate, have demonstrated the same findings concluded that low drug concertation produces higher FPF% (Harjunen et al. 2003; Adi et al. 2008). In addition, this could be explained from the IGC results (Figure 4.6 & 4.7), which has shown the work of cohesion of

unprocessed curcumin particles higher than work of adhesion between curcumin and lactose. Therefore, the effect of agglomeration between drug particles is more pronounced and hence it is difficult to disperse (Ganderton 1992; Steckel and Muller 1997; Adi et al. 2008).

The formulations with a lower particles size of 2.5µm (D_{50}) have illustrated a better inhalation performance compared to curcumin particle size of 3.5µm (D_{50}). The variation between two DPI formulations is attributed to the alteration in the particle size of the curcumin particles, also the formulations with lower particles size have a D_{90} of 5.5µm compared to 7.7µm for formulations with larger particle size. It is reported that the particles above than 5µm will deposit on the throat (Telko and Hickey 2005), therefore the formulations with large particle size demonstrated lower FPF compared to those with 2.5µm particle size.

It is clear from the mass distribution that the formulations with particle size of 2.5µm has more ability to penetrate into both lung zones (central and peripheral zone) which is corresponding to stages 3,4 and 5 of the NGI. Therefore, the formulations with curcumin particles size of 2.5µm (D_{50}) could be more appropriate to target the lung cancer cells that are located in the central or peripheral zone. This is because these formulations showed superior performance with higher FPF%. Also more penetration to lung zones was observed with preparation with the smaller particles.

4.4. Conclusion

In the summary, the air jet milling is a simple and suitable method for inhalable curcumin particles production. In this milling technique, the grinding pressure was more predominant on particles size reduction, therefore, grinding pressure

was kept as low as possible to reduce the mechanical energy applied to the particles and to avoid the polymorphic transformation of the compounds. The thermal analysis and XRPD confirmed that the particles obtained have polymorph1 as in unprocessed materials. The free surface energy of comminuted particles was found to be lower than the unprocessed one; this is because of the reduction on the polar surface energy of agglomerated particles.

The inhalation profile of the DPI formulations which contains curcumin particles with size of 2.5µm (F3 &F4) illustrated better performance compared to formulations with particles size of 3.5µm (F1&F2). The aerodynamic parameter values (FPF%), in F3 and F4, is similar to the published studies. The simple approach as well as no excipients was involved in the production of the curcuminoids particles was an advantage of this study compared to the published one. This makes this work safer and more suitable for respiratory system. Another advantage is that the aerodynamic parameters of curcuminoids components, curcumin (C), demethoxycurcumin (DC) and bisdemethoxycurcumin (BDC) were individually assessed.

CHAPTER FIVE

Sonocrystallisation of Curcuminoids for Inhalation Application

Chapter 5: Sonocrystallisation of curcumin for inhalation application

5.1. Introduction

Ultrasound is a cycle of sound waves which are not detectable by human ears, and this is because it has a frequency greater than the upper limit of human hearing (Leonelli and Mason 2010). Ultrasound (with frequency 20 to 100 KHz) has been used to induce physical and chemical changes in materials (Richards and Loomis 1927; Leonelli and Mason 2010).

The application of ultrasound energy to crystallisation is known as sonocrystallisation (Chen et al. 2011). The main mechanism of sonocrystallisation is cavitation (Suslick 1998; Bund and Pandit 2007; Leonelli and Mason 2010); this cavitation can be either stable or transient. The stable one is associated with small bubbles dissolved in a liquid, whereas the transient cavitation occurs when the bubble size is expanded further and collapses, and as a result locally produces very high pressure (100 MPa) and high temperature (5,000 K) with heat cool rate of 10^{10} K/s (Suslick 1998; McNamara et al. 1999; De Castro and Priego-Capote 2007; Deora et al. 2013). Therefore, during sonocrystallisation, nucleation is initiated at higher temperatures and at the lowest level of supersaturation and in shorter times, which result in more uniform and smaller crystals with narrower size distribution (Guo et al. 2005; Li et al. 2006; Chen et al. 2011).

The particles produced by ultrasound have shown to be suitable for inhalation application and it has been presented to have a superior aerodynamic behaviour over spray dried and milled particles (Abbas et al. 2007; Dhumal et al. 2009). This has been attributed to the smoothness of the sonocrystallised particle surface and the reduction in the cohesive and adhesive forces and also

due to the uniform shape and the narrower particle distribution (Dhumal et al. 2009).

Curcumin polymorph controlled by ultrasound have been recently published (Thorat and Dalvi 2015; Thorat and Dalvi 2016), and it has shown the ability of the ultrasound in production of curcumin particles within 5µm (Thorat and Dalvi 2014). However, this report has not studied the application of these particles for inhalation and has not reported any aerodynamic profile of curcumin particles by sonocrystallisation and also they have not examined the surface energy of the produced particles.

In this chapter, ultrasound is used to obtain a suitable particle of curcumin for inhalation with different cohesive and adhesive energy, therefore different solvents and antisolvents were used (ethanol, isopropanol, acetone, water and heptane). The solid state of the produced particles was characterised using differential scanning calorimetry (DSC) and X-ray powder diffraction (XRPD). The micrometric properties such as particle size and shape were determined using laser diffraction and a scanning electron microscope, respectively. The cohesive, adhesive and surface energy of the processed particles were examined using inverse gas chromatography (IGC). The dry powder inhaler of curcumin was prepared by mixing the sonocrystallised particles with α-lactose monohydrate as a carrier; aerosol performance of the DPI was then tested using a next generation impactor (NGI). The aerodynamic profile (FPF,MMAD and GSD) of curcumin, demethoxycurcumin and bisdemethoxycurcumin has been reported in this work.

5.2. Methods

5.2.1. Sonocrystallisation of curcumin

A supersaturation solution of curcuminoids was prepared in different organic solvents (ethanol, isopropanol and acetone) by adding an extra amount of curcuminoids into the solvents, and then the solvent temperature was increased accordingly (in ethanol increased to 60ºC, in isopropanol increased to 70ºC and in acetone to 45ºC). The solvents were filtered before their use, in crystallisation; to remove any insoluble curcumin particles. The antisolvent (water 80ml) was placed in jacket vessels with a control temperature at 5ºC using a circulating water bath. The ultrasound probe was immersed in the antisolvent and the ultrasound power and timer were set before staring the process. Once curcumin solution (20ml) was added into the antisolvent, the ultrasound power was switched on. The experimental parameters (times and ultrasound amplitude) were shown in tables 5.1, 5.2, and 5.3. The water antisolvent was replaced by heptane, and the setting parameters of the experiment are shown in table 5.4. The precipitated curcuminoid particles were collected using a filter paper and left to dry at room temperature for characterisations.

Table 5.1 Parametrs of sonocrystallisation of curcumionds from ethano and water

Sonocrystallisation from ethanol-water						
Code	Sono1	Sono2	Sono3	Sono4	Sono5	Sono6
Time (min)	5	5	5	5	1	3
Ultrasound amplitude%	25	50	75	100	50	50

Table 5.2 Parameters of sonocrystallisation of curcuminoids from isopropanol and water

Sonocrystallisation from isopropanol-water						
Code	Sono7	Sono8	Sono9	Sono10	Sono11	Sono12
Time (min)	5	5	5	5	1	3
Ultrasound amplitude%	25	50	75	100	50	50

Table 5.3 Parameters of sonocrystallisation of curcuminoids from acetone and water

Sonocrystallisation from acetone-water			
Code	Sono13	Sono14	Sono15
Time (min)	0.5	1	3
Ultrasound amplitude%	50	50	50

Table 5.4 Parameters of sonocrystallisation of curcuminoids using different solvent and heptane as antisolvent

Sonocrystallisation using heptane as antisolvent			
Code	Sono16	Sono17	Sono18
Time (min)	1	1	1
Ultrasound amplitude%	50	50	50
Curcumin solvent	Ethanol	Acetone	Isopropanol

5.3. Results and discussion

5.3.1. Particle size analysis using laser diffraction

The particle size, of sonocrystallised curcumin from each solvent, was measured using laser diffraction. The data are shown in tables 5.5, 5.6, 5.7 and 5.8.

- Particles precipitated from ethanol-water

Table 5.5 shows the particle size of sonocrystallised curcumin using ethanol as organic solvent and water as an antisolvent.

Table5.5 The mean size and the standard deviation (n=3) of the sonocrystallised curcumin particles which precipitated from ethanol and water.

	Code	D_{10} µm +/-std	D_{50} µm +/-std	D_{90} µm +/-std
Sonocrystallisation from ethanol-water	Sono1	0.75 +/- 0.01	1.65 +/- 0.02	4.07 +/- 0.32
	Sono2	0.75 +/- 0.01	1.59 +/- 0.01	3.50 +/- 0.02
	Sono3	0.82 +/- 0.09	2.26 +/- 0.48	11.54 +/- 5.36
	Sono4	0.73 +/- 0.01	1.62 +/- 0.01	4.37 +/- 0.22
	Sono5	0.71 +/- 0.07	1.64 +/- 0.03	4.78 +/- 0.52
	Sono6	0.62 +/- 0.08	1.54 +/- 0.10	18.68 +/- 23.85

Effect of ultrasound amplitude and ultrasound time on the particle size of curcuminoids has been investigated. Different amplitudes (25%, 50%, 75% and 100%) were applied during the sonocrystallisation, the results show no difference between the low and high amplitude of the ultrasound on the particle

size of curcuminoids, this could be attributed to the fact that the supersaturation level is dominant over the sonication irradiation and the cavitation worked here as a high efficiently mixer, which increases the mass transfer and diffusion between the solvents and the antisolvents (Miyasaka et al. 2006), which in turn leads to homogenise and rapid nucleation (Guo et al. 2005; Abbas et al. 2007; Dhumal et al. 2009). The sonocrystallisation has been reported to be more effective during crystallisation at lower level of drug concentrations (Guo et al. 2005; Miyasaka et al. 2006).

Also, the period of sonication suggests that the particle size of curcumin at 1 min (sono5) is similar to particle size at 5 mins (sono3), thus, sonication for 1 min provides sufficient micro mixing during crystallisation to enhance the nucleation and to produce a small crystal. The particle size (D_{90} and D_{50}) is smaller than 5µm which suggests its suitability for inhalation. However, during drying using filter paper, the particle forms cake, this is due to the particles compacting on each other through filtration and due to their size, and also may be due to a long period of drying as the water has low volatility compared with organic solvents, as the particles are kept in contact with each other in the presence of water–ethanol throughout drying.

- Particles precipitated from isopropanol-water

Table 5.6 shows the particle size of sonocrystallised curcumin using isopropanol as organic solvent and water as antisolvent.

Table5. 6 The mean size and the standard deviation (n=3) of the sonocrystallised curcumin particles which precipitated from isopropanol and water.

	Code	D_{10} µm +/-std	D_{50} µm +/-std	D_{90} µm +/-std
Sonocrystallisation from isopropanol-water	Sono7	0.51 +/- 0.01	1.25 +/- 0.04	4.00 +/- 0.34
	Sono8	0.57 +/- 0.04	1.50 +/- 0.23	5.38 +/- 0.14
	Sono9	0.61 +/- 0.04	1.45 +/- 0.01	3.83 +/- 0.36
	Sono10	0.64 +/- 0.00	1.44 +/- 0.01	3.38 +/- 0.07
	Sono11	0.59 +/- 0.05	1.46 +/- 0.25	4.22 +/- 0.37
	Sono12	0.68 +/- 0.02	1.83 +/- 0.14	9.72 +/- 1.06

Changing the organic solvent (from ethanol to isopropanol) during sonocrystallisation of the curcuminoids has not shown any further reduction in particle size of the curcumin.

The range of ultrasound amplitude has been examined in order to determine their effect on the size reduction of curcumin. The data indicates that the increase in the amplitude from 25% to 100% (for a period of time of 5 mins) has no further decrease in the particle size. Also, the effect of the sonication time has been tested; the results present that the sonocrystallisation of curcumin for 1 min gives a similar particle size (D_{50}) to those particles obtained after 5 mins. These findings could suggest that sonocrystallisation at low amplitude and for a short period of time at high supersaturation levels are able to produce a particle below 5µm. The production of small particles during sonocrystallisation using a supersaturation solvent is attributed to the fact that the ultrasound irradiation produces an intensified micro mixing by cavitation bubbles, which in turn leads

to an enhanced mass transfer and diffusion rate between the solvents and the antisolvents , and thus enhances a high supersaturation level, which results in rapid nucleation (Li et al. 2006; Miyasaka et al. 2006). As the number of nuclei increases, the amount of the solute on each nucleus decreases; hence the particle size of the final crystals is reduced (Louhi-Kultanen et al. 2006).

It is noticeable that at a at shorter time (1 min) of sonication was enough to induce rapid nucleation and reduce the crystal growth of the particles and a complete release of the supersaturation has occurred within 1 min, therefore increasing the sonication time has not shown any further change in the particle size.

- Particle precipitated from acetone-water

Table 5.7 shows the particle size of sonocrystallised curcumin using acetone as organic solvent and water as antisolvent.

Table 5.7 The mean size and the standard deviation (n=3) of the sonocrystallised curcumin particles which precipitated from acetone and water.

	Code	D_{10} µm +/-std	D_{50} µm +/-std	D_{90} µm +/-std
Sonocrystallisation from acetone-water	Sono13	0.82 +/- 0.06	2.30 +/- 0.28	10.05 +/- 3.92
	Sono14	0.62 +/- 0.06	1.33 +/- 0.01	3.08 +/- 0.48
	Sono15	0.47 +/- 0.07	1.24 +/- 0.05	4.33 +/- 1.09

The sonication time has been reduced to start from 30 second up to 3 mins, and the amplitude has been set to 50%, as the results from previous data (ethanol and isopropanol) have illustrated that sonication for a short period of time is enough to produce an inhalable particle size. The data have shown an increase

in the particle size when the sonocrystallisation was conducted for 30 seconds, but no alteration in particle size when it was carried out at 1 min and 3 mins. The higher particle size at 30 seconds illustrates that a rapid nucleation occurs and then is followed by crystal growth and agglomeration; this means the ultrasound at 30 seconds was not enough to reduce the crystal growth and to allow a complete liberation of the supersaturation to occur as it does at 1 min. Therefore, the optimum condition was considered to be 50% amplitude for 1 min. The variation in particle size of D_{90} between sono12 and sono13 and sono14 is due to cake formation during drying by filtration.

The particle size obtained from ethanol, isopropanol and acetone at 1 min and 3 mins and 5 mins (in case of ethanol and isopropanol) is very similar and there is no big variance between them. In terms of particle size, it could be concluded that sonocrystallisation is independent of the organic solvent of the solute to obtain inhalable particles.

Drying the processed particles using an ordinary filtration technique like filter paper, is a slow procedure of removing the solvent and the antisolvent from the product, in turn leads to cake formation of the particles. If these cakes do not disperse during mixing with lactose it will produce heterogeneous distribution of the drug in the formulation, which is not suitable for inhalation. Therefore, the antisolvent was replaced with another one with higher vapour pressure and less polar than water to prevent a long contact between the crystal particles with solvents and the antisolvent during filtration and the drying process of the product, which will reduce the possibility of having hard cake particles. Choosing the second antisolvent with no polarity properties (or less polar than water) helps to modify the surface energy of the produced particle. The water

antisolvent was replaced by heptane and three experiments were processed at 50% amplitude and for 1 min sonication.

- Particles precipitated from ethanol, isopropanol, acetone and heptane

Table 5.8 shows the particle size of sonocrystallised curcumin using ethanol, isopropanol and acetone as organic solvents and heptane as an antisolvent.

Table 5. 8 The mean size and the standard deviation (n=3) of the sonocrystallised curcumin particles which precipitated from different solvents and heptane.

	Code	D_{10} µm +/-std	D_{50} µm +/-std	D_{90} µm +/-std
Sonocrystallisation using heptane as antisolvent	Sono19	0.91 +/- 0.01	2.49 +/- 0.05	5.47 +/- 0.21
	Sono20	0.73 +/- 0.01	2.40 +/- 0.06	8.92 +/- 0.47
	Sono21	0.72 +/- 0.11	2.37 +/- 0.05	11.54 +/- 0.02

Replacing water (anti-solvent) by heptane using the optimum conditions which were obtained previously (time 1 min and amplitude 50%). The sonication time is for 1 min and the amplitude is 50%, these conditions produced a suitable particle size for inhalation and there was no need to increase sonication time or power of the ultrasound. However, the particle size of curcuminoids shows some increase in their size when heptane was used. This is because the heptane is volatile during sonication and thus increases the level of the supersaturation and therefore the effect of nucleation by supersaturation becomes more prominent over that of sonication. However, the crashing out of the crystals at concentrations above supersaturation is controlled by both supersaturation nucleation and sonication driving forces (Abbas et al. 2007; Dhumal et al. 2009). The D_{50} is 2.5µm in the heptane system, whereas it was

1.5µm in the water system. D_{90} is 5.4µm when ethanol-heptane (sono19) system was used, which is close to those particles produced by ethanol (sono5), isopropanol (sono11) and acetone-water (sono14) system. The D_{90} for both sono20 and sono21 was higher than sono19, and so higher than those produced from isopropanol-water (sono11) and acetone water (sono14) system.

These findings indicate the ability of the ultrasound to produce a small particle size of curcuminoids within short period of time and even with low amplitude. Furthermore, the sonocrystallisation technique could be a drug solvent independent, as the inhalable particles of the drugs was obtained using three different organic solvents.

5.3.2. Morphology of sonocrystallised curcumin particles using scanning electron microscope (SEM)

The morphology (particle shape) of sonocrystallised curcumin were analysed using SEM. The particle shapes vary depending on the curcumin organic solvent during sonocrystallisation as well as the time of the sonication process.

Figure 5.1 (from sono1 to sono4) shows the SEM images of curcumin particles precipitated using ethanolic curcumin solution and water antisolvent at different applied amplitude (25% to 100%) for 5 mins. The particles exhibit a long plate-like shape. The edge ends of these particles look to be broken down later, which could be as a result of long sonication time (5 min). The SEM images of sono5 and sono6 particles, which are processed at less time of sonication (1 and 3 mins); seem to have different particle morphology. In sono5, a dendritic morphology could be seen. Each particle is composed of a stem–like in the middle from which branches originate, it can be seen that a break occurs in this stem to give a hand shape with its branches and each branch has a needle

structure. This structure/shape (stem–like) has been reported by Alpha without using ultrasound. Therefore, this break could be attributed to sonication energy. These particles have probably started from the middle (stem) point and are then stretched by a secondary nucleation to grow on each side of that stem to form branches (Thorat and Dalvi 2014). In sono6, a rice seed-like shape of curcumin particles could be seen, also this particle shape was reported and it is attributed to that curcumin particle that is made of several layers which are fused by time (Thorat and Dalvi 2014). It seems that sonocrystallisation for a long time (such as 5 mins) has broken down the already formed particles at early stage of precipitations (1 min or 3 mins). It is likely that the curcumin particles have been formed within 3 mins of time and any extra time of ultrasound breaks these particles, which gives them a different shape and plates with irregular edges too as is shown in sono1, 2, 3 and sosn4. This theory was reported by (Dhumal et al. 2009; Chen et al. 2011) that sonocrystallisation could further reduce the particles size (which in turn changes the particle's shape) of formed particles. This hypothesis has also been examined in this work, by precipitating curcumin particles from ethanol-water with absence of the ultrasound, after completion of the precipitation, a gentle sonication (using a sonication bath) was applied into these particles. The SEM images are shown in figure 5.2 and named as after and before sono. It is clear that particle shapes have been modified from long rectangular plates (at zero time) to a square plate by increasing the sonication time to 15 mins.

The results of SEM images of curcumin particles produced using isopropanol solvent are presented in figure 5.1 (sono7, 8, 9, 10, 11 and sono12). The morphology of the particle has shown some changes compared to the one that produced from ethanol solvent. The particles, at power of amplitude from 50%

to 100% for a period of 5 mins process, look like a fusiform muscle as they are wider in the middle and tapered toward the end with small branches at each end. The particle shape of curcumin, at power 25% for 5 mins, look like spindles (they are wider in the middle and narrower at each end with no further branches). The fusiform shape was observed in curcumin particles, which are sonocrystallised for a different period of time too (1, 3 mins), these particles also have small branches on each edge of the particles. It seems these branches are an extension of the single groups of particles arranged (fused) on tope to each other (Thorat and Dalvi 2014).

The SEM results of the curcumin particles obtained from acetone curcumin solution are presented in figures 5.1, sono13, 14 and sono15. The particle shapes with less time of sonication (i.e. 30 sec; sono13) seem to be less uniform in their shape, as they look like a long wide plate with a smaller break on too. The morphology of curcumin particles at longer time process, (time 1 and 3 mins which represent sono14 and 15, respectively), also has a plate like structure, which are further broken down to a smaller one.

Interesting changes in the curcumin morphology were observed when heptane was used as an antisolvent. Figures 5.1 of sono16, sono17 and sono18 are illustrated with curcumin particle shapes produced from ethanol, acetone and isopropanol, respectively. SEM images of particles obtained from ethanol and acetone solvents present plate morphology of curcumin particles with more elongation when acetone solvent is used. More interestingly, a flower shape was observed when isopropanol was used. It is noticed that in both solvents (ethanol and acetone), the crystal particle has been broken down during sonication, but not in the case of isopropanol, this indicates a faster crystal growth is obtained and the particles crashed out later, whereas in isopropanol a

slow crystal growth was gained. This could be attributed to the higher viscosity of isopropanol compared to both acetone and ethanol.

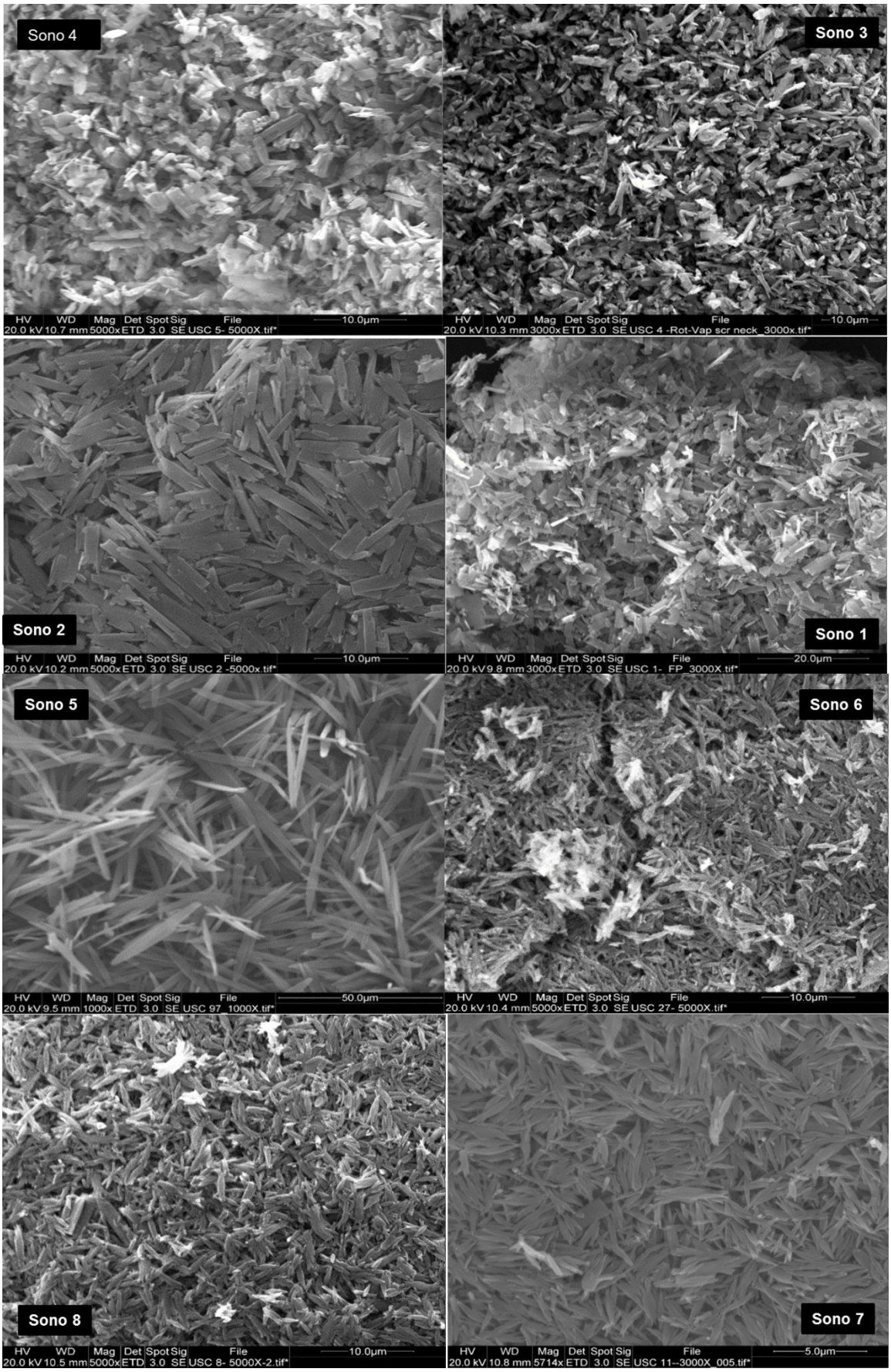
Sono 4
HV WD Mag Det Spot Sig File 10.0µm
20.0 kV 10.7 mm 5000x ETD 3.0 SE USC 5- 5000X.tif*
Sono 3
HV WD Mag Det Spot Sig File 10.0µm
20.0 kV 10.3 mm 3000x ETD 3.0 SE USC 4 -Rot-Vap scr neck_3000x.tif*
Sono 2
HV WD Mag Det Spot Sig File 10.0µm
20.0 kV 10.2 mm 5000x ETD 3.0 SE USC 2 -5000x.tif*
Sono 1
HV WD Mag Det Spot Sig File 20.0µm
20.0 kV 9.8 mm 3000x ETD 3.0 SE USC 1- FP_3000X.tif*
Sono 5
HV WD Mag Det Spot Sig File 50.0µm
20.0 kV 9.5 mm 1000x ETD 3.0 SE USC 97_1000X.tif*
Sono 6
HV WD Mag Det Spot Sig File 10.0µm
20.0 kV 10.4 mm 5000x ETD 3.0 SE USC 27- 5000X.tif*
Sono 8
HV WD Mag Det Spot Sig File 10.0µm
20.0 kV 10.5 mm 5000x ETD 3.0 SE USC 8- 5000X-2.tif*
Sono 7
HV WD Mag Det Spot Sig File 5.0µm
20.0 kV 10.8 mm 5714x ETD 3.0 SE USC 11--3000X_005.tif*

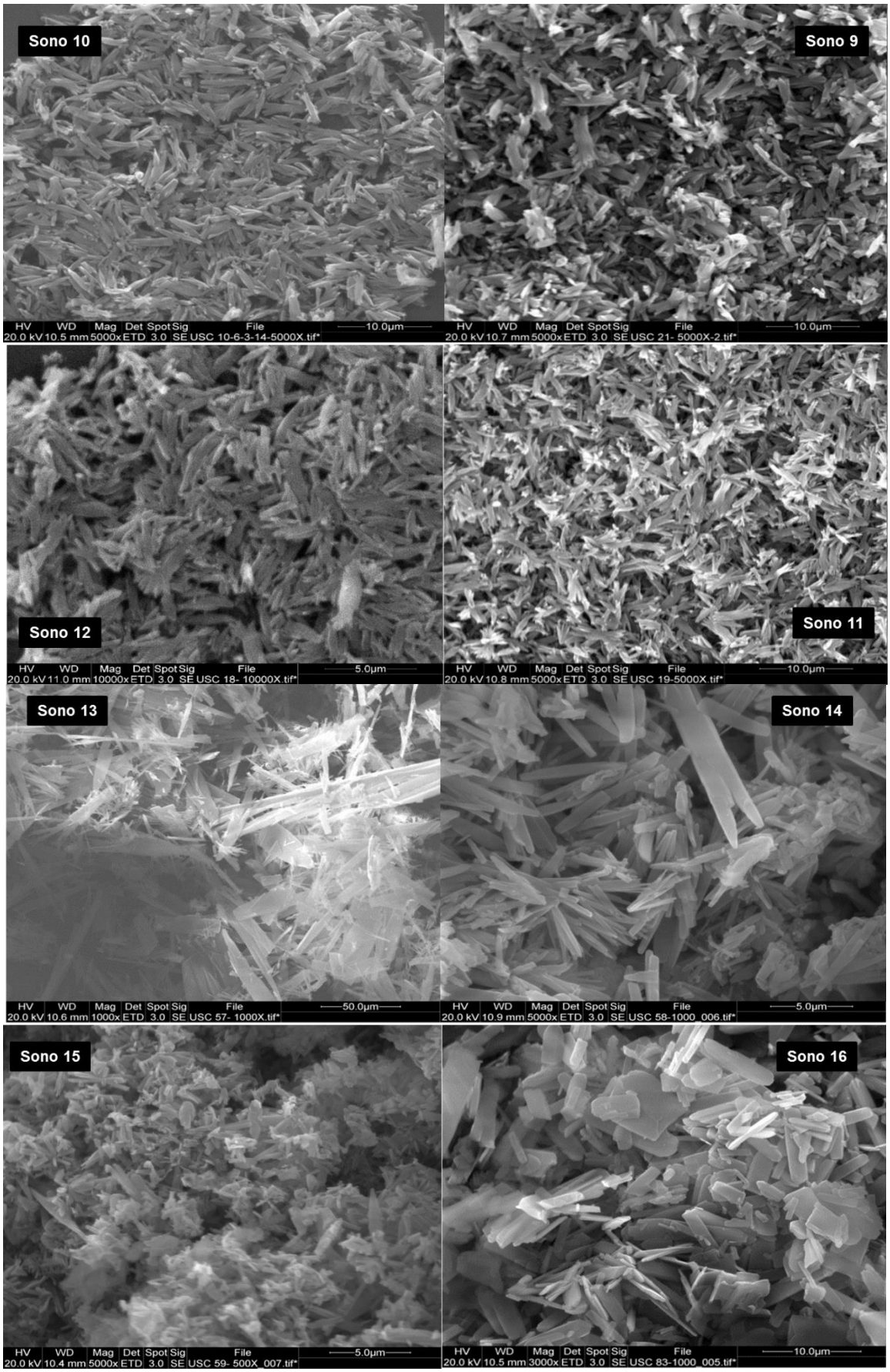
Sono 10
HV WD Mag Det Spot Sig File
20.0 kV 10.5 mm 5000x ETD 3.0 SE USC 10-6-3-14-5000X.tif*
10.0µm
Sono 9
HV WD Mag Det Spot Sig File
20.0 kV 10.7 mm 5000x ETD 3.0 SE USC 21- 5000X-2.tif*
10.0µm
Sono 12
HV WD Mag Det Spot Sig File
20.0 kV 11.0 mm 10000x ETD 3.0 SE USC 18- 10000X.tif*
5.0µm
Sono 11
HV WD Mag Det Spot Sig File
20.0 kV 10.8 mm 5000x ETD 3.0 SE USC 19-5000X.tif*
10.0µm
Sono 13
HV WD Mag Det Spot Sig File
20.0 kV 10.6 mm 1000x ETD 3.0 SE USC 57- 1000X.tif*
50.0µm
Sono 14
HV WD Mag Det Spot Sig File
20.0 kV 10.9 mm 5000x ETD 3.0 SE USC 58-1000_006.tif*
5.0µm
Sono 15
HV WD Mag Det Spot Sig File
20.0 kV 10.4 mm 5000x ETD 3.0 SE USC 59- 500X_007.tif*
5.0µm
Sono 16
HV WD Mag Det Spot Sig File
20.0 kV 10.5 mm 3000x ETD 3.0 SE USC 83-1000_005.tif*
10.0µm

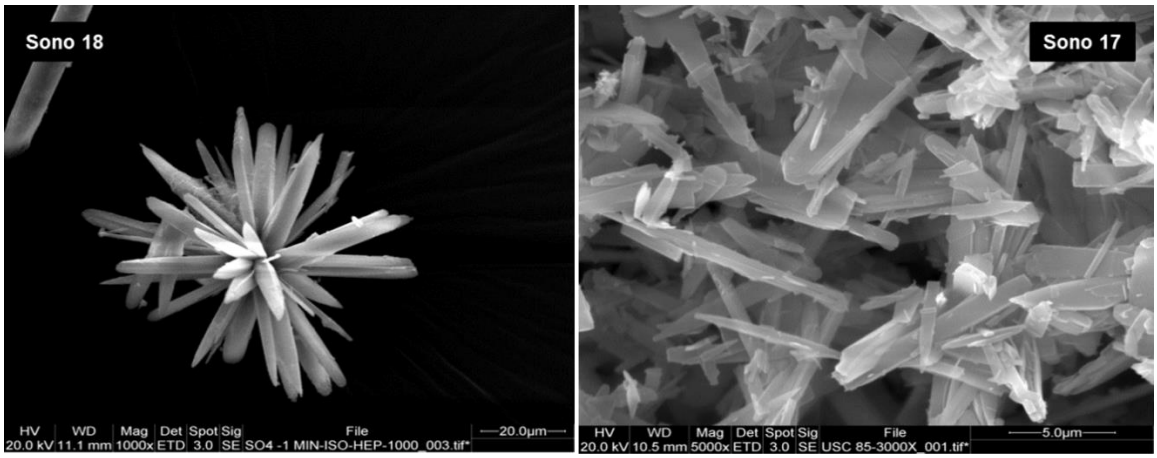

Figure 5.1 SEM images of sonocrystallised curcumin particles which precipitated from different organic solvents with water and heptane.

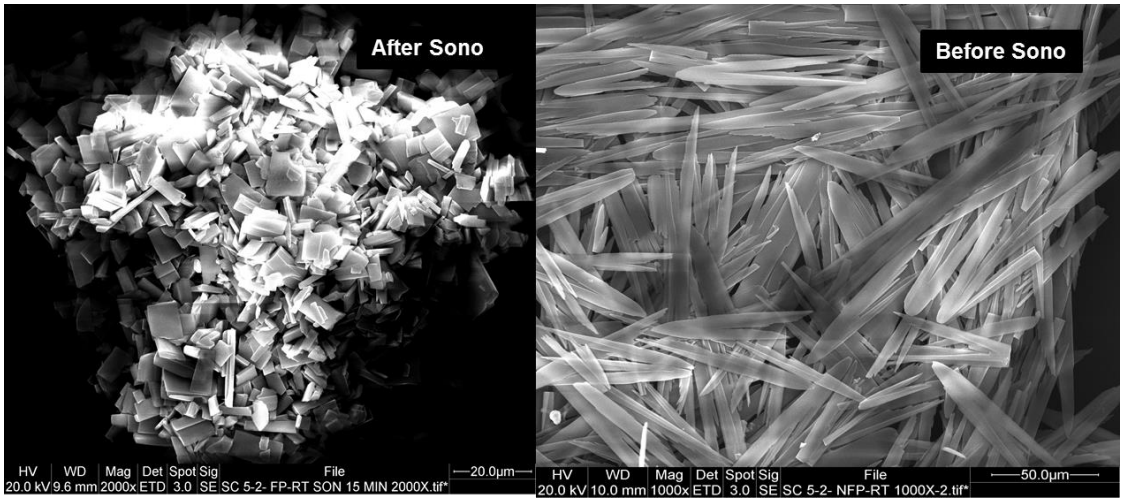

Figure 5. 2 SEM images of curcumin particles which precipitated from ethanol and water without ultrasound. *Before-sono is the curcumin particles prepared without ultrasound,*After-sono is the formed particles sonicated for 15 minutes.

5.3.3. Differential scanning calorimetry (DSC)

Differential scanning calorimetry (DSC) was used to examine any changes in the melting point of the curcumin particle prepared by ultrasound compared to unprocessed material. The unprocessed curcumin particle has an endothermic peak at 175ºC (Sanphui et al. 2011; Liu et al. 2015), which represents the melting point of curcumin polymorph 1 as is shown in chapter 4.

DSC results of sonocrystallised curcumin particles, which were produced by using ethanol curcumin and water as an antisolvent (from sono1 to sono6), are presented in figures 5.3 & 5.4 and table 5.9. The results illustrate one endothermic peak of sonocrystallised curcumin particles, which represent the melting temperature of curcumin form 1 (Thorat and Dalvi 2015). The DSC data indicates no effect of different amplitude of ultrasound on the melting point of the formed particles, as well as the time of sonication.

Table 5. 9 Endothermic peak temperature for precipitated curcumin particles from ethanol-water.

Sample code	Endothermic peak temperature ºC
Sono1	174
Sono2	176
Sono3	176
Sono4	173
Sono5	175
Sono6	179

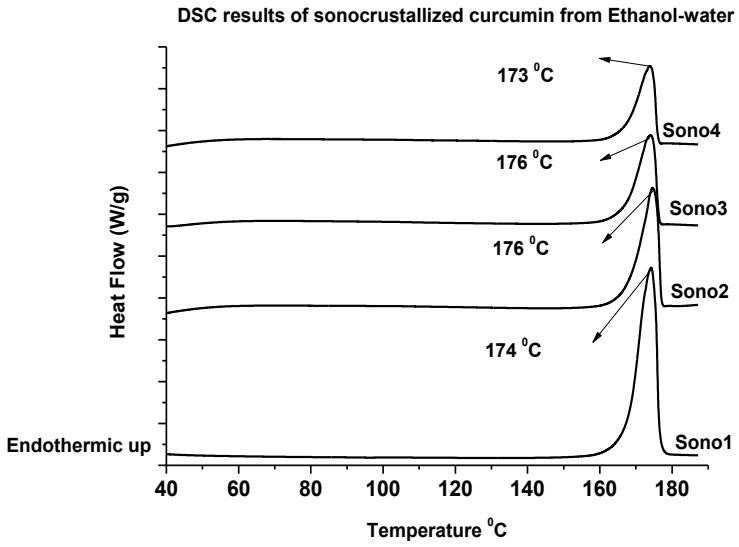

Figure 5. 3 DSC thermograms of precipitated curcumin particles from ethanol-water at different ultrasound amplitude

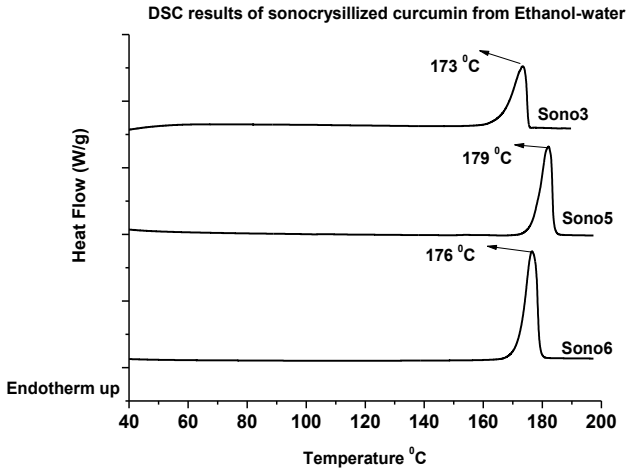

Figure 5.4 DSC thermograms of precipitated curcumin particles from ethanol-water at different sonication time

The DSC data of sonocrystallised curcumin particles, which are produced from isopropanol solvents and water as antisolvents (from sono7 to sono12), are shown in figure 5.5 and 5.6 and the average endothermic melting temperature (n=3) in table 5.10. DSC thermograms present two peaks; the presence of multiple melting peaks is usually associated with polymorphic transformation (Giron 2001; Maher et al. 2012; Thorat and Dalvi 2015). Therefore, the first endothermic peak is around 160ºC, and the second at 177ºC. The former peak is attributed to a polymorph transformation of curcumin particles from form 3 to form 1, and the second peak corresponds to the melting peak of curcumin form 1 (Thorat and Dalvi 2015). This polymorphic transformation was observed in all curcumin samples at either different sonication times or variations of sonication amplitude (sono7 to sono12).

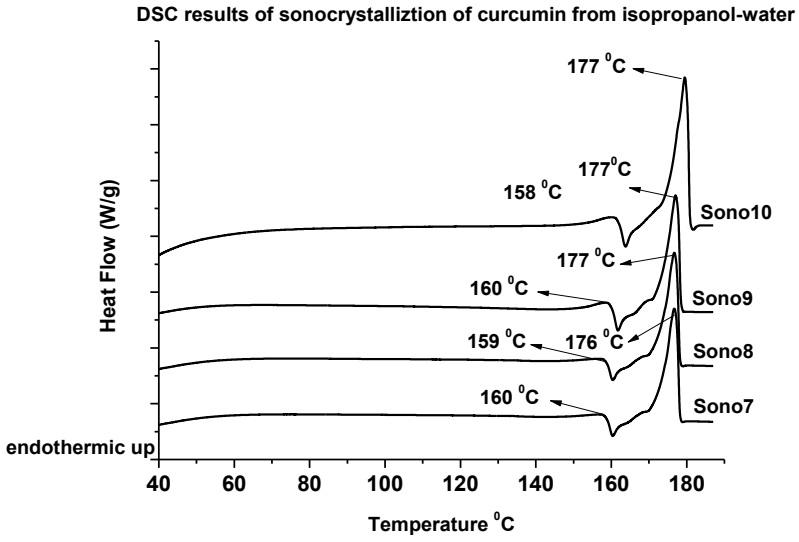

Figure 5. 5 DSC thermograms of precipitated curcumin particles from isopropanol-water at different ultrasound amplitude

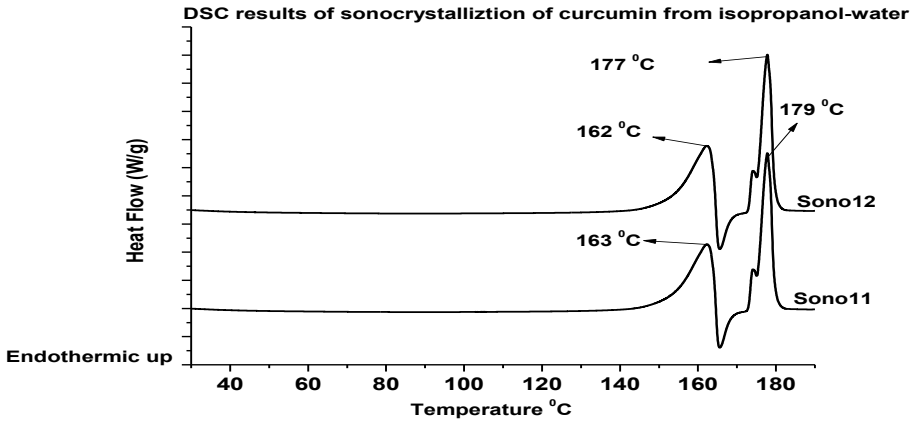

Figure 5.6 DSC thermograms of precipitated curcumin particles from isopropanol-water at different sonication time

Table 5. 10 Polymorph transformation and melting temperature of precipitated curcumin particles from isopropanol-water

Sample code	Transition temperature ºC	Endothermic peak temperature ºC
Sono7	160	176
Sono8	158	177
Sono9	160	177
Sono10	158	177
Sono11	163	179
Sono12	162	177

The DSC thermograms of sono13 to sono15, which are prepared from acetone solvents and water as antisolvents, are illustrated in figure 5.7 and the associated melting peak temperature in table 5.11. The DSC curves exhibit one

endothermic peak at 177ºC, which corresponds to the melting temperature of curcumin particles form 1 (Liu et al. 2015).

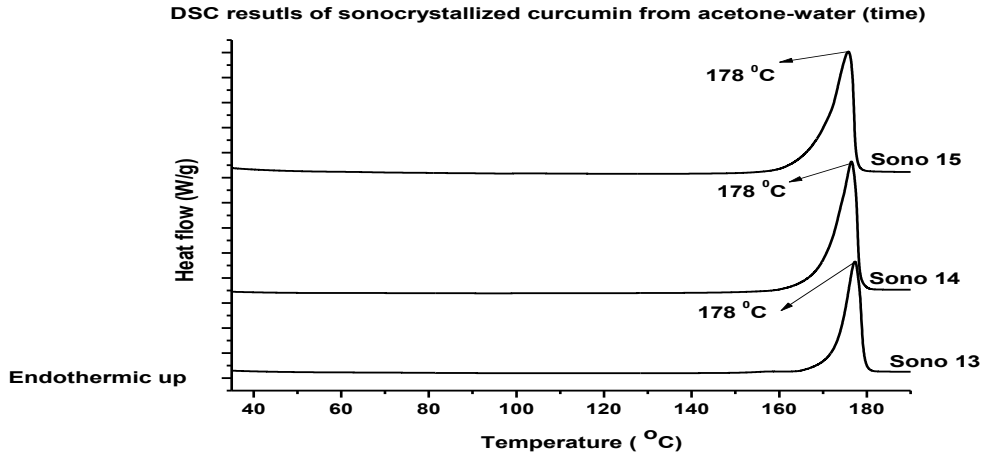

Figure 5. 7 DSC thermograms of precipitated curcumin particles from acetone-water at different sonication time

Table 5. 11 Endothermic peak temperature of precipitated curcumin particles from acetone-water

Sample	Endothermic peak temperature ºC
Sono13	178
Sono14	178
Sono15	178

The DSC data of sono16 to sono18 are shown in figure 5.8 and their melting peak temperature in table5.12. The thermograms of the DSC show only one endothermic peak at 178ºC, this melting peak temperature corresponds to the melting temperature of curcumin particles form 1.

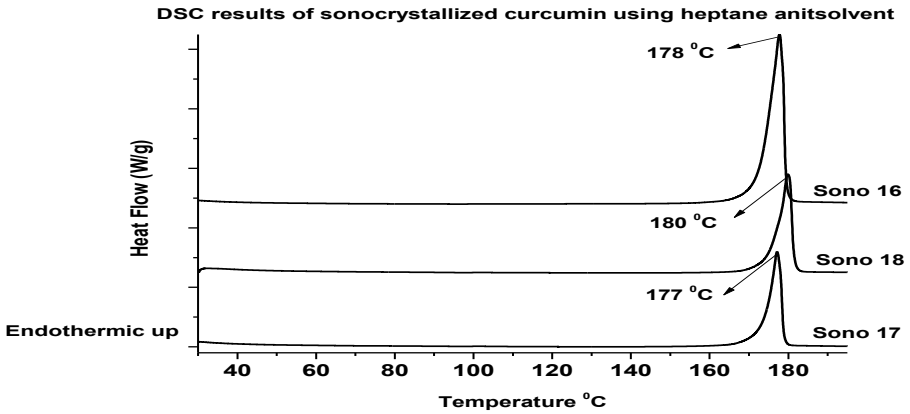

Figure 5. 8 DSC thermograms of sonocrystallised curcumin particles from ethanol, isopropanol and acetone as good solvents and heptane as an antisolvent

Table 5. 12 Endothermic peak temperature of sonocrystallised curcumin particles from ethanol, isopropanol and acetone as good solvents and heptane as an antisolvent

Sample	Endothermic peak temperature ºC
Sono16	178
Sono17	177
Sono18	180

To conclude, the DSC results of the sonocrystallised curcumin, which are prepared from acetone and ethanol solvents and water as an antisolvent, have shown one endothermic peak. Whereas low thermal events were seen when isopropanol solvents were used, in which the first endothermic peak represents curcumin polymorph transformation (form 3 to form 1) and the second melting peak corresponds to the melting temperature of form 1 (Thorat and Dalvi 2015; Thorat and Dalvi 2016). The DSC curves of sonocrystallised curcumin using the

above three solvents (ethanol, isopropanol and acetone) and heptane as an antisolvent, exhibit only one endothermic peak which agrees with the melting temperature of curcumin form 1. These findings were confirmed using XRPD in the next section

5.3.4. X-ray powder diffraction (XRPD)

XRPD is used to determine any changes in curcumin crystal structure. Curcumin crystal structure exists in three different forms (Sanphui et al. 2011), forms 2 and 3 are known as orthorhombic structure (form 2 and 3, and form 1 is a monoclinic structure (Sanphui et al. 2011).

The variation between form 1 and forms 2 and 3 of curcumin is mainly the conformation of a curcumin molecule and its interaction through hydrogen bonding with neighbouring curcumin molecules (Sanphui et al. 2011; Thorat et al. 2014). In form 1, the curcumin molecule has a curved and twisted conformation as a result of hydrogen bonding between neighbouring curcumin molecules (Sanphui et al. 2011; Thorat et al. 2014). In forms 2 and 3, they have a linear and planar conformation (Sanphui et al. 2011). The difference between forms 2 and 3 is only the keto-enol orientation of curcumin molecules packed in the unit cell (Sanphui et al. 2011; Thorat et al. 2014). In form 2 the keto-enol groups in 2 molecules are *cis* in orientation, whereas in form 3 they are in *trans* in orientation (Sanphui et al. 2011; Thorat and Dalvi 2015). Also the colour of the curcumin polymorph is distinguishable visually, as form 1 has a yellow-orange and forms 2 and 3 have a red-orange colour (Liu et al. 2015). The XRPD patterns of these polymorphs are shown in figure 5.9. Curcumin form 1 has characteristics peaks in 2θ region at 8.9º and 17º, form 2 has characteristics peaks at 13.8º and 25.9º- 27º and 27.5º and form 3 at 14.1º and 26.7º and 27.1º (Sanphui et al. 2011; Liu et al. 2015; Thorat and Dalvi 2015).

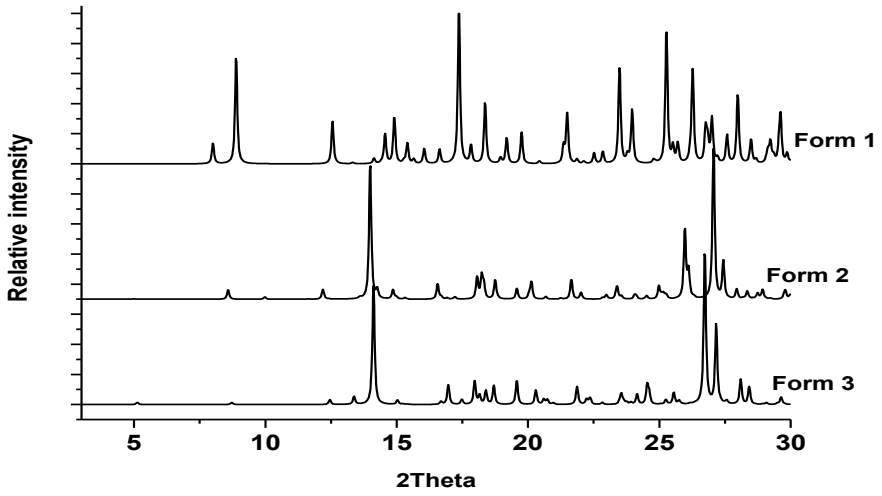

Figure 5. 9 XRPD patterns of curcumin polymorphs reproduced from Cambridge Crystallographic Data Centre (CCDC)

The XRPD patterns of sonocrystallised curcumin, which is produced using an ethanol solvent, (from sono1 to sono6) are illustrated in figures 5.10 and 5.11. The results indicate that curcumin particles formed are similar to curcumin form 1. The different irradiation amplitude (25% to 100%) and time of sonication (1 to 5 min) did not show any changes on curcumin polymorph, these results are in agreement with the DSC data, where both results suggest form 1 is produced. These findings are in disagreement with recent published data (Thorat and Dalvi 2015) which show that curcumin obtained from an ethanol solvent using ultrasound has form 3. This conflict in the results could be attributed to the different levels of supersaturation level of curcumin, as the used curcumin concentration was 5mg/ml, whereas in this work the solution curcumin has a concentration of 15mg/ml. It is clearly that solution concentration that plays a role in the determination of the final polymorph, since the rate of nucleation will be affected by the supersaturation level of the used solution (McCrone 1965; Bernstein et al. 1999; Thorat and Dalvi 2016).

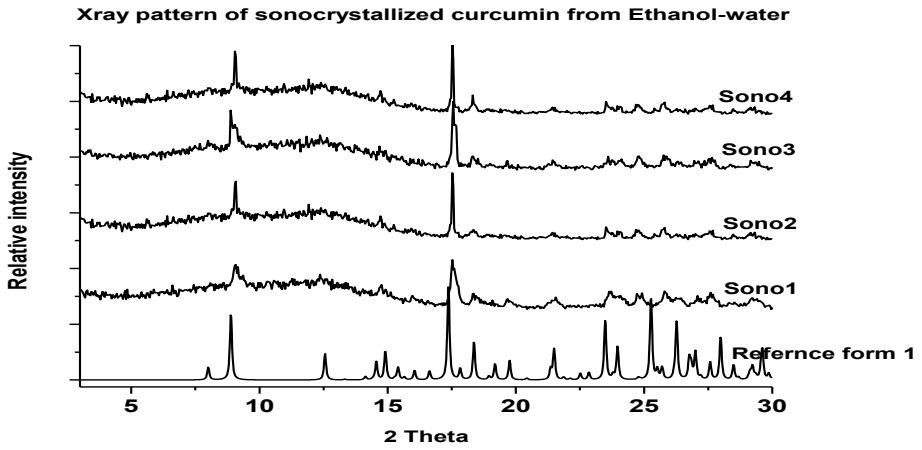

Figure 5. 10 XRPD patterns of sonocrystallised curcumin particles from ethanol-water at different ultrasound amplitude

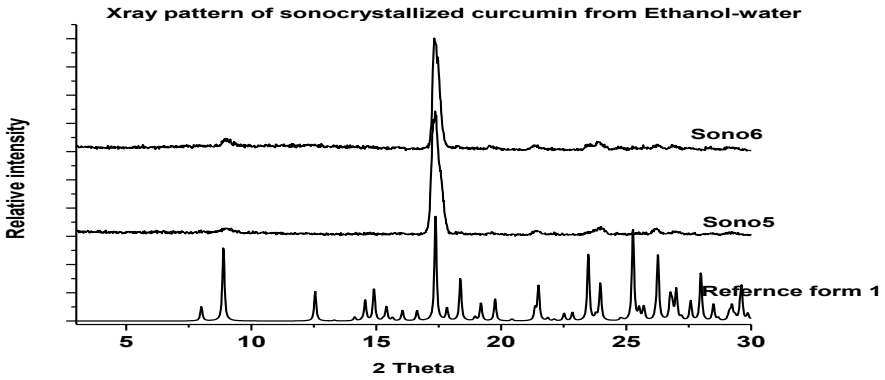

Figure 5. 11 XRPD patterns of sonocrystallised curcumin particles from ethanol-water at different times of sonication

The diffractograms of sonocrystallised curcumin particles, which are obtained from isopropanol solvent and water as an antisolvent, are displayed in figures 5.12 and 5.13. The XRPD patterns have formed in curcumin form 3. Comparing

these patterns with curcumin reference patterns indicates the precipitated curcumin particles have a polymorph 3. Form 3 of curcumin particles was observed among the samples that were produced at different levels of amplitude and sonication time. These results are agreed with DSC thermograms, which showed polymorph transformations. This change of curcumin form during ultrasound was attributed to the ability of the ultrasound irradiation to disturbance and the prevention of hydrogen bonding among curcumin molecules by cavitation (Thorat and Dalvi 2014; Thorat and Dalvi 2015). It is also the processing conditions that could induce polymorphic transformation during crystallisation such as temperature, supersaturation levels and nucleation rate (McCrone 1965; Bernstein et al. 1999).

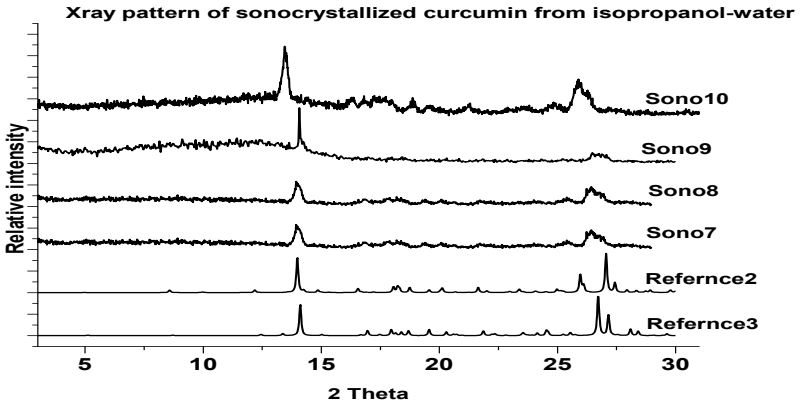

Figure 5. 12 XRPD patterns of sonocrystallised curcumin particles from isopropanol-water at different ultrasound amplitude

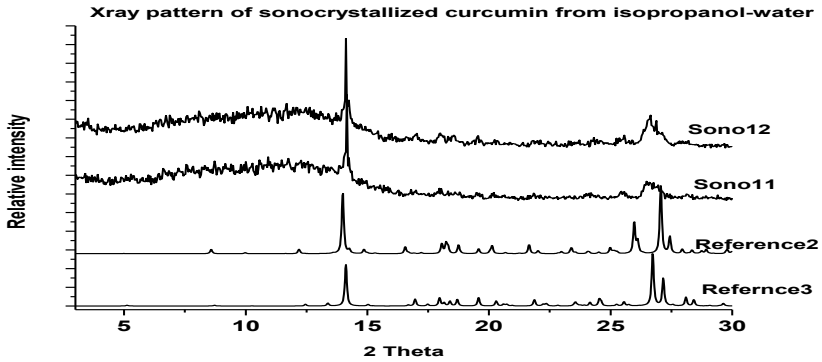

Figure 5.13 XRPD patterns of sonocrystallised curcumin particles from isopropanol-water at different times of sonication

XRPD patterns of curcumin particles (sono13, 14 and 15), which are precipitated from acetone and water, are shown in figure 5.14. The diffractograms of processed particles shows the same trend of curcumin as form 1. These findings support the data of DSC, in which the endothermic peak was related to curcumin form 1.

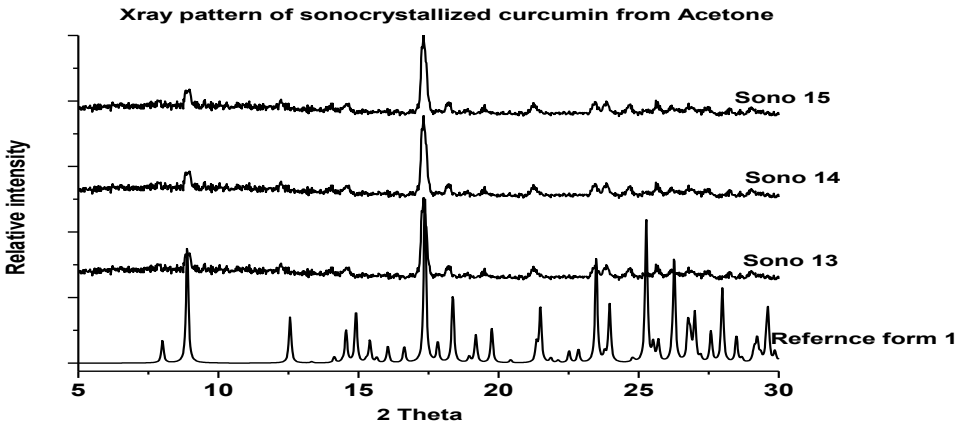

Figure 5. 14 XRPD patterns of sonocrystallised curcumin particles from acetone-water at different times of sonication

Figure 5.15 demonstrates the diffractometer results of sonocrystallised curcumin (sono16, 17, and 18) using ethanol, acetone and isopropanol curcumin solution and heptane as an antisolvent, respectively. The XRPD patterns indicate that obtained curcumin polymorph is form 1, compared to the reference pattern of form 1. Using heptane antisolvent, curcumin form 1 was obtained even with isopropanol solvent, these results are confirmed by thermograms data from DSC, from which a single endothermic peak was present and it corresponds to a melting temperature of curcumin form 1.

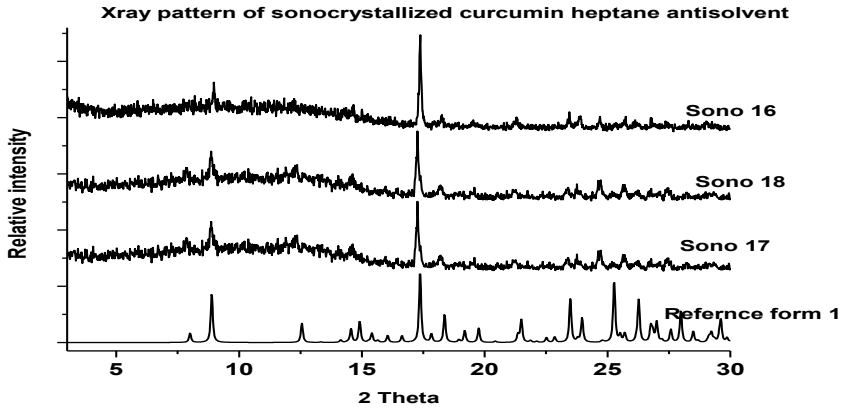

Figure 5. 15 XRPD patterns of sonocrystallised curcumin particles from ethanol, acetone and isopropanol and heptane as an antisolvent.

In conclusion, XRPD data of sonocrystallised curcumin using different solvents and antisolvents are supported by the DSC results. Two curcumin polymorphs, form 1 and form 3, were observed using ultrasound precipitation methods. Curcumin form 1 and form 3 can be identified visually according to their colour, since curcumin form 1 has a yellow-orange colour, and form 3 has a red colour (Liu et al. 2015). Form 3 of curcumin has been observed when isopropanol and water were used as a solvent and antisolvent, respectively. This may be

attributed to the hydrogen bond disturbance between curcumin molecules (Thorat et al. 2014; Thorat and Dalvi 2015) as well as the low level of supersaturation and hence low nucleation rate (McCrone 1965; Bernstein et al. 1999). Whereas in heptane antisolvent with isopropanol, the supersaturation level of curcumin may increase due to the high vapour pressure of heptane solvent compared to water as well as the viscosity of heptane less than water, which could increase the nucleation rate and then crystal growth which in turn reduces the chance of hydrogen bonding to be disturbed. On the other hand, in the case of the ethanol and acetone, the level of the supersaturation was higher than it was in isopropanol, therefore, the nucleation rate could be faster and the ultrasound was unable to prevent hydrogen bonding between the curcumin molecules. The results from the diffractometer and thermal analyses are in agreement, as in form 3, two thermal events were observed and for form 1 a single endothermic peak was seen.

5.3.5. Surface energy analysis of curcumin particles

The free surface energy of curcumin was characterised using inverse gas chromatography (IGC) by injection of a series of n-alkanes (hexane to nonane) and two polar probes (ethyl acetate and chloroform). In this work, we are trying to correlate the free surface energy of curcumin with its performance during inhalation.

The surface free energy or surface energy (γ) is defined as the energy that creates a unit area of surface. The total free surface energy is composed of different physical forces and it is usually divided into several components (Grimsey et al. 2002). All materials have non-polar (dispersive) forces, and most of the materials have polar forces such as hydrogen bonding or acid base

forces (Fowkes 1964; Grimsey et al. 2002). Therefore, the surface free energy is split into dispersive (γ^{d}) and polar (specific γ^{sp}) components, thus the total free energy is the sum of both energies of the dispersive and the specific energy (Fowkes 1964; Van Oss et al. 1988).

The specific, dispersive and total surface energy of sonocrystallised curcumin using water and a heptane antisolvent are presented in figure 5.16 and 5.17, respectively. The lactose carrier free surface energy characterisation is shown in figure 5.18. The work of adhesion between processed curcumin particles and the lactose carrier is illustrated in figure 5.19, and the work of cohesion between the curcumin particles is shown in figure 5.20.

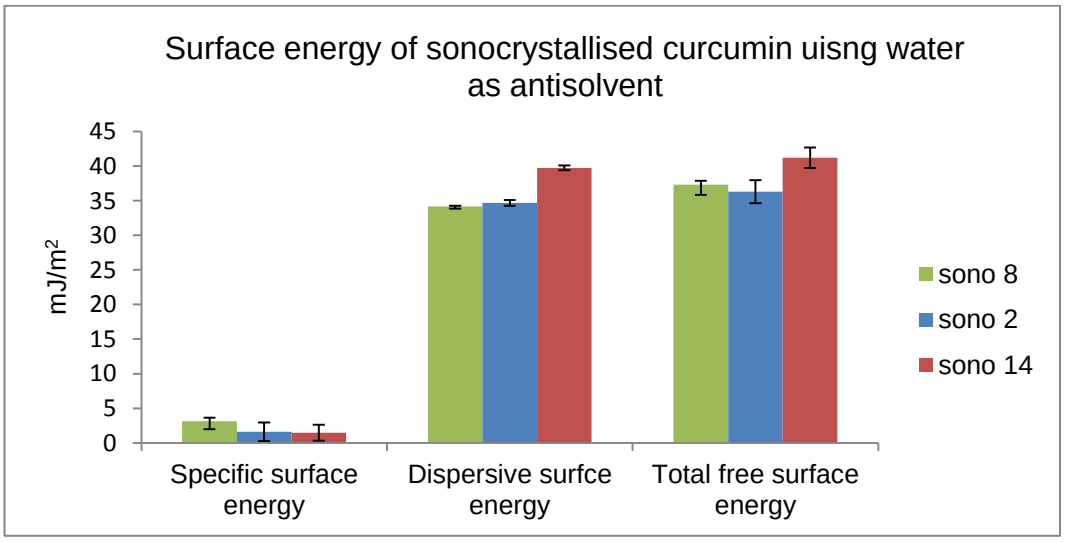

Figure 5. 16 Surface energy of sonocrystallised curcumin, sono8: particles precipitated from isopropanol-water; sono2: particles precipitated from ethanol-water; sono14: particles precipitated from acetone-water.

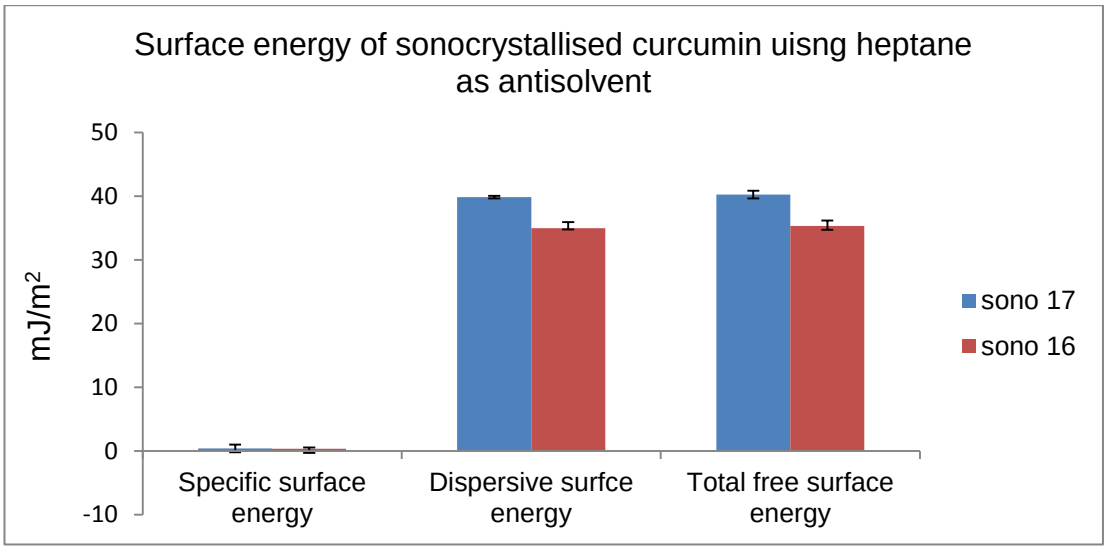

Figure 5. 17 Surface energy of sonocrystallised curcumin, sono16: particles precipitated from ethanol-heptane; sono17: particles precipitated from acetone-heptane.

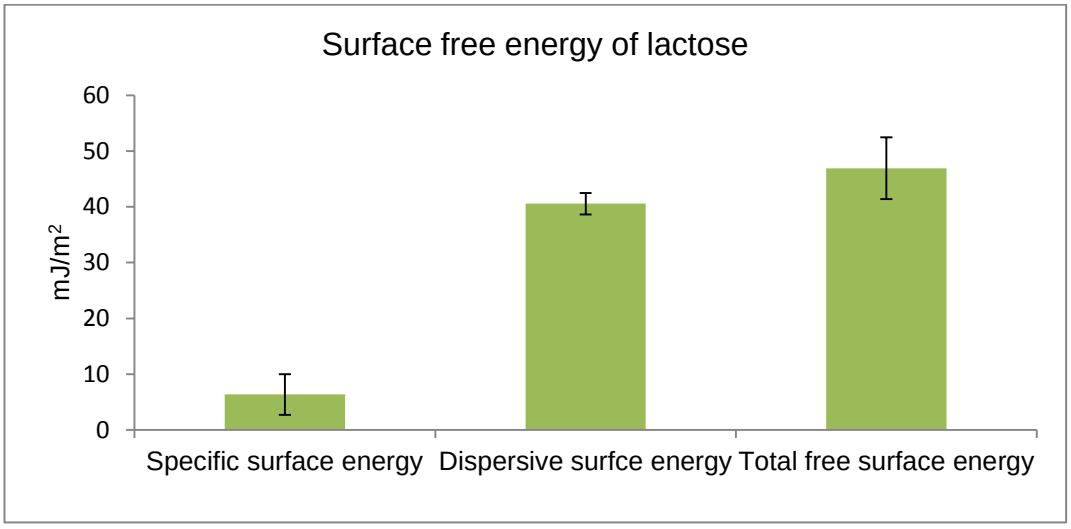

Figure 5. 18 Surface energy of lactose (lactohale200) which is used in DPI formulations of curcumin

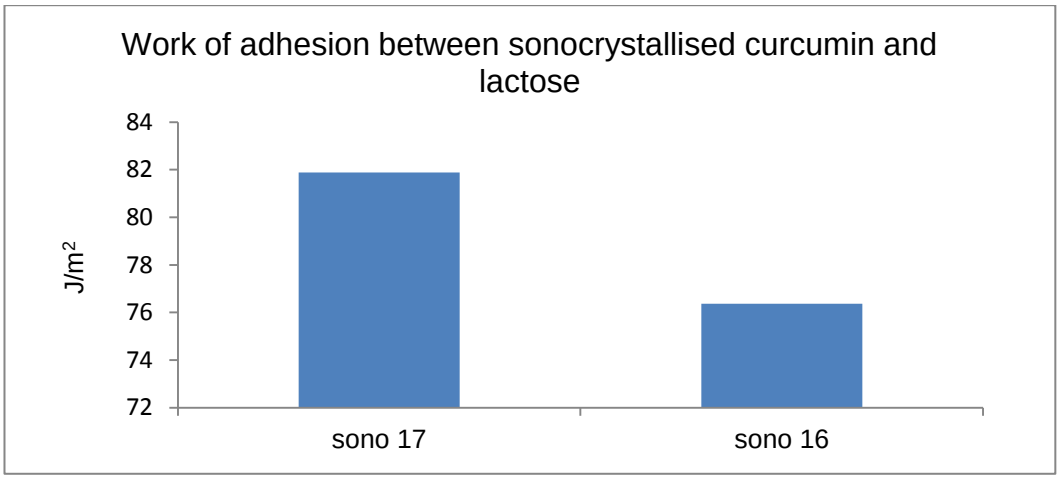

Figure 5. 19 The work of adhesion between sonocrystallised curcumin and lactose, sono16: particles precipitated from ethanol-heptane, sono17: particles precipitated from acetone-heptane.

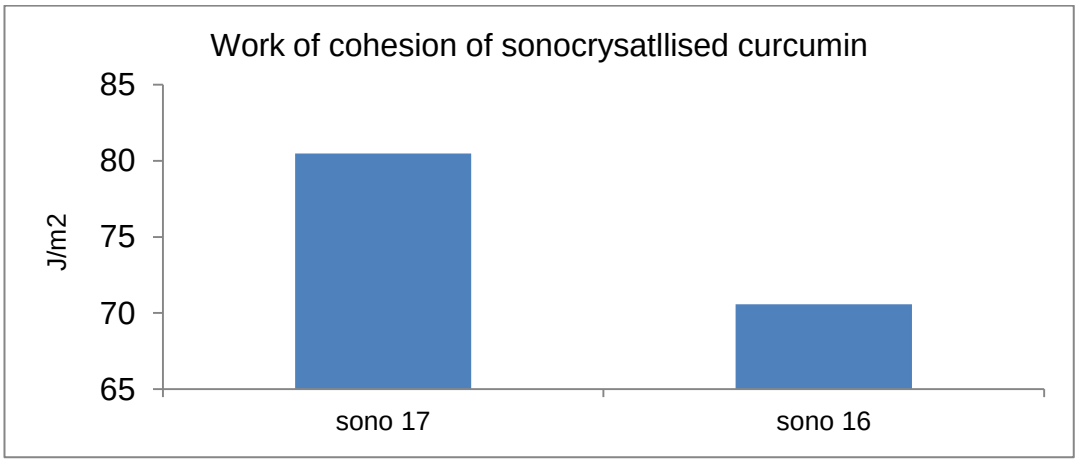

Figure 5. 20 The work of cohesion between sonocrystallised curcumin, sono16: particles precipitated from ethanol-heptane, sono17: particles precipitated from acetone-heptane

The specific components of the sonocrystallised curcumin produced by acetone, ethanol solvent and water antisolvent (sono2 and sono14) are very similar as γ^{sp} for sono2 (by ethanol) is 1.67 mJ/m^2 and 1.47 mJ/m^2 for sono14 (by acetone) acetone, this difference in the γ^{sp} is attributed to the differences in the polarity of both solvents. However, the dispersive components of curcumin (sono2 and sono14) significantly varies, which is 34.7mJ/m^2 for curcumin

obtained from ethanol and 39.7mJ/m^2 from acetone. The differences in the dispersive energy are attributed to the fact that acetone is less polar than ethanol and therefore the dispersive energy in the sonocrystallised curcumin is higher than it is in ethanol. This finding is in agreement with another study which was conducted by Storey (Storey 2008) on ibuprofen, in which the ibuprofen showed a different dispersive and specific energy according to the used solvent polarity.

The specific components of curcumin polymorph 3 (sono8), which is produced by using isopropanol and water as an antisolvent, is notably greater than the one found in sonocrystallised curcumin polymorph 1 (whether it is obtained by acetone (sono14) and ethanol (sono2). The γ^{sp} in sonocrystallised curcumin polymorph 3 is 3.15mJ/m^2, whereas in curcumin polymorph 1 is 1.67mJ/m^2 and 1.47mJ/m^2 for ethanol and acetone solvent, respectively. This finding could be attributed to the rearrangement of curcumin structure to surface of curcumin particles during crystallisation. The non-polar surface energy of the polymorph 3 of curcumin is 34.19mJ/m^2, which is very similar to the dispersive energy of curcumin polymorph 1, which is produced using ethanol (sono2); this is due to the closeness in polarity of ethanol and isopropanol.

Sonocrystallisation of curcumin using a nonpolar antisolvent, such as heptane, has changed the surface energy of curcumin and this was more noticeable on the polar energy rather than dispersive energy of curcumin. The specific energy of curcumin has been reduced from 1.67mJ/m^2 and 1.47mJ/m^2 to 0.33mJ/m^2 and 0.40mJm^2 when the heptane antisolvent was used. The dispersive energy of sonocrystallised curcumin has not changed when the water antisolvent was replaced by heptane, as it was 34.71mJ/m^2 and 39.75mJ/m^2 when water is

used and it is 34.96mJ/m^2 and 39.84mJ/m^2 in the case of heptane antisolvent. This finding is in agreement with Grimsey's work on poly(l-actide)microparticles, in which dispersive surface energy was less sensitive to processing techniques, whereas the polar surface energy has been dramatically changed (Grimsey et al. 1999).

The surface energy characterisation has also been determined for a lactose carrier to work out the work of adhesion between the curcumin particles and the carrier (lactose). The results indicate a low surface energy for lactose, which has polar and non-polar surface energy 6mJ/m^2 and 35mJ/m^2, respectively.

The work of adhesion between the drug particles and the carrier determines the energy that is needed to be applied to detach interest particles from the lactose surface. This energy is related to surface energy of both the curcumin particles and the lactose carrier. The work of adhesion between sonocrystallised curcumin and the lactose (sono16) is lower than the work of adhesion between the carrier and curcumin crystallised from acetone (sono17), this is attributed to the lower free surface energy of curcumin sono16 (which is obtained from ethanol solvent).

5.3.6. Dry powder inhaler preparations

Sonocrystallised curcumin particles were mixed with lactose at two ratios of 10% (1:9, drug to lactose) and 2% (1:67.5, drug to lactose). These ratios illustrated a good performance in the air jet milled curcumin studies (see chapter 4), therefore were used for the sonocrystallisation formulations.

Sono5, Sono11, Sono14, sono16 and sono17 samples were selected to be mixed with lactose at the above ratios. Sono5, sono11, sono14, formed cake particles during filtration and when they were mixed with lactose; the drug

particles did not disperse throughout the carrier. Therefore, those formulations were excluded from any further testing (i.e. aerodynamic characterisation). Formulations using sono16 and sono17 were as well dispersed when they were mixed with lactose.

5.3.7. Aerodynamic characterisation using next generation impactor

- Formulations from acetone (sono17): sono17-1 is the formulation drug-lactose ratio of 1:9, and sono17-2 is the formulation of drug-lactose ratio 1:67.5.

The aerodynamic behaviour (FPF%, MMAD, and GSD) of curcuminoid components (bisdemethoxycurcumin, demethoxycurcumin and curcumin) are presented in table 5.13, the mass distribution of curcuminoids among NGI stages are shown in figures 5.21 and 5.22. The mean (n=3) of fine particles fraction (FPF), mass median aerodynamic diameter (MMAD) and geometric standard deviation (GSD) were calculated using Copley Inhaler Testing Data analysis software (CITDAS).

Table 5. 13 The mean (n=3) of the aerodynamic parameters of DPI formulation of curcuminoids of sono17 (sonocrystallised curcumin particles precipitated from acetone-heptane).

Aerodynamic parameters of curcuminoids DPI Formulations, sono17				
Drug	Formulations	FPF%	MMAD (µm)	GSD
Bisdemethoxycurcumin	Sono17-1 (1:9)	32.12	3.29	2.69
	Sono17-2 (1:67.5)	32.85	2.89	2.96
Demethoxycurcumin	Sono17-1 (1:9)	30.06	3.54	3.04
	Sono17-2 (1:67.5)	30.36	3.06	2.92
Curcumin	Sono17-1 (1:9)	29.94	3.76	2.46
	Sono17-2 (1:67.5)	32.13	3.12	2.69

FPF% is fine particle fraction, MMAD is the mass median aerodynamic diameter, and GSD is the geometric standard deviation.

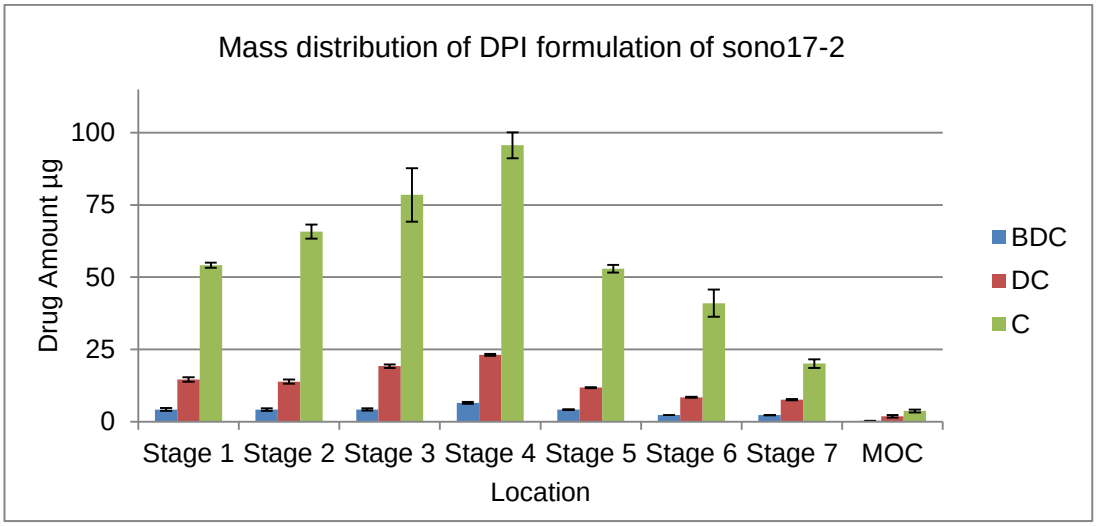

Figure 5. 21 Mass distribution of DPI formulation (sono17-2) of sonocrystallised curcumin particles from acetone-heptane (sono17). BDC: Bisdemethoxycurcumin, DC: Demethoxycurcumin, C: curcumin.

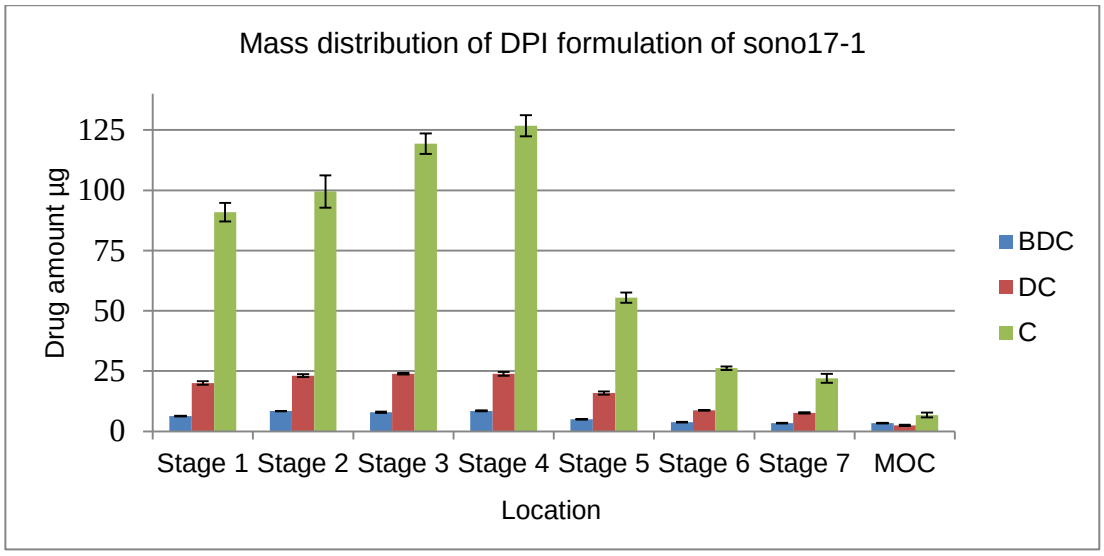

Figure 5. 22 Mass distribution of DPI formulation (sono17-1) of sonocrystallised curcumin particles from acetone-heptane (sono17). BDC: bisdemethoxycurcumin, DC: demethoxycurcumin, C: curcumin

The FPF% of the three curcuminoid components was determined (i.e. curcumin, demethoxycurcumin and bisdemethoxycurcumin), and found to be around 30% throughout both formulations. The MMAD of both formulations is also about 3.2µm, which means 50% of the particles are below 3.2µm. The GSD ranges from 2.4 to 3 for both formulations and among curcuminoid components. These data (FPF 30%) are satisfactory in DPI formulations, because most of the inhaled formulations have a FPF% above 25% (Yakubu, 2009). The low fraction of the fine particle dose in both formulations could be attributed to a high particle size of D_{90}, which has shown to be above 5µm, as any particles above this size (5µm) are usually deposited in on the throat. Also, the free surface energy of sonocrystallised curcumin from acetone was slightly high and therefore, the adhesion force was high too, this usually leads to poor aerodynamic performance of DPI formulations. Both formulations with different ratio of drug-lactose present an almost similar FPF% (30%). This suggests that increasing the amount of the carrier has no significant effect on the FPF% of

curcumin. This similarity of both results (FPF%) could be related to the fact that the work of adhesion (81J/m^2) is very close to the work of cohesion (80.81J/m^2) as shown in section 5.3.3. The energy between the agglomerate sonocrystallised particles curcumin is almost equal to the energy between the curcumin particles and the lactose. Therefore, increasing the ratio of lactose to curcumin in this case has not shown improvement on the formulation performance. This could be attributed to the fact that when the particles are detached from the carriers surface they stay as an agglomeration as shown in figure 5.26 and thus increase the size of the individual particles which leads to low FPF%.

- Formulation from ethanol (sono16): sono16-1 is the formulation of drug:lactose ratio 1:9, and sono16-2 is the formulation of drug:lactose ratio 1:67.5.

The aerodynamic characterisation of the DPI formulations sonocrystallised curcuminoids (curcumin and demethoxycurcumin and bisdemethoxycurcumin) form ethanol (sono16) as represented in table 5.14. The mass distribution of the drugs throughout the NGI stages is shown in figures 5.23 and 5.24. The mean (n=3) of fine particles fraction (FPF), mass median aerodynamic diameter (MMAD) and geometric standard deviation (GSD) were calculated using Copley Inhaler Testing Data analysis software (CITDAS).

Table 5. 14 Aerodynamic characterisation of DPI formulation of curcuminoids of sono16 (sonocrystallised curcumin particles precipitated from ethanol-heptane)

Aerodynamic parameters of curcuminoids DPI Formulations, sono16				
Drug	Formulations	FPF%	MMAD (µm)	GSD
Bisdemethoxycurcumin	Sono16-1 (1:9)	43.41	3.41	2.29
	Sono16-2 (1:67.5)	37.09	2.89	2.90
Demethoxycurcumin	Sono16-1 (1:9)	43.68	3.56	2.11
	Sono16-2 (1:67.5)	34.29	2.81	2.92
Curcumin	Sono16-1 (1:9)	43.49	3.68	1.95
	Sono16-2 (1:67.5)	36.62	2.86	2.77

FPF% is fine particle fraction, MMAD is the mass median aerodynamic diameter, and GSD is the geometric standard deviation.

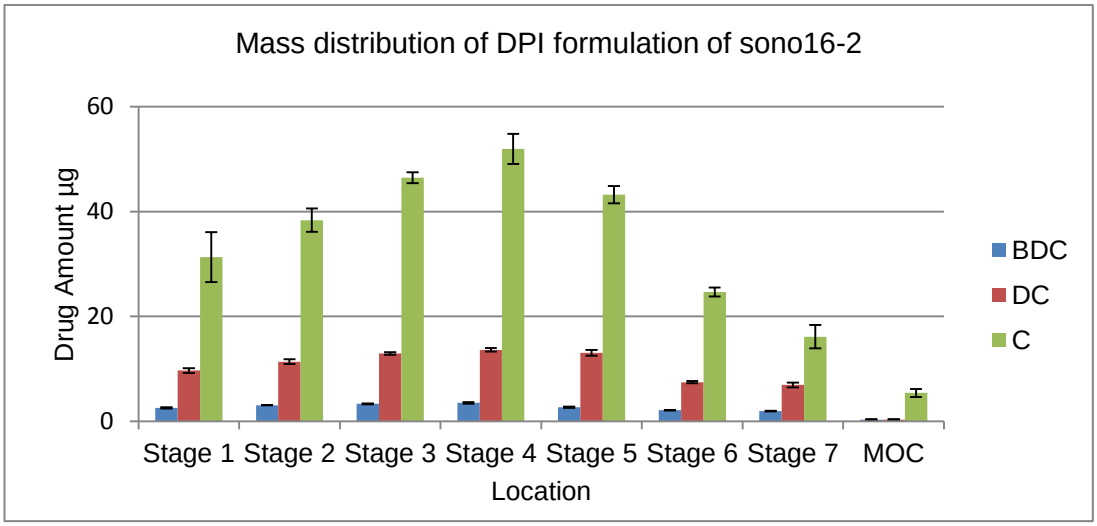

Figure 5. 23 Mass distribution of DPI formulation (sono16-2) of sonocrystallised curcumin particles from ethanol-heptane (sono16). BDC: bisdemethoxycurcumin, DC: demethoxycurcumin, C: curcumin

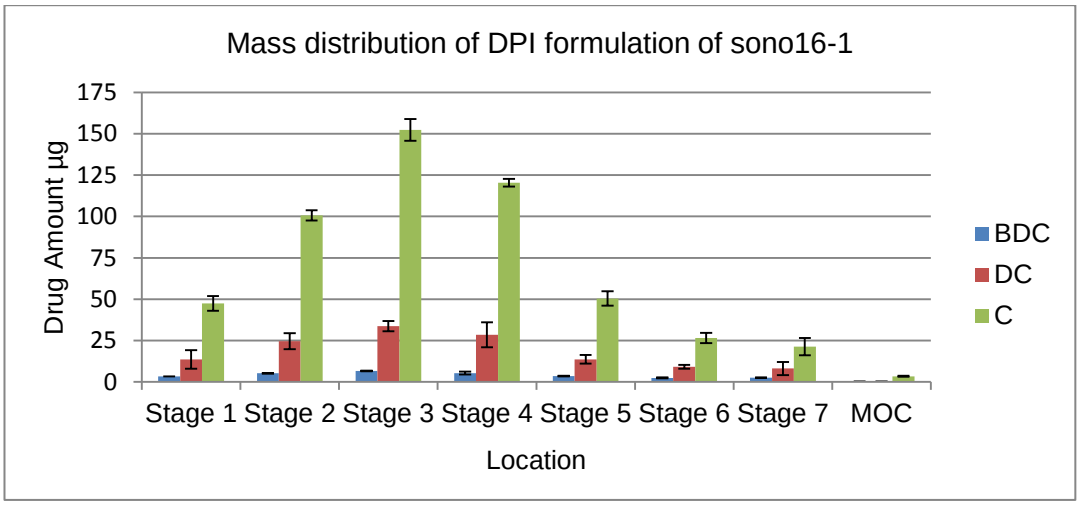

Figure 5. 24 Mass distribution of DPI formulation (sono16-2) of sonocrystallised curcumin particles from ethanol-heptane (sono16). BDC: bisdemethoxycurcumin, DC: demethoxycurcumin, C: curcumin

The results, which were obtained from sonocrystallised curcuminoids from ethanol (sono16), show that FPF% ranges from 43.4% to 43.6% for the formulation sono16-1 (which contains drug: lactose 1:9) among the curcuminoid components, whereas the formulation 16-2 (which contains drug: lactose 1:67.5) has FPF% ranging from 34.2% to 37.0%. The MMAD for the formulation of sono16-1 is between 3.4µm and 3.6µm but for the formulation sono16-2 is 2.8µm. Both DPI formulations demonstrate a well aerosol deposition and performance; this could be related to the low surface energy of the sonocrystallised curcumin particles as well as to the work of cohesion and of adhesion. The first formulation sono16-1 demonstrates a better performance, as FPF is 43%, compared to the second formulation, as its FPF is 37%. This could be as a result of the lower cohesion energy compared to the adhesion energy as shown in section 5.4.5. It is likely the adhesion work is the more dominant force in the second formulation (sono16-2) over cohesion, as the amount of the drug is just enough to cover (less agglomerate) the carrier surface. On the other

hand, in the former formulation (sono16-1), in which the amount of the drug is as high as 10%, the extra amount of the drug is likely to form a second or more layers of the drug particles (agglomerations) on the carrier surface. Therefore, the cohesion force is a dominant force in this formulation over the adhesion energy, as the first layer will be attached to the carrier surface by the adhesion energy and other agglomerate particles or the other layers of the drug will be more controlled by the cohesion force. Since the cohesion energy ($70J/m^2$) is lower than the adhesion work ($76J/m^2$), the particles will be detached from each other before their detachment from the carrier when they inhaled as shown in figure 5.26. Therefore, the performance of first formulation (with 10% of the drug, 1:9 drug: lactose) is superior to the second formulation (with 2% of the drug, 1:67.5, drug: lactose).

From the data, the sonocrystallised curcumin using ethanol (sono16) solvent shows an improvement in the FPF% over the curcumin particles prepared using acetone (sono17). This is attributed to the higher surface energy and work of cohesion and adhesion of the later formulation.

The results of this work led to synthesis a theory of drug particles distribution onto a carrier surface illustrated in Figure 5.25.The theory illustrates the possible effect of the adhesion and cohesion energy on performance of the DPI formulations. Figure 5.25-E and F represent an irregular distribution of the agglomerated drug particles onto the surface of carrier, Figures 5.25-C and D illustrates a regular distribution of drug particles on the carrier. When more drug particles are loaded onto the surface of the carrier, then the aerodynamic behaviour of drug particles will be controlled by the cohesion work, the (either way of regular or irregular distributions).The following points summarise the

relationships between the cohesion and the adhesion forces and with drug-carrier concentration linked to DPI formulation performance:

- When the work of adhesion is equal to the work of cohesion, there will be no difference in the DPI formulation performance between the high or low concentration of the drug on the surface as is it shown in the formulation of sono17-1 and sono17-2.
- When the work of cohesion is smaller than the work of adhesion, the more amounts of the drug onto the surface, the better performance of the formulation as shown in formulation of sono16-1 and sono16-2. This could be attributed to the fact that the particles will be detached from each other before their detachment from the carrier when they inhaled as shown in figure 5.26.
- Results from this work could also suggest that when the work of cohesion is higher than the work of adhesion, the less amounts of drugs onto the surface, the better performance of the DPI formulation would be expected.

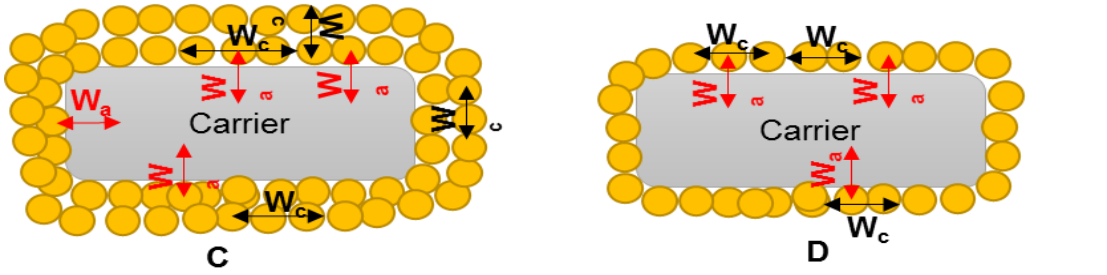

C: regular distribution of a drug particles onto a carrier surface (high % of the drug are loaded).
D: regular distribution of a drug particles onto a carrier surface (low % of the drug are loaded into the surface).
Drug, W_c :is cohesion energy, W_a:is adhesion energy

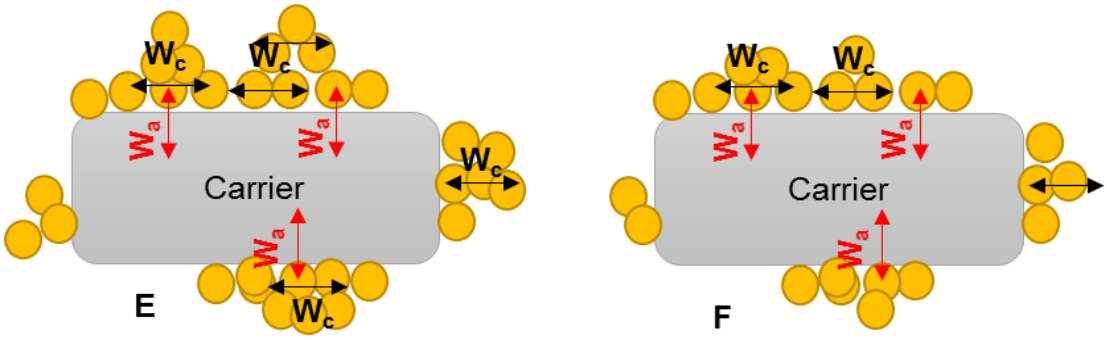

E: irregular distribution of a drug particles onto a carrier surface (high % of the drug are loaded).
F: irregular distribution of a drug particles onto a carrier surface (low % of the drug are loaded).
Drug, W_c :is cohesion energy, W_a:is adhesion energy

Figure 5. 25 drug particles distributed on a carrier surface at low and high concentration of drugs particles in dry powder inhaler formulations

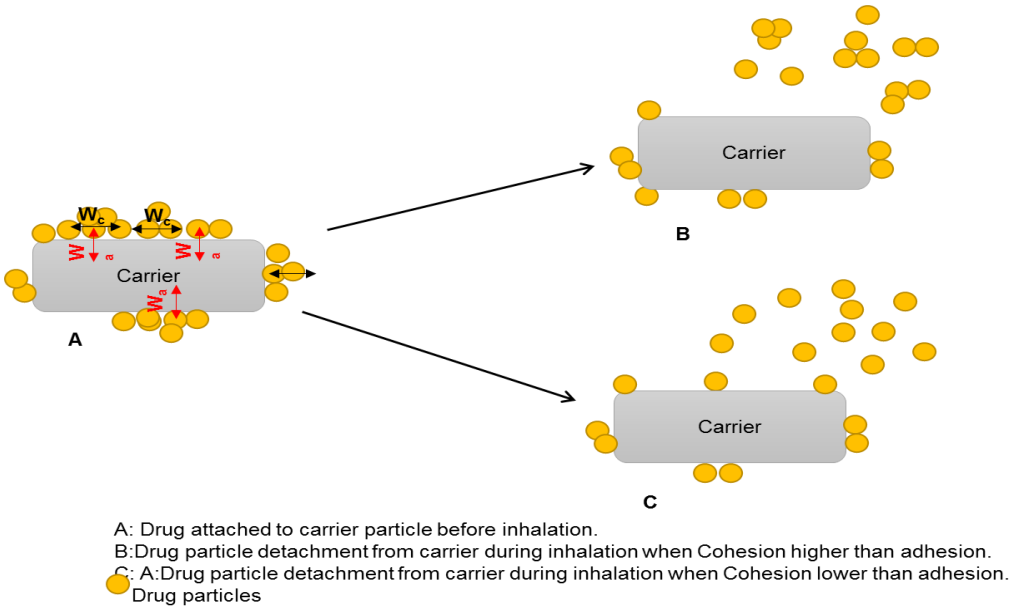

Figure 5. 26 drug detachments from the carrier surface during inhalation

5.4. Conclusion

In conclusion, inhalable curcumin particles were prepared from different solvents (ethanol, isopropanol and acetone) and antisolvents (water and heptane) using ultrasound. The optimum conditions of the ultrasound to produce curcumin particles for inhalation are 1 min of sonication time and 50% of ultrasound irradiation.

The DSC thermograms and diffractograms showed that the precipitated curcumin particles have polymorph 3 (form 3) when it is only produced from isopropanol (solvent) and water (antisolvent) while the ethanol and acetone solvents produce form 1 of curcumin with water antisolvent. On the other hand form 1 of curcumin was also obtained from ethanol, acetone and isopropanol with heptane (antisolvent). The SEM images presented that the sonocrystallised curcumin particles were based on the used solvent and antisolvent system during crystallisation by ultrasound. The crystal morphology of the precipitated particles were in plate shape when ethanol and acetone with water and heptane

systems were used, whereas a rising seed-like shape was observed when isopropanol and water were used, a flower particles shape was seen with an isopropanol-heptane system.

The surface energy of the precipitated curcumin particles varies depending on the solvent and antisolvent system. The total free surface energy for the particles precipitated from ethanol-water was 36.3mJ/m^2, from isopropanol-water (form 3) was 37.3mJ/m^2, from acetone-water was 41.2mJ/m^2, from ethanol-heptane was 35.2mJ/m^2 and from acetone-heptane is 40.2mJ/m^2. The variations in the surface energy were referred to the difference in the polarities of the solvents and antisolvents. The total free surface energy of the carrier is 46.9mJ/m^2.

Dry powder inhaler formulations were prepared by mixing sonocrystallised curcumin particles with lactose, the produced particles using water antisolvent showed poor dispersibility with lactose as they had formed a cake during drying by filtration, whereas the particles obtained from heptane as an antisolvent dispersed very well on the carrier. Therefore particles that produced sonocrystallised using water as an antisolvent were excluded from aerosol characterisations. Also, the produced particles from isopropanol and heptane were excluded due to the large particle size of D_{90} (12µm).

The two formulations of DPI of sonocrystallised curcumin particles (from ethanol and acetone with heptane as antisolvents) at two different ratios (1 to 9 and 1 to 1 to 67.5) of curcumin:lactose, were characterised using NGI. The FPF%, MMAD and GSD of each individual curcuminoid component was determined. The DPI formulations from ethanol showed a better performance compared to the DPI formulation obtained from acetone, this was due to the total free surface

energy of curcumin particles produced from acetone higher than the surface energy of precipitated curcumin particles from ethanol. The higher drug: lactose ratio of the DPI formulation, which its curcumin particles obtained from ethanol and heptane, illustrated better FPF% compared to the one with lower drug: lactose ratio, this was attributed to low cohesion energy compared to the adhesion energy of the curcumin particles and lactose. In the DPI formulation, which the curcumin particles prepared from acetone and heptane, both ratios present very close FPF%, this attributed to the closeness of the cohesion and adhesion energy of curcumin and lactose particles.

CHAPTER SIX

Development and Evaluation of Nanoemulsion and Microsuspension Formulations of Curcuminoids for Lung Cancer by Nebulisers

Chapter 6: Development and evaluation of nanoemulsion and microsuspension formulations of curcuminoids for lung cancer using nebuliser

6.1. Introduction

Liquid-based formulation is usually delivered to the lungs using a nebuliser. Microsuspension is the only approved solution formulation for lipophilic inhaled drugs. Therefore, the nebulised formulations of water insoluble that are available in the market are in suspension form such as budesonide microsuspension. However, several disadvantages have been reported by using microsuspension for inhalation, such as considerable heterodispersity in drug concentration in the aerosol droplet (Knoch and Keller 2005), short drug residence time of drug in the lungs due to the ciliary movement (Patravale and Kulkarni 2004), limited bioavailability of the micronized drug compared to the nanoparticles and variability in drug deposition patterns when using different nebulisers (Nikander et al. 1999). For these reasons, another formulation of curcuminoids in this study has been considered and optimised for inhalation.

Nanoemulsion is a nanometre sized droplet of one liquid dispersed in another immiscible liquid, and it is generally optically transparent and thermodynamically stable (Bryant and Altria 2004). Nanoemulsion drug delivery systems have been used in different administration route, such as oral, parenteral and topical (Lawrence and Rees 2012). In addition to its small particles size (1-100nm), the nanoemulsion has the ability to solubilise both hydrophilic and hydrophobic drugs, hence increasing the bioavailability of the drug (Lawrence and Rees 2012). Nanoemulsion enhanced the curcuminoids bioavailability and its activity

when it was applied locally onto skin or taken orally (Wang et al. 2008; Cui et al. 2009; Liu et al. 2011; Hu et al. 2012).

Curcuminoids nanoemulsion for lung delivery has not been studied before. Therefore, the aim of this work is to prepare curcuminoids nanoemulsion for the treatment of lung cancer and another lung disease. There are few reports of using nanoemulsion for respiratory drug delivery (Amani et al. 2010; Nasr et al. 2012; Nesamony et al. 2014), but these formulations contain high amount of surfactant and hence this limits their suitability for inhalation therapy. In this work, it is proposed to prepare a curcuminoid nanoemulsion using an extremely low amount of surfactant to avoid the formulation toxicity and to make it safe for inhalation.

The *in vitro* genotoxicity of the nanoemulsion of curcuminoids has also been examined using single gel electrophoresis (comet assay) on human lymphocyte cells. The genotoxicity test is required to assess the safety of the formulation and its suitability for animal study in the future.

In this chapter, nebulised formulations of curcuminoid (microsuspension and nanoemulsion) have been prepared. The formulation characterisations such as particle size, zeta potential, viscosity, density, aerosol output and aerodynamic properties were examined and reported. The aerosol output and the aerodynamic assessment have been carried out for all individual curcuminoids (curcumin, demethoxycurcumin and bisdemethoxycurcumin) in each formulation. It is worth reporting that no previous studies have conducted *in vitro* aerodynamic characterisation for all curcuminoids components.

6.2. Methods

6.2.1. Nanoemulsion Preparation

To prepare nanoemulsion that is safe for internal use, accepted pharmaceutical ingredients need to be considered. The reported formulations by Marsh (Marsh et al. 2004), which were composed of octane 0.8% (w/w), butanol 6.6% (w/w) , SDS 3.3% (w/w) and phosphate buffer 89.3% (w/w), and Amani (Amani et al. 2010), which consist of medium 1% of chain triglyceride (w/w), 10% of Tween 80 (w/w), 1% of ethanol (w/w) and 88% normal saline (w/w), were initially followed to prepare the nanoemulsion formulations and then were optimised accordingly to meet respiratory use. The amount of each component of nanoemulsion was reduced to the minimum to produce a formulation that is suitable and safe for respiratory drug delivery.

Nanoemulsion formulations were prepared using different types of oil, limonene and oleic acid oil. Tween 80 and ethanol were used as surfactant and cosurfactant, respectively. Limonene and Oleic acid were used as an oily phase while distilled water was used as an aqueous and continuous phase (see table 6.1). The oil (limonene or oleic acid), surfactant (Tween 80) and cosurfactant (ethanol) were initially mixed and the aqueous phase was then added. A clear solution was formed simultaneously by adding the ultrapure milli-Q water. The nanoemulsion was then sonicated for 10 minutes to ensure that all ingredients had been mixed very well.

Loading capacity of nanoemulsion was studied by adding an excess amount of curcuminoid and then sonicated for 15 mins and left at room temperature for 24 hours. The nanoemulsion was then filtered using 0.45µm syringe filter and

diluted in a HPLC mobile phase then injected into HPLC using a validated HPLC method as mentioned in chapter 3 section 3.1.2.1.

Table 6. 1 Nanoemulsion compositions (NE: Nanoemulsion)

Formulations	Surfactant% (w/w)	Cosurfacnt% (w/w)	Oil% (w/w)	Water% (w/w)
NE1	Tween 80 (3.3)	Ethanol (6.6)	Limonene (0.8)	Water (89.4)
NE2	Tween 80 (3.3)	Ethanol (2.5)	Limonene (0.8)	Water (93.4)
NE3	Tween 80 (1.65)	Ethanol (1.25)	Limonene (0.4)	Water (96.7)
NE4	Tween 80 (0.82)	Ethanol (0.62)	Limonene (0.2)	Water (98.4)
NE5	Tween 80 (0.33)	Ethanol (0.25)	Limonene (0.08)	Water (99.2)
NE6	Tween 80 (3.3)	Ethanol (6.6)	Oleic acid (0.8)	Water (89.3)
NE7	Tween 80 (3.3)	Ethanol (6.6)	Oleic acid (0.3)	Water (89.8)
NE8	Tween 80 (3.3)	Ethanol (2.5)	Oleic acid (0.3)	Water (93.9)
NE9	Tween 80 (1.65)	Ethanol (1.25)	Oleic acid (0.15)	Water (96.95)
NE10	Tween 80 (0.82)	Ethanol (0.62)	Oleic acid(0.075)	Water (98.48)
NE11	Tween 80 (0.33)	Ethanol (0.25)	Oleic acid (0.03)	Water (99.39)

6.2.2. Microsuspension preparation

Saline solution was prepared by dissolving 0.9% of sodium chloride in distilled water. A sufficient amount of micronized curcuminoids was suspended in 0.2% (w/w) of Tween 80 and then diluted with saline solution to obtain a 0.02% of tween 80 with final concentration of 500, 250 and 100 µg of curcuminoids.

Suspension formulation of curcuminoids was prepared to study the difference in the aerodynamic behaviour between the nanoemulsion and suspension when they are nebulised.

Suspension is a dispersion of fine insoluble solid particles (the disperse phase) in a fluid which is called the dispersion medium. The suspension formulations are usually composed of an aqueous dispersion phase and suspending agent like surfactant such as polysorbate 80. The suspension remains homogenous after shaking for the period of filling the nebulised chamber and during nebulisation time. The amount of Tween 80 was used according to FDA regulations.

6.2.3. Osmolality and PH

The osmolality and pH of the nanoemulsion samples was determined at room temperature using Advanced 3320 Micro-Osmometer (Model 3320) and a pH meter (details), respectively. The Osmometer was calibrated using a standard solution (50 mOsm Calibration Standard). Samples were measured in triplicate and the mean was then calculated. Sodium chloride was used to adjust the osmolality of the samples.

6.2.4. Physical stability studies

The selected formulation was monitored for stability studies at room temperature for six months. The nanoemulsion solutions were kept in sealed glass vials at room temperature of (22ºC +/- 2ºC) and were visually examined every two weeks for any turbidity in the formulation. The stability was conducted for any changed in the physical appearance of the nanoemulsion, phase separation and any turbidity during the storage period at room temperature.

6.2.5. Particles size measurement

The nanoemulsion particle size was measured using Malvern Zetasizer Nano-Zs dynamic light scattering (DLS) instrument. The average particle size was determined from three measurements. The instrument was calibrated by using Nanospher TM (with average diameter 59.0nm±2.5) and duke standard TM (with average diameter 500.0nm±0.2).

6.2.6. Zeta potential determination

The zeta potential of the nanoemulsion formulations was carried out at 25°C using a Malvern Zetasizer dynamic light scattering (DLS) instrument. The mean of the zeta potential was determined from three reading for each formulation. The samples were loaded in covet cell designed for zeta potential measurement and inserted into the instrument. The machine was calibrated using standard polystyrene latex (with zeta potential of – 50 mV±5 mV.)

6.2.7. Density

The density of the formulation was examined by filling samples into a 10ml volumetric flask and weighing them at room temperature. Distilled water was filled into the same volumetric flask and weighed too. The relative density was determined according to the following equation:

$$Relative\ Density = \frac{weight\ of\ the\ sample}{weight\ of\ the\ distilled\ water}$$

6.2.8. Viscosity

The viscosity of the samples was measured using vibrating viscometer (SV-10) at 25 ^{0} C. The sample was loaded into viscometer container (35ml) and attached into the base of the instrument.

6.2.9. CEN method for measuring aerosol output

Figure 6.1 displays the European Standard methodology setup for measuring the nebuliser aerosol output (Boe et al. 2001). The aerosol output of the nanoemulsion was carried out using the Sidestream jet nebuliser. The chamber of the nebuliser was filled with 5ml of nanoemulsion sample and connected to a breathing simulation machine. The breathing machine was set up at sinus flow of 15 breathes per minute and a tidal volume of 500ml with an inspiration to expiration ratio of 1:1. A filter holder containing filter (A) was attached between the breathing machine and the nebuliser. This filter would collect the inhaled aerosol during the breathing cycle. A second holder containing filter (B) was connected to a vacuum pump set at 25L/min, and was placed at 4cm from the other end of the nebuliser to collect the exhaled particles without interfering with inhaled aerosol. The breathing machine and vacuum pump were switched on 30 second before starting on the compressor of the nebuliser. Nebulisation time was recorded and the nebuliser was allowed to operate until the sputtering occurred. The sputtering is when the sidestream jet nebuliser produces an intermittent sound which indicates discontinues stream of the aerosols from the nebuliser. On completion of each run, both filters (A) and (B) were transferred into separate beakers and dissolved in appropriate solvent to collect the inhaled and exhaled aerosol particles of the nebulised formulation. Each sample was run in triplicate (n=3); the mean and the SD were calculated. Among all samples the amount and the percentage of the inhaled, exhaled and remaining drug in the nebuliser chamber were calculated.

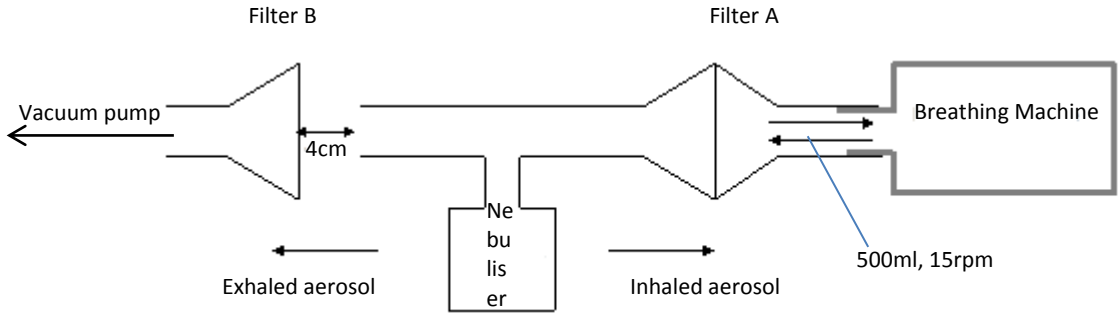

Figure 6.1 Schematic diagram of aerosol output system, adapted from Boe (Boe et al. 2001)

6.2.10. Aerodynamic diameter measurements and particles lungs depositions

Figure 6.2 illustrates next generation impactor setup for measuring the aerodynamic particles size of nebulised curcuminoids formulations according to pharmacopeia (USP 2012, Ph. Eur 2012). NGI was placed in a cooler system at 5°C for 30 mins before nebulisation. The jet sidestream nebuliser was kept outside the cooler system and connected to the NGI by T-piece as it is shown in figure 6.2. The NGI was connected form the other side to a flow controller which was already attached to a vacuum pump. The flow rate was adjusted to be 15 L/min. The pump and the flow controller were switched on before starting the nebulisation. The nebuliser chamber was filled with 5ml of nanoemulsion samples and run after switching the pump and the controller on. The nebulisation was stopped first after the sputtering sound is heard and then the controller and the pump. The NGI cups and the nebuliser chamber were then washed with 20ml of the emodin solution (internal standard). Samples were assessed in triplicate and the nebulisation time for each one was recorded.

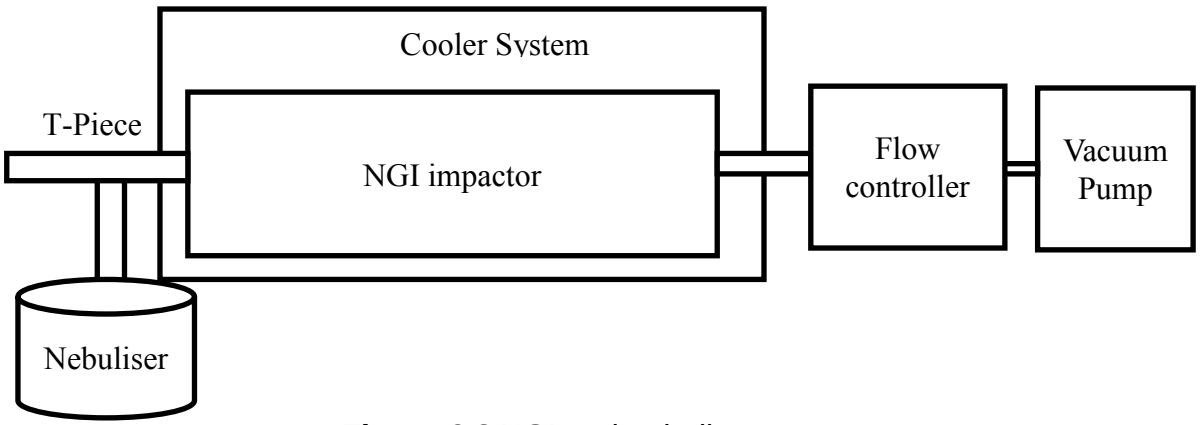

Figure 6.2 NGI and nebuliser set up

6.2.11. Genotoxicity

Comet assay is a simple and sensitive method for the detection of DNA breakage in individual cells (Ostling and Johanson 1984). This method was produced by Ostling and Johanson (Ostling and Johanson 1984) and it has been developed further by Singh and Olive (Singh et al. 1988; Olive et al. 1990). It has been found that DNA damages (fragments) stretches from the nucleus, in the form of a comet, towards the anode in alkaline electrophoresis gel. The DNA migration is the function of the intensity of DNA breakage. Tail moment, a measure of tail length and the fraction of DNA in the Comet tail, was used as the arbitrary unit of assessment (Anderson et al. 2003; Kumaravel and Jha 2006). Tail moment measures both the smallest detectable size of migrating DNA (reflected in the comet tail length) and the number of relaxed/broken pieces of DNA (represented by the intensity of DNA in the tail)

$$Olive\ Tail\ Moment = (Tail.mean - Head.mean)\ X\ Tail\ \%\ DNA/100$$

The assay was carried out using lymphocytes cells because they are excellent carriers for examining genomic sensitivity of any cell as their sub-populations have a lengthy life span and are capable of carrying mutagen-induced genetic

aberrations for over 40 years (Neel et al. 1989). Also, the World Health Organisation/International Programme for Chemical Safety recommends the use of lymphocytes for the detection of genotoxic insult (Albertini et al. 2000).

Protocol

The protocol which was carried out for comet assay was as described by Tice (Tice et al. 2000), and it is as follows:

A glass slide was covered with 1% normal melting point agarose (NMP) and left to dry overnight. 890µl PRMI 1640 was added into Eppendorf tube, 10µl of curcumin nanoemulsion (NE3, NE4, NE5, NE9, NE10 and NE11) was added to the cell media then 100µl of whole blood sample was added to the previous mixture and incubated for 30 mins at 37ºC. The samples were moved to a centrifuge for 5 mins at 3000 rpm. 900µl from the supernatant was removed from the samples and 100µl of 0.5% low melting point of agarose (at 40ºC) was added to each sample. The cell pellets were disrupted gently and 100µl of the suspended cells was transferred into previous coated glass slide with 1% NMP and distributed by a cover slip, and left on ice for around 5 min. The cover slip was removed carefully from the slide and then the slide was kept in a lysis solution (2.5M NaCl, 100mM EDTA, 10mM Tris, 10% DMSO, 1% Triton X-100, pH 10) at 4ºC for overnight. The slide then transferred into gel electrophoresis tank with cold alkaline buffer solution (300mM NaOH, 1mM EDTA, pH <13) and left for about 30 mins at 4ºC. The electrophoresis was conducted at 25 voltages and 300mA for 30 mins at 4ºC. The samples slide was washed with neutralising buffer solution (400mM Tris, pH 7.5) and left for 5 min. Ethidium bromide (60µl, 20µg/ml) was added into the sample slides with a cover slip and incubated for 5 mins and then examined with a fluorescent microscope equipped with CCD

camera. A computerised image analysis system, Komet 4.0 (Kinetic Imaging, Liverpool, UK), was employed to measure the Comet parameters; the % Olive tail moment was then used for statistical analysis.

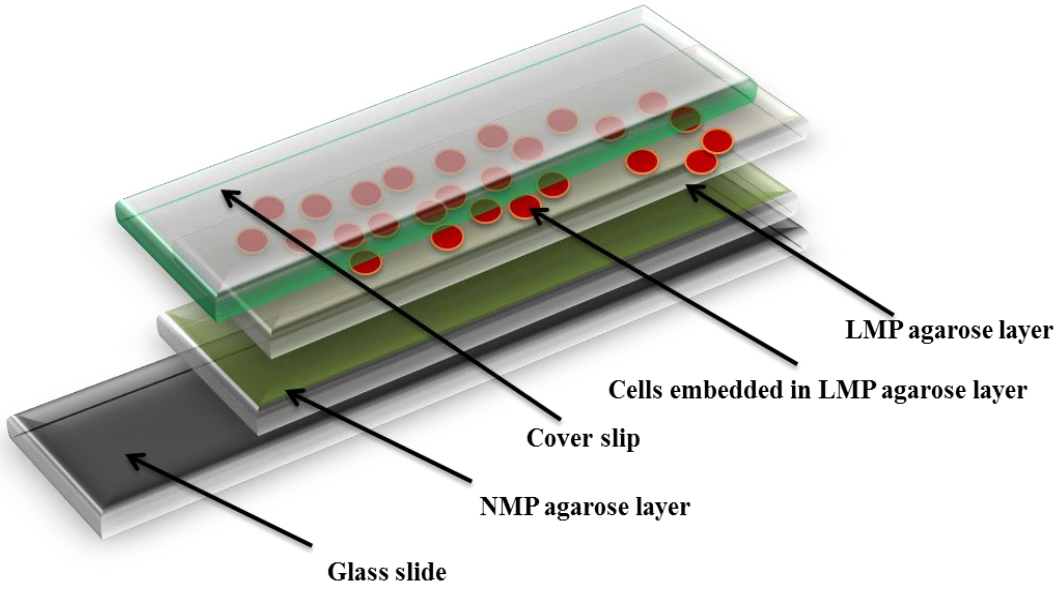

Figure 6.3 Schematic structure of glass slide preparation for comet assay

6.3. Results and discussions

6.3.1. Nanoemulsion preparation and optimization

Table 6.2 shows the visual observation of the nanoemulsion preparations. The limonene nanoemulsion was clear in all formulations. The oleic acid nanoemulsion was not formed with 0.8% of oleic acid as oil, so the oil percentage was reduced gradually to 0.3% to obtain a clear transparent nanoemulsion.

Table 6. 2 Results of visual observation for nanoemulsion reported in table 6.1

Formulation	Appearance
NE1	Clear
NE2	Clear
NE3	Clear
NE4	Clear
NE5	Clear
NE6	Turbid
NE7	Clear
NE8	Clear
NE9	Clear
NE10	Clear
NE11	Clear

The study target was to prepare nanoemulsion with the lowest possible amount of ingredients (i.e. surfactant, cosurfactant and oil). Therefore, the amount of each nanoemulsion components was decreased to the minimum.

Curcuminiods were dissolved in the oily phase (surfactant, cosurfactant and oil) and then sonicated for a few minutes to assure that the drug was completely dissolved. The distilled water was added gradually to the oily phase; a spontaneous clear transparent solution was formed. The loading capacity of

curcuminoids in nanoemulsion (NE9, 10 and 11) was 500µg/ml, 250µg/ml and 100µg/ml of curcuminoid respectively. Loading capacity of NE3, 4 and NE5 was 500, 250 and 100µg/ml, respectively.

The oleic acid is approved by the FDA to be used in respiratory preparations at a concentration of 0.28%. Also Tween 80 was approved to be used at 0.02% of formulations. In this work the minimum amount of surfactant used was 0.33% (NE5&11).The cosurfactant (ethanol) also was reduced from 6.6% (NE1&NE7) to 0.25% (NE5&NE11).There was no change on nanoemulsion appearance when the surfactant, cosurfacnt and oil reduced to the minimum. However, nanoemulsion was not formed when reducing the percentage of the Tween 80 or ethanol less than 0.33% and 0.25% respectively; this was because of insufficient amounts of the surfactant and cosurfactant to solubilise the oil.

Limonene was also used in this research as an oil phase to produce the nanoemulsion. It was reported that limonene did not show any irritation or central nervous system related-symptoms when inhaled by human subjects (Falk-Filipsson et al. 1993) and it was also reported that limonene reduces the air way inflammation in mice (Hirota et al. 2012). Additionally, limonene has chemopreventive and chemotherapeutic activity against many types of cancer in rodents (Gould 1997) and has antioxidant activity (Bacanlı et al. 2015).

Nanoemulsion formulations, for drug delivery, have been widely used for oral, parenteral and intravenous route. However, very limited studies were reported by using nanoemulsion formulations for lung delivery, which is likely attributed to the high concentration of nanoemulsion ingredients, which are not suitable for lungs or it is not proved to be safe for the lungs. For example, budesonide has been formulated in nanoemulsion to be delivered to the lungs (Amani et al.

2010), but the Tween 80 were about 10% w/w of the formulation which is not suitable for the lungs according to the FDA. In other reported studies, the combination of surfactants (25% to 65%) were required to be used along with cosurfactants (12% to 44%) to produce the nanoemulsion (Nesamony et al. 2014), this is also likely to be harmful to human lungs. Whereas, in this work, the amount of Tween 80 (surfactant) used was ten and thirty times less than it was used in the reported work, which could be suitable and safer for the respiratory system.

6.3.2. Osmolality

Osmolality of nebulised formulations has an effect on the respiratory systems by producing bronchoconstriction and a cough; hence, it decreases the delivery of the drug to the lungs (Weber et al. 1997). The suitable osmolality of aerosols solution should be between130mOsm/kg and 500mOsm/kg, and the formulation should also have permeant ions (such as chloride) in concentrations of 31mM to 300mM to ensure the airways tolerability of such formulation (Weber et al. 1997).

The nebulised nanoemulsion has been formulated using ultrapure milli-Q water as an aqueous phase (continues phase) and then osmolality was adjusted for each formulation by adding a suitable amount of sodium chloride. The suspension formulations were prepared in a saline solution by dissolving sodium chloride (0.9%) in distilled water. The osmolality was measured for nanoemulsion and suspension with curcuminiods and without it. Table 6.3 presents the osmolality with curcuminiods.

Table 6.3 Osmolality results for the nanoemulsion and suspension preparations and Sodium chloride concentrations in each formulation

Formulations	Concentration of NaCl mM	Osmolality (mOsm/kg)
NE2 (1000µg/ml)	0	600 ± 3.0
NE3 (500µg/ml)	35	350 ± 2.1
NE4 (250µg/ml)	95	345 ± 3.2
NE5 (100µg/ml)	150	340 ± 4.5
NE8 (1000µg/ml)	0	600 ± 4.0
NE9 (500µg/ml)	35	353 ± 3.6
NE10 (250µg/ml)	95	343 ± 5.8
NE11 (100µg/ml)	150	335 ± 2.1
Suspension1 (500µg/ml)	160	286 ± 4.0
Suspension2 (250µg/ml)	160	285 ± 3.4
Suspension3 (100µg/ml)	160	283 ± 2.5

From the results in table 6.3, it is clear that all the formulations of nanoemulsion and suspension (with concentration of 500, 250 and100µg/ml) are in the ideal range of the osmolality. The only two formulations out of the accepted osmolality range for nebulisation are NE2 and NE8; this is attributed to a high amount of ethanol in the formulations. The ethanol forms 2.5% of the formulations NE2 and NE8. Therefore, these formulations with high osmolality and zero sodium chloride were excluded from further studies.

6.3.3. pH

The pH for nebulisation solutions need to be adjusted before approaching the respiratory system, because the low and high pH causes a bronchoconstriction and a cough. Cough is undesirable as the deposited particles may be expectorated before it takes effect (Weber et al. 1997). The bronchoconstriction can cause hypoxemia in some patients and reduces the aerosols delivered into the airways (Weber et al. 1997). The ideal pH for nebulised preparations should be between 3 and 8.5, according to USA pharmacopeia. Table 6.4 shows the pH for the selected formulations for both suspensions and nanoemulsion. The results show that all formulations have a pH in the acceptable range for solutions for nebulisation.

Table 6.4 pH results of nanoemulsion and suspension formulations

Formulations	pH
NE3 (500µg/ml)	6.93
NE4 (250µg/ml)	6.74
NE5 (100µg/ml)	6.33
NE9 (500µg/ml)	6.84
NE10 (250µg/ml)	6.77
NE11 (100µg/ml)	6.34
Suspension1 (500µg/ml)	5.90
Suspension2 (250µg/ml)	5.11
Suspension3 (100µg/ml)	5.15

6.3.4. Viscosity

Viscosity is the resistance of the fluid to a flow; therefore, the viscosity is important in aerosols formulations. Ingredients of the formulations and concentration of the drugs may change the viscosity of the preparations, hence this could alter the aerosol output and the aerodynamic distributions of the particles (Mc Callion and Patel 1996; Weber et al. 1997).Viscosity measurements of the nanoemulsions and suspension preparations with curcuminoids at different concentrations are presented in table 6.5.

Table 6.5 Viscosity results of nanoemulsion and suspension formulation using viscometer

Formulations	Viscosity (mPas)
NE3 (500µg/ml)	1.21
NE4 (250µg/ml)	1.13
NE5 (100µg/ml)	1.07
NE9 (500µg/ml)	1.28
NE10 (250µg/ml)	1.16
NE11 (100µg/ml)	1.08
Suspension1 (500µg/ml)	1.04
Suspension2 (250µg/ml)	1.05
Suspension3 (100µg/ml)	1.04

The results illustrate that the viscosity of the nanoemulsion formulations with either limonene oil or oleic acid oil increases as the concentration of the

ingredients (oil, surfactant and co-surfactant) increases. The suspension formulation did not show any further raise in the viscosity, this is because of the amount of the surfactant, which was used in each formulation, and was constant at the of level 0.02% w/w.

6.3.5. Density

The density results of the nanoemulsions formulations and suspensions are shown in table 6.6. The results show no change in the formulations density; this is attributed to fact that the 98% of the formulation is water (saline)

Table 6. 6 Density results of both preparations nanoemulsion and suspension

Formulations	Density (g/ml)
NE3 (500µg/ml)	1.0001
NE4 (250µg/ml)	1.0019
NE5 (100µg/ml)	1.001
NE9 (500µg/ml)	1.0003
NE10 (250µg/ml)	1.0022
NE11 (100µg/ml)	1.0036
Suspension1 (500µg/ml)	1.00010
Suspension2 (250µg/ml)	1.00018
Suspension3 (100µg/ml)	1.00020

6.3.6. Particle size analysis using malvern (zetasizer)

The results of the particles size of the nanoemulsion and suspension formulations were given in table 6.7.

Table 6.7 Particles size results and polydispersity index for nanoemulsion and suspension formulations using Zetasizer

Formulations	Particle size (nm) ± SD	PDI
NE3 (500µg/ml)	13 ± 4.83	0.13
NE4 (250µg/ml)	12 ± 3.34	0.05
NE5 (100µg/ml)	12 ± 3.64	0.06
NE9 (500µg/ml)	39 ± 25.16	0.23
NE10 (250µg/ml)	32 ± 17.67	0.15
NE11 (100µg/ml)	31 ± 15.42	0.15
Suspension1 (500µg/ml)	1650 ± 1015	0.19
Suspension2 (250µg/ml)	1650 ± 1015	0.19
Suspension3 (100µg/ml)	1650 ± 1015	0.19

The particle size of the nanoemulsion prepared by limonene oil (NE3, 4 and 5) is smaller than the nanoemulsion produced by oleic acid (NE9, 10 and 11). The particle size of NE3, 4 &5 is about 12nm whereas the size of the particles in NE9, 10 & 11 is around 35nm. The difference in the particle droplet size is attributed to the difference in physicochemical properties of the oils (viscosity). The viscosity of limonene is about 0.923mPa at 25ºC (Haynes 2014), whereas the viscosity of oleic acid is 30mPa at 25ºC (Noureddini et al. 1992). Increasing

the viscosity of the fluid, increases the resistance to the deformation of the particles, hence the oleic acid is more resistant to be deformed (disperse into smaller droplet size) than limonene oil. The viscosity of oils has a significant effects on the droplet size of emulsions, as a less viscose oil produced a smaller droplet size of emulsion (Wooster et al. 2008; Khatibi 2013). The particle size of microsuspension was about 1.6µm, which was the same micronized solid particle of curcuminoids that were prepared beforehand and then were suspended in ultrapure milli-Q water containing Tween 80 and 0.9% sodium chloride.

The polydispersity index (PDI) value for the NE3, NE4 and NE5 was very small around 0.1 to 0.05 which indicates that the particle size of nebulised formulation was monodispersed. Also, the low value of the PDI was shown for NE10 and NE11 formulations, which contains lower concentrations of drugs (100 & 250 µg/ml) than NE9 (500µg/ml). PDI in the suspension formulation is about 0.2 which indicates a narrow distribution of the particles size of curcuminoids in the formulations.

Figure 6.4 gives some illustrative data from analysis of nanoemulsion using Malvern Zetasizer.

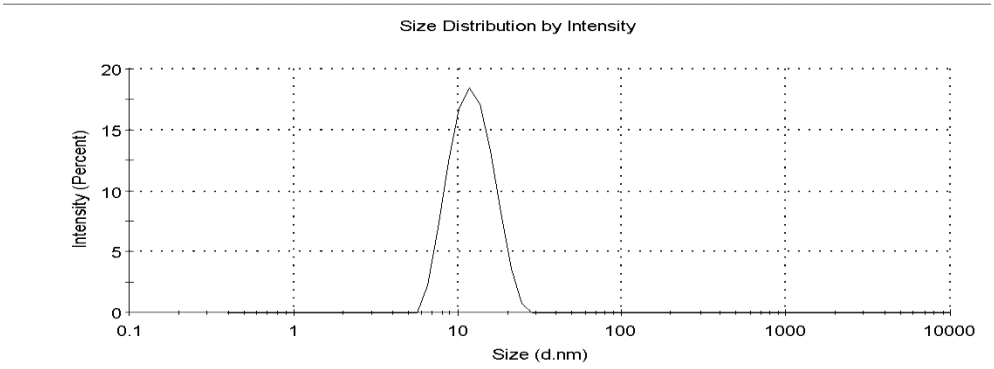

Figure 6.4 An example of illustrative data analysis obtained from malvern zeta sizer for NE11

6.3.7. Zeta potential

Table 6.8 shows the zeta potential data of both formulations nanoemulsion and suspension

Table 6.8 Zeta potential data for nanoemulsion and suspension formulations

Formulations	Zeta potential (mV)
NE3 (500µg/ml)	-6.14 (0.87)
NE4 (250µg/ml)	-3.59 (0.33)
NE5 (100µg/ml)	-2.75 (0.33)
NE9 (500µg/ml)	-7.79 (0.59)
NE10 (250µg/ml)	-5.75 (0.50)
NE11 (100µg/ml)	-5.46 (0.45)
Suspension1 (500µg/ml)	-5.20 (0.36)
Suspension2 (250µg/ml)	-5.13 (0.37)
Suspension3 (100µg/ml)	-4.25 (0.88)

Values from -20mV, to 20mV for surface charge on particles (zeta potential), have been considered to provide a sufficient electrostatic activity to maintain the physical stability of nanoemulsion (Müller and Heinemann 1992).

The zeta potential for nanoemulsion ranged from -6mV to -2mV in case of (NE3, NE4 andNE5) where the limonene oil was used, the zeta was decreased by decreasing the concentration of the drug. In the case of oleic acid, NE9, NE10 and NE11, the zeta potential of nanoemulsion ranged from -7.7mV to -5.4mV.

The microsuspension zeta potential is about -5mV among the different concentrations of the formulations. The low value of the zeta potential is because there are no ionic ingredients in the preparations. All the measured zeta potential is within the range of -20mv to +20mv. These data are in agreement with Amani's work on nanoemulsion formulations (Amani et al. 2008)

6.3.8. Physical stability results

The physical instability of a colloidal system could be one of the phenomena explained in figure 6.5. Since the nanoemulsion is a transparent thermodynamically stable system, it is not expected to predicate instability of the formulation (McClements 2012). The instability could appear if any of the nanoemulsion ingredients are degraded or due to the storage conditions (McClements 2012). Flocculation is when the disperse phase droplets aggregate. Coalescence is when the aggregated droplets fuse and produce a large droplet. Creaming and breaking is a phase separations, as the dispersed phase separates and floats on the top of continuous phase. Nanoemulsion is usually transparent and clear from any turbidity; therefore any turbidity of the nanoemulsion could be an indication of poor stability of the formulation, the turbidity occurs because of oil droplet aggregates (Flocculation) and produces a larger oil droplet (coalescence) (Rahn-Chique et al. 2012).

The data from the nanoemulsion samples, (NE3, NE4, NE5, NE9, NE10 and NE11), showed no phase separation during six months storage at room temperature (22ºC +/+ 2ºC). Moreover, the samples were clear and no turbidity appeared during the storage conditions. This could prove the possibility of preparation of a stable nanoemulsion with very low amount of surfactants which could be suitable and safe for inhalation.

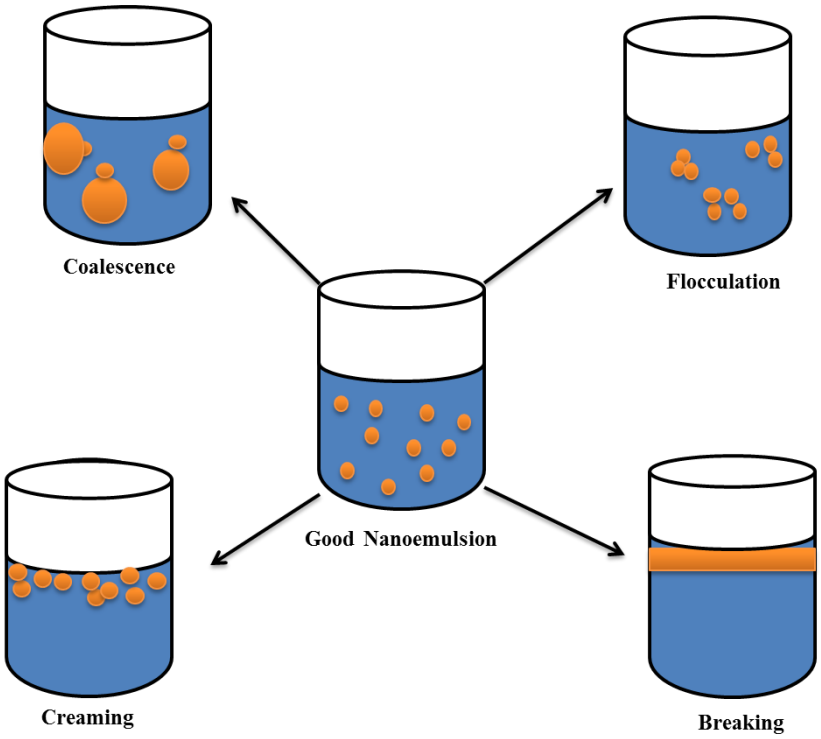

Figure 6.5 Schematic diagram of physical instability of emulsion

6.3.9. Aerosol output using the jet nebuliser

The aerosol output was determined for the individual components of curcuminoids, i.e. curcumin, demethoxycurcumin and bisdemethoxycurcumin, in each formulation (nanoemulsions and suspension) using CEN methodology described in section 6.2.9.

Table 6.9 shows the percentage of bisdemethoxycurcumin, which inhaled, exhaled and remained in the chamber after nebulisation of suspension and nanoemulsion (limonene or oleic acid) formulations at concentrations of 100µg/ml, 250µg/ml and 500µg/ml, of curcuminoids using jet nebuliser. Table 6.10 shows the nebulisation time of each formulation and the percentage rate of inhaled and exhaled bisdemethoxycurcumin per minute at concentrations of

100µg/ml, 250µg/ml and 500µg/ml of curcuminoids by using the same nebuliser.

Table 6.9 The percentage of bisdemethoxycurcumin (BDC) that was nebulised from jet nebuliser at dose of 100µg/ml, 250µg/ml and 500µg/ml of 5ml of curcuminiods (n=3)

Formulations	Concentrations (of curcuminoid)	% Inhalation	% Exhalation	% Chamber	% Connector
NE5	100µg/ml (contains 5µg/ml of BDC)	33.85	31.49	33.25	1.42
NE11		37.17	27.04	31.18	2.72
Suspension3		27.74	21.34	49.12	1.79
NE4	250µg/ml (contains 12.5µg/ml of BDC)	36.31	30.77	31.34	1.84
NE10		37.52	29.36	30.44	2.63
Suspension2		29.99	22.66	44.79	2.55
NE3	500µg/ml (contains 25µg/ml of BDC)	33.40	34.72	29.65	2.23
NE9		37.11	32.90	27.45	2.54
Suspension1		22.75	21.40	53.84	2.01

Table 6.10 The nebulisation time and the percentage of inhaled and exhaled BDC per minute using jet nebuliser

Formulations	Concentrations (of curcuminoid)	Nebulisation time (min)	Inhalation rate (% drug/min)	Exhalation rate (% drug/min)
NE5	100µg/ml (contains 5µg/ml of BDC)	13.00	2.60	2.42
NE11		12.50	2.97	2.16
Suspension3		14.50	1.91	1.47
NE4	250µg/ml (contains 12.5µg/ml of BDC)	12.50	2.90	2.46
NE10		12.00	3.13	2.45
Suspension2		14.50	2.07	1.56
NE3	500µg/ml (contains 25µg/ml of BDC)	13.00	2.57	2.67
NE9		12.50	2.97	2.63
Suspension1		14.50	1.57	1.48

Table 6.11 shows the percentage of demethoxycurcumin, which is inhaled, exhaled and remained in the chamber after nebulisation of suspension and nanoemulsion (limonene or oleic acid) formulations at concentrations of 100µg/ml, 250µg/ml and 500µg/ml, of curcuminoids using jet nebuliser. Table 6.12 presents the nebulisation time of each formulation and the percentage rate of inhaled and exhaled bisdemethoxycurcumin per minute at concentrations of 100µg/ml, 250µg/ml and 500µg/ml, of curcuminoids using the same nebuliser.

Table 6.11 The percentage of demethoxycurcumin (DC) that nebulised from jet nebuliser at dose of 100µg/ml, 250µg/ml and 500 µg/ml of 5ml of curcuminoids

Formulations	Concentrations (of curcuminoid)	% Inhalation	% Exhalation	% Chamber	% Connector
NE5	100µg/ml (contains 17µg/ml of DC)	34.75	35.73	28.79	1.09
NE11		31.20	33.36	32.60	2.83
Suspension3		25.92	18.30	53.74	2.04
NE4	250µg/ml (contains 42.5µg/ml of DC)	33.93	33.59	30.45	2.04
NE10		32.78	33.00	30.94	3.29
Suspension2		28.42	24.13	44.65	2.80
NE3	500µg/ml (contains 85µg/ml of DC)	33.40	34.72	29.65	2.23
NE9		37.11	32.90	27.45	2.54
Suspension1		22.75	21.40	53.84	2.01

Table 6.12 The nebulisation time and the percentage of inhaled and exhaled DC per minute using jet nebuliser

Formulations	Concentrations (of curcuminoid)	Nebulisation time (min)	Inhalation rate (%/min)	Exhalation rate (%/min)
NE5	100µg/ml (contains 17µg/ml of DC)	13.00	2.67	2.75
NE11		12.50	2.50	2.67
Suspension3		14.50	1.79	1.26
NE4	250µg/ml (contains 42.5µg/ml of DC)	12.50	2.71	2.69
NE10		12.00	2.73	2.75
Suspension2		14.50	1.96	1.66
NE3	500µg/ml (contains 45µg/ml of DC)	13.00	2.57	2.67
NE9		12.50	2.97	2.63
Suspension1		14.50	1.57	1.48

Table 6.13 and shows the percentage of curcumin, which is inhaled, exhaled and remained in the chamber after nebulisation of suspension and nanoemulsion (limonene or oleic acid) formulations at concentrations of 100µg/ml, 250µg/ml and 500µg/ml, of curcuminoids using jet nebuliser. Table 6.14 shows the nebulisation time of each formulation and the percentage rate of inhaled and exhaled bisdemethoxycurcumin per minute at concentrations of 100µg/ml, 250µg/ml and 500µg/ml of curcuminoids y using the same nebuliser.

Table 6.13 The percentage of curcumin (C) that nebulised from jet nebuliser at dose of 100µg/ml, 250µg/ml and 500µg/ml of 5 ml of curcuminoids

Formulations	Concentrations (of curcuminoid)	% Inhalation	% Exhalation	% Chamber	% Connector
NE5	100µg/ml (contains 78µg/ml of C)	33.85	31.49	33.25	1.42
NE11		37.17	27.04	31.18	2.72
Suspension3		27.74	21.34	49.12	1.79
NE4	250µg/ml (contains 195µg/ml of C)	33.07	36.03	29.49	1.41
NE10		30.63	35.69	30.56	3.12
Suspension2		27.09	26.72	43.54	2.64
NE3	500µg/ml (contains 390µg/ml of C)	33.52	34.53	30.05	1.91
NE9		36.53	34.03	27.05	2.40
Suspension1		21.49	22.51	54.01	1.99

Table 6.14 The nebulisation time and the percentage of inhaled and exhaled curcumin (C) per minute using jet nebuliser

Formulations	Concentrations (of curcuminoid)	Nebulisation time (min)	Inhalation rate (%/min)	Exhalation rate (%/min)
NE5	100µg/ml (contains 78µg/ml of C)	13.00	2.60	2.42
NE11		12.50	2.97	2.16
Suspension3		14.50	1.91	1.47
NE4	250µg/ml (contains 195µg/ml of C)	12.50	2.65	2.88
NE10		12.00	2.55	2.97
Suspension2		14.50	1.87	1.84
NE3	500µg/ml (contains 390µg/ml of C)	13.00	2.58	2.66
NE9		12.50	2.92	2.72
Suspension1		14.50	1.48	1.55

The aerosols output results of bisdemethoxycurcumin, demthoxycurcumin and curcumin (compnents of curcuminiods) have the same trend throughtout the nanoemulsion and suspension formulations.

The results in table 6.19,6.11 and 6.13 demonstrated that slight differences in the percentage of curcumionids that are entrained into inhalation and exhalation filters or left in the nebuilser chamber between nanoemulsion formulations with either limoenene or oleic acid oil. The amount of the drug, which is entraind in the inhalation filter using nanoemulsion formulation with oleic acid oil, was three % higher compared to formulations with limonene oil.

In comparing both formulations, suspension and nanoemulsion, there is a significant increase in the performance of the curcumionids nanoemulsion formulations (either with limonene or oelic acid oil) over the suspension preparations. In the suspension formulations, the percentage of the drug, which left in the nebuliser chamber, was almost 50% of the deleivered dose whereas in the nanemulsion it was about 30%. Also the percentage of drug entrained into the inhalation filter from the nanoemulsion preparation ranged from 33% to 37%, whereas in the suspension formulation it was about 21% to 27%. This is because the particles size of the nanoemulsion is smaller than the particles on suspension formulation. Furthermore, the nanoemulsion exists in liquid form, the nebulised droplet will be fully filled with a liquid form rather than soild form (suspension). This finding is in agreement with previous studies which were done on nanoemulsion of budesonide by Amani (Amani et al. 2010).

Tables 6.10,6.12 and 6.14 show an improvement on the inahalation rate, which is an important factor in regard to pateint compliance, because of the duration of the required time for the nebulised dose to be taken. The rate of inhalation (%drug/min) is faster in the nanoemulsion formulations (NE3,NE4, NE5, NE9,NE10 and NE11) than the suspension prepartions (suspension 1,2 and 3). Also, this finding is in agreement with Amani's work, in which commercial budsonide suspension was compared to the budesionde nanoemulsion formulation using the same nebuliser (jet nebuliser) (Amani et al. 2010).

Among the nanoemulsion formulation limonene (NE 3,4 and 5) and oelic acid (NE 9, NE10 and NE11), there was no significant variation in the inhalation rate or in the amount of the inhaled drug between the nanoemulsion formulations with limonene oil (NE3, NE4 and NE5) and formulations with oleic acid oil (NE9, NE10 and NE11) which have 0.33%, 0.82% and 1.65% of Tween 80,

respectively. Besides, the aerosol output of the these nanoemulsion formulations was similar to those obtained by Amani et al using nanoemulsions in which 10% of Tween 80 was used as surfactant. From both studies, it could be noticed that using high concentration of surfactant in the nanoemulsion formulations does not improve the aerosol output of the formulation (percentage of the inhaled drug, exhaled drug and left in the chamber). However, it may affect the nebulisation time. The average of the nebulisation time in the present study for 5ml of the nanoemulsion solution was in the range of 12mins to 13 mins whereas Amani et al (Amani et al. 2010) reported the same nebulisation time but for 4ml of nanoemulsion formulation using 10%w/w of surfactant.

Additionally, curcumiond suspension formulation have shown a superior aerosl output performance compared to the available budesoniod suspesnion formulation in the market (Amani et al. 2010) which has been charactersied by the jet nebuliser .

6.3.10. Aerodynamic particles size characterisation

Suspension formulations: the aerodynamic characterisation for suspension formulations (suspension 1, 2 and 3) of curcumin, demethoxycurcumin and bisdemethoxycurcumin are presented in table 6.15. The effect of the drug concentrations, of the suspension formulations, on the FPF and MMAD is described in figures 6.6 and 6.7. The mean (n=3) of the fine particles fraction (FPF), mass median aerodynamic diameter (MMAD) and geometric standard deviation (GSD) were calculated using Copley Inhaler Testing Data analysis software (CITDAS). The mass distribution of the drugs throughout the NGI stages is shown in figures 6.8, 6.9 and 6.10.

Table6.15 The mean (n=3) of the aerodynamic data of suspension formulations using jet nebuliser at flow 15 L/min

Drug	Formulations	FPF%	MMAD (µm)	GSD
Bisdemethoxycurcumin	Suspension3 (100µg/ml)	40.19	5.83	2.07
	Suspension2 (250µg/ml)	34.91	6.45	2.17
	Suspension1 (500µg/ml)	32.50	6.59	2.03
	Suspension4 (1000µg/ml)	26.28	7.08	2.03
Demethoxycurcumin	Suspension3 (100µg/ml)	37.82	6.08	2.21
	Suspension2 (250µg/ml)	33.44	6.43	2.05
	Suspension1 (500µg/ml)	30.66	6.69	2.01
	(1000µg/ml)	25.46	7.09	1.99
Curcumin	Suspension3 (100µg/ml)	43.05	5.31	2.59
	Suspension2 (250µg/ml)	36.00	6.20	2.19
	Suspension1 (500µg/ml)	32.13	6.64	2.12
	(1000µg/ml)	26.01	7.05	2.01

FPF%*: the percentage of Fine Particle Fraction. MMAD*: Mass Median Aerodynamic Diameter. GSD*: Geometric Standard Deviation. FPD*: Fine Particle Dose.

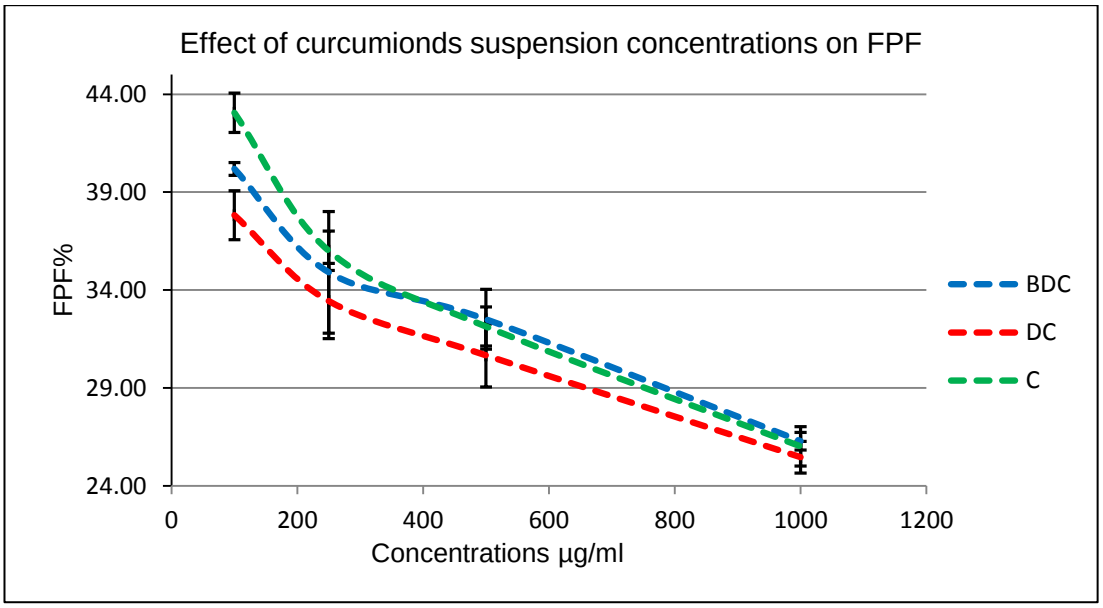

Figure 6.6 The relationships between the suspension concentrations and the Fine Particle Fraction of curcuminoids. BDC*: Bisdemethoxycurcumin. DC*: Demethoxycurcumin. C*: Curcumin. FPF*: Fine Particle Fraction.

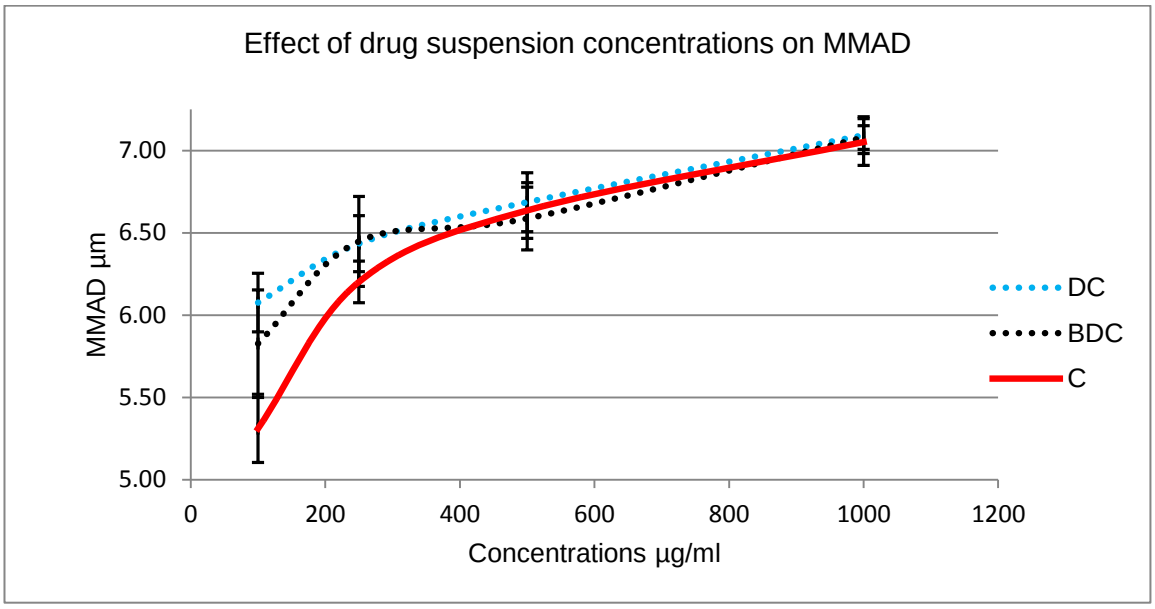

Figure 6.7 The relationships between the suspension concentrations and the Mass Median Aerodynamic Diameters (MMAD) of curcuminoids. BDC*: Bisdemethoxycurcumin. DC*: Demethoxycurcumin. C*: Curcumin

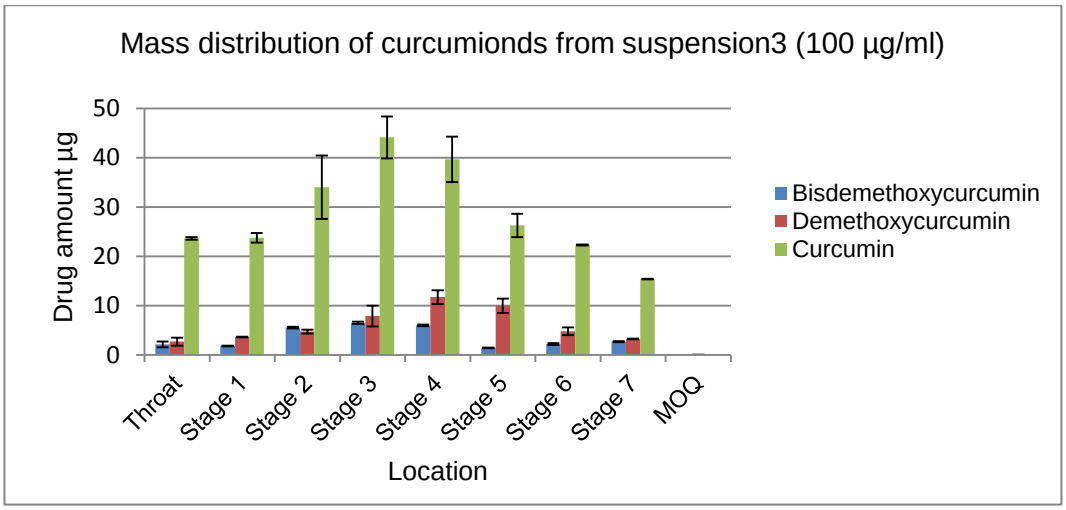

Figure 6.8 The mean (n=3, SD) of mass distribution of curcuminoids from suspension 3 in NGI using jet nebuliser at flow 15 L/min

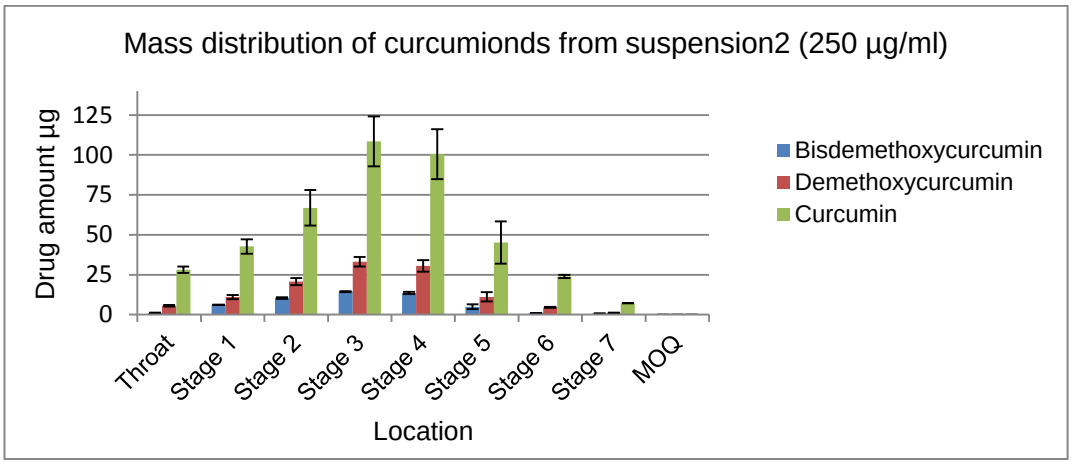

Figure 6.9 The mean (n=3, SD) of mass distribution of curcuminoids from suspension 2 in NGI using jet nebuliser at flow 15 L/min.

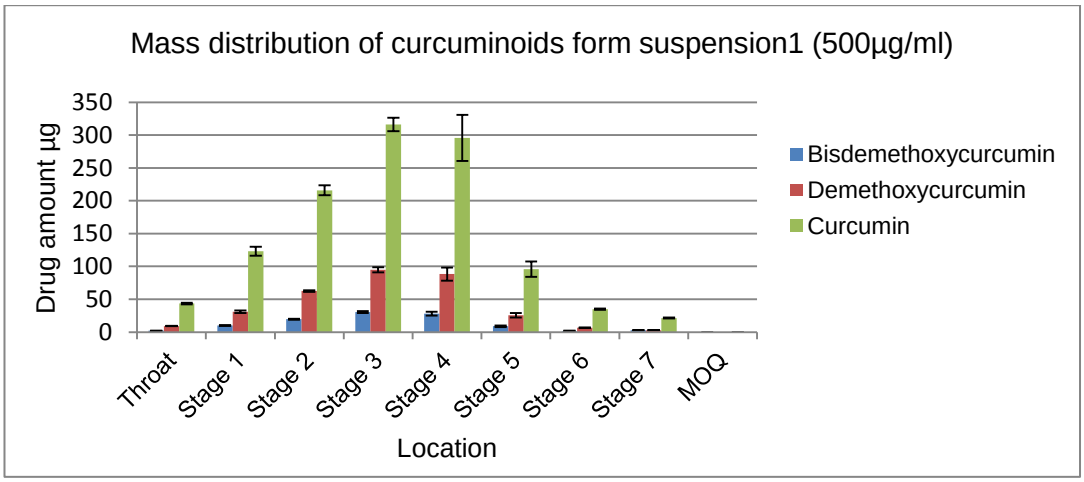

Figure 6.10 The mean (n=3, SD) of mass distribution of curcuminoids from suspension 1 in NGI using jet nebuliser at flow 15 L/min.

The aerodynamic results of the suspension formulation indicate a satisfactory drug deposition behaviour (for concentrations of 0.1mg/ml to 0.5mg/ml), as it shows that about 30 to 40%of the delivered doses were able to reach the lungs. FPF% decreases by increasing the drug concentrations; the FPF, of curcuminoid ingredients, was reduced from 40% at drug concentration of 0.1mg/ml to 26% at curcuminoids concentration of 1mg/ml. This indicates a poor performance for a high drug concentration of suspension during nebulisation (low FPF and high MMAD), whereas the same formulation with low drug concentration showed suprior performance in FPF% and MMAD. This could be due to the the fact that nebulisers produce droplets size range from1 to 5µm, these droplets usually carry the drug particles during nebulisation. In the author openion, nebulised droplets, at low drug concentrations, carry the suspended particles based on the actual size of suspended drug particles (1.6µm). For example, if the drug has a particle size of 1.6µm, it will likely reside in a nebulised droplets size of 2µm and above, as it is explained in figure 6.11. However, at higher drug concentrations, as the number of the drug particles

increased, the nebulised droplets are enforced to carry more drug particles within droplets. Consequently, more particles have to move at the same time inside the large droplets, which leads to particles agglomeration and hence increasing their size (for example, if the individual particles has a size of 1.6µm the agglomerated may have a size of 2.5µm or bigger). Therefore, the small droplets will remain free from the agglomerated drug particles. This theory could explain the poor aerosolisation performance with low FPF and large MMAD of the formulated microsuspension of high drug concentrations. Similar aerosolistion perfermnce was reported by Hemmandez-Trejo (Hernández-Trejo et al. 2005). They found that the agglomeration of particles in suspended solution is a significant issue during nebulisation from jet nebuliser.

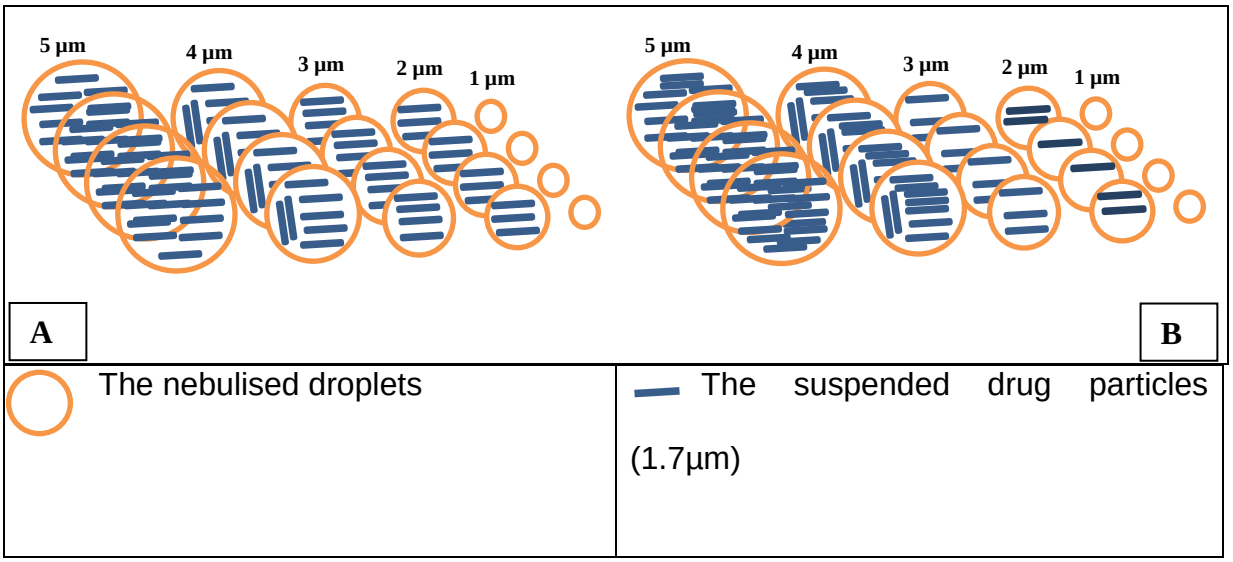

Figure 6.11 Nebulised droplets form microsuspension formulations at low drug concentration (A) and at high drug concentration (B)

Nanoemulsion formulations using oleic acid: The aerodynamic characterisation of the nanoemulsion formulations using oleic acid (NE11, NE10 and NE9) for curcumin and demethoxycurcumin and bisdemethoxycurcumin are

presented in table 6.16. Figures (6.12 and 6.13) show the effect of the drug concentrations, of the nanoemulsion formulations, on the FPF and MMAD. The mass distribution of the drugs throughout the NGI stages is presented in figures 6.14, 6.15, 6.16. The mean (n=3) of the fine particles fraction (FPF), mass median aerodynamic diameter (MMAD) and geometric standard deviation (GSD) were calculated using Copley Inhaler Testing Data analysis software (CITDAS).

Table 6.16 The mean (n=3) of the aerodynamic characterisation of curcuminoids nanoemulsion nanoemulsion with oleic acid oil formulations using jet nebuliser at flow 15 L/min

Drug	Formulations	FPF%	MMAD (µm)	GSD
Bisdemethoxycurcumin	NE11(100µg/ml)	45.69	4.88	2.30
	NE10 (250µg/ml)	43.78	5.39	2.36
	NE9 (500µg/ml)	42.57	5.78	2.15
Demethoxycurcumin	NE11(100µg/ml)	44.05	5.50	2.45
	NE10 (250µg/ml)	42.75	5.72	2.52
	NE9 (500µg/ml)	41.78	5.83	2.16
Curcumin	NE11(100µg/ml)	48.45	4.39	2.62
	NE10 (250µg/ml)	47.15	4.83	2.85
	NE9 (500µg/ml)	46.60	5.25	2.14

FPF%*: the percentage of Fine Particle Fraction. MMAD*: Mass Median Aerodynamic Diameter. GSD*: Geometric Standard Deviation. FPD*: Fine Particle Dose.

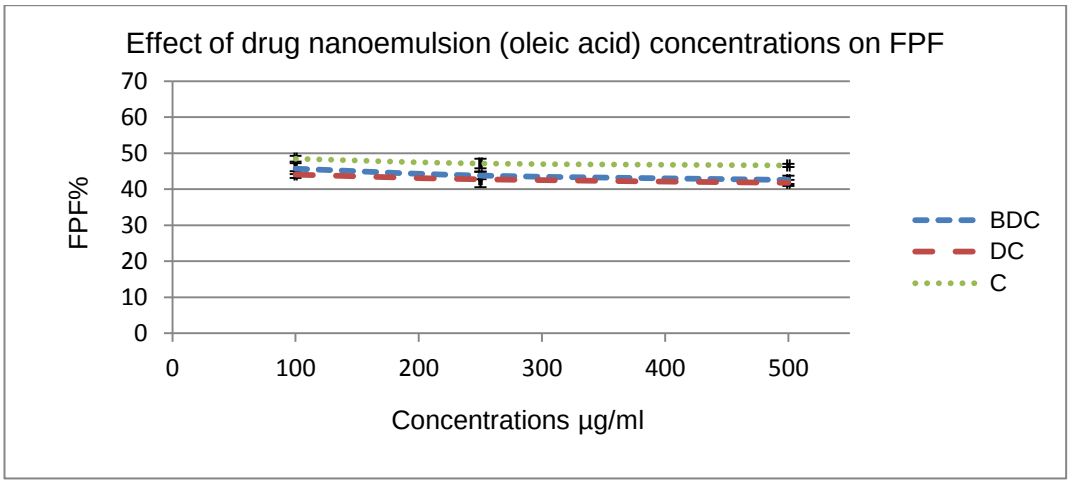

Figure 6.12 The relationships between the drug nanoemulsion concentrations (using oleic acid oil) and the Fine Particle Fraction of curcuminoids. BDC*: Bisdemethoxycurcumin. DC*: Demethoxycurcumin. C*: Curcumin. FPF*: Fine Particle Fraction.

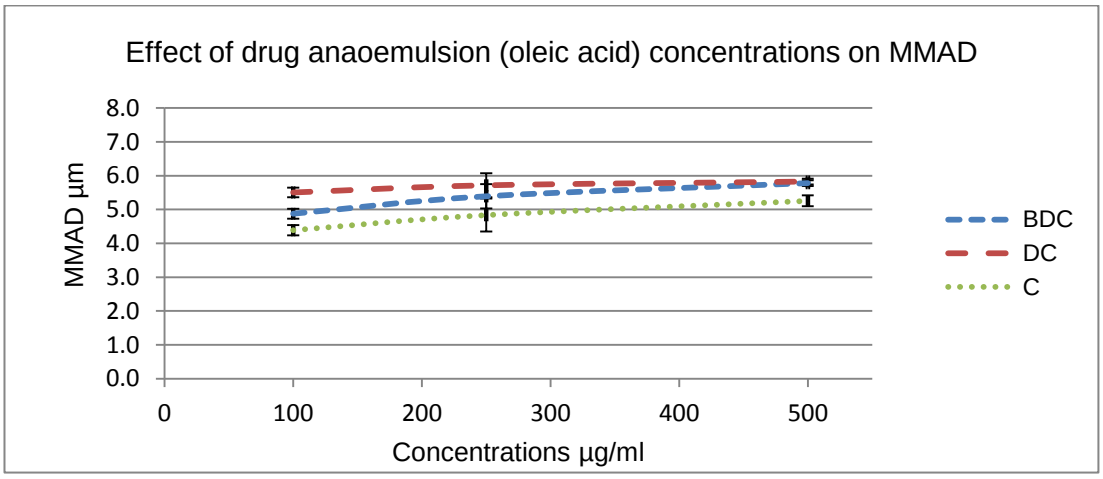

Figure 6.13 The relationship between the nanoemulsion concentrations (using oleic acid oil) and the Mass Median Aerodynamic Diameters (MMAD) of curcuminoids. BDC*: Bisdemethoxycurcumin. DC*: Demethoxycurcumin. C*: Curcumin.

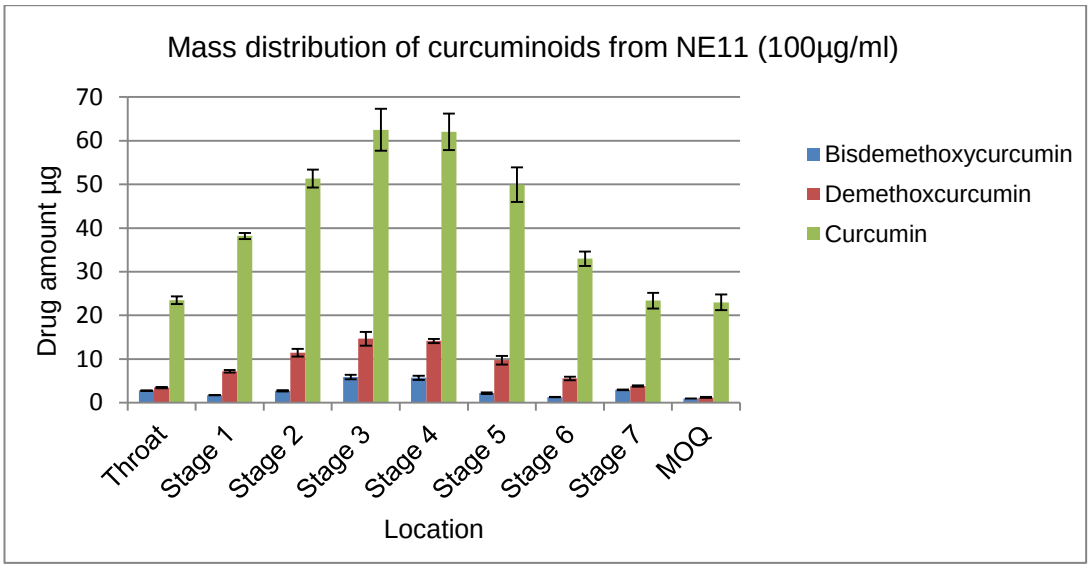

Figure 6.14 The mean (n=3, SD) of mass distribution of curcuminoids nanoemulsion (NE11, with oleic acid oil) in NGI using jet nebuliser at flow 15 L/min.

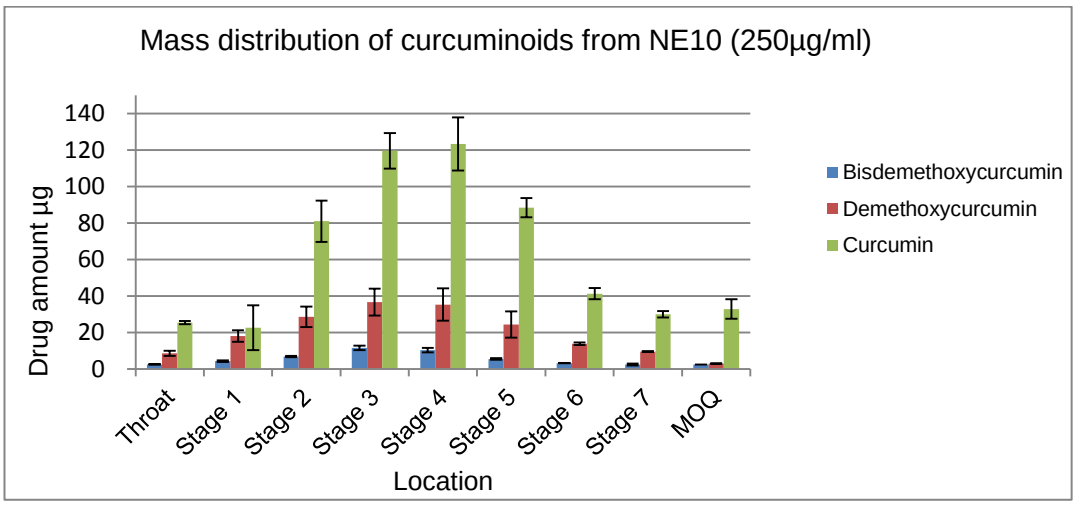

Figure 6.15 The mean (n=3, SD) of mass distribution of curcuminoids nanoemulsion (NE10, with oleic acid oil) in NGI using jet nebuliser at flow 15 L/min

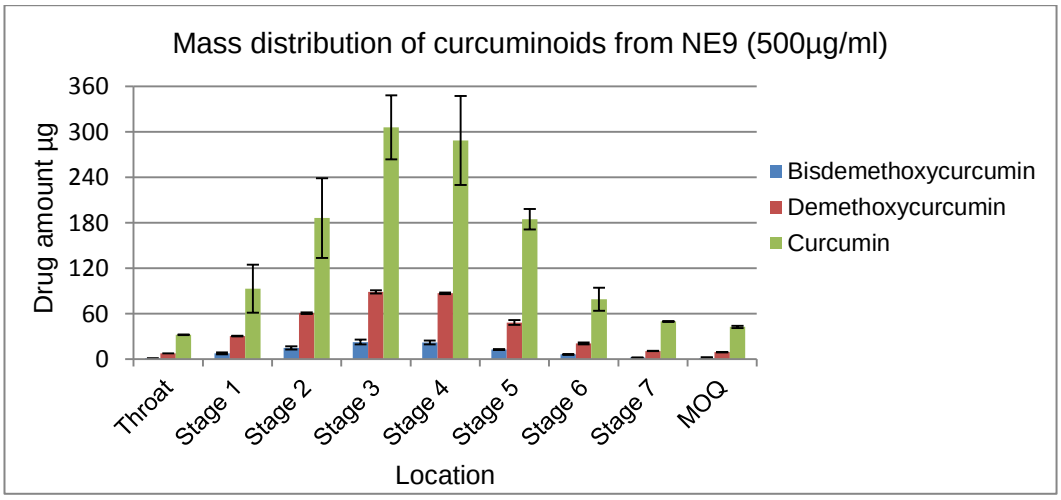

Figure 6.16 The mean (n=3, SD) of mass distribution of curcuminoids nanoemulsion (NE9, with oleic acid oil) in NGI using jet nebuliser at flow 15 L/min.

The results illustrate an improvement in FPF (%) and MMAD compared to suspension formulations. The FPF (%) ranged from 48% to 46% for curcumin and from 44% to 41% for demethoxycurcumin and 45% to 42% for bisdemethoxycurcumin. The variation in MMAD was very small throughout the nanoemulsion formulations for different curcuminoid concentrations (NE9, NE10 and NE11), The lowest MMAD was 4.3µm for the NE11 (100µg/ml) and the highest was 5.8µm for the NE9 (500µg/ml) whereas in suspension formulation the lowest MMAD was 5.8µm and the highest was 6.66µm (for concentration of 500µg/ml) and 7.0µm (for 1000µg/ml). This shows that the suspension formulation containing curcuminoid at a concentration above 500µg/ml is not suitable for inhalation due to low FPF (%) and high MMAD. These findings are in agreement with Amani's results that were reported for commercial budesonides suspension using jet nebuliser device.

Nanoemulsion formulations using limonene oil: The aerodynamic characterisation of the nanoemulsion formulations using limonene (NE5, NE4

and NE3) for curcumin and demethoxycurcumin and bisdemethoxycurcumin are presented in table 6.17. Figures (6.17 and 6.18) display the effect of the drug concentrations, of the nanoemulsion, on the FPF and MMAD. The mass distribution of the drugs throughout the NGI stages is illustrated in figures 6.19, 6.20 and 6.21.

Table 6.17 The mean (n=3) of the aerodynamic characterisation of curcuminoids nanoemulsion with limonene oil formulations using jet nebuliser at flow 15 L/min

Drug	Formulations	FPF%	MMAD (µm)	GSD
Bisdemethoxycurcumin	NE5 (100µg/ml)	51.32	4.52	2.75
	NE4 (250µg/ml)	46.17	5.34	2.35
	NE3 (500µg/ml)	44.86	5.53	2.20
Demethoxycurcumin	NE5 (100µg/ml)	47.30	4.97	2.20
	NE4 (250µg/ml)	46.12	5.12	2.16
	NE3 (500µg/ml)	44.07	5.63	2.19
Curcumin	NE5 (100µg/ml)	50.72	4.50	2.42
	NE4 (250µg/ml)	50.15	4.73	2.24
	NE3 (500µg/ml)	44.70	5.55	2.20

FPF%*: the percentage of Fine Particle Fraction. MMAD*: Mass Median Aerodynamic Diameter. GSD*: Geometric Standard Deviation. FPD*: Fine Particle Dose.

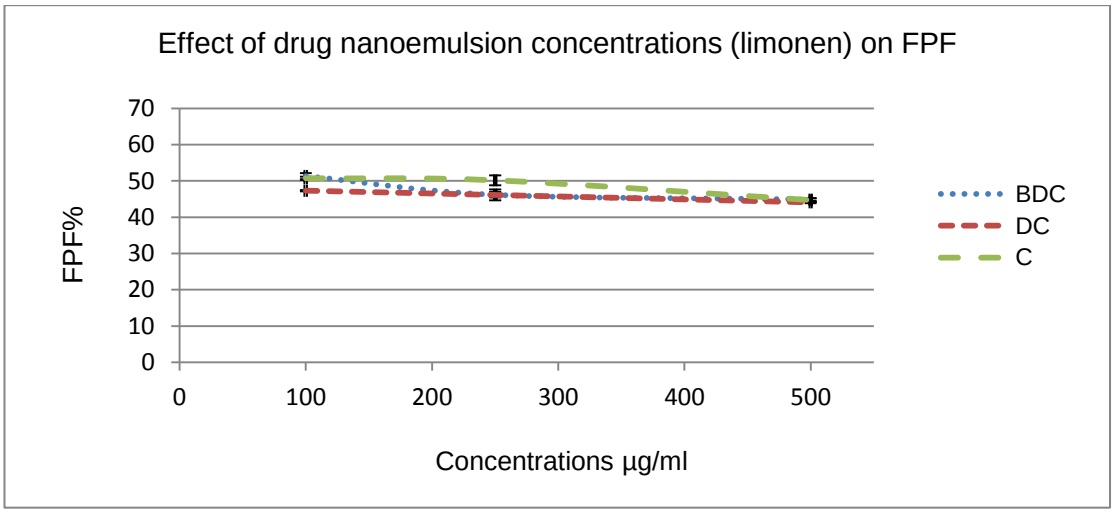

Figure 6.17 The relationship between the drug nanoemulsion concentrations (using limonene oil) and the Fine Particle Fraction of curcuminoids. BDC*: Bisdemethoxycurcumin. DC*: Demethoxycurcumin. C*: Curcumin. FPF*: Fine Particle Fraction

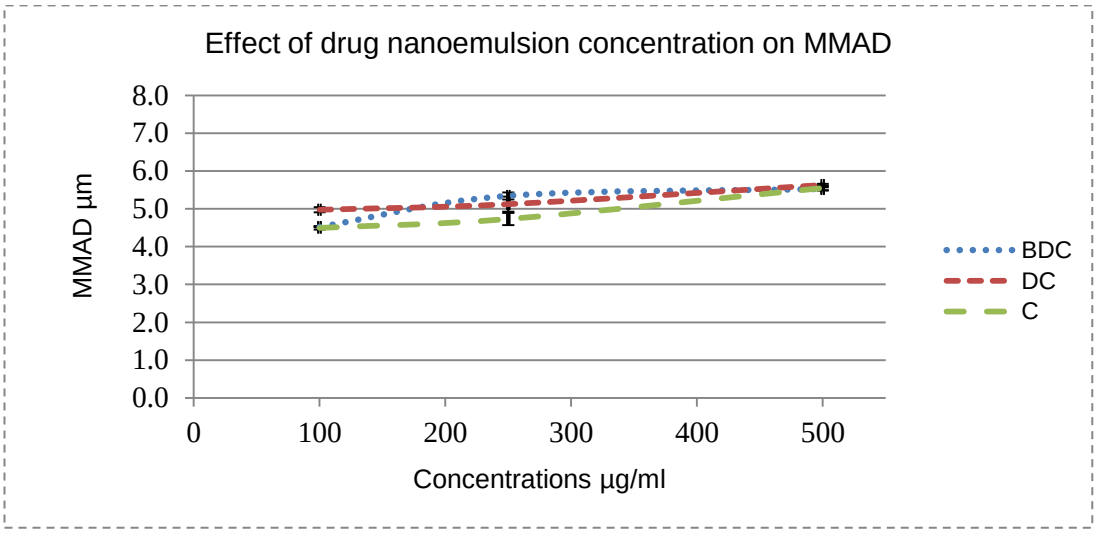

Figure 6.18 The relationship between the drug nanoemulsion concentrations (using limonene oil) and the Mass Median Aerodynamic Diameters (MMAD) of curcuminoids. BDC*: Bisdemethoxycurcumin. DC*: Demethoxycurcumin. C*: Curcumin.

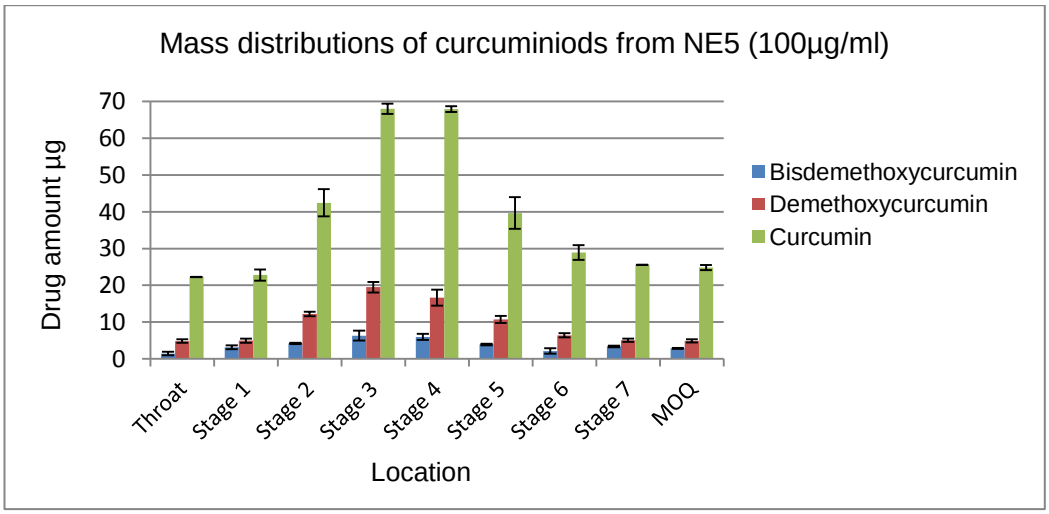

Figure 6.19 The mean (n=3, SD) of mass distribution of curcuminoids nanoemulsion (NE5, with limonene oil) in NGI using jet nebuliser at flow 15 L/min.

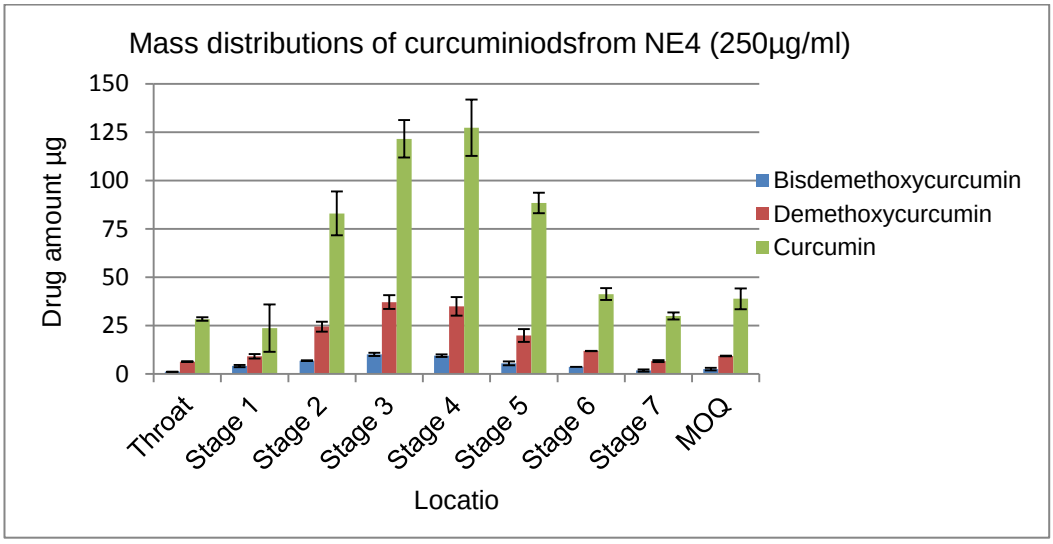

Figure 6.20 The mean (n=3, SD) of mass distribution of curcuminoids nanoemulsion (NE4, with limonene oil) in NGI using jet nebuliser at flow 15 L/min.

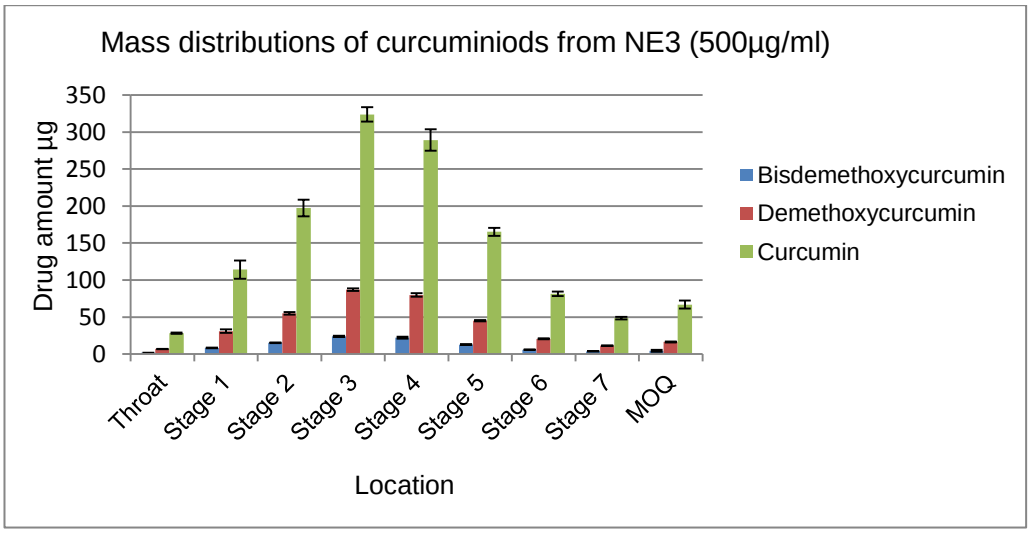

Figure 6.21 The mean (n=3, SD) of mass distribution of curcuminoids nanoemulsion (NE3, with limonene oil) in NGI using jet nebuliser at flow 15 L/min.

The results of the limonene nanoemulsion formulation demonstrate an improvement in FPF and the MMAD compared to suspension formulations. Also the limonene nanoemulsion indicates a slight improvement in FPF over the oleic acid nanoemulsion formulations.

The FPF (%) ranged from 44% to 50% for curcumin and from 44% to 47% for demethoxycurcumin and 45% to 51% for bisdemethoxycurcumin. The variation in MMAD was very small throughout the nanoemulsion formulations for different curcuminoid concentrations (NE3, NE4 and NE5). The lowest MMAD was 4.5µm for the NE5 (100µg/ml) and the highest was 5.6µm for the NE3 (500µg/ml) whereas in suspension formulation the lowest MMAD was 5.8µm and the highest was 6.66µm (for concentration of 500µg/ml) and 7.0µm (for 1000µg/ml). These results are similar to the oleic acid nanoemulsion formulation (NE9, NE10 and NE11) and in agreement with Amani's results when nanoemulsion was used for budesonides formulation using a jet nebuliser device.

The summary of the comparison of FPF, for the three formulations, suspension, limonene nanoemulsion and oleic acid nanoemulsion, is demonstrated in figures 6.22, 6.23, and 6.24.

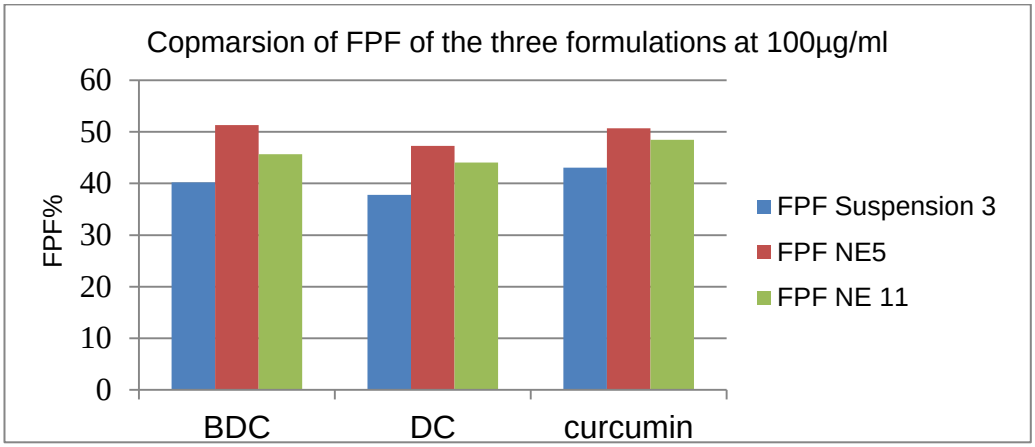

Figure 6.22 Comparison of fine particle fraction (FPF) between nanoemulsion formulations (NE5: limonene oil, NE11: oleic acid oil) and suspension 3 of curcuminoids for the same concentration (100µg/ml). BDC*: bisdemethoxycurcumin, DC*: demethoxycurcumin

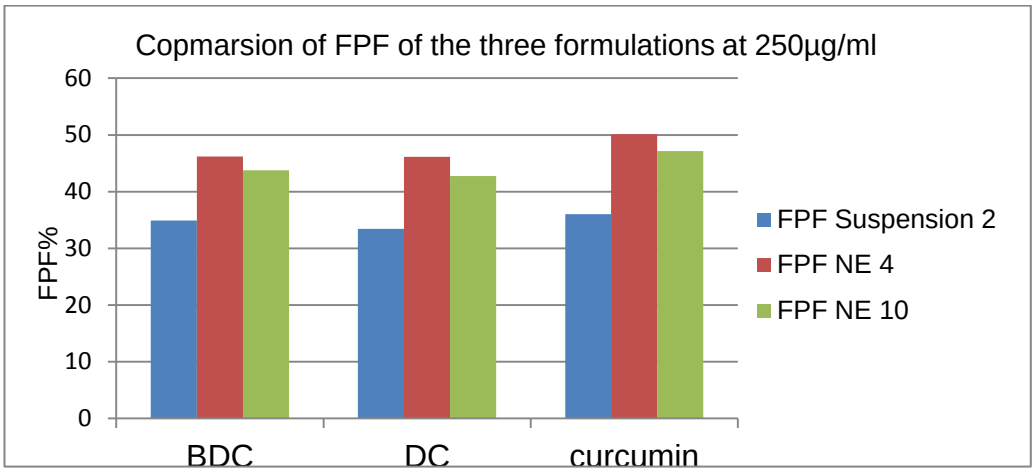

Figure 6.23 Comparison of fine particle fraction (FPF) between nanoemulsion formulations (NE4: limonene oil, NE10: oleic acid oil) and suspension 2 of curcuminoids for the same concentration (250µg/ml). BDC*: bisdemethoxycurcumin, DC*: demethoxycurcumin.

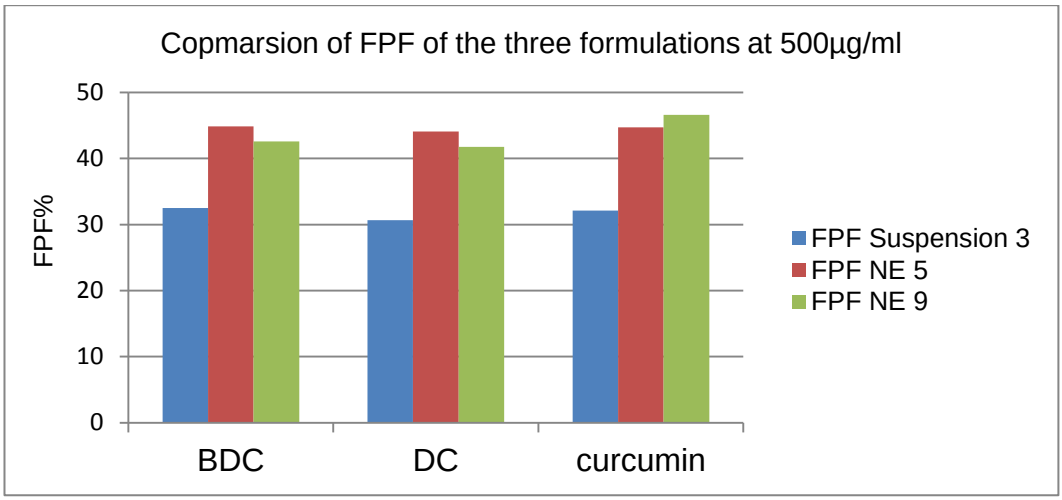

Figure 6.24 fine particle fraction (FPF) comparison between nanoemulsion formulations (NE5: limonene oil, NE11: oleic acid oil) and suspension 3 of curcuminoids for the same concentration (100µg/ml). BDC*: bisdemethoxycurcumin, DC*: demethoxycurcumin.

In all nanoemulsion formulations, the FPF (%) and MMAD were independent of the drug concentration, whereas in the suspension formulations FPF (%) and MMAD greatly varied with respect to the drug concentrations.

In the nanoemulsion formulations, the respirable fraction was larger compared to the suspension formulation, and the mass median diameter value was smaller. The drug amount which remained in the nebuliser chamber was significantly greater in the suspension formulations compared to nanoemulsion formulations. These findings were in agreement with the study reported by (Amani et al. 2010). The difference in the aerodynamic performance between the nanoemulsion and suspension formulations is attributed to the particle size of the drug in each formulation, as the particle size in the nanoemulsion is in the range of 12nm and 35nm but in the suspension, the particle size was 1.6µm. Since nebulisers produce droplets sized from 5µm to almost 1µm. The author theory for explaining the differences in the aerodynamic performance between suspension and nanoemulsion formulations is that when the drug in a

suspension form, it will occupy the droplet based on its size. For example, if the drug particles are 1.6-2µm, the drug will be carried in the larger nebulised droplet only as is demonstrated in figure 6.25, therefore the smaller nebulised droplet will be free of the drugs. Consequently, the microsuspension formulations exhibit a lower FPF (%) and higher MMAD. In the case of nanoemulsion particles, the drug is very small in size (12nm to 35nm) and the particles size is more uniformed, therefore all nebulised droplets will be fully filled with nanoparticles of the drug. For these reasons, nanoemulsion formulations exhibited much better fine particle fractions (FPF) and hence achieved deeper particle deposition compared to microsuspension formulations.

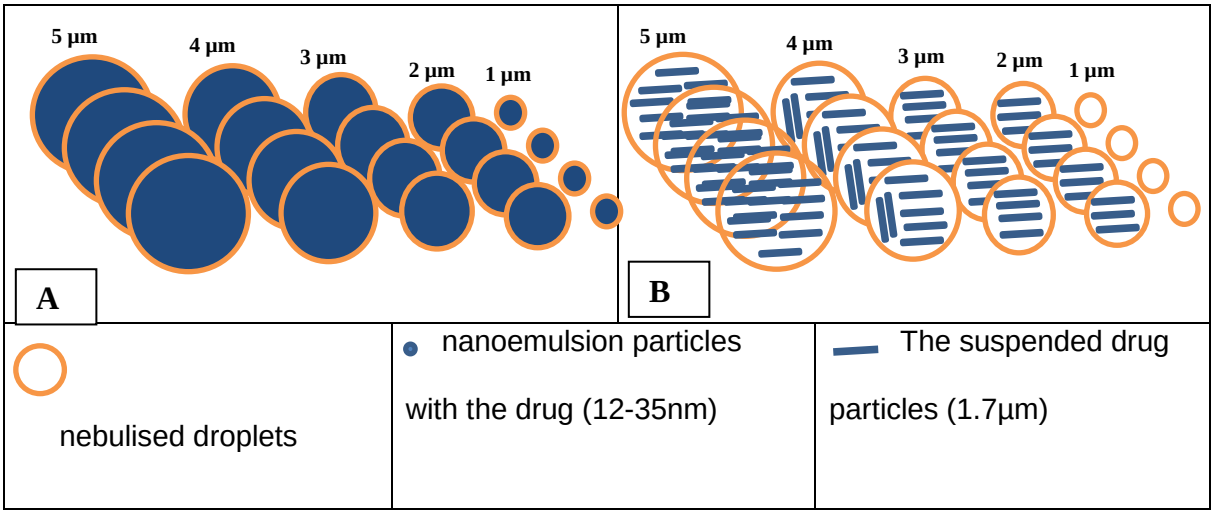

Figure 6.25. Nebulised droplets from nanoemulsion formulation (A) and from microsuspension formulation (B)

The nanoemulsion formulation demonstrates its ability to reach to a deep lung deposition as particles reached to stage7 and MOQ (and the filter that is placed after the MOQ) in the *in vitro* studies which represent the alveoli. This clearly shows that aerosol nanoemulsion formulation has the potential to be used for the treatment of both central and peripheral lung cancer.

6.3.11. Genotoxicity of curcumin nanoemulsion

Genotoxicity tests of pharmaceutical products before commercialisation are required by regulatory agencies worldwide (Snyder and Green 2001). Nanoparticles were reported to have a potential harmful side effect to humans and could be genotoxic too (Chan 2006; Magdolenova et al. 2013). This could be attributed to a direct interaction of the nanoparticles with genetic material, or indirect damage from nanoparticle-induced reactive oxygen species, or by releasing toxic ions (Kisin et al. 2007; Barnes et al. 2008). Nanoparticles, due to their unique size, have the ability to cross the cellular membrane and may reach the nucleus by diffusion across the nuclear membrane or by transportation through nuclear pore complex, and directly interact with DNA (Barillet et al. 2010). Nanoparticles with size 8nm to 10nm enter through a nuclear pore, whereas larger nanoparticle size 15nm to 60nm may access to the DNA in the dividing cells during the mitosis when the nuclear membrane dissolves (Xing-Jie Liang 2008; Singh et al. 2009; Magdolenova et al. 2013).

Nanoemulsion of curcumin genotoxicity, DNA damage, has not been examined before. The genotoxicity of NE3, NE4 and NE5 is presented in figure 6.26 and NE9, NE10, and NE11) is shown in figure 6.27. The data indicates that there is no genotoxicity for the curcumin nanoemulsion on lymphocytes cells compared to the negative control. Changing the oil in the nanoemulsion also did not show any changes in the DNA damage too. DNA seems to be intact as is expressed in figure 6.28, as there was no comet for DNA. This finding is in agreement with an *in vivo* study which reported that solid nanoparticles (in suspension form) of curcumin are not genotoxic (Dandekar et al. 2010). Moreover, it was reported that curcumin protect lymphocytes cells from genotoxicity induced by 131 radioiodine (Shafaghati et al. 2014), and was also used to reduce the

genotoxicity of chemotherapies as Mitomycin C and Cisplatin (Antunes et al. 2005; Siddique et al. 2010). This protection of curcumin to the cells that being damaged is attributed to its antioxidant activity and the potential free radical scavengers (Srinivasan et al. 2006).

These results could confirm the safety of the developed curcuminoids nanoemulsion formulations. Comet assay demonstrated that there is no DNA damage when the cells treated with curcumin nanoemulsion.

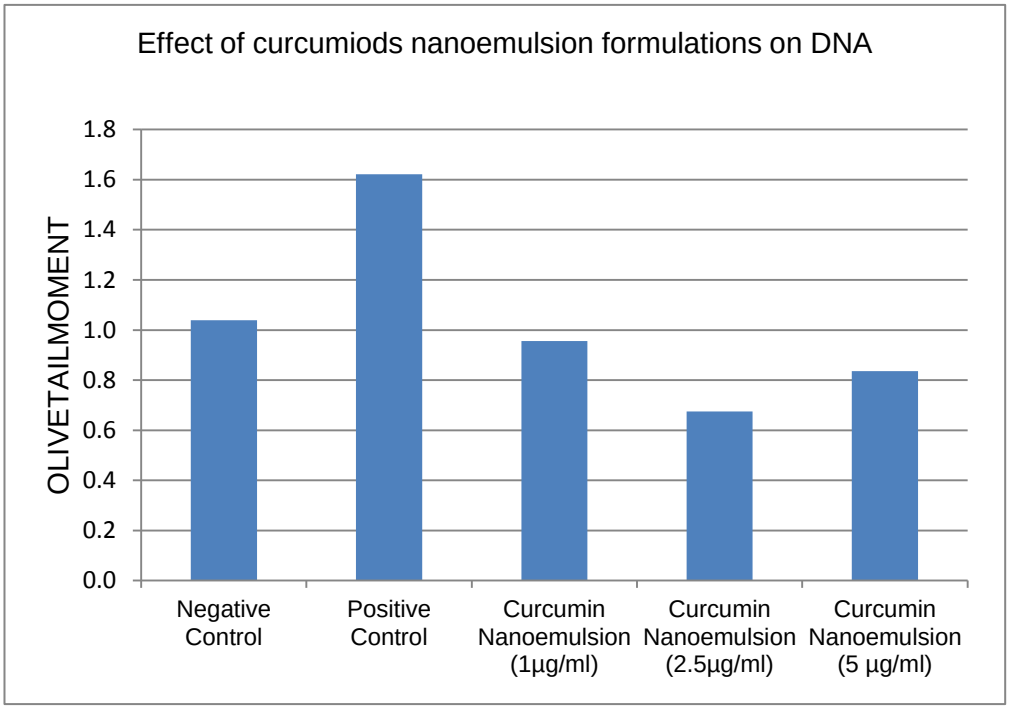

Figure 6.26 Effect of curcuminoids nanoemulsion (with limonene oil) formulations on lymphocyte's DNA

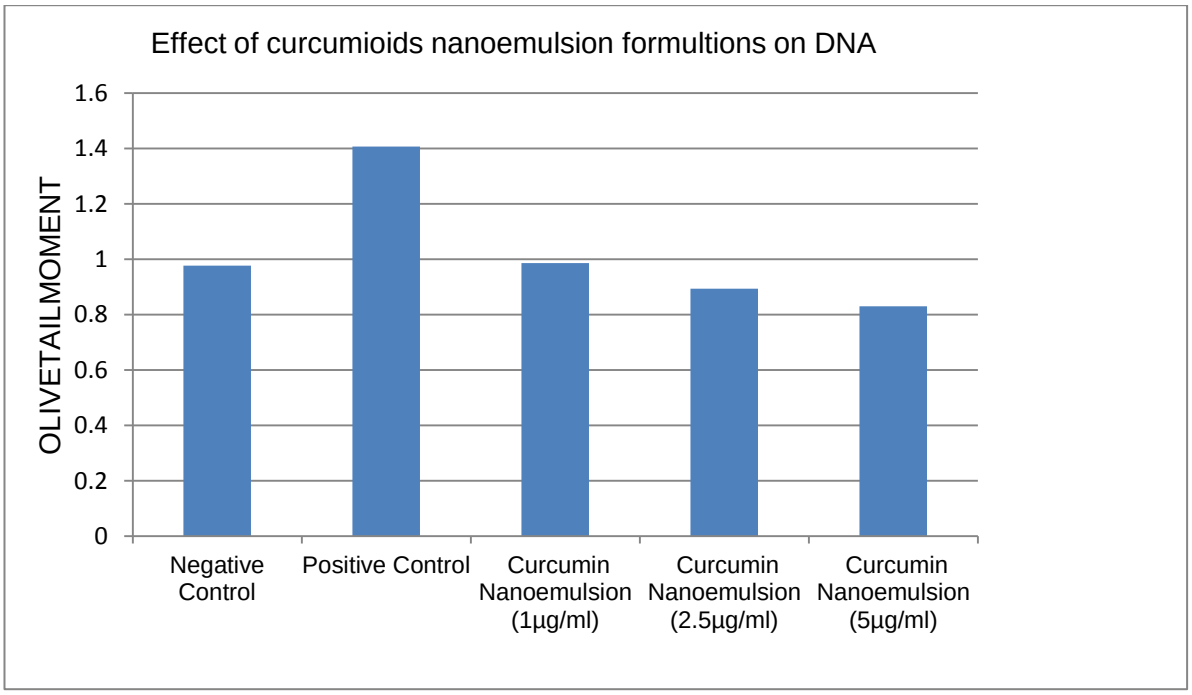

Figure 6.27 Effect of curcuminoids nanoemulsion (with oleic acid oil) formulations on lymphocyte's DNA

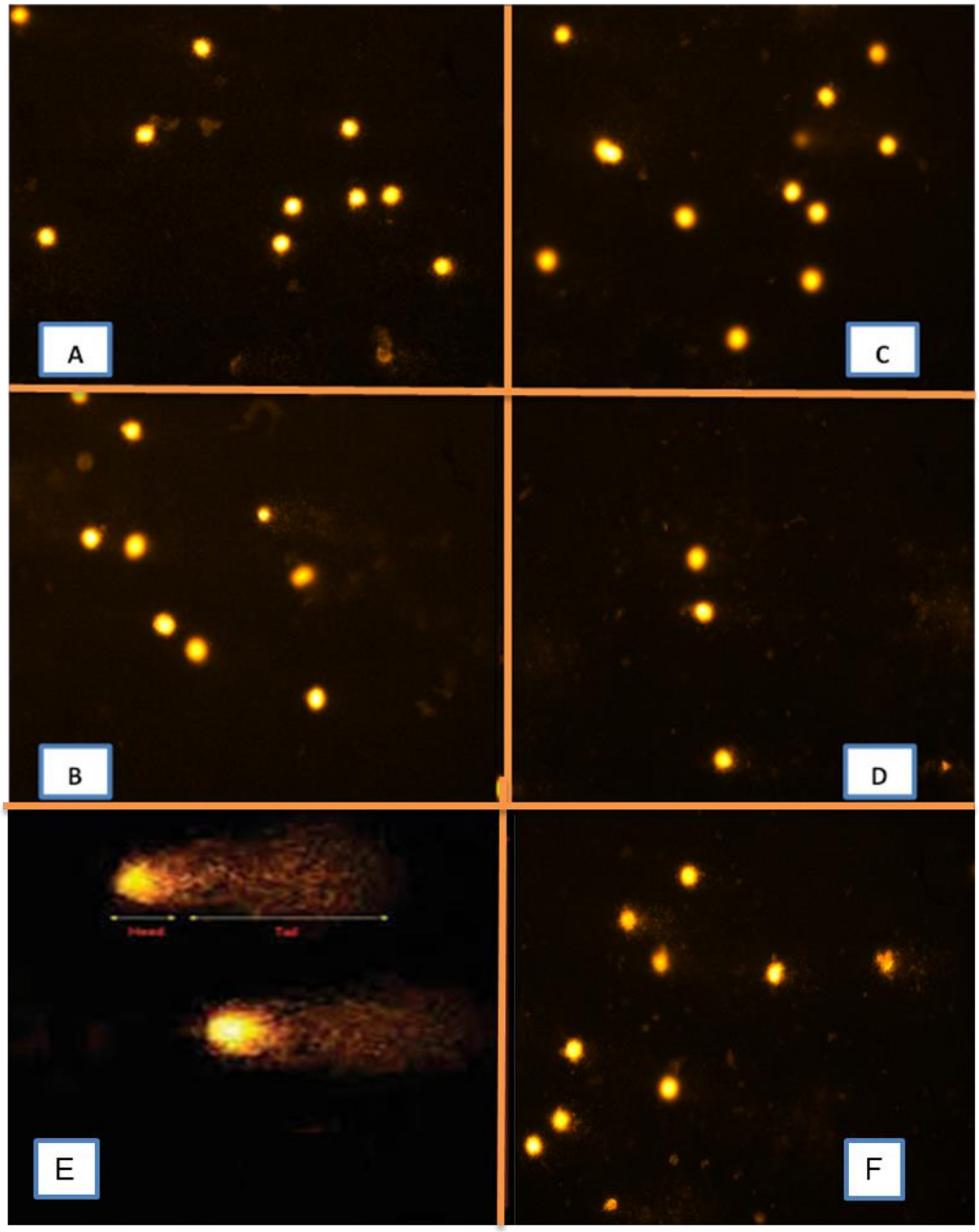

Figure 6. 28 Lymphocyte DNA under a fluorescence microscope after treatment with curcuminoids nanoemulsion formulations, A & C: treated with curcuminoids nanoemulsion using oleic acid oil at concentrations 1 & 5 µg/ml. B &D: treated with curcuminoids nanoemulsion using limonene oil at concentration 1 & 5 µg/ml. E is an example of positive control, and F is a negative control.

6.4. Conclusion

The curcuminoids nanoemulsion formulations were prepared using a very small amount of surfactants (ranging from 1.6% to 0.33%). The formulations were found to be stable at room temperature. The particle size ranged from 12nm to

35nm. The osmolality and pH of the formulations are suitable for inhalation; the viscosity was determined. The suspension formulations were also prepared according to FDA regulations (i.e. in regards of the amount of surfactant). The osmolality and pH of the suspension are presented to be suitable for the respiratory system.

The aerosol output for nanoemulsion was far superior to suspension formulation, as 50% of the drug (suspension) remained in the nebuliser chamber upon completion of the run, while the residual nanoemulsion remaining in the chamber was less than 30%. Moreover, suspension formulation would be less convenient to patients as it took longer to complete nebulisation compared to nanoemulsion nebulised formulations. The *in vitro* aerosolisation performances for all formulations of curcuminoids were examined using NGI. The performance of the suspension was found to be drug concentration dependent, whereas the performance of nebulised nanoemulsion was independent. The fine particle fraction of the nanoemulsion was much better than the suspension formulation.

It is clear that nanoemulsion has the ability to penetrate into both lung zones (central and peripheral zone), therefore, nanoemulsion could be used for lung cancers, whether they are located in the central or peripheral zone. On the other hand, suspension would be more located in the lung central zone, therefore, could be an option for those cancers located in the lung central zone. Since, curcuminoid particles in nanoemulsions (12nm and 35nm) are smaller than in the suspension (1.6µm); therefore, the nanoemulsion could be more effective against cancer cells. In addition, curcuminoid particles in the nanoemulsion formulation are in liquid form, so this increases both activity and onset of action of the drug compared to solid particles in the suspension form.

The nanoemulsion formulation with the small amount of surfactants was found to be safe to DNA and did not cause any damage to genetic information of the lymphocyte cells. Therefore, this could indicate the safety and suitability of the nanoemulsion formulation to be used for further inhalation studies in both animals and in humans.

CHAPTER SEVEN

General Conclusion and Future Work

Chapter 7: General conclusion and future work

7.1 General Conclusion

This thesis is considered the first study to assess the suitability of using curcuminoids (curcumin, demethoxycurcumin and bisdemethoxycurcumin) for inhalation as dry powder inhalers without excipients and nebulisers, in which FPF% and the MMAD of curcumin, demethoxycurcumin and bisdemethoxycurcumin have been determined. The need for such formulations for curcuminoids originated from two points, firstly curcuminoids have strong anticancer activities but they have low bioavailability. Secondly, lung cancer is considered responsible for the highest rate of cancer deaths, also, [1]when anticancer agents are taken orally or IV; they reach the lungs in low concentrations which limit their effects. Therefore, delivering curcuminoids directly into the lungs will treat the lung (disease) cancer locally; the concentrations of curcumin will be high at the cancer sites and low in the systemic circulations.

The new dry powder inhaler formulation of curcumin, without excipient, is safer than any other formulations that contain additives (excipients which are not approved by FDA). The nebuliser formulation of curcuminoids, using nanoemulsion and microsuspension preparations, covers the needs of elderly and child patients and those who are unable to use DPI. These new inhaled formulations (DPI and nebuliser) show a promising *in vitro* aerodynamic behaviour, which makes these formulations available for *in vivo* studies. As the characteristics of inhalable particles, such as size, shapes and surface energy, have an impact on the formulation performance and deposition profile of the

[1] The low drug concentration, is expected, at the lung cancer site, when the anticancer agents are administrated IV or orally.

inhaled drug, theses formulations were prepared by air jet milling and sonocrystallisation, which are considered the most simple and fastest techniques in producing the desired particles. Furthermore, they are known as easy, less time consuming and an inexpensive process of particle production. The output of the *in vitro* samples was analysed using a developed and validated HPLC method.

Environment friendly HPLC (Microemulsion high performance liquid chromatography) and conventional methods have been developed and validated for curcuminoid solution analysis, according to ICH guidelines. Both methods were sensitive, linear, precipices and accurate. The separation of curcuminoids (curcumin, demethoxycurcumin and bisdemethoxycurcumin), in both methods, was achieved in about 10 mins. The mobile phase of the microemulsion method offers several advantages over the conventional method that has a mobile phase composed of 55% acetonitrile and 45% phosphate buffer. These advantages due to the fact that 90% of the mobile phase was composed of phosphate buffer which makes the method inexpensive and nature-friendly and green as it has very low organic solvents.

A dry powder inhaler of curcuminoids was prepared using micronized particles which are produced by an air jet milling process. The formulation that contains the curcumin particle size of D_{50} 2.5µm (D_{90}=5.5µm) illustrated higher inhalation performance compared to the formulation with a particle size of D_{50} 3.5µm (D_{90} 7.7µm). The obtained FPF% of the micronized DPI formulations (D_{50} 2.5µm) was very close to the recent published formulations with additives. The crystal structure of milled curcumin particles was found to be in form 1. The structural analysis (XRPD, DSC) has confirmed that the micronized curcumin particles have polymorph1 as the unprocessed material.

A dry powder inhaler of curcuminoids using a sonocrystallisation technique was successfully achieved without any excipients. Dry powder inhaler formulations, which contain curcuminoid particles that were obtained from ethanol as a solvent and heptane as antisolvents, have shown a superior deposition profile compared to those formulations with jet milled particles and with those contained particles precipitated from acetone (solvent) and heptane as an antisolvent. Moreover, the aerodynamic behaviour of this formulation, which showed the best inhalation performance, was similar to the recent published work with excipients, which are not approved by the FDA for inhalation (Myrdal et al. 2014). The particle structure analysis (DSC&XRPD) of sonocrystallised curcumin particles has shown curcumin crystal structure in form 3, when the particles were obtained from isopropanol and water, and curcumin polymorph 1, when the curcumin particles were precipitated from ethanol and water as an antisolvent, and also curcumin polymorph 1 was formed when curcumin particles were precipitated from ethanol, acetone, and isopropanol solvents with heptane as antisolvent. The surface energy of the sonocrystallised particles from ethanol was lower than the surface energy of particles obtained from acetone and from the unprocessed materials. The particle shapes varied depending on the solvent-antisolvent used in the system during sonocrystallisation.

The simple approaches of obtaining inhalable curcuminoid particles without involving any extra excipients were an advantage of this study compared to the recently published one. This makes the dry powder inhaler formulations of curcumin safer and suitable for the respiratory system. Another advantage is that the aerodynamic parameters of curcuminoid components, curcumin (C),

Demethoxycurcumin (DC) and Bisdemethoxycurcumin (BDC) were individually measured in this thesis.

Nanoemulsions for nebulisation of curcuminoids were successfully prepared with a very low amount of surfactant (tween 80), which ranged from 1.25% to 0.31%. This nanoemulsion system has the lowest tween 80, compared to the published nanoemulsion for budesonide formulation, which contains 10% of tween 80. Also, a microsuspension of curcuminoids was prepared according to the FDA regulations (tween 80 is 0.02%). The osmolality, pH and the viscosity of the nebuliser formulations meet the inhalation criteria. The aerodynamic behaviour of suspension formulation has been found to be drug concentration dependent, e.g. the low drug suspension concentration shows better performance on the higher drug concentration as FPF% decreased as the drug concentration increased. In the nanoemulsion preparations, the aerodynamic performance was independent of the drug concentrations. The inhalation profile of the nebulised nanoemulsion was far superior on suspensions formulations; this is because of lower particle size as well as the surface tension of the nanoemulsion formulations. Moreover, the aerosol output of the nanoemulsion increased as the amount which was left in the nebuliser chamber decreased compared to the suspension formulations. The nanoemulsion of curcumin has been found not to be genotoxic on lymphocyte blood cells of human. The lung deposition of the nebulised nanoemulsion has shown deep lung penetrations, this could make the nanoemulsion formulation suitable for both lung cancer types which exist in either the peripheral or central zones of the lungs. The aerodynamic parameters (FPF%, MMAD and GSD) of curcuminoid components, curcumin, demethoxycurcumin and bisdemethoxycurcumin were individually determined.

7.2 Future Work

The *in vitro* results present a promising aerodynamic behaviour of dry powder inhaler and nebuliser of curcuminoid formulations. Therefore, it would be useful to extend these *in vitro* findings to *in vivo* study on animals with lung cancer.

The *in vitro* testing of the inhaled dry powder of curcumin was carried out with one flow rate and volume inhalation, which is according to standard compendial methodology. It would be interesting to do the test with different inhalation flows and inhalation volumes, as patients have different stages of the disease, and hence they have different lung capacity and different inhalation force. This study was also carried out using one type of DPI device (which is a multi-dose reservoir). However, Inhaler devices have different resistance which has an effect on the formulation preference as they could require more or less inspiration flow to disperse the drug particles from the carrier. Hence, it is suggested to extend this work to include different inhaler devices such as a single dose inhaler device.

In general, in dry powder inhaler formulation, formulators consider D_{50} to represent the drug particle size for inhalation formulation. It states that the D_{50} needs to be less than 5µm. From this work, it would be recommended to consider the D_{90} too, which should be 5µm or less to obtain a better inhalation performance (FPF%).

In this project, we have established a relation between the work of adhesion and cohesion and with drug concentration onto the carrier that affects the aerodynamic behaviour of the inhaled particles. This relation was examined when the work of cohesion is equal or smaller than the work of adhesion. It is suggested to extend this work further to investigate the performance of DPI

formulation when the work of cohesion is higher than the work of adhesion as we are expecting in this case that the less amount of the drug onto the surface, the better performance of the formulation of the DPI. In the nebuliser formulation, only one type of nebuliser devices was used which is Sidestream; there are other nebuliser devices such as Omron and Aeroneb, which may give different performance of the formulations.

Studies using a combination therapy of curcumin and anticancer agents, such as paclitaxel, doxorubicin and cisplatin, have shown that curcumin produces synergistic effects with chemotherapeutic drugs against various cancer cell lines (Ganta and Amiji 2009; Duarte et al. 2010; Wang et al. 2013), therefore it would interesting to investigate the feasibility of producing inhaled formulation which contains the combination therapy.

CHAPTER EIGHT

References

Chapter 8: References

8.1 References

Abbas, A., Srour, M., Tang, P., Chiou, H., Chan, H.-K. and Romagnoli, J. A. (2007) Sonocrystallisation of sodium chloride particles for inhalation. *Chemical Engineering Science* 62 (9), 2445-2453.

Adi, H., Larson, I., Chiou, H., Young, P., Traini, D. and Stewart, P. (2008) Role of agglomeration in the dispersion of salmeterol xinafoate from mixtures for inhalation with differing drug to fine lactose ratios. *Journal of Pharmaceutical Sciences* 97 (8), 3140-3152.

Aggarwal, B. B., Kumar, A. and Bharti, A. C. (2003) Anticancer potential of curcumin: preclinical and clinical studies. *Anticancer Research* 23 (1A), 363-398.

Aggarwal, B. B., Surh, Y.-J. and Shishodia, S. (2007) *The molecular targets and therapeutic uses of curcumin in health and disease.* Vol. 595. Springer.

Ahmad, F., Khar, R., Sultana, S. and Bhatnagar, A. (2009) Techniques to develop and characterize nanosized formulation for salbutamol sulfate. *Journal of Materials Science: Materials in Medicine* 20, 71-76.

AL-Jammal, M., Al Ayoub, Y. and Assi, K. (2015) Development and Validation of Micro Emulsion High Performance Liquid Chromatography (MELC) Method for the Determination of Nifedipine in Pharmaceutical Preparation. *Pharmaceutica Analytica Acta* 2015.

Albertini, R. J., Anderson, D., Douglas, G. R., Hagmar, L., Hemminki, K., Merlo, F., Natarajan, A., Norppa, H., Shuker, D. E. and Tice, R. (2000) IPCS guidelines for the monitoring of genotoxic effects of carcinogens in humans. *Mutation Research/Reviews in Mutation Research* 463 (2), 111-172.

Allen, T. (1990) Sampling and sizing from the atmosphere. *Particle size measurement.* Springer. 72-123.

Almeida, C. and Barry, S. (2010) *Cancer : basic science and clinical aspects.* S 616 006 6. Oxford: Wiley-Blackwell.

Althanyan, M., Assi, K., Clark, B. and Hanaee, J. (2011) Microemulsion high performance liquid chromatography (MELC) method for the

determination of terbutaline in pharmaceutical preparation. *Journal of pharmaceutical and biomedical analysis* 55 (3), 397-402.

Althanyan, M., Nasser, A., Assi, H., Clark, B. and Assi, K. H. (2016) Microemulsion High Performance Liquid Chromatography (MELC) for Determination of Terbutaline in Urine Samples. *International Journal of Pharmaceutical Sciences Review and Research*

Althanyan, M. S. (2011) Use of nanoemulsion liquid chromatography (NELC) for the analysis of inhaled drugs: investigation into the application of oil-in-water nanoemulsion as mobile phase for determination of inhaled drugs in dosage forms and in clinical samples.PhD.Thesis. The University of Bradford.

Altria, K. D. (1999) Overview of capillary electrophoresis and capillary electrochromatography. *Journal of Chromatography A* 856 (1), 443-463.

Amani, A., York, P., Chrystyn, H. and Clark, B. J. (2010) Evaluation of a Nanoemulsion-Based Formulation for Respiratory Delivery of Budesonide by Nebulizers. *AAPS PharmSciTech* 11 (3), 1147-51.

Amani, A., York, P., Chrystyn, H., Clark, B. J. and Do, D. Q. (2008) Design, characterization and in vitro aerosolisation performance of a nanoemulsion for nebulisation of hydrophobic drugs. *Thesis, University of Bradford*.

AmericanCancerSociety (2012) Lung Cancer Fact Sheet | American Lung Association.

Ammon, H. P. and Wahl, M. A. (1991) Pharmacology of Curcuma longa. *Planta medica* 57 (01), 1-7.

Anand, P., Kunnumakkara, A. B., Newman, R. A. and Aggarwal, B. B. (2007) Bioavailability of curcumin: Problems and promises. *Molecular Pharmaceutics* 4 (6), 807-818.

Anand, P., Nair, H. B., Sung, B., Kunnumakkara, A. B., Yadav, V. R., Tekmal, R. R. and Aggarwal, B. B. (2010) Design of curcumin-loaded PLGA nanoparticles formulation with enhanced cellular uptake, and increased bioactivity in vitro and superior bioavailability in vivo. *Biochemical Pharmacology* 79 (3), 330-338.

Anand, P., Sundaram, C., Jhurani, S., Kunnumakkara, A. B. and Aggarwal, B. B. (2008) Curcumin and cancer: An "old-age" disease with an "age-old" solution. *Cancer Letters* 267 (1), 133-164.

Anderson, D., Schmid, T. E., Baumgartner, A., Cemeli-Carratala, E., Brinkworth, M. H. and Wood, J. M. (2003) Oestrogenic compounds and oxidative stress (in human sperm and lymphocytes in the Comet assay). *Mutation Research/Reviews in Mutation Research* 544 (2), 173-178.

Angelidis, G., Protonotariou, S., Mandala, I. and Rosell, C. M. (2016) Jet milling effect on wheat flour characteristics and starch hydrolysis. *Journal of food science and technology* 53 (1), 784-791.

Antunes, L. M. G., Araújo, M. C. P., Dias, F. d. L. and Takahashi, C. S. (2005) Effects of H2O2, Fe2+ and Fe3+ on curcumin-induced chromosomal aberrations in CHO cells. *Genetics and Molecular Biology* 28 (1), 161-164.

Ardizzoni, A., Hansen, H., Dombernowsky, P., Gamucci, T., Kaplan, S., Postmus, P., Giaccone, G., Schaefer, B., Wanders, J. and Verweij, J. (1997) Topotecan, a new active drug in the second-line treatment of small-cell lung cancer: a phase II study in patients with refractory and sensitive disease. The European Organization for Research and Treatment of Cancer Early Clinical Studies Group and New Drug Development Office, and the Lung Cancer Cooperative Group. *Journal of clinical oncology* 15 (5), 2090-2096.

Aulton, M. E. (2009) *Aulton's pharmaceutics : the design and manufacture of medicines.* 3rd edition. Edinburgh: Churchill Livingstone Elsevier.

Ayres, J., Forsberg, B., Annesi-Maesano, I., Dey, R., Ebi, K., Helms, P., Medina-Ramón, M., Windt, M. and Forastiere, F. (2009) Climate change and respiratory disease: European Respiratory Society position statement. *Eur Respir J* 34 (2), 295-302.

Bacanlı, M., Başaran, A. A. and Başaran, N. (2015) The antioxidant and antigenotoxic properties of citrus phenolics limonene and naringin. *Food and Chemical Toxicology* 81, 160-170.

Barillet, S., Jugan, M. L., Laye, M., Leconte, Y., Herlin-Boime, N., Reynaud, C. and Carriere, M. (2010) In vitro evaluation of SiC nanoparticles impact on

A549 pulmonary cells: cyto-, genotoxicity and oxidative stress. *Toxicol Lett* 198 (3), 324-30.

Barnes, C. A., Elsaesser, A., Arkusz, J., Smok, A., Palus, J., Lesniak, A., Salvati, A., Hanrahan, J. P., Jong, W. H., Dziubaltowska, E., Stepnik, M., Rydzynski, K., McKerr, G., Lynch, I., Dawson, K. A. and Howard, C. V. (2008) Reproducible comet assay of amorphous silica nanoparticles detects no genotoxicity. *Nano Lett* 8 (9), 3069-74.

Barry, P. and O'Callaghan, C. (2003) The influence of inhaler selection on efficacy of asthma therapies. *Advanced drug delivery reviews* 55 (7), 879-923.

Bates, D. V., Fish, B., Hatch, T., Mercer, T. and Morrow, P. (1966) Deposition and retention models for internal dosimetry of the human respiratory tract. *Health Physics (England)* 12.

Bernstein, J., Davey, R. J. and Henck, J. O. (1999) Concomitant polymorphs. *Angewandte Chemie International Edition* 38 (23), 3440-3461.

Berthod, A., Laserna, J. and Carretero, I. (1992) Oil-in-water microemulsions as mobile phases for rapid screening of illegal drugs in sports. *Journal of Liquid Chromatography & Related Technologies* 15 (17), 3115-3127.

Bharat B. Aggarwal, Indra D. Bhatt and Haruyo Ichikawa (2006) Curcumin — Biological and Medicinal Properties.

Bharat B. Aggarwal, I. D. B., Haruyo Ichikawa, (July 24, 2006) Curcumin — Biological and Medicinal Properties.

Boe, J., Dennis, J., O'Driscoll, B., Bauer, T., Carone, M., Dautzenberg, B., Diot, P., Heslop, K. and Lannefors, L. (2001) European Respiratory Society Guidelines on the use of nebulizers. *European Respiratory Journal* 18 (1), 228-242.

Boldyrev, V. (2004) Mechanochemical modification and synthesis of drugs. *Journal of materials science* 39 (16-17), 5117-5120.

Booth, S., Anderson, H., Swannick, M., Wade, R., Kite, S. and Johnson, M. (2004) The use of oxygen in the palliation of breathlessness. A report of the expert working group of the Scientific Committee of the Association of Palliative Medicine. *Respiratory medicine* 98 (1), 66-77.

Borgstrom, L., Bondesson, E., Moren, F., Trofast, E. and Newman, S. (1994) Lung deposition of budesonide inhaled via Turbuhaler: a comparison with

terbutaline sulphate in normal subjects. *European Respiratory Journal* 7 (1), 69-73.

Bosquillon, C., Lombry, C., Preat, V. and Vanbever, R. (2001) Influence of formulation excipients and physical characteristics of inhalation dry powders on their aerosolization performance. *Journal of controlled release* 70 (3), 329-339.

Boussat, S., El'rini, T., Dubiez, A., Depierre, A., Barale, F. and Capellier, G. (2000) Predictive factors of death in primary lung cancer patients on admission to the intensive care unit. *Intensive care medicine* 26 (12), 1811-1816.

Brito, A. and Giulietti, M. (2007) Study of lactose crystallization in water-acetone solutions. *Crystal Research and Technology* 42 (6), 583-588.

Brodka-Pfeiffer, K., Haeusler, H., Grass, P. and Langguth, P. (2005) Air jet milling with homogeneous premixes of fenoterol hydrobromide and glucose for the application in dry powder inhalers. *Pharmazeutische Industrie* 67 (6), 713-719.

Brodka-Pfeiffer, K., Langguth, P., Graβ, P. and Häusler, H. (2003) Influence of mechanical activation on the physical stability of salbutamol sulphate. *European journal of pharmaceutics and biopharmaceutics* 56 (3), 393-400.

Brouet, I. and Ohshima, H. (1995) Curcumin, an anti-tumor promoter and anti-inflammatory agent, inhibits induction of nitric oxide synthase in activated macrophages. *Biochemical and biophysical research communications* 206 (2), 533-540.

Bryant, S. M. and Altria, K. D. (2004) An initial assessment of the use of gradient elution in microemulsion and micellar liquid chromatography. *Journal of separation science* 27 (17-18), 1498-1502.

Bund, R. K. and Pandit, A. B. (2007) Rapid lactose recovery from paneer whey using sonocrystallization: a process optimization. *Chemical Engineering and Processing: Process Intensification* 46 (9), 846-850.

Cains, P. W., Martin, P. D. and Price, C. J. (1998) The use of ultrasound in industrial chemical synthesis and crystallization. 1. Applications to synthetic chemistry. *Organic process research & development* 2 (1), 34-48.

Cella, D. F., Tulsky, D. S., Gray, G., Sarafian, B., Linn, E., Bonomi, A., Silberman, M., Yellen, S. B., Winicour, P. and Brannon, J. (1993) The Functional Assessment of Cancer Therapy scale: development and validation of the general measure. *Journal of clinical oncology* 11 (3), 570-579.

Chainani-Wu, N. (2003) Safety and anti-inflammatory activity of curcumin: a component of tumeric (Curcuma longa). *The Journal of Alternative & Complementary Medicine* 9 (1), 161-168.

Chan, M. M.-Y., Adapala, N. S. and Fong, D. (2005) Curcumin overcomes the inhibitory effect of nitric oxide on Leishmania. *Parasitology research* 96 (1), 49-56.

Chan, M. M., Huang, H. I., Fenton, M. R. and Fong, D. (1998) In vivo inhibition of nitric oxide synthase gene expression by curcumin, a cancer preventive natural product with anti-inflammatory properties. *Biochem Pharmacol* 55 (12), 1955-62.

Chan, V. S. (2006) Nanomedicine: An unresolved regulatory issue. *Regul Toxicol Pharmacol* 46 (3), 218-24.

Chattopadhyay, I., Biswas, K., Bandyopadhyay, U. and Banerjee, R. K. (2004) Turmeric and curcumin: Biological actions and medicinal applications. *Current science* 87 (1), 44-53.

Chen, A., Xu, J. and Johnson, A. (2006) Curcumin inhibits human colon cancer cell growth by suppressing gene expression of epidermal growth factor receptor through reducing the activity of the transcription factor Egr-1. *Oncogene* 25 (2), 278-287.

Chen, D., Sharma, S. K. and Mudhoo, A. (2011) *Handbook on applications of ultrasound: sonochemistry for sustainability.* CRC press.

Chen, H.-C., Lin, H.-Y., Lin, C.-C. and Lee, M.-H. (2005) The encapsulation of curcumin in micelles. *Bioengineering Conference, 2005. Proceedings of the IEEE 31st Annual Northeast.* IEEE.

Chen, H.-W., Lee, J.-Y., Huang, J.-Y., Wang, C.-C., Chen, W.-J., Su, S.-F., Huang, C.-W., Ho, C.-C., Chen, J. J. W., Tsai, M.-F., Yu, S.-L. and Yang, P.-C. (2008) Curcumin inhibits lung cancer cell invasion and metastasis through the tumor suppressor HLJ1. *Cancer Research* 68 (18), 7428-7438.

Chougule, M. B., Padhi, B. K., Jinturkar, K. A. and Misra, A. (2007) Development of dry powder inhalers. *Recent Patents on drug delivery & formulation* 1 (1), 11-21.

Chrystyn, H. (2003) Is inhalation rate important for a dry powder inhaler? Using the In-Check Dial to identify these rates. *Respiratory medicine* 97 (2), 181-187.

Conney, A. H. (2003) Enzyme induction and dietary chemicals as approaches to cancer chemoprevention: the Seventh DeWitt S. Goodman Lecture. *Cancer research* 63 (21), 7005-7031.

Crompton, G. (1982) Problems patients have using pressurized aerosol inhalers. *European journal of respiratory diseases. Supplement* 119, 101.

Cui, J., Yu, B., Zhao, Y., Zhu, W., Li, H., Lou, H. and Zhai, G. (2009) Enhancement of oral absorption of curcumin by self-microemulsifying drug delivery systems. *International Journal of Pharmaceutics* 371 (1), 148-155.

Dandekar, P., Dhumal, R., Jain, R., Tiwari, D., Vanage, G. and Patravale, V. (2010) Toxicological evaluation of pH-sensitive nanoparticles of curcumin: acute, sub-acute and genotoxicity studies. *Food and Chemical Toxicology* 48 (8), 2073-2089.

Das, S., Larson, I., Young, P. and Stewart, P. (2009) Surface energy changes and their relationship with the dispersibility of salmeterol xinafoate powders for inhalation after storage at high RH. *European Journal of Pharmaceutical Sciences* 38 (4), 347-354.

Das, S. C., Larson, I., Morton, D. A. and Stewart, P. J. (2010) Determination of the polar and total surface energy distributions of particulates by inverse gas chromatography. *Langmuir* 27 (2), 521-523.

Dcodhar, S., Sethi, R. and Srimal, R. (2013) Preliminary study on antirheumatic activity of curcumin (diferuloyl methane). *Indian journal of medical research* 138 (1).

De Boer, A., Gjaltema, D. and Hagedoorn, P. (1996) Inhalation characteristics and their effects on in vitro drug delivery from dry powder inhalers Part 2: Effect of peak flow rate (PIFR) and inspiration time on the in vitro drug release from three different types of commercial dry powder inhalers. *International journal of pharmaceutics* 138 (1), 45-56.

De Castro, M. L. and Priego-Capote, F. (2007) Ultrasound-assisted crystallization (sonocrystallization). *Ultrasonics sonochemistry* 14 (6), 717-724.

Della Volpe, C., Maniglio, D., Brugnara, M., Siboni, S. and Morra, M. (2004) The solid surface free energy calculation: I. In defense of the multicomponent approach. *Journal of Colloid and Interface Science* 271 (2), 434-453.

Della Volpe, C. and Siboni, S. (1997) Some reflections on acid–base solid surface free energy theories. *Journal of Colloid and Interface Science* 195 (1), 121-136.

Deora, N., Misra, N., Deswal, A., Mishra, H., Cullen, P. and Tiwari, B. (2013) Ultrasound for improved crystallisation in food processing. *Food Engineering Reviews* 5 (1), 36-44.

Desai, A. and Mitchison, T. J. (1997) Microtubule polymerization dynamics. *Annual review of cell and developmental biology* 13 (1), 83-117.

Dhumal, R. S., Biradar, S. V., Paradkar, A. R. and York, P. (2009) Particle engineering using sonocrystallization: salbutamol sulphate for pulmonary delivery. *International journal of pharmaceutics* 368 (1), 129-137.

Dikshit, M., Rastogi, L., Shukla, R. and Srimal, R. (1995) Prevention of ischaemia-induced biochemical changes by curcumin & quinidine in the cat heart. *The Indian journal of medical research* 101, 31-35.

Divya, C. S. and Pillai, M. R. (2006) Antitumor action of curcumin in human papillomavirus associated cells involves downregulation of viral oncogenes, prevention of NFkB and AP-1 translocation, and modulation of apoptosis. *Molecular carcinogenesis* 45 (5), 320-332.

Duarte, V. M., Han, E., Veena, M. S., Salvado, A., Suh, J. D., Liang, L.-J., Faull, K. F., Srivatsan, E. S. and Wang, M. B. (2010) Curcumin enhances the effect of cisplatin in suppression of head and neck squamous cell carcinoma via inhibition of IKKβ protein of the NFκB pathway. *Molecular cancer therapeutics* 9 (10), 2665-2675.

Duvoix, A., Blasius, R., Delhalle, S., Schnekenburger, M., Morceau, F., Henry, E., Dicato, M. and Diederich, M. (2005) Chemopreventive and therapeutic effects of curcumin. *Cancer letters* 223 (2), 181-190.

El-Gendy, N. and Berkland, C. (2009) Combination Chemotherapeutic Dry Powder Aerosols via Controlled Nanoparticle Agglomeration. *Pharmaceutical Research* 26 (7), 1752-1763.

El-Sherbiny, D. T., El-Enany, N., Belal, F. F. and Hansen, S. H. (2007) Simultaneous determination of loratadine and desloratadine in pharmaceutical preparations using liquid chromatography with a microemulsion as eluent. *Journal of pharmaceutical and biomedical analysis* 43 (4), 1236-1242.

El-Sherbiny, D. T., Eid, M. I., El-Wasseef, D. R., Al-Ashan, R. M. and Belal, F. (2005) Analysis of flunarizine in the presence of some of its degradation products using micellar liquid chromatography (MLC) or microemulsion liquid chromatography (MELC)–Application to dosage forms. *Journal of separation science* 28 (2), 197-202.

El-Sherbiny, D. T. M., El-Ashry, S. M., Mustafa, M. A., Abd-El-Rahman El-Emam, A. and Hansen, S. H. (2003) Evaluation of the use of microemulsions as eluents in high-performance liquid chromatography. *Journal of separation science* 26 (6-7), 503-509.

Ellison-Loschmann, L. (2004) *Asthma in Māori.* Centre for Public Health Research, Massey University.

Eramo, A., Lotti, F., Sette, G., Pilozzi, E., Biffoni, M., Di Virgilio, A., Conticello, C., Ruco, L., Peschle, C. and De Maria, R. (2008) Identification and expansion of the tumorigenic lung cancer stem cell population. *Cell Death and Differentiation* 15 (3), 504-514.

European Directorate for the Quality of Medicines & HealthCare. (2008) *European pharmacopoeia.* 6th edition. European treaty series. Strasbourg: Council of Europe.

European Parliament, C. (2010) EUR-Lex - Recherche simple.

Falk-Filipsson, A., Lof, A., Hagberg, M., Hjelm, E. W. and Wang, Z. (1993) d-limonene exposure to humans by inhalation: uptake, distribution, elimination, and effects on the pulmonary function. *J Toxicol Environ Health* 38 (1), 77-88.

FDA (2016) *Inactive Ingredient Search for Approved Drug Products.* http://www.accessdata.fda.gov/scripts/cder/iig/index.Cfm

Feng, Z., Hu, W., Hu, Y. and Tang, M.-s. (2006) Acrolein is a major cigarette-related lung cancer agent: Preferential binding at p53 mutational hotspots and inhibition of DNA repair. *Proceedings of the National Academy of Sciences* 103 (42), 15404-15409.

Fink, J. B. (2000) Metered-dose inhalers, dry powder inhalers, and transitions. *Respiratory care* 45 (6), 623.

Fowkes, F. M. (1964) Attractive forces at interfaces. *Industrial & Engineering Chemistry* 56 (12), 40-52.

Furukawa, Y., Kobuke, K. and Matsumori, A. (2001) Role of cytokines in autoimmune myocarditis and cardiomyopathy. *Autoimmunity* 34 (3), 165-168.

Ganderton, D. (1992) The generation of respirable clouds from coarse powder aggregates.

Ganta, S. and Amiji, M. (2009) Coadministration of paclitaxel and curcumin in nanoemulsion formulations to overcome multidrug resistance in tumor cells. *Molecular pharmaceutics* 6 (3), 928-939.

Garcea, G., Jones, D., Singh, R., Dennison, A., Farmer, P., Sharma, R., Steward, W., Gescher, A. and Berry, D. (2004) Detection of curcumin and its metabolites in hepatic tissue and portal blood of patients following oral administration. *British journal of cancer* 90 (5), 1011-1015.

Garti, N., Yaghmur, A., Leser, M. E., Clement, V. and Watzke, H. J. (2001) Improved oil solubilization in oil/water food grade microemulsions in the presence of polyols and ethanol. *Journal of agricultural and food chemistry* 49 (5), 2552-2562.

Giron, D. (2001) Investigations of polymorphism and pseudo-polymorphism in pharmaceuticals by combined thermoanalytical techniques. *Journal of thermal analysis and calorimetry* 64 (1), 37-60.

Goel, A., Kunnumakkara, A. B. and Aggarwal, B. B. (2008) Curcumin as “< i> Curecumin</i>”: From kitchen to clinic. *Biochemical pharmacology* 75 (4), 787-809.

Gould, M. N. (1997) Cancer chemoprevention and therapy by monoterpenes. *Environmental Health Perspectives* 105 (Suppl 4), 977-979.

Grimsey, I., Edwards, A., Shekunov, B., Forbes, R. and York, P. (1999) The effect of processing on the surface energetics of poly (l-lactide)

microparticles as determined by inverse gas chromatography (igc). *Pharm Sci (Suppl)* 1 (4).

Grimsey, I. M., Feeley, J. C. and York, P. (2002) Analysis of the surface energy of pharmaceutical powders by inverse gas chromatography. *Journal of pharmaceutical sciences* 91 (2), 571-583.

Grosser, T. (2006) The pharmacology of selective inhibition of COX-2. *THROMBOSIS AND HAEMOSTASIS-STUTTGART-* 96 (4), 393.

Guilleminault, L., Hervé-Grépinet, V., Heuzé-Vourc'h, N. and Lemarié, E. (2011) *The Airways: A Promising Route for the Pulmonary Delivery of Anticancer Agents.* INTECH Open Access Publisher.

Guinot, S. and Leveiller, F. (1999) The use of MTDSC to assess the amorphous phase content of a micronised drug substance. *International journal of pharmaceutics* 192 (1), 63-75.

Guo, Z., Zhang, M., Li, H., Wang, J. and Kougoulos, E. (2005) Effect of ultrasound on anti-solvent crystallization process. *Journal of Crystal Growth* 273 (3), 555-563.

Gustavsson, P., Jakobsson, R., Nyberg, F., Pershagen, G., Järup, L. and Schéele, P. (2000) Occupational exposure and lung cancer risk: a population-based case-referent study in Sweden. *American journal of epidemiology* 152 (1), 32-40.

Hansen, H. H. (2008) *Textbook of lung cancer.* Informa Healthcare.

Harjunen, P., Lankinen, T., Salonen, H., Lehto, V. P. and Jarvinen, K. (2003) Effects of carriers and storage of formulation on the lung deposition of a hydrophobic and hydrophilic drug from a DPI. *International Journal of Pharmaceutics* 263 (1-2), 151-163.

Harwood, M., Aldington, S. and Beasley, R. (2005) Lung cancer in Maori: a neglected priority. *NZ Med J* 1213.

Haynes, W. M. (2014) *CRC handbook of chemistry and physics.* CRC press.

Hernández-Trejo, N., Kayser, O., Steckel, H. and Müller, R. H. (2005) Characterization of nebulized buparvaquone nanosuspensions—effect of nebulization technology. *Journal of drug targeting* 13 (8-9), 499-507.

Hersey, J. and Krycer, I. (1980) Biopharmaceutical implications of technological change. *Int. J. Pharm. Tech. & Prod. Mfr* 1, 18-21.

Hickey, A. J. (2003) *Pharmaceutical inhalation aerosol technology.* Vol. 134. Informa HealthCare.

Hirota, R., Nakamura, H., Bhatti, S. A., Ngatu, N. R., Muzembo, B. A., Dumavibhat, N., Eitoku, M., Sawamura, M. and Suganuma, N. (2012) Limonene inhalation reduces allergic airway inflammation in Dermatophagoides farinae-treated mice. *Inhal Toxicol* 24 (6), 373-81.

Hitzman, C. J., Wattenberg, L. W. and Wiedmann, T. S. (2006) Pharmacokinetics of 5-fluorouracil in the hamster following inhalation delivery of lipid-coated nanoparticles. *Journal of Pharmaceutical Sciences* 95 (6), 1196-1211.

Hoehle, S. I., Pfeiffer, E., Sólyom, A. M. and Metzler, M. (2006) Metabolism of curcuminoids in tissue slices and subcellular fractions from rat liver. *Journal of agricultural and food chemistry* 54 (3), 756-764.

Holder, G. M., Plummer, J. L. and Ryan, A. J. (1978) The metabolism and excretion of curcumin (1, 7-bis-(4-hydroxy-3-methoxyphenyl)-1, 6-heptadiene-3, 5-dione) in the rat. *Xenobiotica* 8 (12), 761-768.

Hu, A., Zheng, J. and Qiu, T. (2006) Industrial experiments for the application of ultrasound on scale control in the Chinese sugar industry. *Ultrasonics sonochemistry* 13 (4), 329-333.

Hu, L., Jia, Y., Niu, F., Jia, Z., Yang, X. and Jiao, K. (2012) Preparation and enhancement of oral bioavailability of curcumin using microemulsions vehicle. *Journal of agricultural and food chemistry* 60 (29), 7137-7141.

Hu, L., Kong, D., Hu, Q., Gao, N. and Pang, S. (2015) Evaluation of high-performance curcumin nanocrystals for pulmonary drug delivery both in vitro and in vivo. *Nanoscale research letters* 10 (1), 1-9.

Huang, M.-T., Lou, Y.-R., Ma, W., Newmark, H. L., Reuhl, K. R. and Conney, A. H. (1994) Inhibitory effects of dietary curcumin on forestomach, duodenal, and colon carcinogenesis in mice. *Cancer research* 54 (22), 5841-5847.

Huang, T., Chen, Z. and Fang, L. (2013) Curcumin inhibits LPS-induced EMT through downregulation of NF-κB-Snail signaling in breast cancer cells. *Oncology reports* 29 (1), 117-124.

ICH (1996) Validation of Analytical Procedures. *ICH Official web site : ICH*.

Jadhav, B. K., Mahadik, K. R. and Paradkar, A. R. (2007) Development and validation of improved reversed phase-HPLC method for simultaneous determination of curcumin, demethoxycurcumin and bis-demethoxycurcumin. *Chromatographia* 65 (7-8), 483-488.

Jayaprakasha, G. K., Jagan Mohan Rao, L. and Sakariah, K. K. (2002) Improved HPLC method for the determination of curcumin, demethoxycurcumin, and bisdemethoxycurcumin. *Journal of Agricultural and Food Chemistry* 50 (13), 3668-3672.

Jemal, A., Siegel, R., Ward, E., Hao, Y., Xu, J., Murray, T. and Thun, M. J. (2008) Cancer statistics, 2008. *CA: A Cancer Journal for Clinicians* 58 (2), 71-96.

Johnson, D. H. (1999a) Management of small cell lung cancer: current state of the art. *Chest* 116 (6 Suppl), 525s-530s.

Johnson, D. H. (1999b) Management of Small Cell Lung CancerCurrent State of the Art. *CHEST Journal* 116 (suppl_3), 525S-530S.

Kasi, P. D., Tamilselvam, R., Skalicka-Woźniak, K., Nabavi, S. F., Daglia, M., Bishayee, A., Pazoki-toroudi, H. and Nabavi, S. M. (2016) Molecular targets of curcumin for cancer therapy: an updated review. *Tumor Biology* 37 (10), 13017-13028.

Khanna, N. (1999) Turmeric-nature's precious gift. *Current Science* 76 (10), 1351-1356.

Khar, A., Ali, A. M., Pardhasaradhi, B., Begum, Z. and Anjum, R. (1999) Antitumor activity of curcumin is mediated through the induction of apoptosis in AK-5 tumor cells. *FEBS letters* 445 (1), 165-168.

Khatibi, M. (2013) Experimental study on droplet size of dispersed oil-water flow.

Kim, D. W., Yousaf, A. M., Li, D. X., Kim, J. O., Yong, C. S., Cho, K. H. and Choi, H.-G. (2016) Development of RP-HPLC method for simultaneous determination of docetaxel and curcumin in rat plasma: Validation and stability. *Asian Journal of Pharmaceutical Sciences*.

Kisin, E. R., Murray, A. R., Keane, M. J., Shi, X. C., Schwegler-Berry, D., Gorelik, O., Arepalli, S., Castranova, V., Wallace, W. E., Kagan, V. E. and Shvedova, A. A. (2007) Single-walled carbon nanotubes: geno- and

cytotoxic effects in lung fibroblast V79 cells. *J Toxicol Environ Health A* 70 (24), 2071-9.

Kiso, Y., Suzuki, Y., Watanabe, N., Oshima, Y. and Hikino, H. (1983) Antihepatotoxic principles of Curcuma longa rhizomes. *Planta medica* 49 (11), 185-187.

Knoch, M. and Keller, M. (2005) The customised electronic nebuliser: a new category of liquid aerosol drug delivery systems. *Expert Opinion on Drug Delivery* 2 (2), 377-390.

Kou, X., Chan, L. W., Steckel, H. and Heng, P. W. S. (2012) Physico-chemical aspects of lactose for inhalation. *Advanced Drug Delivery Reviews* 64 (3), 220-232.

Kou, X., Chan, L. W., Sun, C. C. and Heng, P. W. S. (2016) Preparation of slab-shaped lactose carrier particles for dry powder inhalers by air jet milling. *Asian Journal of Pharmaceutical Sciences*.

Kulyal, P., Kuchibhatla, L. N., Maheshwari, K. U., Babu, K. N., Tetali, S. D. and Raghavendra, A. S. (2016) Highly sensitive HPLC method for estimation of total or individual curcuminoids in Curcuma cultivars and commercial turmeric powders. *CURRENT SCIENCE* 111 (11), 1816.

Kumaravel, T. and Jha, A. N. (2006) Reliable Comet assay measurements for detecting DNA damage induced by ionising radiation and chemicals. *Mutation Research/Genetic Toxicology and Environmental Mutagenesis* 605 (1), 7-16.

Kunnumakkara, A. B., Anand, P. and Aggarwal, B. B. (2008) Curcumin inhibits proliferation, invasion, angiogenesis and metastasis of different cancers through interaction with multiple cell signaling proteins. *Cancer letters* 269 (2), 199-225.

Kurniawansyah, F., Duong, H. T., Luu, T. D., Mammucari, R., Vittorio, O., Boyer, C. and Foster, N. (2015) Inhalable curcumin formulations: Micronization and bioassay. *Chemical Engineering Journal* 279, 799-808.

Labiris, N. and Dolovich, M. (2003) Pulmonary drug delivery. Part I: physiological factors affecting therapeutic effectiveness of aerosolized medications. *British journal of clinical pharmacology* 56 (6), 588-599.

Lawrence, M. J. and Rees, G. D. (2012) Microemulsion-based media as novel drug delivery systems. *Advanced drug delivery reviews* 64, 175-193.

Lee, A. Y.-L., Fan, C.-C., Chen, Y.-A., Cheng, C.-W., Sung, Y.-J., Hsu, C.-P. and Kao, T.-Y. (2015) Curcumin inhibits invasiveness and epithelial-mesenchymal transition in oral squamous cell carcinoma through reducing matrix metalloproteinase 2, 9 and modulating p53-E-cadherin pathway. *Integrative cancer therapies* 14 (5), 484-490.

Leonelli, C. and Mason, T. J. (2010) Microwave and ultrasonic processing: now a realistic option for industry. *Chemical Engineering and Processing: Process Intensification* 49 (9), 885-900.

Letang, C., Samson, M.-F., Lasserre, T.-M., Chaurand, M. and Abecassis, J. (2002) Production of starch with very low protein content from soft and hard wheat flours by jet milling and air classification. *Cereal Chemistry* 79 (4), 535-543.

Levitzky, M. G. (2007) *Pulmonary physiology.* 7th edition. A LANGE medical book. New York ; London: McGraw-Hill.

Li, H., Li, H., Guo, Z. and Liu, Y. (2006) The application of power ultrasound to reaction crystallization. *Ultrasonics sonochemistry* 13 (4), 359-363.

Li, J., Jiang, Y., Wen, J., Fan, G., Wu, Y. and Zhang, C. (2009) A rapid and simple HPLC method for the determination of curcumin in rat plasma: assay development, validation and application to a pharmacokinetic study of curcumin liposome. *Biomedical chromatography* 23 (11), 1201-1207.

Li, L., Lai, C., Xuan, X., Gao, C. and Li, N. (2016) Simultaneous Determination of Hydrochlorothiazide and Losartan Potassium in Osmotic Pump Tablets by Microemulsion Liquid Chromatography. *Journal of Chromatographic Science*, bmw101.

Li, N., Chen, X., Liao, J., Yang, G., Wang, S., Josephson, Y., Han, C., Chen, J., Huang, M.-T. and Yang, C. S. (2002) Inhibition of 7, 12-dimethylbenz [a] anthracene (DMBA)-induced oral carcinogenesis in hamsters by tea and curcumin. *Carcinogenesis* 23 (8), 1307-1313.

Liu, C.-H., Chang, F.-Y. and Hung, D.-K. (2011) Terpene microemulsions for transdermal curcumin delivery: effects of terpenes and cosurfactants. *Colloids and Surfaces B: Biointerfaces* 82 (1), 63-70.

Liu et al. , D. (2013) Engineering nano-curcumin with enhanced solubility and in-vitro anti-cancer bioactivity.

Liu, J., Svärd, M., Hippen, P. and Rasmuson, Å. C. (2015) Solubility and Crystal Nucleation in Organic Solvents of Two Polymorphs of Curcumin. *Journal of pharmaceutical sciences* 104 (7), 2183-2189.

Loh, Z. H., Samanta, A. K. and Heng, P. W. S. (2015) Overview of milling techniques for improving the solubility of poorly water-soluble drugs. *asian journal of pharmaceutical sciences* 10 (4), 255-274.

Louhi-Kultanen, M., Karjalainen, M., Rantanen, J., Huhtanen, M. and Kallas, J. (2006) Crystallization of glycine with ultrasound. *International journal of pharmaceutics* 320 (1), 23-29.

Lyczko, N., Espitalier, F., Louisnard, O. and Schwartzentruber, J. (2002) Effect of ultrasound on the induction time and the metastable zone widths of potassium sulphate. *Chemical Engineering Journal* 86 (3), 233-241.

Ma, Z., Shayeganpour, A., Brocks, D. R., Lavasanifar, A. and Samuel, J. (2007) High-performance liquid chromatography analysis of curcumin in rat plasma: application to pharmacokinetics of polymeric micellar formulation of curcumin. *Biomedical Chromatography* 21 (5), 546-552.

Magdolenova, Z., Collins, A., Kumar, A., Dhawan, A., Stone, V. and Dusinska, M. (2013) Mechanisms of genotoxicity. A review of in vitro and in vivo studies with engineered nanoparticles. *Nanotoxicology* 8 (3), 233-78.

Maher, A., Seaton, C. C., Hudson, S., Croker, D. M., Rasmuson, Å. C. and Hodnett, B. K. (2012) Investigation of the solid-state polymorphic transformations of piracetam. *Crystal Growth & Design* 12 (12), 6223-6233.

Maheshwari, R. K., Singh, A. K., Gaddipati, J. and Srimal, R. C. (2006) Multiple biological activities of curcumin: A short review. *Life Sciences* 78 (18), 2081-2087.

Mahuzier, P. E., Clark, B. J., Bryant, S. M. and Altria, K. D. (2001) High-speed microemulsion electrokinetic chromatography. *Electrophoresis* 22 (17), 3819-3823.

Maillet, A., Congy-Jolivet, N., Le Guellec, S., Vecellio, L., Hamard, S., Courty, Y., Courtois, A., Gauthier, F., Diot, P., Thibault, G., Lemarie, E. and Heuze-Vourc'h, N. (2008) Aerodynamical, immunological and pharmacological properties of the anticancer antibody cetuximab. *Pharmaceutical Research* 25 (6), 1318-1326.

Malam, Y., Loizidou, M. and Seifalian, A. M. (2009) Liposomes and nanoparticles: nanosized vehicles for drug delivery in cancer. *Trends in pharmacological sciences* 30 (11), 592-599.

Mao, Y. and Carr, P. W. (2001) Separation of selected basic pharmaceuticals by reversed-phase and ion-exchange chromatography using thermally tuned tandem columns. *Analytical chemistry* 73 (18), 4478-4485.

Marple, V. A., Roberts, D. L., Romay, F. J., Miller, N. C., Truman, K. G., Van Oort, M., Olsson, B., Holroyd, M. J., Mitchell, J. P. and Hochrainer, D. (2003) Next generation pharmaceutical impactor (a new impactor for pharmaceutical inhaler testing). Part I: Design. *Journal of aerosol medicine* 16 (3), 283-299.

Marsh, A. (2005) *Oil-in-water microemulsions as separation media for pharmaceutical analysis by high performance liquid chromatography and capillary electrophoresis : the investigation and optimisation of operating parameters in oil-in-water microemulsion high performance liquid ... related substances and preservatives in phamaceutical formulations.* Bradford: University of Bradford.

Marsh, A., Clark, B. and Altria, K. (2004) Oil-in-water microemulsion high performance liquid chromatographic analysis of pharmaceuticals. *Chromatographia* 59 (9), 531-542.

Marsh, A., Clark, B. and Altria, K. D. (2005) A review of the background, operating parameters and applications of microemulsion liquid chromatography (MELC). *Journal of separation science* 28 (15), 2023-2032.

Mason, T. G., Wilking, J., Meleson, K., Chang, C. and Graves, S. (2006) Nanoemulsions: formation, structure, and physical properties. *Journal of Physics: Condensed Matter* 18 (41), R635.

Mc Callion, O. and Patel, M. (1996) Viscosity effects on nebulisation of aqueous solutions. *International journal of pharmaceutics* 130 (2), 245-249.

McClements, D. J. (2012) Nanoemulsions versus microemulsions: terminology, differences, and similarities. *Soft matter* 8 (6), 1719-1729.

McCrone, W. (1965) Physics and Chemistry of the Organic Solid State, Vol. 2, edited by D. *Fox, MM Labes & A. Weissberger*, 725-767.

McEvoy, E., Marsh, A., Altria, K., Donegan, S. and Power, J. (2006) Recent advances in the development and application of microemulsion EKC. *Electrophoresis* 28 (1-2), 193-207.

McNamara, W. B., Didenko, Y. T. and Suslick, K. S. (1999) Sonoluminescence temperatures during multi-bubble cavitation. *Nature* 401 (6755), 772-775.

Miola, M. F., Snowden, M. J. and Altria, K. D. (1998) The use of microemulsion electrokinetic chromatography in pharmaceutical analysis. *Journal of pharmaceutical and biomedical analysis* 18 (4), 785-797.

Miyasaka, E., Kato, Y., Hagisawa, M. and Hirasawa, I. (2006) Effect of ultrasonic irradiation on the number of acetylsalicylic acid crystals produced under the supersaturated condition and the ability of controlling the final crystal size via primary nucleation. *Journal of crystal growth* 289 (1), 324-330.

Mohamed, N. N. A. (2009) *Pharmaceutical analysis and in-vitro aerodynamic characterisation of inhaled theophylline formulations containing drug particles prepared by supercritical fluid processing : chromatographic, spectroscopic, and thermal analysis of micron-sized theophylline particles prepared by supercritical fluid technology and in-vitro evaluation of their performance as inhaled dry powder formulations*. Bradford: University of Bradford,.

Mohammad, M. A. (2013) Chromatographic adhesion law to simplify surface energy calculation. *Journal of Chromatography A* 1318, 270-275.

Mohammad, M. A. (2015) An equation to calculate the actual methylene middle parameter as a function of temperature. *Journal of Chromatography A* 1408, 267-271.

Morita, S., Kobayashi, K., Eguchi, K., Matsumoto, T., Shibuya, M., Yamaji, Y., Sakamoto, J. and Ohashi, Y. (2003) Influence of clinical parameters on quality of life during chemotherapy in patients with advanced non-small cell lung cancer: application of a general linear model. *Japanese journal of clinical oncology* 33 (9), 470-476.

Müller, R. and Heinemann, S. (1992) Fat emulsions for parenteral nutrition. I: Evaluation of microscopic and laser light scattering methods for the determination of the physical stability. *Clinical Nutrition* 11 (4), 223-236.

Mullin, J. W. (2001) *Crystallization.* Butterworth-Heinemann.

Myrdal, P. B., Sheth, P. and Stein, S. W. (2014) Advances in metered dose inhaler technology: formulation development. *AAPS PharmSciTech* 15 (2), 434-455.

Nagabhushan, M. and Bhide, S. (1992) Curcumin as an inhibitor of cancer. *Journal of the American College of Nutrition* 11 (2), 192-198.

Nasr, M., Nawaz, S. and Elhissi, A. (2012) Amphotericin B lipid nanoemulsion aerosols for targeting peripheral respiratory airways via nebulization. *International journal of pharmaceutics* 436 (1), 611-616.

Natarajan, C. and Bright, J. J. (2002) Curcumin inhibits experimental allergic encephalomyelitis by blocking IL-12 signaling through Janus kinase-STAT pathway in T lymphocytes. *The Journal of Immunology* 168 (12), 6506-6513.

Neel, J., Schull, W., Awa, A. A., Satoh, C., Otake, M., Kato, H. and Yoshimoto, Y. (1989) Implications of the Hiroshima-Nagasaki genetic studies for the estimation of the human" doubling dose" of radiation. *Genome* 31 (2), 853-859.

Nesamony, J., Shah, I. S., Kalra, A. and Jung, R. (2014) Nebulized oil-in-water nanoemulsion mists for pulmonary delivery: development, physico-chemical characterization and in vitro evaluation. *Drug Dev Ind Pharm* 40 (9), 1253-63.

Newell, H. E., Buckton, G., Butler, D. A., Thielmann, F. and Williams, D. R. (2001) The use of inverse phase gas chromatography to study the change of surface energy of amorphous lactose as a function of relative humidity and the processes of collapse and crystallisation. *International journal of pharmaceutics* 217 (1), 45-56.

Newman, S., Talaee, N. and Clarke, S. (1991a) Salbutamol aerosol delivery in man with the Rondo Spacer. *Acta therapeutica* 17 (1), 49-58.

Newman, S. P., Morén, F., Trofast, E., Talaee, N. and Clarke, S. W. (1991b) Terbutaline sulphate Turbuhaler: effect of inhaled flow rate on drug deposition and efficacy. *International journal of pharmaceutics* 74 (2), 209-213.

Nikander, K., Turpeinen, M. and Wollmer, P. (1999) The conventional ultrasonic nebulizer proved inefficient in nebulizing a suspension. *Journal of aerosol medicine* 12 (2), 47-53.

Nirmala, C. and Puvanakrishnan, R. (1996) Protective role of curcumin against isoproterenol induced myocardial infarction in rats. *Molecular and cellular biochemistry* 159 (2), 85-93.

Noureddini, H., Teoh, B. and Clements, L. D. (1992) Viscosities of vegetable oils and fatty acids. *Journal of the American Oil Chemists Society* 69 (12), 1189-1191.

Oetari, S., Sudibyo, M., Commandeur, J. N., Samhoedi, R. and Vermeulen, N. P. (1996) Effects of curcumin on cytochrome P450 and glutathione S-transferase activities in rat liver. *Biochemical pharmacology* 51 (1), 39-45.

Olive, P. L., Banáth, J. P. and Durand, R. E. (1990) Heterogeneity in radiation-induced DNA damage and repair in tumor and normal cells measured using the" comet" assay. *Radiation research* 122 (1), 86-94.

Osawa, T. and Namiki, M. (1985) Natural antioxidants isolated from Eucalyptus leaf waxes. *Journal of Agricultural and Food Chemistry* 33 (5), 777-780.

Ostling, O. and Johanson, K. (1984) Microelectrophoretic study of radiation-induced DNA damages in individual mammalian cells. *Biochemical and biophysical research communications* 123 (1), 291-298.

Paccagnella, A., Favaretto, A., Oniga, F., Barbieri, F., Ceresoli, G., Torri, W., Villa, E., Verusio, C., Cetto, G. and Santo, A. (2004) Cisplatin versus carboplatin in combination with mitomycin and vinblastine in advanced non small cell lung cancer. A multicenter, randomized phase III trial. *Lung cancer (Amsterdam, Netherlands)* 43 (1), 83.

Paradkar, A., Ambike, A. A., Jadhav, B. K. and Mahadik, K. R. (2004) Characterization of curcumin-PVP solid dispersion obtained by spray drying. *International Journal of Pharmaceutics* 271 (1-2), 281-286.

Patel, S. R. and Murthy, Z. (2009) Ultrasound assisted crystallization for the recovery of lactose in an anti-solvent acetone. *Crystal Research and Technology* 44 (8), 889-896.

Patravale, V. and Kulkarni, R. (2004) Nanosuspensions: a promising drug delivery strategy. *Journal of pharmacy and pharmacology* 56 (7), 827-840.

Pharmacopoeia, B. (2001) *The Stationary Office Ltd*. London.

Pilcer, G., Wauthoz, N. and Amighi, K. (2012) Lactose characteristics and the generation of the aerosol. *Advanced Drug Delivery Reviews* 64 (3), 233-256.

Pitcairn, G., Lunghetti, G., Ventura, P. and Newman, S. (1994) A comparison of the lung deposition of salbutamol inhaled from a new dry powder inhaler, at two inhaled flow rates. *International journal of pharmaceutics* 102 (1), 11-18.

Pond, S. M. and Tozer, T. N. (1984) First-pass elimination basic concepts and clinical consequences. *Clinical pharmacokinetics* 9 (1), 1-25.

Pritchard, J. (2001) The influence of lung deposition on clinical response. *Journal of Aerosol Medicine* 14 (1, Supplement 1), 19-26.

Priyadarsini, K. I. (2014) The chemistry of curcumin: from extraction to therapeutic agent. *Molecules* 19 (12), 20091-20112.

Protonotariou, S., Mandala, I. and Rosell, C. M. (2015) Jet milling effect on functionality, quality and in vitro digestibility of whole wheat flour and bread. *Food and Bioprocess Technology* 8 (6), 1319-1329.

Raaschou-Nielsen, O., Andersen, Z. J., Hvidberg, M., Jensen, S. S., Ketzel, M., Sørensen, M., Loft, S., Overvad, K. and Tjønneland, A. (2011) Lung cancer incidence and long-term exposure to air pollution from traffic. *Environmental health perspectives* 119 (6), 860.

Rahn-Chique, K., Puertas, A. M., Romero-Cano, M. S., Rojas, C. and Urbina-Villalba, G. (2012) Nanoemulsion stability: experimental evaluation of the flocculation rate from turbidity measurements. *Advances in colloid and interface science* 178, 1-20.

Rao, M. (1997) Nitric oxide scavenging by curcuminoids. *Journal of pharmacy and Pharmacology* 49 (1), 105-107.

Rayleigh, L. (1884) On the circulation of air observed in Kundt's tubes, and on some allied acoustical problems. *Philosophical Transactions of the Royal Society of London* 175, 1-21.

Rees, P., Clark, T. and Moren, F. (1982) The importance of particle size in response to inhaled bronchodilators. *Eur J Respir Dis* 63 (suppl 119), 73-8.

Richards, W. T. and Loomis, A. L. (1927) The chemical effects of high frequency sound waves I. A preliminary survey. *Journal of the American Chemical Society* 49 (12), 3086-3100.

Ritter, J. M. (2008) *A textbook of clinical pharmacology and therapeutics.* 5th edition. London: Hodder Education.

Rodríguez-hornedo, N. and Murphy, D. (1999) Significance of controlling crystallization mechanisms and kinetics in pharmaceutical systems. *Journal of pharmaceutical sciences* 88 (7), 651-660.

Ruby, A., Kuttan, G., Babu, K. D., Rajasekharan, K. and Kuttan, R. (1995) Anti-tumour and antioxidant activity of natural curcuminoids. *Cancer letters* 94 (1), 79-83.

Sa, G. and Das, T. (2008) Anti cancer effects of curcumin: cycle of life and death. *Cell Division* 3.

Saleem, I. Y. and Smyth, H. D. (2010) Micronization of a soft material: air-jet and micro-ball milling. *AAPS PharmSciTech* 11 (4), 1642-1649.

Sanphui, P., Goud, N. R., Khandavilli, U. R. and Nangia, A. (2011) Fast dissolving curcumin cocrystals. *Crystal Growth & Design* 11 (9), 4135-4145.

Scagliotti, G., De Marinis, F., Rinaldi, M., Crino, L., Gridelli, C., Ricci, S., Matano, E., Boni, C., Marangolo, M. and Failla, G. (2002) Phase III randomized trial comparing three platinum-based doublets in advanced non–small-cell lung cancer. *Journal of clinical oncology* 20 (21), 4285-4291.

Schultheis, C. P., Raheem, M. A. and Perry, M. C. (2001) Second-line chemotherapy for small-cell lung cancer: a review. *Clin Lung Cancer* 3 (2), 118-24.

Schultz, J., Lavielle, L. and Martin, C. (1987) The role of the interface in carbon fibre-epoxy composites. *The Journal of Adhesion* 23 (1), 45-60.

Sculier, J.-P. (1995) Intensive care and oncology. *Supportive Care in Cancer* 3 (2), 93-105.

Sculier, J.-P. and Fry, W. A. (2004) *Malignant tumors of the lung : evidence-based management.* Berlin ; London: Springer.

Sculier, J. and Markiewicz, E. (1993) Cardiopulmonary resuscitation in medical cancer patients: the experience of a medical intensive-care unit of a cancer centre. *Supportive Care in Cancer* 1 (3), 135-138.

Seo, J.-a., Kim, B., Dhanasekaran, D. N., Tsang, B. K. and Song, Y. S. (2016) Curcumin induces apoptosis by inhibiting sarco/endoplasmic reticulum Ca 2+ ATPase activity in ovarian cancer cells. *Cancer letters* 371 (1), 30-37.

Shafaghati, N., Hedayati, M. and Hosseinimehr, S. J. (2014) Protective effects of curcumin against genotoxicity induced by 131-iodine in human cultured lymphocyte cells. *Pharmacognosy magazine* 10 (38), 106-110.

Shankar, T. B., Shantha, N., Ramesh, H., Murthy, I. A. and Murthy, V. S. (1980) Toxicity studies on turmeric (Curcuma longa): acute toxicity studies in rats, guineapigs and monkeys. *Indian journal of experimental biology* 18 (1), 73-75.

Shanmugam, M. K., Kannaiyan, R. and Sethi, G. (2011) Targeting cell signaling and apoptotic pathways by dietary agents: role in the prevention and treatment of cancer. *Nutrition and cancer* 63 (2), 161-173.

Shanmugam, M. K., Rane, G., Kanchi, M. M., Arfuso, F., Chinnathambi, A., Zayed, M., Alharbi, S. A., Tan, B. K., Kumar, A. P. and Sethi, G. (2015) The multifaceted role of curcumin in cancer prevention and treatment. *Molecules* 20 (2), 2728-2769.

Shariare, M., De Matas, M. and York, P. (2011a) Effect of crystallisation conditions and feedstock morphology on the aerosolization performance of micronised salbutamol sulphate. *International journal of pharmaceutics* 415 (1), 62-72.

Shariare, M. H. (2011) *The rational design of drug crystals to facilitate particle size reduction. : Investigation of crystallisation conditions and crystal properties to enable optimised particle processing and comminution*. Bradford: University of Bradford,.

Shariare, M. H., de Matas, M., York, P. and Shao, Q. (2011b) The impact of material attributes and process parameters on the micronisation of lactose monohydrate. *International Journal of Pharmaceutics* 408 (1–2), 58-66.

Sharma, C. P., Behera, D., Aggarwal, A. N., Gupta, D. and Jindal, S. K. (2002) Radiographic patterns in lung cancer. *Indian J Chest Dis Allied Sci* 44 (1), 25-30.

Sharma, R., McLelland, H., Hill, K., Ireson, C., Euden, S., Manson, M., Pirmohamed, M., Marnett, L., Gescher, A. and Steward, W. (2005) Pharmacodynamic and pharmacokinetic study of oral Curcuma extract in patients with colorectal cancer.

Sharma, R. A., Euden, S. A., Platton, S. L., Cooke, D. N., Shafayat, A., Hewitt, H. R., Marczylo, T. H., Morgan, B., Hemingway, D. and Plummer, S. M. (2004) Phase I Clinical Trial of Oral Curcumin Biomarkers of Systemic Activity and Compliance. *Clinical Cancer Research* 10 (20), 6847-6854.

Shen, L. and Ji, H.-F. (2007) Theoretical study on physicochemical properties of curcumin. *Spectrochimica Acta Part A: Molecular and Biomolecular Spectroscopy* 67 (3), 619-623.

Shi, B. and Qi, D. (2012) A method for improving the calculation accuracy of acid–base constants by inverse gas chromatography. *Journal of Chromatography A* 1231, 73-76.

Shi, Y., Hartel, R. and Liang, B. (1989) Formation and growth phenomena of lactose nuclei under contact nucleation conditions. *Journal of Dairy Science* 72 (11), 2906-2915.

Shi, Y., Liang, B. and Hartel, R. (2005) *Crystal refining technologies by controlled crystallization*. Google Patents.

Shishodia, S., Chaturvedi, M. M. and Aggarwal, B. B. (2007a) Role of curcumin in cancer therapy. *Current problems in cancer* 31 (4), 243-305.

Shishodia, S., Singh, T. and Chaturvedi, M. M. (2007b) Modulation of transcription factors by curcumin. *The Molecular Targets and Therapeutic Uses of Curcumin in Health and Disease*, 127-148.

Siddique, Y. H., Ara, G., Beg, T., Gupta, J. and Afzal, M. (2010) Assessment of cell viability, lipid peroxidation and quantification of DNA fragmentation after the treatment of anticancerous drug mitomycin C and curcumin in cultured human blood lymphocytes. *Experimental and Toxicologic Pathology* 62 (5), 503-508.

Siegel, R., Naishadham, D. and Jemal, A. (2012) Cancer statistics, 2012. *CA: A Cancer Journal for Clinicians*.

Singh, N., Manshian, B., Jenkins, G. J., Griffiths, S. M., Williams, P. M., Maffeis, T. G., Wright, C. J. and Doak, S. H. (2009) NanoGenotoxicology: the DNA damaging potential of engineered nanomaterials. *Biomaterials* 30 (23-24), 3891-914.

Singh, N. P., McCoy, M. T., Tice, R. R. and Schneider, E. L. (1988) A simple technique for quantitation of low levels of DNA damage in individual cells. *Experimental cell research* 175 (1), 184-191.

Skalko-Basnet, Purusotam Basnet and Natasa (2011) Curcumin: An Anti-Inflammatory Molecule from a Curry Spice on the Path to Cancer Treatment. *Molecules* 16 (6), 4567-4598.

Smit, E., Fokkema, E., Biesma, B., Groen, H., Snoek, W. and Postmus, P. (1998) A phase II study of paclitaxel in heavily pretreated patients with small-cell lung cancer. *British journal of cancer* 77 (2), 347.

Smoke, I. and Smoking, I. (2004) IARC monographs on the evaluation of carcinogenic risks to humans. *IARC, Lyon*, 1-1452.

Snyder, R. D. and Green, J. W. (2001) A review of the genotoxicity of marketed pharmaceuticals. *Mutat Res* 488 (2), 151-69.

Srinivasan, M., Prasad, N. R. and Menon, V. P. (2006) Protective effect of curcumin on γ-radiation induced DNA damage and lipid peroxidation in cultured human lymphocytes. *Mutation Research/Genetic Toxicology and Environmental Mutagenesis* 611 (1), 96-103.

Srivastava, K., Bordia, A. and Verma, S. (1995) Curcumin, a major component of food spice turmeric (< i> Curcuma longa</i>) inhibits aggregation and alters eicosanoid metabolism in human blood platelets. *Prostaglandins, leukotrienes and essential fatty acids* 52 (4), 223-227.

Srivastava, R., Dikshit, M., Srimal, R. and Dhawan, B. (1985) Anti-thrombotic effect of curcumin. *Thrombosis research* 40 (3), 413-417.

Steckel, H. and Muller, B. W. (1997) In vitro evaluation of dry powder inhalers .2. Influence of carrier particle size and concentration on in vitro deposition. *International Journal of Pharmaceutics* 154 (1), 31-37.

Steenland, K., Loomis, D., Shy, C. and Simonsen, N. (1996) Review of occupational lung carcinogens. *American journal of industrial medicine* 29 (5), 474-490.

Storey, R. A. (2008) *The Nucleation, Growth and Solid State Properties of Particulate Pharmaceuticals: Studies of the Molecular Clustering, Nucleation and Crystal Growth of Ibuprofen and the Role of the Crystallisation Environment on the Solid State, Surface, Physical and Mechanical Properties of Particles.* University of Bradford.

Suslick, K. S. (1998) Sonochemistry. *Kirk-othmer encyclopedia of chemical technology*.

Taylor, K. M. G., Pancholi, K. and Wong, D. Y. T. (1999) In-vitro evaluation of dry powder inhaler formulations of micronized and milled nedocromil sodium. *Pharmacy and Pharmacology Communications* 5 (4), 255-257.

Teixeira, C., Mendonça, L., Bergamaschi, M., Queiroz, R., Souza, G., Antunes, L. and Freitas, L. (2016) Microparticles containing curcumin solid dispersion: stability, bioavailability and anti-Inflammatory activity. *AAPS PharmSciTech* 17 (2), 252-261.

Telko, M. J. and Hickey, A. J. (2005) Dry powder inhaler formulation. *Respiratory care* 50 (9), 1209-1227.

Thompson, L. H. and Doraiswamy, L. (2000) The rate enhancing effect of ultrasound by inducing supersaturation in a solid–liquid system. *Chemical Engineering Science* 55 (16), 3085-3090.

Thongprasert, S., Sanguanmitra, P., Juthapan, W. and Clinch, J. (1999) Relationship between quality of life and clinical outcomes in advanced non-small cell lung cancer: best supportive care (BSC) versus BSC plus chemotherapy. *Lung Cancer* 24 (1), 17-24.

Thorat, A. A. and Dalvi, S. V. (2014) Particle formation pathways and polymorphism of curcumin induced by ultrasound and additives during liquid antisolvent precipitation. *CrystEngComm* 16 (48), 11102-11114.

Thorat, A. A. and Dalvi, S. V. (2015) Non-classical crystallization of curcumin.

Thorat, A. A. and Dalvi, S. V. (2016) Ultrasound-assisted modulation of concomitant polymorphism of curcumin during liquid antisolvent precipitation. *Ultrasonics sonochemistry* 30, 35-43.

Thorat, A. A., Yadav, M. D. and Dalvi, S. V. (2014) Simple Criterion for Stability of Aqueous Suspensions of Ultrafine Particles of a Poorly Water Soluble Drug. *Langmuir* 30 (16), 4576-4592.

Tice, R., Agurell, E., Anderson, D., Burlinson, B., Hartmann, A., Kobayashi, H., Miyamae, Y., Rojas, E., Ryu, J. and Sasaki, Y. (2000) Single cell gel/comet assay: guidelines for in vitro and in vivo genetic toxicology testing. *Environmental and Molecular Mutagenesis* 35 (3), 206-221.

Tikhomirov, O. and Carpenter, G. (2003) Identification of ErbB-2 kinase domain motifs required for geldanamycin-induced degradation. *Cancer research* 63 (1), 39-43.

Timsina, M., Martin, G., Marriott, C., Ganderton, D. and Yianneskis, M. (1994) Drug delivery to the respiratory tract using dry powder inhalers. *International journal of pharmaceutics* 101 (1), 1-13.

Tomatis, L., Agthe, C., Bartsch, H., Huff, J., Montesano, R., Saracci, R., Walker, E. and Wilbourn, J. (1978) Evaluation of the carcinogenicity of chemicals: a review of the Monograph Program of the International Agency for Research on Cancer (1971 to 1977). *Cancer Research* 38 (4), 877-885.

Tønnesen, H. H., Másson, M. and Loftsson, T. (2002) Studies of curcumin and curcuminoids. XXVII. Cyclodextrin complexation: solubility, chemical and photochemical stability. *International Journal of Pharmaceutics* 244 (1), 127-135.

Torchilin, V. (2009) Multifunctional and stimuli-sensitive pharmaceutical nanocarriers. *European Journal of Pharmaceutics and Biopharmaceutics* 71 (3), 431-444.

Torchilin, V. P. (2005) Recent advances with liposomes as pharmaceutical carriers. *Nature reviews Drug discovery* 4 (2), 145-160.

Uchitomi, Y., Mikami, I., Nagai, K., Nishiwaki, Y., Akechi, T. and Okamura, H. (2003) Depression and psychological distress in patients during the year after curative resection of non–small-cell lung cancer. *Journal of Clinical Oncology* 21 (1), 69-77.

United States Pharmacopeial Convention. (2004) *The United States Pharmacopeia : the National Formulary.* Rockville, Md.: United States Pharmacopeial Convention.

Usmani, O. S., Biddiscombe, M. F., Nightingale, J. A., Underwood, S. R. and Barnes, P. J. (2003) Effects of bronchodilator particle size in asthmatic patients using monodisperse aerosols. *Journal of Applied Physiology* 95 (5), 2106-2112.

Van Eerdenbrugh, B., Van den Mooter, G. and Augustijns, P. (2008) Top-down production of drug nanocrystals: nanosuspension stabilization, miniaturization and transformation into solid products. *International journal of pharmaceutics* 364 (1), 64-75.

Van Oss, C. (1993) Acid—base interfacial interactions in aqueous media. *Colloids and Surfaces A: Physicochemical and Engineering Aspects* 78, 1-49.

Van Oss, C., Good, R. and Chaudhury, M. (1988) Additive and nonadditive surface tension components and the interpretation of contact angles. *Langmuir* 4 (4), 884-891.

Vaswani, S. K. and Creticos, P. S. (1998) Metered Dost Inhaler: Past, Present, and Future. *Annals of Allergy, Asthma & Immunology* 80 (1), 11-23.

Venkatesan, N. (1998) Curcumin attenuation of acute adriamycin myocardial toxicity in rats. *British journal of pharmacology* 124 (3), 425-427.

Visser, R. (1982) Supersaturation of alpha-lactose in aqueous solutions in mutarotation equilibrium. *Netherlands Milk and Dairy Journal*.

Wahlström, B. and Blennow, G. (1978) A study on the fate of curcumin in the rat. *Acta pharmacologica et toxicologica* 43 (2), 86-92.

Wang, B.-L., Shen, Y.-m., Zhang, Q.-w., Li, Y.-l., Luo, M., Liu, Z., Li, Y., Qian, Z.-y., Gao, X. and Shi, H.-s. (2013) Codelivery of curcumin and doxorubicin by MPEG-PCL results in improved efficacy of systemically administered chemotherapy in mice with lung cancer. *International Journal of Nanomedicine* 8, 3521.

Wang, X., Jiang, Y., Wang, Y.-W., Huang, M.-T., Ho, C.-T. and Huang, Q. (2008) Enhancing anti-inflammation activity of curcumin through O/W nanoemulsions. *Food Chemistry* 108 (2), 419-424.

Wang, Y.-J., Pan, M.-H., Cheng, A.-L., Lin, L.-I., Ho, Y.-S., Hsieh, C.-Y. and Lin, J.-K. (1997) Stability of curcumin in buffer solutions and characterization of its degradation products. *Journal of Pharmaceutical and Biomedical Analysis* 15 (12), 1867-1876.

Ward, G. H. and Schultz, R. K. (1995) PROCESS-INDUCED CRYSTALLINITY CHANGES IN ALBUTEROL SULFATE AND ITS EFFECT ON POWDER PHYSICAL STABILITY. *Pharmaceutical Research* 12 (5), 773-779.

Weber, A., Morlin, G., Cohen, M., Williams-Warren, J., Ramsey, B. and Smith, A. (1997) Effect of nebulizer type and antibiotic concentration on device performance. *Pediatr Pulmonol* 23 (4), 249-60.

Wichitnithad, W., Jongaroonngamsang, N., Pummangura, S. and Rojsitthisak, P. (2009) A simple isocratic HPLC method for the simultaneous determination of curcuminoids in commercial turmeric extracts. *Phytochemical Analysis* 20 (4), 314-319.

Wooster, T. J., Golding, M. and Sanguansri, P. (2008) Impact of oil type on nanoemulsion formation and Ostwald ripening stability. *Langmuir* 24 (22), 12758-12765.

Xing-Jie Liang, C. C. Y. Z. L. J. P. C. W. (2008) Biopharmaceutics and Therapeutic Potential of Engineered Nanomaterials. *Current Drug Metabolism* 9 (8).

Yakubu, S. I. (2009) *Investigations to identify the influence of the inhalation manoeuvre on the ex-vivo dose emission and the in-vitro aerodynamic dose emission characteristics of dry powder inhalers : studies to identify the influence of inhalation flow, inhalation volume and the number of inhalations per dose on the ex-vivo dose emission and the in-vitro aerodynamic dose emission characteristics of dry powder inhalers*. Bradford: University of Bradford,.

Yu, H., Tran, T.-T., Teo, J. and Hadinoto, K. (2016) Dry powder aerosols of curcumin-chitosan nanoparticle complex prepared by spray freeze drying and their antimicrobial efficacy against common respiratory bacterial pathogens. *Colloids and Surfaces A: Physicochemical and Engineering Aspects* 504, 34-42.

Yu, L. (2001) Amorphous pharmaceutical solids: preparation, characterization and stabilization. *Advanced Drug Delivery Reviews* 48 (1), 27-42.